THE UNIVERSITY OF ALBERTA

RELEASE FORM

NAME OF AUTHOR   Siu-Ki Stephen Au

TITLE OF THESIS   An investigation of the propagation of a focused laser beam

in a magnetically confined plasma using ray tracing techniques

DEGREE FOR WHICH THESIS WAS PRESENTED  Master of Science

YEAR THIS DEGREE GRANTED  Fall 1981

Permission is hereby granted to THE UNIVERSITY OF ALBERTA LIBRARY to reproduce single copies of this thesis and to lend or sell such copies for private, scholarly or scientific research purposes only.

The author reserves other publication rights, and neither the thesis nor extensive extracts from it may be printed or otherwise reproduced without the author's written permission.

THE UNIVERSITY OF ALBERTA

An investigation of the propagation of a focused laser beam in a magnetically confined

plasma using ray tracing techniques

by

$\left( C \right)$ Siu-Ki Stephen Au

A THESIS

SUBMITTED TO THE FACULTY OF GRADUATE STUDIES AND RESEARCH

IN PARTIAL FULFILMENT OF THE REQUIREMENTS FOR THE DEGREE

OF Master of Science

IN

Plasma Studies

Department of Electrical Engineering

EDMONTON, ALBERTA

Fall, 1981

THE UNIVERSITY OF ALBERTA

FACULTY OF GRADUATE STUDIES AND RESEARCH

The undersigned certify that they have read, and recommend to the Faculty
of Graduate Studies and Research, for acceptance, a thesis entitled An investigation of
the propagation of a focused laser beam in a magnetically confined plasma using ray
tracing techniques submitted by Siu-Ki Stephen Au in partial fulfilment of the
requirements for the degree of Master of Science in Plasma Studies.

## Dedication

*To my parents*

*and*

*To the goodwill of mankind*

## Abstract

The propagation of a focused laser beam in a magnetically confined plasma is studied using ray tracing techniques. The transport of beam energy along rays in a vacuum is described in terms of a phase space distribution function which includes the beam diffraction effects. Solutions for ray trajectories in the plasma are solved for various density profiles. These solutions are used to match into corresponding density distributions within the medium. Energy deposition and ponderomotive forces are evaluated accordingly. Program packages are designed to be used with the magnetic shell flux code developed by McMullin, Milroy and Capjack.

## Acknowledgement

# Table of Contents

## List of Figures

# Chapter 1

## Introduction

### 1.1 Significance of the problem

The utilization of lasers as energy sources for heating plasmas in a thermonuclear fusion reaction has been studied extensively in the past years. J. Nuckolls et. al.[1] proposed the scheme of using laser beams to heat plasmas confined within a spherical pellet (inertial confinement), while Dawson[2] et. al. reported the feasibility of heating magnetically confined plasmas by lasers(laser heating with magnetic confinement). In both schemes, as the laser beam propagates within the plasma, energy is transferred to the medium. The plasma is heated up upon absorbing the energy and as a result, thermo-expansion of the plasma will take place. The disturbance in the plasma density affects the refractive index and hence a change in the propagation of the beam. This, in turn, will change the heating pattern for the plasma and a self-consistent system will be set up between the plasma and the beam. In order to understand the heating mechanism, it is essential to study the problem of laser beam propagation within a plasma medium. Before introducing the research objectives, a survey of the recent investigations on this problem will be carried out in the following section.

### 1.2 Review of past work

In 1974, Humphries[3] studied the propagation of a laser beam parallel to the magnetic field in a $\theta$ pinch plasma column. He found that waveguide type solutions are necessary for describing the beam condition within a plasma which was assumed to have a radially parabolic density profile. Mani et.al.[4] used the method of normal mode analysis to describe laser beam propagation within a plasma column having a parabolic density variation. They evaluated the maximum number of modes that can be trapped within the plasma. Their analysis showed that the beam propagates periodically along the column. Feit et.al.[5,6,7,8] developed a self-consistent treatment for the relation between laser beam propagation and plasma hydrodynamics. They found that the beam trapped itself as it heats up the medium. In their further investigations, they showed that an axial density

changes were also found in the beam after it traversed the column. They also studied the case of a beam propagating through a region with an electron density profile determined from a detailed time-dependent hydrodynamic calculation. The beam was found to exhibit aperiodic properties along the column but remained trapped. McMullin et.al.[9] used normal mode analysis to derive a general expression for the field of a laser beam in a quadratic waveguide. The electric field amplitude was shown to exhibit periodic property along the column. For an axially varying parabolic density profile, the electric field was expressed as a linear combination of the normal modes for a quadratic profile. They found that the electric field of the beam displays aperiodic axial variation.

Instead of using wave optics to treat the problem, Steinhauer and Ahlstrom[10, 11] made a detailed study on the problem by means of geometrical optics. They considered the propagation of rays along a cylindrical plasma column with azimuthal symmetry. They found that rays would oscillate within a plasma column which has a parabolic density profile with an on axis minimum. The beam trapping phenomena were experimentally observed by several research groups[12, 13, 14].

Dudder and Henderson[15] developed a two dimensional (radial and axial) simulation model, RAMSES, for studying the propagation of a laser pulse through a background gas or plasma. Ray optics was used in the model. The ray trajectories were solved from the ray equation. Hubbard and Montes[16] also developed a program to trace the beam in a continuously varying refracting medium. They used the method of Taylor expansion about the initial position to approximate the new ray position. Acccording to the analysis, by knowing the refractive index of the medium, its gradient, the co-ordinates and tangent vector of an initial point on the ray, the co-ordinates of the ray path can be found. However, diffraction and phase information of the radiation were not included in the program and the initial positions and directions of the rays were chosen in a definite pattern.

Rinker and Bohannon[17] recently presented a description of the finite size focal spot of a laser beam. Rays were chosen to be normally distributed at the focal plane so that a Gaussian beam intensity profile was ensured at the spot. In the analysis, the rays are traced within a cylindrical symmetric medium by means of a two step procedure. The first step gives the ray positions at the boundaries of a plasma zone and the second step

computes the ray path within the zone. Their overall treatment does not include the diffraction effects of the beam.

Tappert[18] developed a method to trace rays for a focused laser beam with the inclusion of diffraction effects. Formulae were derived for the spread of ray angles that yield the correct diffraction patterns for coherent and partially coherent beams. With this method, the size of the beam was found to reach the diffraction limit in the case of an ideal lens.

### 1.3 Purpose of present work

The purpose of the present work is to investigate the propagation of a focused laser beam in a plasma confined within a solenoidal magnetic field by using geometrical optics. The use of ray optics to describe beam propagation gives an alternate approach for obtaining the propagation behaviour of the beam. The objective can be divided into three parts:

1.    *Description of a focused laser beam in vacuum using ray optics*

By using rays to describe the focusing action of an ideal lens, one has to solve the problem of infinite intensity at the focus as all rays will merge into that point. Tappert suggested including the diffraction effects of a focused beam in the ray tracing technique so that a finite size focal spot can be attained. Based upon this idea, rays emerging from a converging lens are assigned a direction which deviate from the direction pointing at the focus. This deviation is chosen to follow a Gaussian distribution. With such chosen directions, rays will spread out at the focus in a Gaussian manner, avoiding the problem of infinite intensity.

2.    *Beam propagation within a magnetically confined plasma column*

The propagation of the beam within the plasma are studied in terms of ray optics. Past work has been done for the case of a parabolic density profile. The present objective is to trace rays within the plasma which has an arbitrary profile. This tracing is intended for implementing the magnetohydrodynamic(MHD) code for a plasma column developed by McMullin, Milroy and Capjack [19]. In the code, the spatial beam intensity profile and hence the laser power is assumed to be a constant of time within the column. This assumption does not include the effect of

a changing refractive index which alters the beam profile. The tracing routine will be used to modify the laser power computation routine in the MHD code by including refractions. In this way, a more realistic simulation of the plasma can be obtained.

3.   *Calculation of absorbed energy and ponderomotive forces*

Upon knowing how the beam propagates inside the column, energy deposition and absorption can be described more accurately. An energy absorption package is designed based upon the computed ray trajectories, since energy interchanges are taken place along the ray paths. Moreover, the MHD code is also designed for studying the magnetohydrodynamics for a gas target, the ponderomotive force becomes an important component affecting the dynamics of the plasma as high intensity laser beams are used in this case.

Discussions and derivations of the above objectives are presented in the following chapters. In chapter two, an explanation of Tappert's diffractive ray tracing technique is given. Here, rays can be chosen accordingly to simulate a focused laser beam propagating in vacuum. Cases for coherent and incoherent Gaussian beam are presented. The propagation of these rays inside the plasma is discussed in chapter three. Solutions to the ray trajectories in regions with different densities are derived. Chapter four gives a discussion on the energy absorption and ponderomotive forces within the plasma. Energy absorption is based on inverse Bremstrahlung process. Derivations of ponderomotive forces are based on the work of Chen[20]. The conversion of the analytical results obtained in previous chapters into numerical computations is presented in chapter five. Descriptions of program routines for generation of ray locations and directions, ray tracing and energy absorption are given and discussed. Results computed for a tested density profile within the plasma column are discussed in chapter six.

CGS units are adopted throughout the work, except power is given in watts.

# Chapter 2

## Diffractive ray tracing

The focusing action of an ideal converging lens can be determined by tracing rays according to the theory of geometrical optics. Ideally, rays parallel to the optical axis of a converging lens will all converge to the focus resulting with an infinite intensity at that point. However, according to the theory of diffraction[1], a light beam parallel to the optical axis of the lens is not focused to just a point but to a sizable area. The beam intensity at the geometrical focus is found to be

$$I = (\frac{\pi a^2 A}{\lambda f_L^2})^2$$

where A is the amplitude of a spherical wave front, $\frac{Ae^{ikr}}{r}$ at unit distance from the source; $f_L$ and a are focal length and aperture of lens respectively; $\lambda$ is the wavelength of the incident beam. As can be seen from the expression, the focal intensity goes to infinity as the wavelength $\lambda$ goes to zero which is the basic assumption used in geometrical optics.

A more accurate description of the lens focusing action can be provided by the ray tracing techniques if the diffraction effects are incorporated into the picture. This chapter discusses how rays can be chosen to take the diffraction effect into account by introducing the idea of a phase space distribution function. Based on this function, formulae for ray directions and for beam size are derived for a beam with a Gaussian amplitude and a coherent phase in the first case and an incoherent phase in the second case. Section 2.1 explains how the radiation energy of a beam can be distributed into particular locations and directions according to the above distribution function. This latter function for a Gaussian beam will be derived in section 2.2. Section 2.3 discusses how the distributed radiation energy can be assigned to rays with particular directions and locations. It also gives a description of the ray distribution at the lens and focal planes. Section 2.4 discusses the distribution function for a Gaussian beam with incoherent phases due to instrument limitations.

## 2.1 Tappert's phase-space distribution function

In this section, Tappert's phase space distribution function is defined. The significance of this function in the ray tracing technique is discussed. The energy density and energy flux of a laser beam are found to be the zero and first moments respectively of this function with respect to direction.

In conventional ray tracing of light propagation through a converging lens, each point at the lens plane can be associated with a ray directed towards the focus so that all rays will meet at one spot. In order to obtain the diffraction limited focus size, the directions of rays were chosen in such a way that not all the rays would intersect at the focus. Tappert's phase space distribution function provides a method of solving this problem.

Before defining the distribution function, a review on the derivation of energy flux and energy density from Helmoltz equation for the vacuum case is given in here for future reference.

The wave equation for a laser beam propagating in vacuum is given by the Helmoltz equation

$$\vec{\nabla}^2 \vec{E} + k^2 \vec{E} = 0$$

$$\vec{E} = \vec{\epsilon}(\vec{r})\exp(i\vec{k}\cdot\vec{r} - i\omega t) \tag{2.1.1}$$
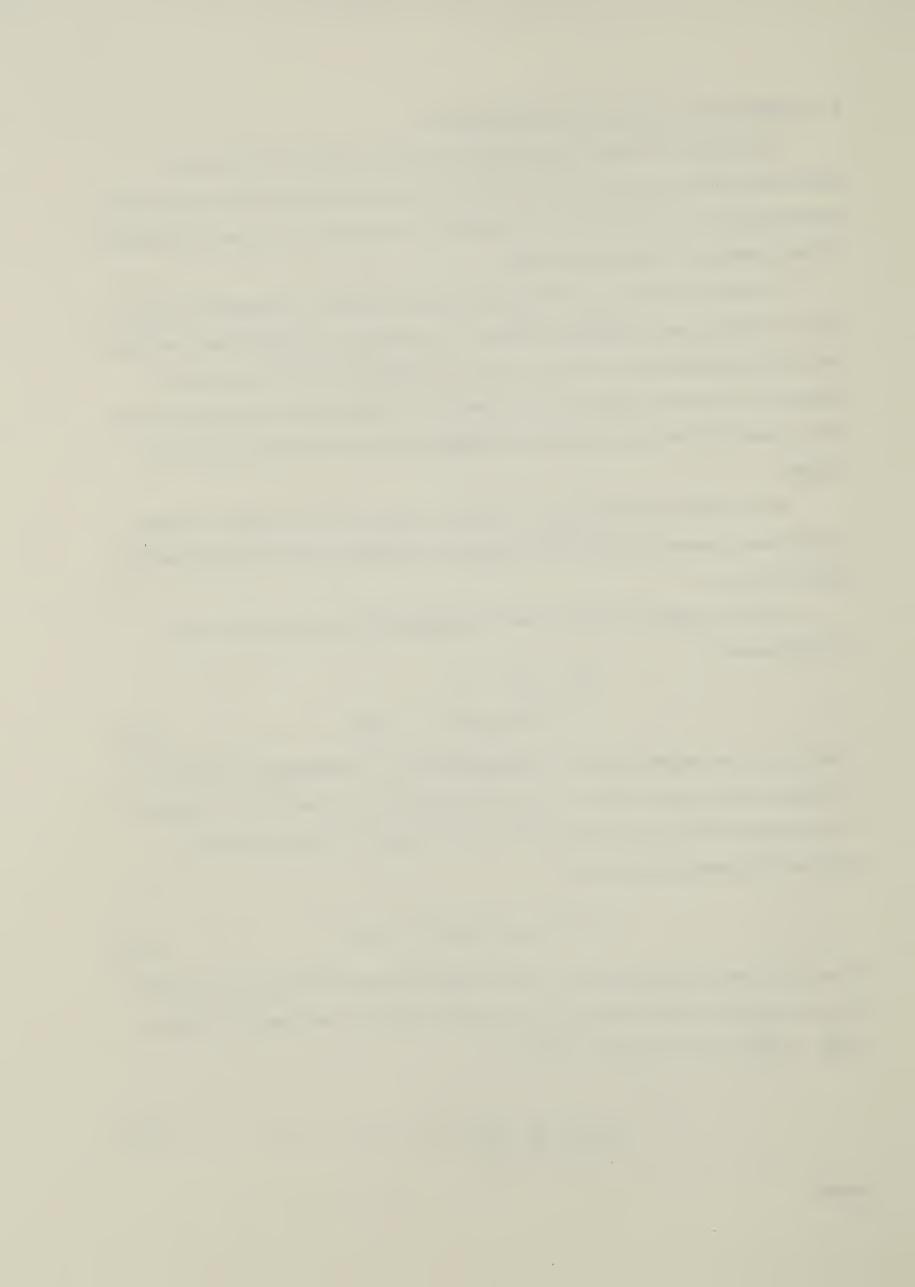
where $\vec{k}$ is the propagation vector in vacuum, and $|k|=\omega/c$; $\omega$ is the angular frequency of the wave; $c$ is the speed of light; $\vec{r}$ is the position vector of a wavefront at a distance $r$ from the source. Through assuming that the wave propagates primarily along the $\vec{z}$ direction, $\vec{E}$ is taken to have the form

$$\vec{E} = \vec{\epsilon}(x,y,z)\exp(ikz - i\omega t) \tag{2.1.2}$$

By using the parabolic approximation (which states that the axial field amplitude variation over a wavelength is much smaller than the variation over the axial scale length, that is,
$(\frac{\partial^2 \epsilon}{\partial z^2} \ll k\frac{\partial \epsilon}{\partial z}$ ), eq. (2.1.1) is then reduced to

$$i\frac{\partial \epsilon}{\partial z} + \frac{1}{2k} \frac{\partial^2 \epsilon}{\partial \vec{x}_\perp^2} = 0 \tag{2.1.3}$$

where

By taking the Fourier Transform of eq. (2.1.3) with respect to $\vec{k} = k_x\vec{i} + k_y\vec{j}$ and using the boundary conditions : (1)at infinity, the integrals of $\frac{\partial \varepsilon}{\partial x_\perp}$ and $\varepsilon$ vanish over a surface perpendicular to the direction of propagation (see footnote) , the equation becomes

$$\frac{d\varepsilon_F}{dz} = -a^2 k_\perp^2 \varepsilon_F$$

(2.1.3a)

On solving eq. (2.1.3a) with the boundary condition that the electric field at the lens plane is $\varepsilon(x,y,z_0)$, the solution of the transformed equation is

$$\varepsilon_F(k_x,k_y,z) = \varepsilon_F(k_x,k_y,z_0)\exp[-a^2k_\perp^2(z-z_0)]$$

(2.1.4)

where

$$\varepsilon_F(k_x,k_y,z) = \frac{1}{2\pi} \int\int_{-\infty-\infty}^{\infty\ \infty} \exp(i\vec{k_\perp}\cdot\vec{x_\perp})\varepsilon(\vec{x_\perp},z)d^2\vec{x_\perp}$$

$$a^2 = -\frac{1}{2ik}$$

(2.1.5)

By taking the inverse Fourier transform of eq. (2.1.4) and applying the convolution theorem, the amplitude of the electric field at $z>z_0$ is given by

$$\varepsilon(x,y,z) = \frac{k}{2\pi i (z-z_0)} \int\int_{-\infty-\infty}^{\infty\ \infty} \varepsilon(\vec{x_\perp'},z_0)\exp[\frac{ik(\vec{x_\perp}-\vec{x_\perp'})^2}{2(z-z_0)}]d^2\vec{x_\perp'}$$

(2.1.6)

According to the electromagnetic theory, the time average energy density U and flux $\vec{S}$ of the radiation field which is characterized by eq. (2.1.2) are

$$U = \frac{1}{8\pi} |\varepsilon|^2$$

(2.1.7)

$$\vec{S} = \frac{c}{8\pi} [|\varepsilon|^2\vec{z} - \frac{i}{2k}(\varepsilon^*\vec{\nabla_\perp}\varepsilon - \varepsilon\vec{\nabla_\perp}\varepsilon^*)]$$

(2.1.8)
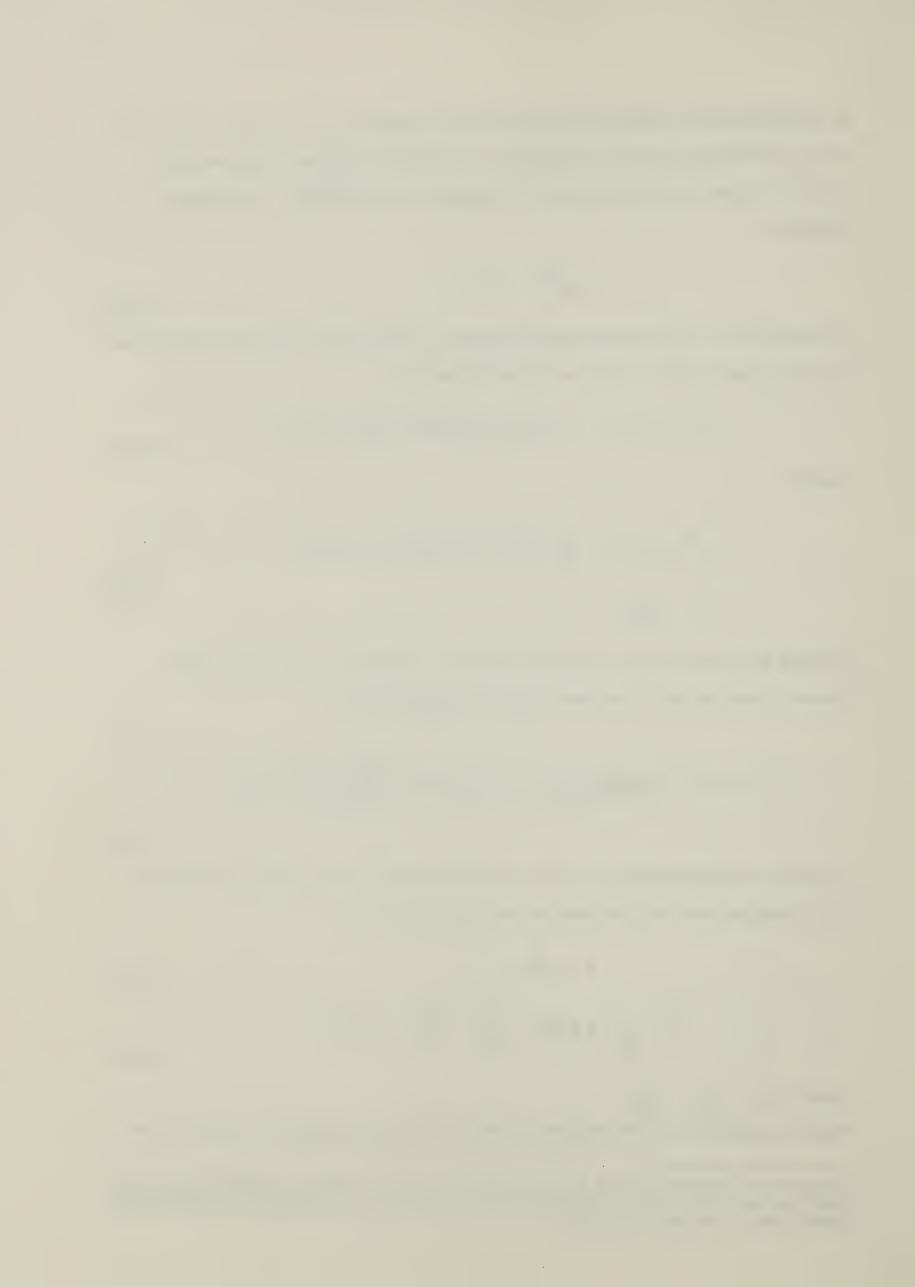
where $\vec{\nabla_\perp}$ is $\frac{\partial}{\partial x}\vec{i} + \frac{\partial}{\partial y}\vec{j}$

These two quantities can be evaluated in terms of the integral derived in eq. (2.1.6). The

--------------------------

The boundary condition can be imposed because of the finiteness of field energy. At any time t, the wavefront from a source reaches a distance ct. If the boundary is taken to be further than ct, the field will be zero.

derivation of $\vec{S}$ is given in Appendix(1).

Instead of obtaining the energy density and flux by directly evaluating eq. (2.1.7) and eq. (2.1.8) with the electric field given by eq. (2.1.6), Tappert introduced the idea of using a phase space distribution function to evaluate the quantities. This distribution function was originated from Wigner[2] who introduced it in finding the probability of a particle having its location and momentum defined simultaneously.

Adopting this idea from Wigner[2,3], Tappert[4] was able to describe the propagation of beam energy in terms of a set of rays continuously distributed over space and directions by using a phase space distribution function in the form

$$f(\vec{x}_\perp,\vec{u}_\perp,z) = \frac{k^2}{(2\pi)^2}\iint_{-\infty -\infty}^{\infty \infty} d^2\vec{x}_\perp' e^{ik\vec{u}_\perp\cdot\vec{x}_\perp'} \epsilon(\vec{x}_\perp-\tfrac{1}{2}\vec{x}_\perp',z)\epsilon^*(\vec{x}_\perp+\tfrac{1}{2}\vec{x}_\perp',z) \qquad (2.1.9)$$

$\epsilon(\vec{x}_\perp,z)$ is defined in eq. (2.1.2); $\vec{u}_\perp$ is a two dimensional unit vector whose x and y components denote the direction cosines of the ray direction (see fig. 2.1)

$$u_{\perp x} = \sin\theta\cos\phi$$

$$u_{\perp y} = \sin\theta\sin\phi$$

For rays propagating close to the axis of propagation, the magnitude of $\vec{u}_\perp$ is

$$|\vec{u}_\perp| = \sqrt{u_{\perp x}^2 + u_{\perp y}^2}$$

$$= |\sin\theta| = \theta$$

For small angle $\theta$, the magnitude of $\vec{u}_\perp$ approximately equals to the angle which is the angle the ray subtends at the z-axis.

This function gives a description of the distribution of beam energy over space and direction. The amount of beam energy which is located at the point (x,y) and propagates in the direction $\vec{u}_\perp=\vec{u}_\perp+\vec{z}$ is determined from the function. The trajectory which is traced out by this pack of energy is a ray with defined origin $\vec{x}$ and direction $\vec{u}_\perp+\vec{z}$. Tappert's function is a real function and may take negative values. It has the following properties:
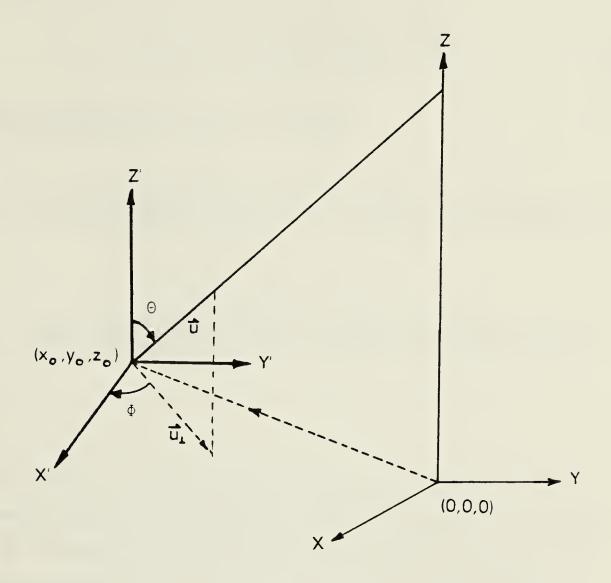
Figure 2.1 Co-ordinate system adopted for rays.

1. When it is integrated over all transverse directions $\vec{u}_\perp$, it gives the energy density over a volume element at location $(\vec{x}_\perp,z)$, that is,

$$U(\vec{x}_\perp,z) = \frac{1}{8\pi} \int\int_{-1}^{1} f(\vec{x}_\perp,\vec{u}_\perp,z)d^2\vec{u}_\perp \qquad (2.1.10)$$

which after substituting f from eq. (2.1.9), gives

$$U(\vec{x}_\perp, z) = \frac{1}{8\pi}\int_{-\infty}^{\infty}\int_{-\infty}^{\infty} \frac{k^2}{(2\pi)^2}d^2\vec{x}'_\perp \int_{-1}^{1}\int_{-1}^{1} e^{i k\vec{u}_\perp \cdot \vec{x}'_\perp}\varepsilon(\vec{x}_\perp-\tfrac{1}{2}\vec{x}'_\perp, z)\varepsilon^*(\vec{x}_\perp+\tfrac{1}{2}\vec{x}'_\perp, z) \, d^2\vec{u}_\perp$$

$$=\frac{1}{8\pi}\frac{k^2}{(\pi)^2}\int_{-\infty}^{\infty}\int_{-\infty}^{\infty}\frac{\sin kx'}{kx'}\frac{\sin ky'}{ky'}\varepsilon(\vec{x}_\perp-\tfrac{1}{2}\vec{x}'_\perp,z)\varepsilon^*(\vec{x}_\perp+\tfrac{1}{2}\vec{x}'_\perp,z)dx'dy'$$

Since the amplitude of the electric field is assumed to vary slowly over a wavelength, the field can be considered constant over the region of integration $(\frac{-\pi}{k}, \frac{\pi}{k})$. The value of the electric field at $\vec{x}'_\perp=0$ is taken to be the field value throughout the region $(\frac{-\pi}{k}, \frac{\pi}{k})$. Thus, the integral can be approximated as

$$U(\vec{x}_\perp, z) = \frac{1}{8\pi}\frac{k^2}{(\pi)^2}[\int\int_{-\infty}^{\infty}\frac{\sin kx'}{kx'}\frac{\sin ky'}{ky'}]dx'dy'\,\varepsilon(\vec{x}_\perp,z)\varepsilon^*(\vec{x}_\perp,z)$$

$$= \frac{\varepsilon(\vec{x}_\perp,z)\varepsilon^*(\vec{x}_\perp,z)}{8\pi}\frac{k^2}{\pi^2}\int\int_{0}^{\infty}\frac{\sin ky'\,4\sin kx'}{ky'\,kx'}dx'dy'$$
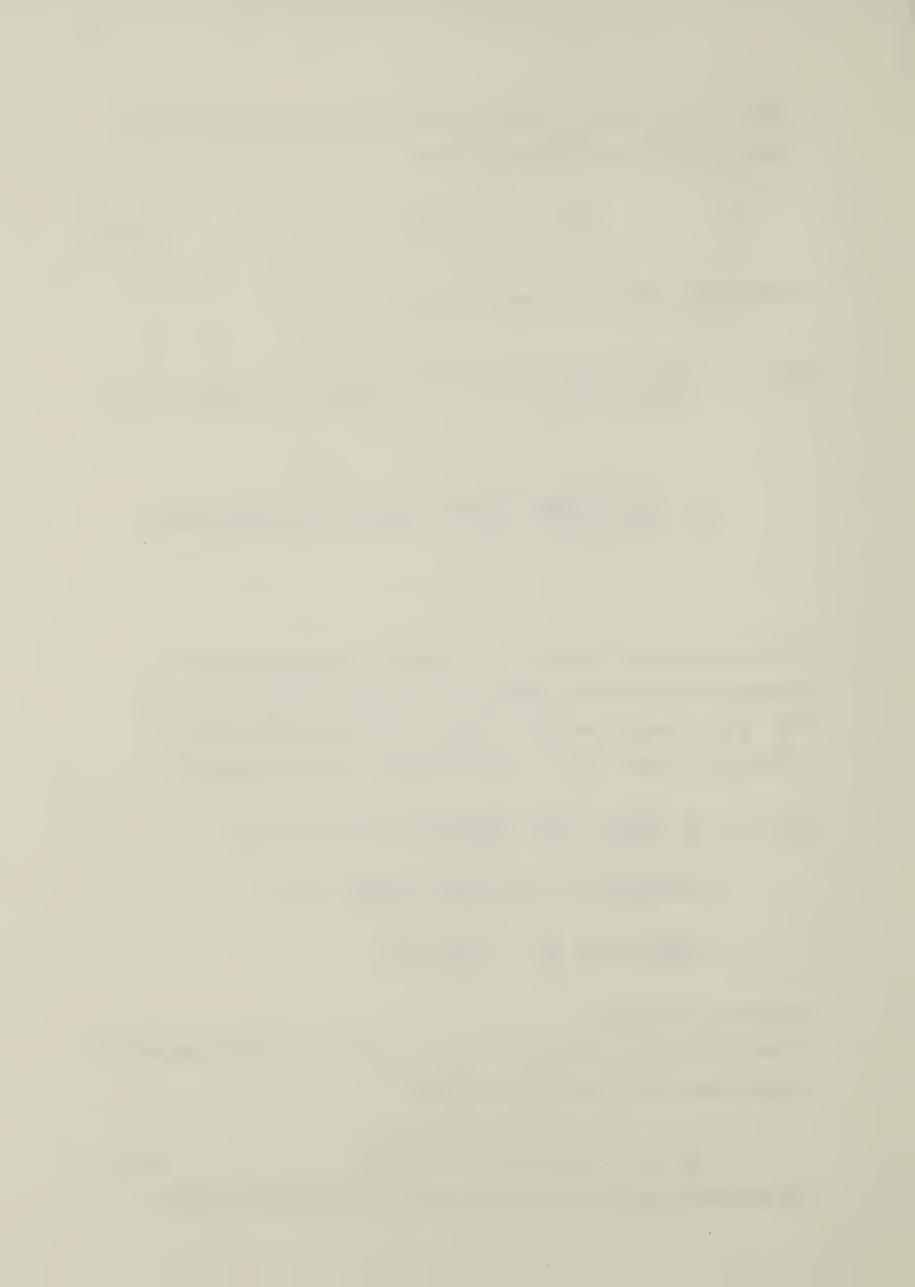
$$= \frac{|\varepsilon(\vec{x}_\perp,z)|^2}{8\pi}\frac{k^2}{\pi^2}\frac{4\pi^2}{4k^2} = \frac{|\varepsilon(\vec{x}_\perp,z)|^2}{8\pi}$$

which is the energy density.

2. When $\vec{u}_\perp f$ is integrated with respect to $u_{\perp x}, u_{\perp y}$ the transverse flux components of the light beam along x , y directions is obtained

$$\vec{S}_\perp(\vec{x}_\perp,z) = \frac{c}{8\pi}\int_{-1}^{1}\int_{-1}^{1} f(\vec{x}_\perp,\vec{u}_\perp,z)\vec{u}_\perp d^2\vec{u}_\perp \qquad (2.1.11)$$

The aforemented statement is verified by substituting f into eq. (2.1.11) giving

$$\vec{S}_{\perp}(\vec{x}_{\perp},z) = \frac{c}{8\pi} \int_{-\infty}^{\infty}\int_{-\infty}^{\infty}dx'dy'\,\epsilon(\vec{x}_{\perp}-\tfrac{1}{2}\vec{x}_{\perp}',z)\epsilon*(\vec{x}_{\perp}+\tfrac{1}{2}\vec{x}_{\perp}',z)$$

$$\times(\frac{k}{2\pi})^2\int_{-1}^{1}\int_{-1}^{1}(u_{\perp x}\vec{i}+u_{\perp y}\vec{j})e^{ik(u_{\perp x}x'+u_{\perp y}y')}du_{\perp x}du_{\perp y} \qquad (2.1.12)$$

Consider the x component of $S_{\perp}$,

$$S_{x}(\vec{x}_{\perp},z) = \frac{c}{8\pi} \iint_{-\infty}^{\infty}dx'dy'\,\epsilon(\vec{x}_{\perp}-\tfrac{1}{2}\vec{x}_{\perp}',z)\epsilon*(\vec{x}_{\perp}+\tfrac{1}{2}\vec{x}_{\perp}',z)$$

$$\times\frac{k^2}{(2\pi)^2}\iint_{-1}^{1}u_{\perp x}e^{ik(u_{\perp x}x'+u_{\perp y}y')}du_{\perp x}du_{\perp y}$$

$$= \frac{c}{8\pi}\frac{k^2}{(2\pi)^2}\int_{-\infty}^{\infty}\int_{-\infty}^{\infty}dx'dy'\,\epsilon(\vec{x}_{\perp}-\tfrac{1}{2}\vec{x}_{\perp}',z)\epsilon*(\vec{x}_{\perp}+\tfrac{1}{2}\vec{x}_{\perp}',z)$$

$$\times\int_{-1}^{1}u_{\perp x}e^{iku_{\perp x}x'}du_{\perp x}\int_{-1}^{1}e^{iku_{\perp y}y'}du_{\perp y}$$

$$= \frac{c}{8\pi}(\frac{k}{2\pi})^2\int_{-\infty}^{\infty}\int_{-\infty}^{\infty}dx'dy'\,\epsilon(\vec{x}_{\perp}-\tfrac{1}{2}\vec{x}_{\perp}',z)\epsilon*(\vec{x}_{\perp}+\tfrac{1}{2}\vec{x}_{\perp}',z)$$

$$\times\frac{d}{dx'}\int_{-1}^{1}\frac{e^{iku_{\perp x}x'}}{ik}du_{\perp x}\frac{2\sin ky'}{ky'}$$

$$= \frac{c}{8\pi}(\frac{k}{2\pi})^2\frac{4}{ik}\int_{-\infty}^{\infty}\frac{d}{dx'}\frac{\sin kx'}{kx'}dx'$$

$$\times\int_{-\infty}^{\infty}\frac{\sin ky'}{ky'}\epsilon(\vec{x}_{\perp}-\tfrac{1}{2}\vec{x}_{\perp}',z)\epsilon*(\vec{x}_{\perp}+\tfrac{1}{2}\vec{x}_{\perp}',z)dy'$$

By the same argument as in (i),

$$S_{x}(\vec{x}_{\perp}',z) = \frac{c}{8\pi}(\frac{k}{2\pi})^2\frac{4}{ik}\frac{\pi}{k}\int_{-\infty}^{\infty}\epsilon(x-\tfrac{1}{2}x',y-\tfrac{1}{2}y',z)_{y'=0}$$

$$\times\epsilon*(x+\tfrac{1}{2}x',y+\tfrac{1}{2}y',z)_{y'=0}[\frac{d}{dx'}\frac{\sin kx'}{kx'}]dx'$$

$$= \frac{c}{8\pi} \left(\frac{k}{2\pi}\right)^2 \frac{4\pi}{ik^2} [-\int_{-\infty}^{\infty} \frac{\sin kx'}{kx'} \frac{\partial}{\partial x'} \epsilon \epsilon^* dx']$$

Since the field is assumed to vary slowly in space, the derivative of the product of the field amplitudes, $\frac{\partial}{\partial x'}(\epsilon \epsilon^*)$ can be considered constant and taken to be the value at $x'=0$, Thus, after integrating,

$$S_x(\vec{x}_\perp, z) = \frac{c}{8\pi} \frac{1}{ik} \frac{\partial}{\partial x'}(\epsilon \epsilon^*)\Big|_{x'=0}$$

Similarly, for the y component of $\vec{S}$,

$$S_y(\vec{x}_\perp, z) = \frac{c}{8\pi} \frac{1}{ik} \frac{\partial}{\partial y'}(\epsilon \epsilon^*)\Big|_{y'=0}$$

By adding the x and y components, the transverse flux component is given by

$$\vec{S}_\perp = S_x \vec{i} + S_y \vec{j}$$

$$= \frac{c}{8\pi} \frac{1}{ik} \vec{\nabla}_\perp'(\epsilon \epsilon^*)\Big|_{x'=0,y'=0}$$

By using the transform of the co-ordinates,

$$\vec{\nabla}_\perp' \epsilon(\vec{x}_\perp - \frac{1}{2}\vec{x}_\perp', z) = -\frac{1}{2}\vec{\nabla}_\perp \epsilon(\vec{x}_\perp - \frac{1}{2}\vec{x}_\perp', z) \qquad (2.1.12a)$$
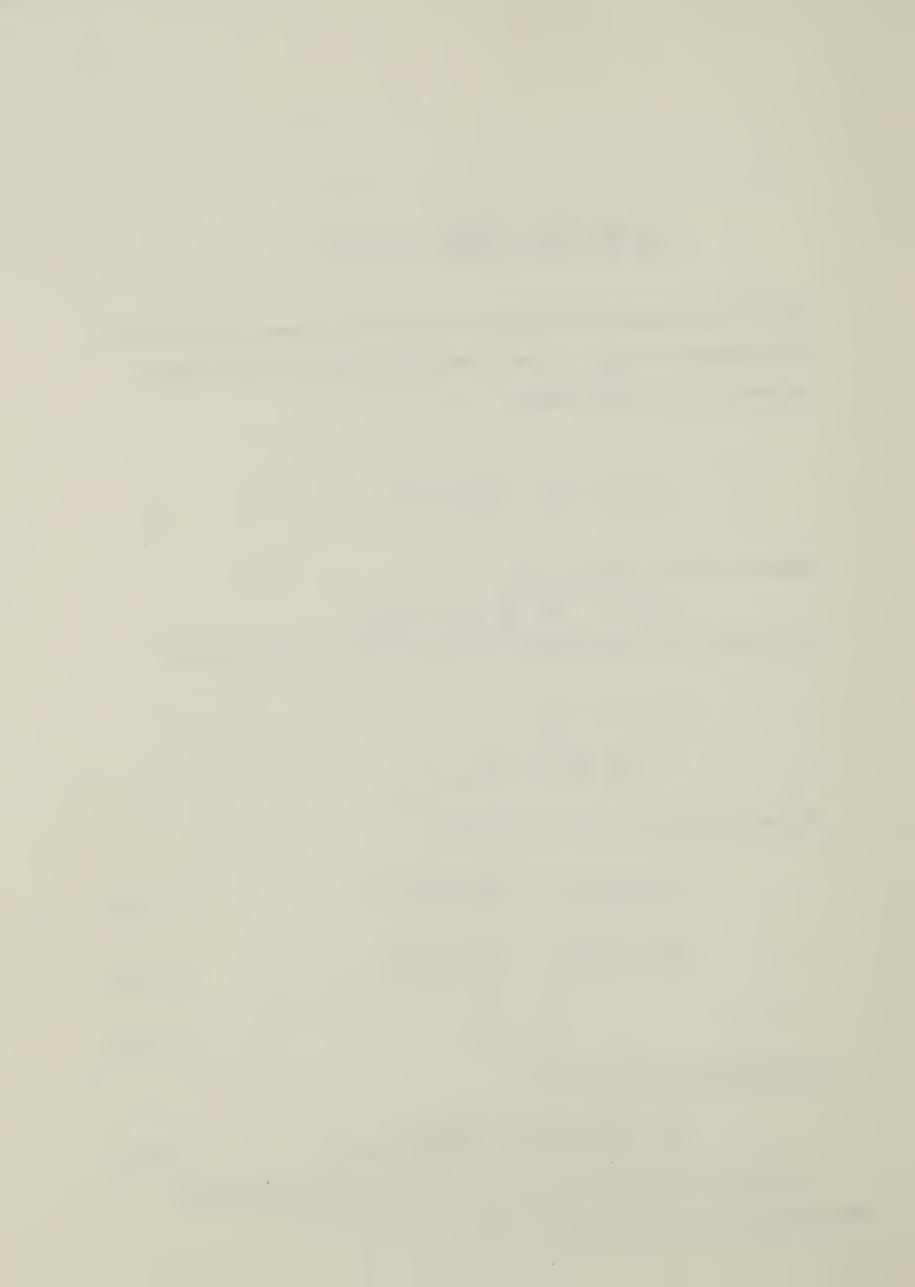
$$\vec{\nabla}_\perp' \epsilon^*(\vec{x}_\perp + \frac{1}{2}\vec{x}_\perp', z) = \frac{1}{2}\vec{\nabla}_\perp \epsilon^*(\vec{x}_\perp + \frac{1}{2}\vec{x}_\perp', z) \qquad (2.1.12b)$$

$$\vec{\nabla}_\perp^2 = 4\vec{\nabla}_\perp'^2 \qquad (2.1.13)$$

the transverse flux vector becomes

$$\vec{S}_\perp = \frac{c}{8\pi} \frac{i}{2k} [\epsilon \vec{\nabla}_\perp \epsilon^* - \epsilon^* \vec{\nabla}_\perp \epsilon]\Big|_{x'=0,y'=0} \qquad (2.1.14)$$

The variation of the distribution function along a trajectory can be found by differentiating eq. (2.1.9) with respect to z, that is,

$$\frac{\partial f}{\partial z} = \frac{k^2}{(2\pi)^2}\int_{-\infty}^{\infty}\int_{-\infty}^{\infty}d^2\vec{x}_\perp' e^{ik\vec{u}_\perp\cdot\vec{x}_\perp'}\left(\varepsilon\frac{\partial\varepsilon^*}{\partial z} + \varepsilon^*\frac{\partial\varepsilon}{\partial z}\right)$$ (2.1.15)

Multiply eq. (2.1.3) by $\varepsilon^*$ and its complex conjugate by $\varepsilon$ ,

$$i\varepsilon^*\frac{\partial\varepsilon}{\partial z} + \frac{\varepsilon^*}{2k}\vec{\nabla}_\perp^2\varepsilon = 0$$ (2.1.16)

$$-i\varepsilon\frac{\partial\varepsilon^*}{\partial z} + \frac{\varepsilon}{2k}\vec{\nabla}_\perp^2\varepsilon^* = 0$$ (2.1.17)

eq. (2.1.15) becomes

$$\frac{\partial f}{\partial z} = \frac{1}{2ik}\frac{k^2}{(2\pi)^2}\int_{-\infty}^{\infty}\int_{-\infty}^{\infty}d^2\vec{x}_\perp' e^{ik\vec{u}_\perp\cdot\vec{x}_\perp'}(\varepsilon\vec{\nabla}_\perp^2\varepsilon^* - \varepsilon^*\vec{\nabla}_\perp^2\varepsilon)$$ (2.1.18)

And from eq (2.1.12) and eq. (2.1.13), $\frac{\partial f}{\partial z}$ becomes

$$\frac{\partial f}{\partial z} = \frac{2}{ik}\left(\frac{k}{2\pi}\right)^2\int_{-\infty}^{\infty}\int_{-\infty}^{\infty}d^2\vec{x}_\perp' e^{ik\vec{u}_\perp\cdot\vec{x}_\perp'}(\varepsilon\vec{\nabla}_\perp'^2\varepsilon^* - \varepsilon^*\vec{\nabla}_\perp'^2\varepsilon)$$ (2.1.19)

Integrating each term by parts and using the boundary condition $\varepsilon(x,y,z)\underset{\substack{x\to-\infty\\y\to-\infty}}{=}0$, one gets

$$\frac{\partial f}{\partial z} = \frac{k^2}{(2\pi)^2}\left(\frac{2}{ik}\right)\left[\int_{-\infty}^{\infty}\int_{-\infty}^{\infty}\vec{\nabla}_\perp'(\varepsilon^* e^{ik\vec{u}_\perp\cdot\vec{x}_\perp'})\vec{\nabla}_\perp'\varepsilon\,d^2\vec{x}_\perp'\right.$$

$$\left.-\int_{-\infty}^{\infty}\int_{-\infty}^{\infty}\vec{\nabla}_\perp'(\varepsilon e^{ik\vec{u}_\perp\cdot\vec{x}_\perp'})\vec{\nabla}_\perp'\varepsilon^*\,d^2\vec{x}_\perp'\right]$$ (2.1.20)

Expanding the integrand,

$$\frac{\partial f}{\partial z} = 2\int_{-\infty}^{\infty}\int_{-\infty}^{\infty}\left(\frac{k}{2\pi}\right)^2[\varepsilon^*\vec{u}_\perp\cdot\vec{\nabla}_\perp'\varepsilon - \vec{u}_\perp\cdot\vec{\nabla}_\perp'\varepsilon^*]e^{ik\vec{u}_\perp\cdot\vec{x}_\perp'}d^2\vec{x}_\perp'$$ (2.1.21)
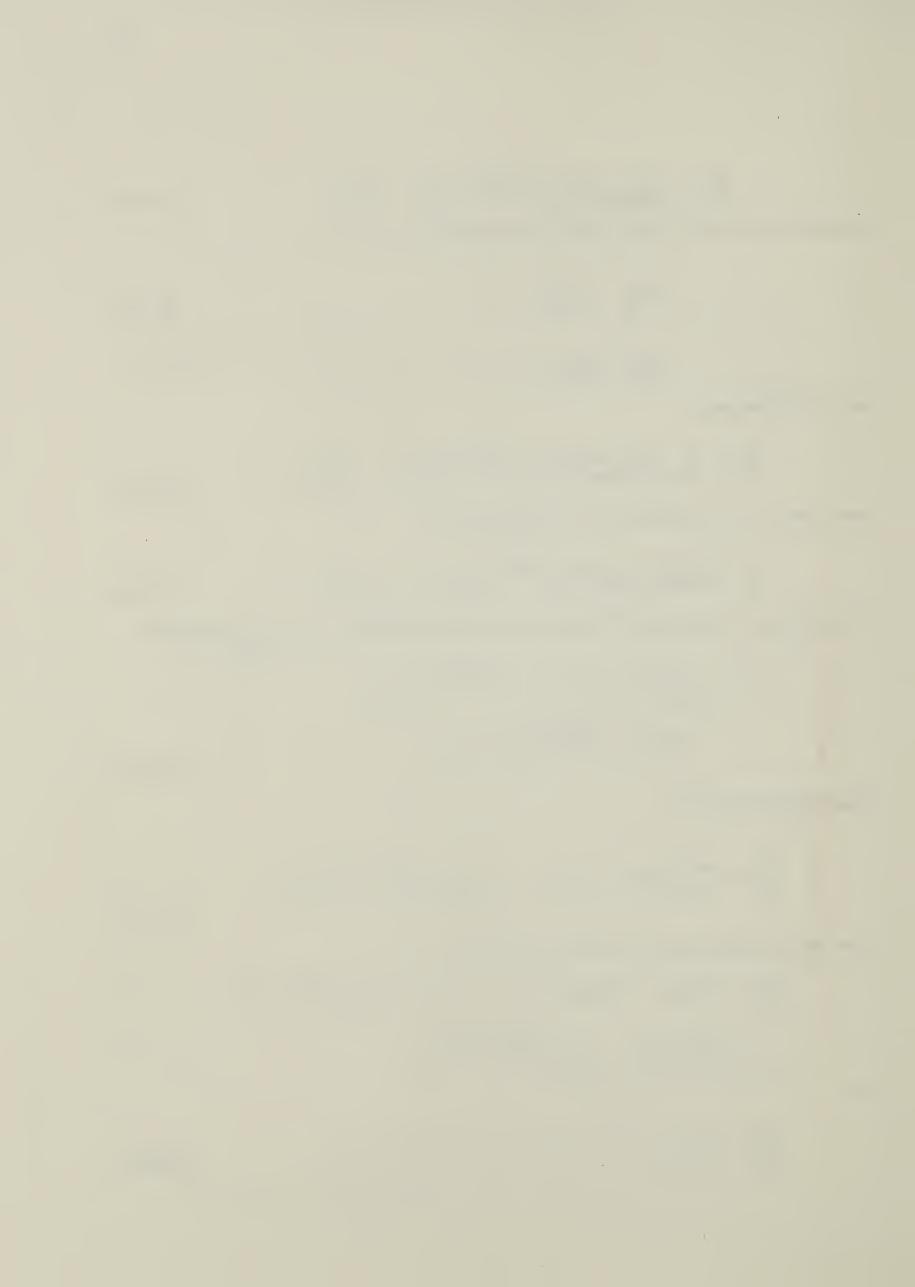
From eq. (2.1.12a) and eq. (2.1.12b), replace $\vec{\nabla}_\perp'$ by $\vec{\nabla}_\perp$ ,

$$\frac{\partial f}{\partial z} = \frac{-k^2}{4\pi^2}\int_{-\infty}^{\infty}\int_{-\infty}^{\infty}d^2\vec{x}_\perp'[\varepsilon^*(\vec{u}_\perp\cdot\vec{\nabla}_\perp\varepsilon) + \varepsilon(\vec{u}_\perp\cdot\vec{\nabla}_\perp\varepsilon^*)]e^{ik\vec{u}_\perp\cdot\vec{x}_\perp'}$$

$$= \frac{-k^2}{4\pi^2}\int_{-\infty}^{\infty}\int_{-\infty}^{\infty}(\vec{u}_\perp\cdot\vec{\nabla}_\perp\varepsilon\varepsilon^*)e^{ik\vec{u}_\perp\cdot\vec{x}_\perp'}d^2\vec{x}_\perp'$$

or

$$\frac{\partial f}{\partial z} = -\vec{u}_\perp\cdot\vec{\nabla}_\perp f$$ (2.1.22)

Using the method of characteristics in partial differential equations to solve eq. (2.1.22), the corresponding characteristic equations for eq. (2.1.22) are

$$\frac{dx}{dt} = u_{\perp x}$$

$$\frac{dy}{dt} = u_{\perp y}$$

$$\frac{dz}{dt} = 1 \tag{2.1.23}$$

where t is a parameter. On integrating, the solution to eq. (2.1.23) is,

$$x = u_{\perp x} t + c_1$$

$$y = u_{\perp y} t + c_2$$

$$z = t + c_3 \tag{2.1.24}$$

This set of equations denotes a parametric curve on which eq. (2.1.22) is satisfied. In other words, the value of f remains constant along this set of curves.

By using the initial conditions for x, y, z, namely, at $t=0$, $x=x_0, y=y_0, z=z_0$, the family of curves can be written as

$$x = x_0 + u_{\perp x} t$$

$$y = y_0 + u_{\perp y} t$$

$$z = z_0 + t$$

$$\tag{2.1.25}$$
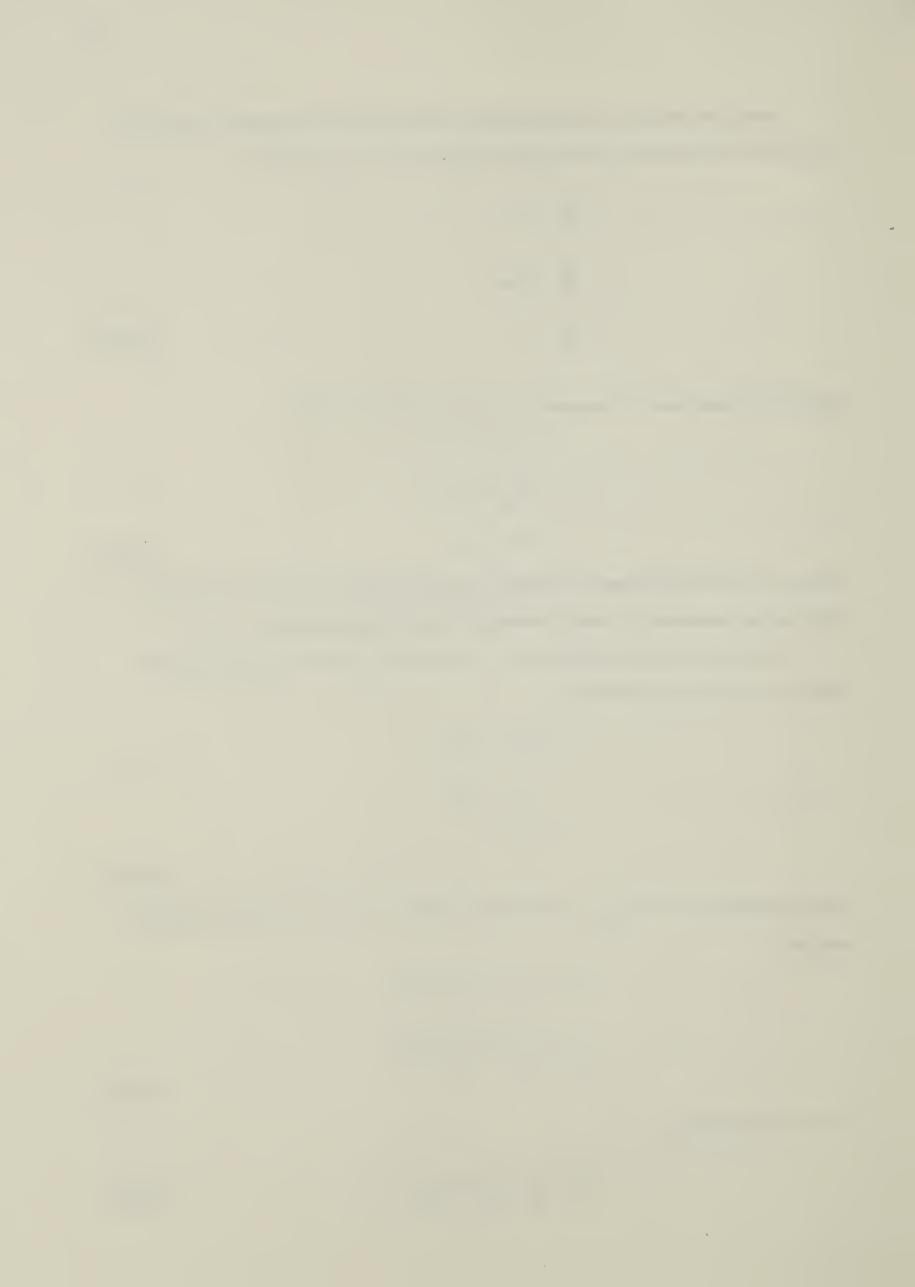
Through replacing t with $z-z_0$ from the last equation of (2.1.25), the above equations become

$$x = x_0 + u_{\perp x}(z-z_0)$$

$$y = y_0 + u_{\perp y}(z-z_0)$$

$$\tag{2.1.26}$$

Or, in vector notation,

$$\vec{x} = \vec{x}_0 + \vec{u}_\perp(z-z_0) \tag{2.1.27}$$

Since according to eq. (2.1.22), f remains unchanged along the path, one can write

$$f(\vec{x}_{\perp 0} + \vec{u}_{\perp}(z-z_0), \vec{u}_{\perp}, z) = f(\vec{x}_{\perp 0}, \vec{u}_{\perp}, z_0)$$

(2.1.28)

By substituting for the arguments of f from eq. (2.1.26), eq. (2.1.28) becomes

$$f(\vec{x}_{\perp}, \vec{u}_{\perp}, z) = f(\vec{x}_{\perp} - \vec{u}_{\perp}(z-z_0), \vec{u}_{\perp}, z_0)$$

(2.1.29)

The path given by eq. (2.1.26) may be regarded as a trajectory for energy packets with the same initial positions $\vec{x}_{\perp 0}$ and the same initial direction $\vec{u}_{\perp}$.

## 2.2 Tappert's distribution function of a coherent Gaussian beam

In this section, the phase space distribution function for a coherent Gaussian beam is derived. From this distribution function, the average directions of the rays, beam energy density and spot size are deduced.

Under the far field approximation, the wave amplitude of a collimated Gaussian laser beam before passing through a converging lens at a distance $z_0$ from the lens[5], is given by,

$$\epsilon(x,y,z_0) = \sqrt{\frac{2}{\pi}} \frac{1}{w(z_0)} e^{i(kz_0 - \phi)} e^{-r^2/w^2(z_0)} e^{-ikr^2/2R(z_0)}$$

(2.2.1)

where

$$\Phi = \tan^{-1}(\frac{\lambda z_0}{\pi w_0^2})$$

$$R(z_0) = z_0[ 1 + (\frac{\pi w_0^2}{\lambda z_0})^2]$$

$$w^2(z_0) = w_0^2[1 + (\frac{\lambda z_0}{\pi w^2})^2]$$

$$r^2 = x^2 + y^2$$

$r << R$ and $w_0$ is the beam waist of the laser.

On passing through the lens which is assumed to be thin, the field amplitude just after the lens($z=z_1$), becomes(see Appendix 2)

$$\epsilon(x,y,z_1) = E_0 e^{-r^2/a_0^2} e^{-ikr^2/2f_L}$$

(2.2.2)

where $E_0$ is

$$\sqrt{\frac{2}{\pi}} \frac{1}{a_0} e^{-i(kz_0^- \phi)}$$

$a_0$ is $w(z_0)$ ; $f_L$ is the focal length of the lens.

By substituting this expression into eq. (2.1.9), the distribution function at a particular point $(x_0, y_0, z_1)$ becomes

$$f(x_0, y_0, u_x, u_y, z_1) = \frac{|E_0|^2 k^2 a_0^2}{2\pi} e^{-2r_0^2/a_0^2} e^{-\frac{k^2 a_0^2}{2}(u_x + \frac{x_0}{f_L})^2} e^{-\frac{k^2 a_0^2}{2}(u_y + \frac{y_0}{f_L})^2}$$

(2.2.3)

At any particular location on x-y plane(constant r), the function has a maximum value at

$$u_x = -\frac{x_0}{f_L}$$

$$u_y = -\frac{y_0}{f_L}$$

(2.2.4)
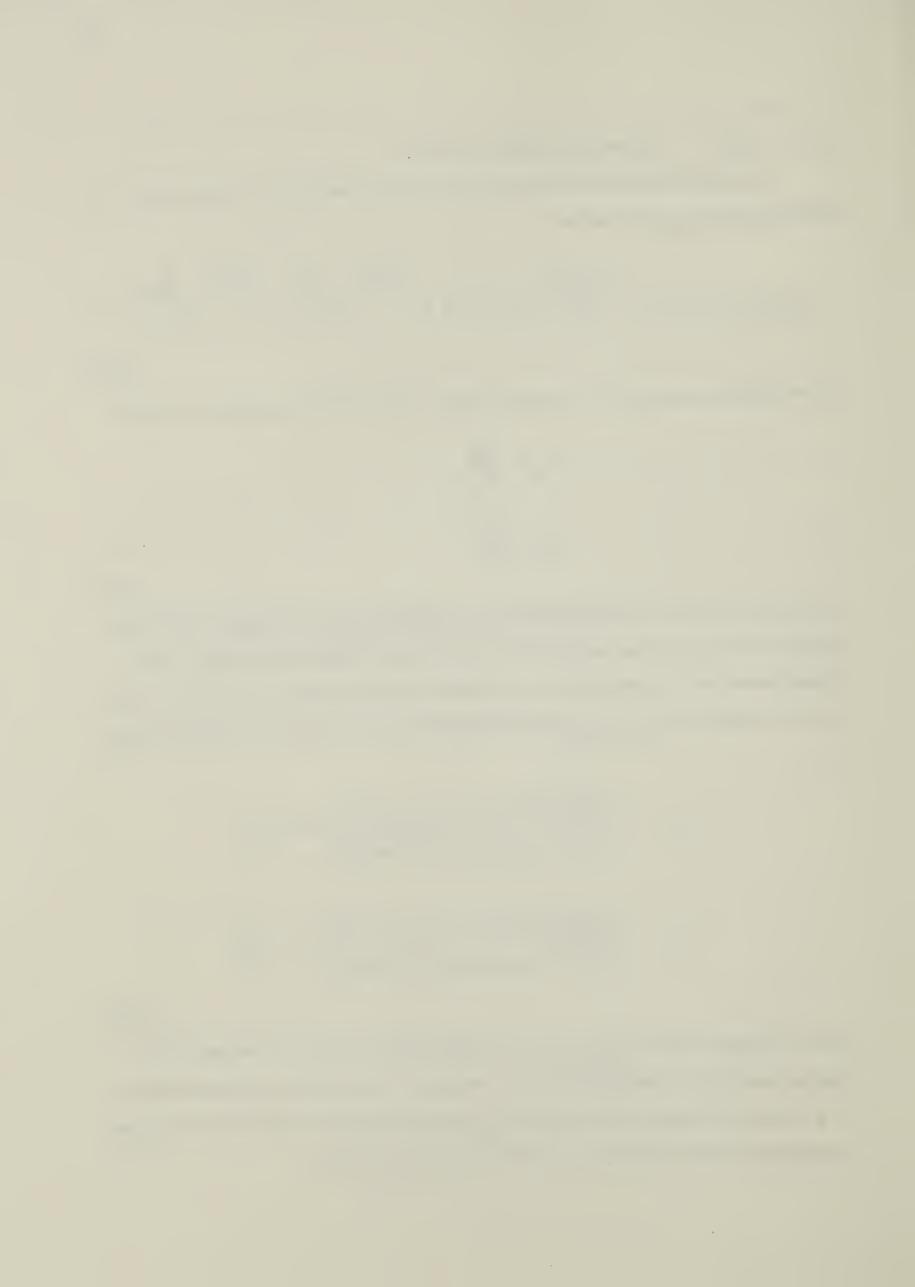
This shows that most of the radiation energy at location $(x_0, y_0)$ is associated with the ray pointing towards the focus (see fig. 2.2), while the rest of the radiation energy will be spread around this ray according to the distribution function given in eq. (2.2.3). By taking the first moment of $f(x_0, y_0, u_x, u_y, z_1)$, the average direction of the rays at the point $(x_0, y_0, z_1)$ is

$$< u_x > = \frac{\int_{-\infty}^{\infty}\int_{-\infty}^{\infty} u_x f(x_0, y_0, u_x, u_y, z_1) du_x du_y}{\int_{-\infty}^{\infty}\int_{-\infty}^{\infty} f(x_0, y_0, u_x, u_y, z_1) du_x du_y} = \frac{-x_0}{f_L}$$

$$< u_y > = \frac{\int_{-\infty}^{\infty}\int_{-\infty}^{\infty} u_y f(x_0, y_0, u_x, u_y, z_1) du_x du_y}{\int_{-\infty}^{\infty}\int_{-\infty}^{\infty} f(x_0, y_0, u_x, u_y, z_1) du_x du_y} = \frac{-y_0}{f_L}$$

(2.2.5)

which is the peak value of $f(x_0, y_0, u_x, u_y, z_1)$. Thus, the average direction of the rays is the direction along which most rays will follow. Moreover, this direction is the same as that for a single ray emerging from the point $(x_0, y_0)$ passing through the focus. Thus, the beam focusing action can be described in terms of a collection of rays.
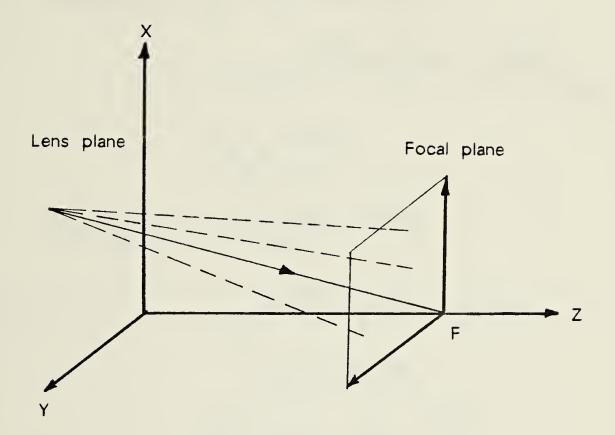
Figure 2.2 Spread of rays at focal plane.

By using eqs.(2.1.10), (2.1.11), the energy density and transverse flux components of the beam at a point $(x_0, y_0)$ are given as,

$$U(x_0, y_0, z_1) = \frac{1}{8\pi} \frac{|E_0^2| k^2 a_0^2}{2\pi} e^{-2r_0^2/a_0^2}$$

$$\times \int_{-\infty}^{\infty}\int_{-\infty}^{\infty} e^{\frac{-k^2 a_0^2}{2}[(u_x + \frac{x_0}{f_L})^2 + (u_y + \frac{y_0}{f_L})^2]} du_x du_y$$

$$= \frac{|E_0|^2 e^{-2r_0^2/a_0^2}}{8\pi} \tag{2.2.6}$$

$$\vec{S}_\perp(x_0, y_0, z_1) = \frac{c}{8\pi} \frac{|E_0|^2 k^2 a_0^2}{2\pi} e^{-2r_0^2/a_0^2}$$

$$\times \int_{-\infty}^{\infty}\int_{-\infty}^{\infty} e^{\frac{-k^2 a_0^2}{2}[(u_x + \frac{x_0}{f_L})^2 + (u_y + \frac{y_0}{f_L})^2]}$$

$$\times (u_x \vec{i} + u_y \vec{j}) du_x du_y$$

$$= \frac{c|E_0|^2}{8\pi} (\frac{-x_0}{f_L}\vec{i} - \frac{y_0}{f_L}\vec{j}) e^{-2r_0^2/a_0^2} \tag{2.2.7}$$
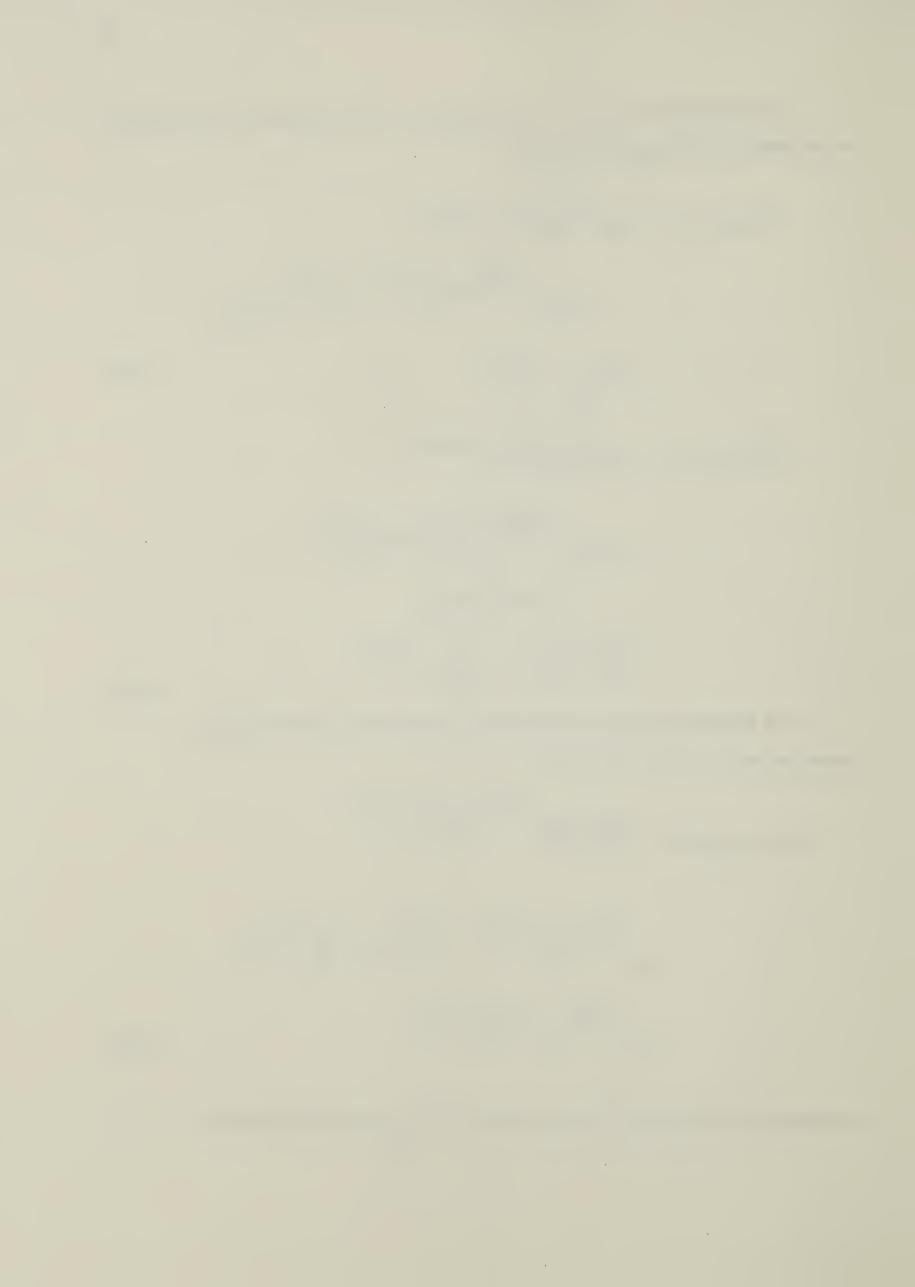
The distribution function from the lens plane onward can be derived by substituting eq. (2.1.26) into eq. (2.2.3)

$$f(x, y, u_x, u_y, z) = \frac{|E_0|^2 k^2 a_0^2}{2\pi} e^{\frac{-2[(x - u_x(z - z_0))^2]}{a_0^2}}$$

$$\times e^{\frac{-2(y - u_y(z - z_0))^2}{a_0^2}} e^{\frac{-k^2 a_0^2}{2}(u_x + \frac{x - u_x(z - z_0)}{f_L})^2}$$

$$\times e^{\frac{-k^2 a_0^2}{2}(u_y + \frac{y - u_y(z - z_0)}{f_L})^2} \tag{2.2.8}$$

Expanding the exponent and combining terms in $x^2, y^2, u_x, u_y$, eq. (2.2.8) becomes

$$f(x,y,u_x,u_y,z) = \frac{|E_0|^2 k^2 a_0^2}{2} e^{\frac{-2(x^2+y^2)}{a^2(z)}} e^{\frac{-k^2 a^2(z)}{2}(u_x + \frac{x}{F(z)})^2}$$

$$\times e^{\frac{-k^2 a^2(z)}{2}(u_y + \frac{y}{F(z)})^2} \tag{2.2.9}$$

where

$$a^2(z) = a_0^2 [(1-\frac{z-z_0}{f_L})^2 + \frac{4(z-z_0)^2}{k^2 a_0^4}] \tag{2.2.10}$$

$$F(z) = f_L [\frac{(1-\frac{z-z_0}{f_L})^2 + \frac{4(z-z_0)^2}{k^2 a_0^4}}{1-\frac{z-z_0}{f_L}(1+\frac{4f_L^2}{k^2 a_0^4})}] \tag{2.2.11}$$

By substituting for $f$ from eq. (2.2.9) into eq. (2.2.5), the average value for $u_x, u_y$ are evaluated to be

$$<u_x> = \frac{-x}{F(z)} \tag{2.2.12}$$

$$<u_y> = \frac{-y}{F(z)} \tag{2.2.13}$$

Moreover, by similar integration procedure as in eq. (2.2.6), and eq. (2.2.7), the energy density and transverse flux components are found to be
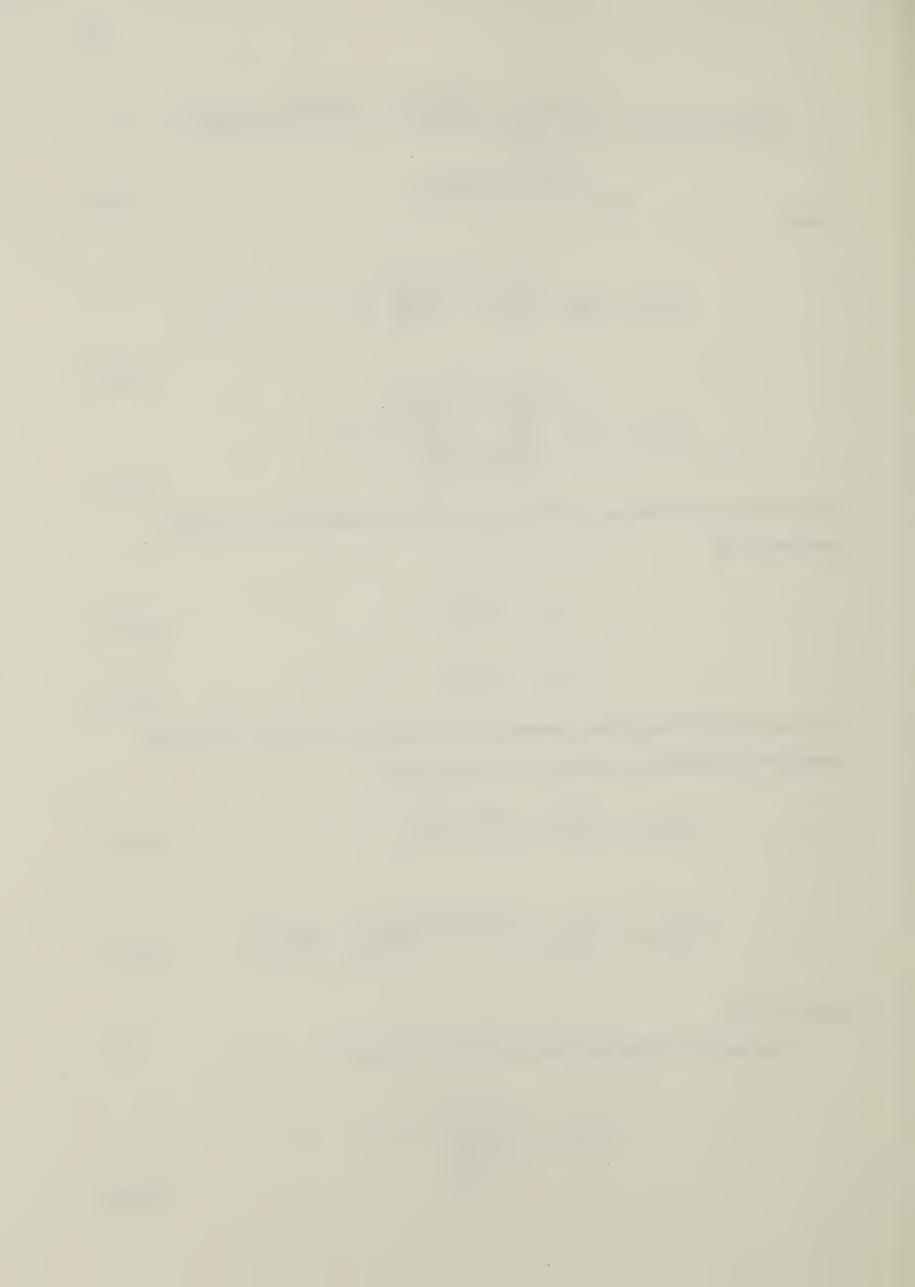
$$U(\vec{x}_\perp,z) = \frac{|E_0|^2}{8\pi} e^{-2r^2/a^2(z)} \tag{2.2.14}$$

$$\vec{S}_\perp(\vec{x}_\perp,z) = \frac{c}{8\pi}|E_0|^2 e^{-2r^2/a^2(z)} [\frac{-x}{F(z)}\vec{i} - \frac{y}{F(z)}\vec{j}] \tag{2.2.15}$$

where $r^2 = x^2 + y^2$.

From eq. (2.2.10) the minimum spotsize is found to be

$$a_{min}^2 = \frac{4f_L^2/k^2 a_0^2}{1 + \frac{4f_L^2}{k^2 a_0^4}} \tag{2.2.16}$$

at an axial distance

$$z = z_0 + \frac{f_L}{1 + \frac{4f_L^2}{k^2 a_0^4}}$$

(2.2.17)

From such a distribution function, the beam size at the focus reaches a limit which is governed by the wavelength of the beam. Moreover, the beam is focused within a focal region with radius $a_{min}$ located at a distance slightly less than the focal length of the lens.
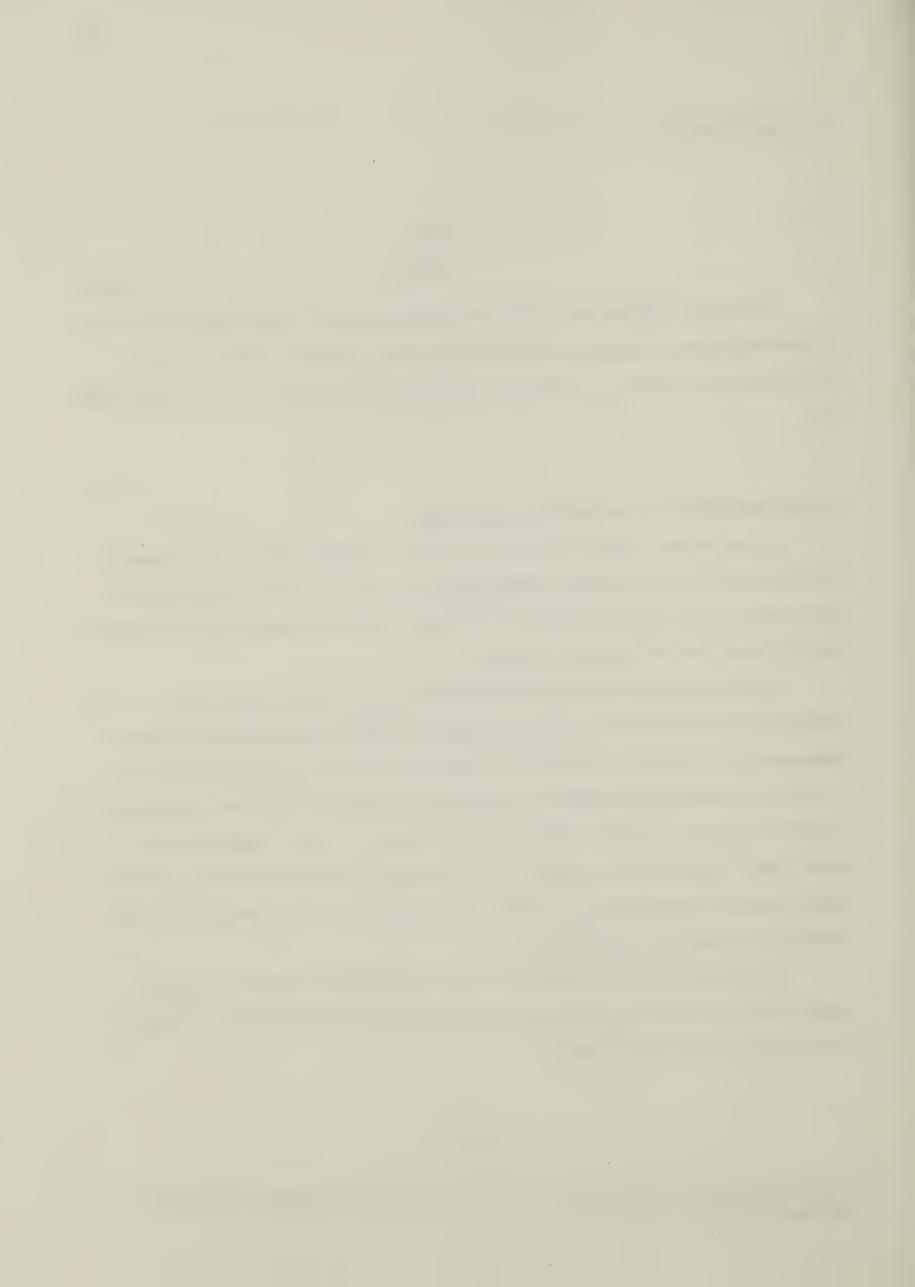
## 2.3 Ray description of a coherent Gaussian beam

In this section, Tappert's distribution function is represented as a sum of energy packages. Each of these packages is associated with a particular direction and location, determined from a sampling of Tappert's distribution function. These sampled values give the initial directions and locations of the rays.

As shown in the previous section, the energy flux of a laser beam can be evaluated from the first moment of the distribution function. This evaluation involves an integration over a continuous variation of transverse directions and positions. However, in using rays to trace the propagation of beam flux, a finite set of discrete directions and locations is chosen since only a finite number of rays can be used for describing the beam. These rays provide trajectories for the propagation of energy flux (macrophotons) (see footnote). The total energy flux over an area can be found by summing over all the macrophotons passing through that area.

Based on this idea, the distribution function is expressed in terms of a sum of macrophotons defined in particular locations and directions. The distribution function at the lens plane can be represented as

---

The term,macrophotons,are used in the work of Dudder and Henderson. [7]The term represents a group of photons.

$$f(\vec{x}_\perp \vec{u}_\perp, z_1) = \sum_{j=1}^{N} \omega_j \delta^2(\vec{x}_\perp - \vec{x}_{\perp j}) \delta^2(\vec{u}_\perp - \vec{u}_{\perp j}) \tag{2.3.1}$$

where $\vec{x}_\perp$ is the position vector of a macrophoton; $\vec{u}_\perp$ is the direction vector of the macrophoton; $\omega_j$ is the amount of energy carried by the macrophoton; N is the number of macrophotons describing the laser beam; $\delta^2$ is a two dimensional delta function. By substituting eq. (2.3.1) for f in eq. (2.1.10), the energy density is found to be

$$U(\vec{x}_\perp, z_1) = \frac{1}{8\pi} \int f(\vec{x}_\perp, \vec{u}_\perp, z_1) \, d^2\vec{u}_\perp$$

$$= \frac{1}{8\pi} \sum_{j=1}^{N} \omega_j \delta^2(\vec{x}_\perp - \vec{x}_{\perp j}) \int \delta^2(\vec{u}_\perp - \vec{u}_{\perp j}) \, d^2\vec{u}_\perp$$

$$= \frac{1}{8\pi} \sum_{j=1}^{N} \omega_j \delta^2(\vec{x}_\perp - \vec{x}_{\perp j}) \tag{2.3.2}$$

The power flowing across an area $\Delta A$ along the direction of propagation is

$$P = \int_{\Delta A} \vec{S} \cdot \vec{z} \, d^2\vec{x}_\perp = \int_{\Delta A} S_z \, dxdy$$

where $\vec{S} = \vec{S}_\perp + \vec{S}_z$ and $\vec{z}$ is the unit vector along the direction of propagation. From Appendix 1, the z-component of $\vec{S}$ is

$$S_z = cU(\vec{x}_\perp, z_1)$$

Therefore, the power is given by

$$P = \int_{\Delta A} cU(\vec{x}_\perp, z_1) \, dx \, dy$$

From eq. (2.3.2),

$$P = c \int_{\Delta A} \frac{1}{8\pi} \sum_{j=1}^{N} \omega_j \delta^2(\vec{x}_\perp - \vec{x}_{\perp j}) \, dx \, dy$$

$$= \frac{c}{8\pi} \sum_{j=1}^{N'} \omega_j \tag{2.3.3}$$

where N' denotes those macrophotons lying within an area $\Delta A$.

As discussed previously, rays emerge from each point on the lens plane as a bundle. Each of these rays will be assigned a particular direction. The choice of these

directions is based on a Gaussian distribution of the directions of rays around the average direction of the ray bundle. As will be shown next, for such a choice, the beam intensity profile at the focal plane will also follow a Gaussian distribution.

Let U be a random variable representing the set of transverse directions of rays. Recalling from eq. (2.2.5) that the average transverse direction of a set of rays emerging from a point $(x_0, y_0)$ at the lens plane is

$$< U_\perp > = \frac{-(x_0 \vec{i} + y_0 \vec{j})}{f_L}$$

(2.3.4)

For each ray, the direction will be

$$\vec{u}_\perp = < U_\perp > + \Delta \vec{u}_\perp$$

(2.3.5)

where $\Delta \vec{u}_\perp$ is the direction deviation from the average value. By combining eq. (2.3.4) and eq. (2.3.5), the ray direction is given by

$$\vec{u}_\perp = \frac{-(x_0 \vec{i} + y_0 \vec{j})}{f_L} + \Delta \vec{u}_\perp$$

(2.3.6)

The location of such a ray at the focal plane will be

$$\vec{x}_\perp = \vec{u}_\perp f_L + x_0 \vec{i} + y_0 \vec{j}$$
$$= \Delta \vec{u}_\perp f_L$$

(2.3.7)

According to eq. (2.3.7), the ray location is only proportional to the deviation of the ray direction from the average value. For a ray with an average direction $<U_\perp>$, it crosses the axis of propagation at the focal plane. Rays with directions other than this will resume a location different from the origin. Since the number of rays decreases in a Gaussian manner with respect to the deviation of directions, the number of rays which resume locations away from the origin will consequently vary in a Gaussian manner.

## 2.4 Ray description of an incoherent Gaussian beam

In this section, the phase space distribution function and the formula for the beam width of an incoherent Gaussian beam is derived. The expression for the distribution

function is found to be very similar to that for the coherent case except for a coherence factor. This factor accounts for the degree of coherence of the electric fields at different locations at the lens plane.

In practice, the beam can hardly be focussed to the diffraction limited spotsize due to instrumental limitations and imperfections. According to Tappert, these defects can be incorporated into the phase fluctuations of the electric field amplitudes at the lens plane. With such phase fluctuations, the field diffraction pattern at the focus changes. The energy distribution at the focus and accordingly, the spotsize can then be varied.

Phase fluctuations are accounted for by considering an ensemble (see footnote) of fields at the lens plane. Each member of the ensemble consists of electric fields over the plane transverse to the beam. A random phase is associated with the electric field at each location on the plane. As a result, the electric field amplitude used in eq. (2.1.9) is replaced by the average of the ensemble of field amplitudes. Upon substitution, the phase space distribution function then becomes

$$< f(\vec{x}_\perp,\vec{u}_\perp,z) > = \frac{k^2}{(2\pi)^2}\int_{-\infty}^{\infty}\int_{-\infty}^{\infty}d^2\vec{x}_\perp' e^{ik\vec{u}_\perp\cdot\vec{x}_\perp'}<\epsilon(\vec{x}_\perp-\tfrac{1}{2}\vec{x}_\perp',z)\epsilon^*(\vec{x}_\perp+\tfrac{1}{2}\vec{x}_\perp',z)>$$

(2.4.1)

where the brackets,< >,denote ensemble averages of the bracketed quantity. The energy density and flux of the field are respectively

$$< U > = \frac{1}{8\pi}\int_{-1}^{1}\int_{-1}^{1}<f(\vec{x}_\perp,\vec{u}_\perp,z)>d^2\vec{u}_\perp = \frac{<|\epsilon|^2>}{8\pi}$$

(2.4.2)

$$< \vec{S}_\perp > = \frac{c}{8\pi}\int_{-1}^{1}\int_{-1}^{1}\vec{u}_\perp<f(\vec{x}_\perp,\vec{u}_\perp,z)>d^2\vec{u}_\perp$$

(2.4.3)

$$=\frac{c}{8\pi}\frac{i}{2k}<(\epsilon\vec{\nabla}_\perp\epsilon^* - \epsilon^*\vec{\nabla}_\perp\epsilon)>$$

By applying this idea of random phase to a Gaussian beam, the electric field amplitude at the lens plane will be given by

$$\epsilon(x,y,z_1) = E_0 e^{-r^2/a_0^2} e^{-ikr^2/2f_L} e^{i\psi(x,y)}$$
$$= \epsilon_1 e^{i\psi(x,y)}$$

(2.4.4)

where $\psi(x,y)$ is the random phase of the electric field at the location (x,y); $\epsilon_1$ is the

---

An ensemble is a collection of identical systems

quantity $E_0 e^{\frac{-r^2}{2a_0^2}} e^{\frac{-ikr^2}{2f_L}}$. Although the phase values are regarded as random, they are assumed to be Gaussianly correlated in a small area with radius L within the beam cross sectional area. Within such a region, the phase value at any point (x,y) is given by

$$\psi(x,y) = \psi_0 e^{\frac{-(x-x_c)^2+(y-y_c)^2}{L^2}}$$

(2.4.5)

where $(x_c, y_c)$ is the location at which the phase value is maximum. The phase values are assumed to be isotropic in the sense that the values within a localized area of radius L do not change regardless of the location of the area within the beam. Under such assumption, for any two points within the beam, the correlation function between the phase values is given by

$$\rho(x_2-x_1, y_2-y_1) = \frac{2}{\psi_0^2 \pi L^2} \int_{-\infty}^{\infty}\int_{-\infty}^{\infty} dx_c dy_c \psi_0^2 e^{-\frac{(x_1-x_c)^2+(y_1-y_c)^2}{L^2}} e^{-\frac{(x_2-x_c)^2+(y_2-y_c)^2}{L^2}}$$

$$= e^{\frac{-1}{2L^2}[(x_2-x_1)^2 + (y_2-y_1)^2]}$$
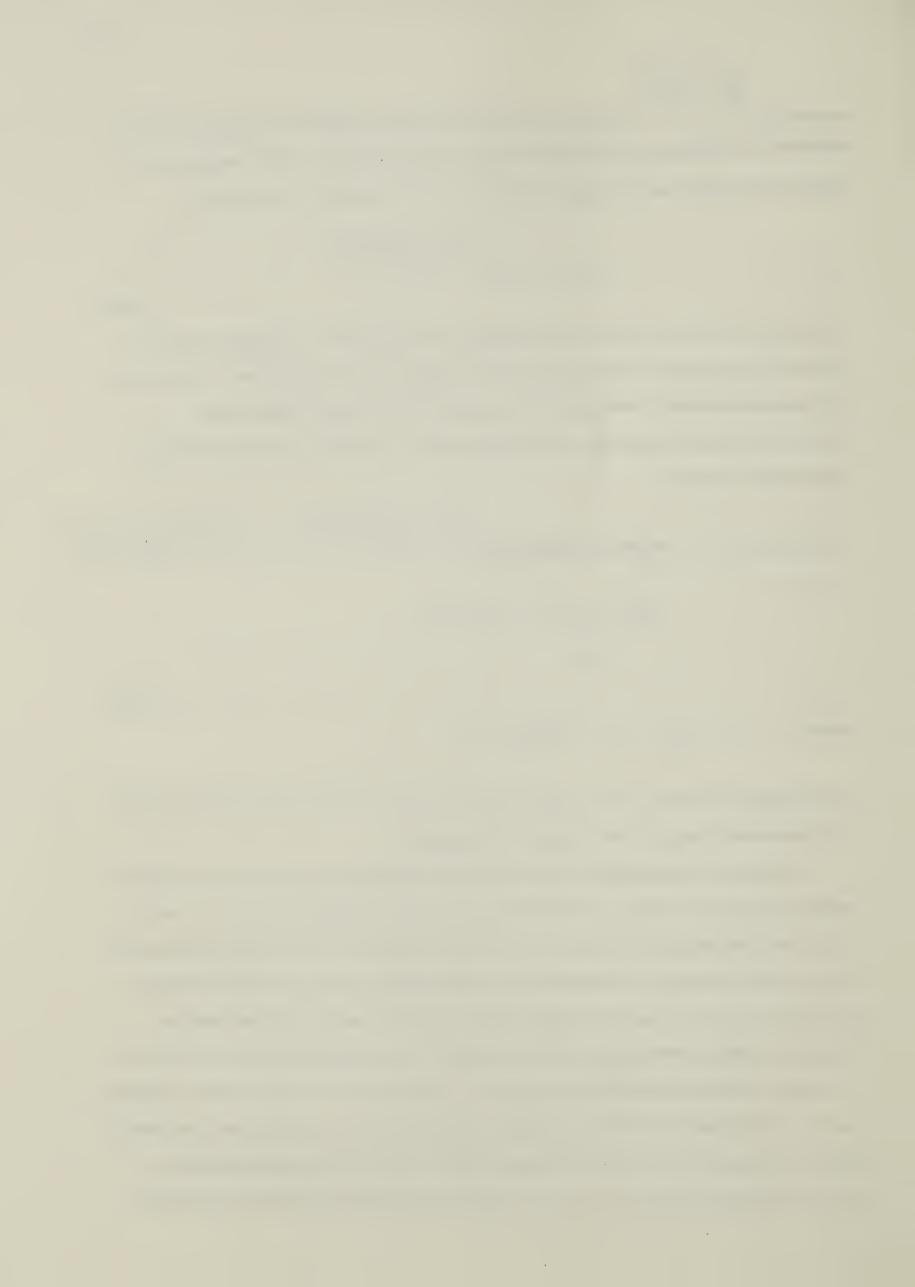
$$= e^{-r'^2/2L^2}$$

(2.4.6)

where $\quad r' = \sqrt{(x_2 - x_1)^2 + (y_2 - y_1)^2}$

The correlation function for the phases at any two points is readily seen from eq. (2.4.6) to be dependent only upon the distance between them.

However, this correlation function can be formulated according to the concept of ensemble average as follows. Let the continuous range of possible values of $\psi$ be $\psi_1$, $\psi_2$, $\psi_3$ ,etc. The phase for the electric field in each member of the ensemble can take any of the values. Consider the phase values of each member at any two particular points $(x_1,y_1)$ and $(x_2,y_2)$. Let $\Phi_1$ be the random variable to denote the set of phase values at $(x_1,y_1)$, $\Phi_2$ to denote those at $(x_2,y_2)$. Since the phase values are restricted only to the set of $\psi$ values mentioned, the values of $\Phi_1$ and $\Phi_2$ will lie within the range of the $\psi$ values as well. A joint probability distribution function, $P_{\Phi_1\Phi_2}(\psi_1,\psi_2;x_2-x_1,y_2-y_1)$ can then be set up for the product of the random variables $\Phi_1\Phi_2$. $\psi_1$, $\psi_2$ are the values taken by $\Phi_1$, $\Phi_2$ respectively; and $(x_2-x_1)$, $(y_2-y_1)$ represent the spatial difference between the

two points. Thus, the ensemble average of $\phi_1\phi_2$ or $<\phi_1\phi_2>$ can be calculated in terms of this distribution function as follows:

$$<\phi_1\phi_2> = \int_{-\infty}^{\infty}\int_{-\infty}^{\infty}\psi_1\psi_2 P_{\phi_1\phi_2}(\psi_1,\psi_2;x_2-x_1,y_2-y_1)d\psi_1 d\psi_2$$

(2.4.7)
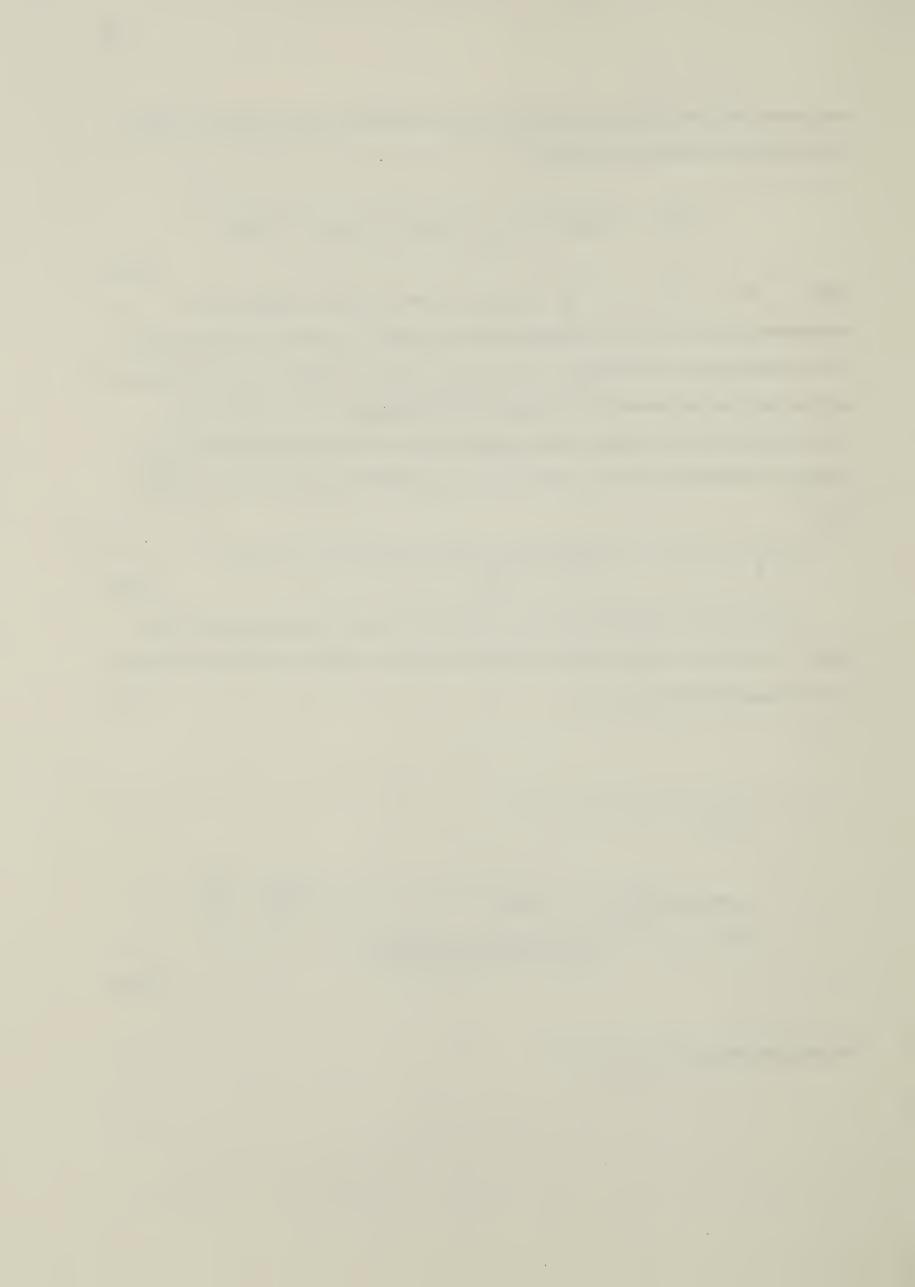
where $\psi^2 =< \phi_1^2 >$ or$< \phi_2^2 >$ because $\phi_1$ and $\phi_2$ have the same kind of distribution. Since as it was mentioned earlier, the range of $\phi$ values is the same as that for $\psi$, the average of the product $\psi(x_1, y_1)\psi(x_2, y_2)$ for a member of the ensemble is the same as the ensemble average. From eq. (2.4.6), the average of $\psi(x_1, y_1)\psi(x_2, y_2)$ over all points within the beam is the correlation function for the phase values at $(x_1,y_1)$ and $(x_2,y_2)$. Thus, the ensemble average of $\phi_1\phi_2$ is equivalent to the correlation function, that is,

$$\rho(x_2-x_1,y_2-y_1) = \int_{-\infty}^{\infty}\int_{-\infty}^{\infty}\psi_1\psi_2 P_{\phi_1\phi_2}(\psi_1,\psi_2;x_2-x_1,y_2-y_1)d\psi_1 d\psi_2$$

(2.4.8)

The distribution functions for $\phi_1$ and $\phi_2$ are chosen to be Gaussian so that Tappert's distribution function can be simplified. The joint probability distribution function for $\phi_1\phi_2$ has the following form[s]

$$P_{\phi_1\phi_2}(\psi_1,\psi_2;x_2-x_1,y_2-y_1)$$

$$= \frac{e^{\frac{-1}{2[1-\rho^2(x_2-x_1,y_2-y_1)]}[\frac{\psi_1^2}{\psi_0^2} - 2\rho(x_2-x_1,y_2-y_1)\frac{\psi_1\psi_2}{\psi_0^2} + \frac{\psi_2^2}{\psi_0^2}]}}{2\pi\psi_0^2\sqrt{1-\rho^2(x_2-x_1,y_2-y_1)}}$$

(2.4.9)

The marginal probability, $P_{\phi_1}(\psi_1)$ will be

$$P_{\Phi_1}(\psi_1) = \int_{-\infty}^{\infty} P_{\Phi_1 \Phi_2}(\psi_1, \psi_2; x_2 - x_1, y_2 - y_1) d\psi_2$$

$$= \frac{\int_{-\infty}^{\infty} e^{-\left[\frac{\psi_1^2}{\psi_0^2} - \frac{2\rho(x_2-x_1,y_2-y_1)\psi_1\psi_2}{\psi_0^2} + \frac{\psi_2^2}{\psi_0^2}\right]} d\psi_2}{2\pi\psi_0^2 \sqrt{1 - \rho^2(x_2-x_1, y_2-y_1)}}$$

$$= \frac{\int_{-\infty}^{\infty} e^{\frac{-1}{2\psi_0^2}\left[\psi_1^2 + \frac{(\rho(x_2-x_1,y_2-y_1)\psi_1 - \psi_2)^2}{1 - \rho^2(x_2-x_1,y_2-y_1)}\right]} d\psi_2}{2\pi\psi_0^2 \sqrt{1 - \rho^2(x_2-x_1, y_2-y_1)}}$$

$$= \frac{e^{-\psi_1^2/2\psi_0^2}}{\psi_0\sqrt{2\pi}} \tag{2.4.10}$$

Hence the set of phase values represented by the random variable $\Phi_1(x, y)$ follows a Gaussian distribution as expected. This Gaussian property of $\Phi_1$ gives the average value of $e^{i\Phi_1}$ to be

$$< e^{i\Phi_1} > = \frac{1}{\sqrt{2\pi}\psi_0} \int_{-\infty}^{\infty} e^{-\psi_1^2/2\psi_0^2} e^{i\psi_1} d\psi_1$$

$$= e^{-\psi_0^2/2} = e^{\frac{-1}{2}<\Phi_1^2>} \tag{2.4.11}$$
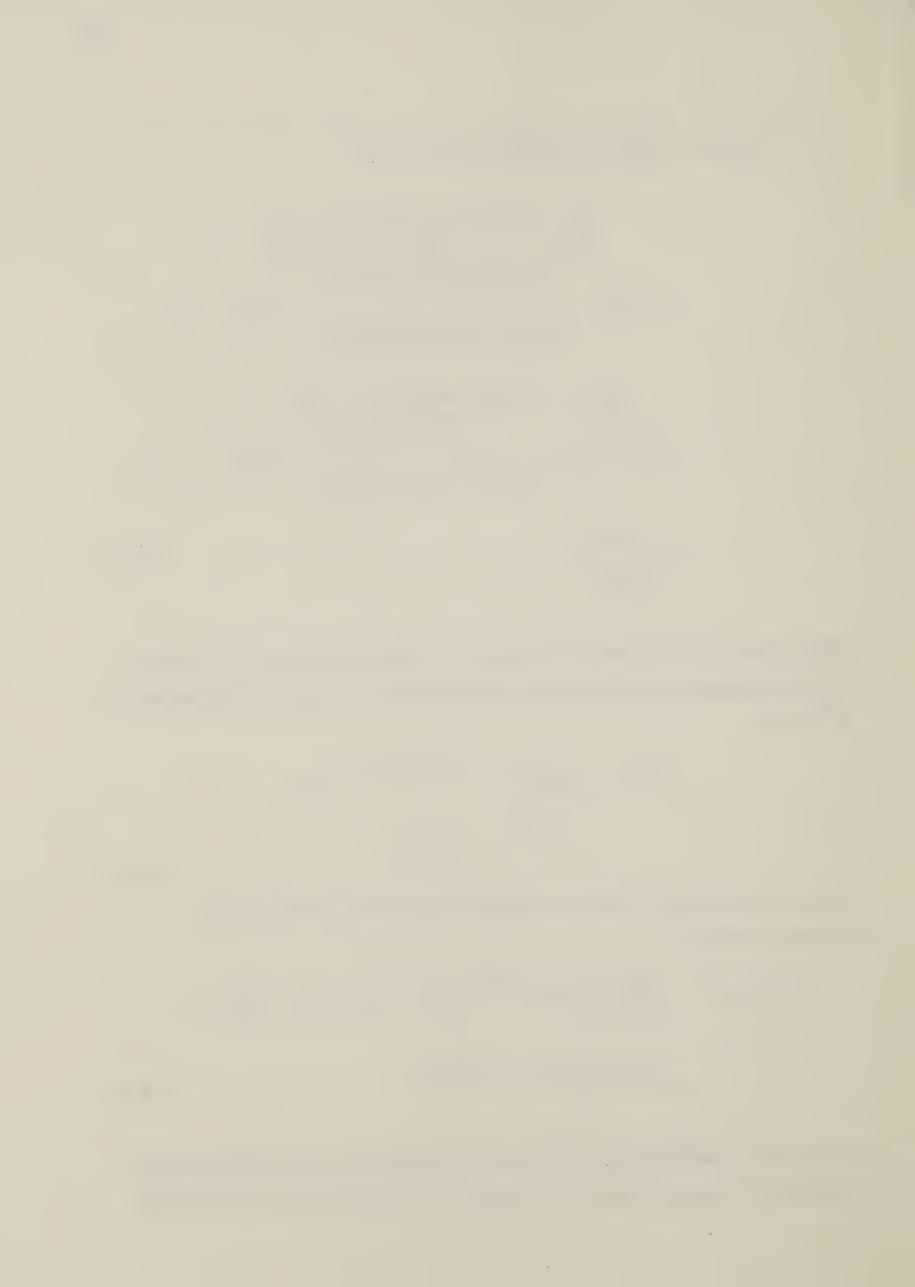
From eq. (2.4.4) and eq. (2.1.9), for a member of the ensemble the phase space distribution function is

$$f(\vec{x}_\perp, \vec{u}_\perp, z) = \frac{k^2}{(2\pi)^2}\int_{-\infty}^{\infty}\int_{-\infty}^{\infty} d^2\vec{x}_\perp' e^{i k \vec{u}_\perp \cdot \vec{x}_\perp'} \epsilon_1(\vec{x}_\perp - \tfrac{1}{2}\vec{x}_\perp', z)\epsilon_1^*(\vec{x}_\perp + \tfrac{1}{2}\vec{x}_\perp', z)$$

$$\times e^{i[\psi(\vec{x}_\perp - \frac{1}{2}\vec{x}_\perp') - \psi(\vec{x}_\perp + \frac{1}{2}\vec{x}_\perp')]} \tag{2.4.12}$$

Moreover, the ensemble average of $f(\vec{x}_\perp, \vec{u}_\perp, z)$ may be derived as follows. Since the range of values of $\psi$ is always the same for any point in x-y plane, the values of $\psi(\vec{x}_\perp - \tfrac{1}{2}\vec{x}_\perp')$

and $\Psi(\vec{x}_\perp + \frac{1}{2}\vec{x}'_\perp)$ can be represented by $\Phi_1$ and $\Phi_2$ respectively. In this case, the joint probability distribution function given previously becomes $P_{\Phi_1 \Phi_2}(\psi_1, \psi_2; x', y')$. The ensemble average of $< e^{i(\Phi_1 - \Phi_2)} >$ is given by

$$< e^{i(\Phi_1 - \Phi_2)} > = \int_{-\infty}^{\infty}\int_{-\infty}^{\infty} e^{i(\psi_1 - \psi_2)} P_{\Phi_1 \Phi_2}(\psi_1, \psi_2; x', y') d\psi_1 d\psi_2$$

(2.4.13)

Substituting for $P_{\Phi_1 \Phi_2}(\psi_1, \psi_2; x', y')$ from eq. (2.4.9),

$$< e^{i(\Phi_1 - \Phi_2)} > = \int_{-\infty}^{\infty}\int_{-\infty}^{\infty} \frac{e^{i(\psi_1 - \psi_2)} e^{\frac{-1}{2\psi_0^2}[\psi_1^2 + \frac{(\rho(x',y')\psi_1 - \psi_2)^2}{1 - \rho^2(x',y')}]}}{2\pi\psi_0^2\sqrt{1 - \rho^2(x',y')}} d\psi_1 d\psi_2$$

$$= \int_{-\infty}^{\infty}\int_{-\infty}^{\infty} \frac{e^{i(\psi_1 - \psi_2)} e^{\frac{-1}{2\psi_0^2}[\psi_1^2 + \frac{(\rho(r')\psi_1 - \psi_2)^2}{1 - \rho^2(r')}]}}{2\pi \psi_0^2\sqrt{1 - \rho^2(r')}} d\psi_1 d\psi_2$$

(2.4.14)

where $\rho(r') = \frac{< \Phi_1 \Phi_2 >}{\psi_0^2}$ and $r' = \sqrt{(x - \frac{1}{2}x' - (x + \frac{1}{2}x'))^2 + (y - \frac{1}{2}y' - (y + \frac{1}{2}y'))^2}$. Integrating eq. (2.4.14) with respect to $\psi_2$, $< e^{i(\Phi_1 - \Phi_2)} >$ becomes

$$< e^{i(\Phi_1 - \Phi_2)} > = \frac{e^{\psi_0^2(1 - \rho(r'))/2}}{\psi_0\sqrt{2\pi}} \int_{-\infty}^{\infty} e^{-i(1 - \rho(r'))\psi_1 - \psi_1^2/2\psi_0^2} d\psi_1$$

$$= e^{-\psi_0^2(1 - \rho(r'))}$$
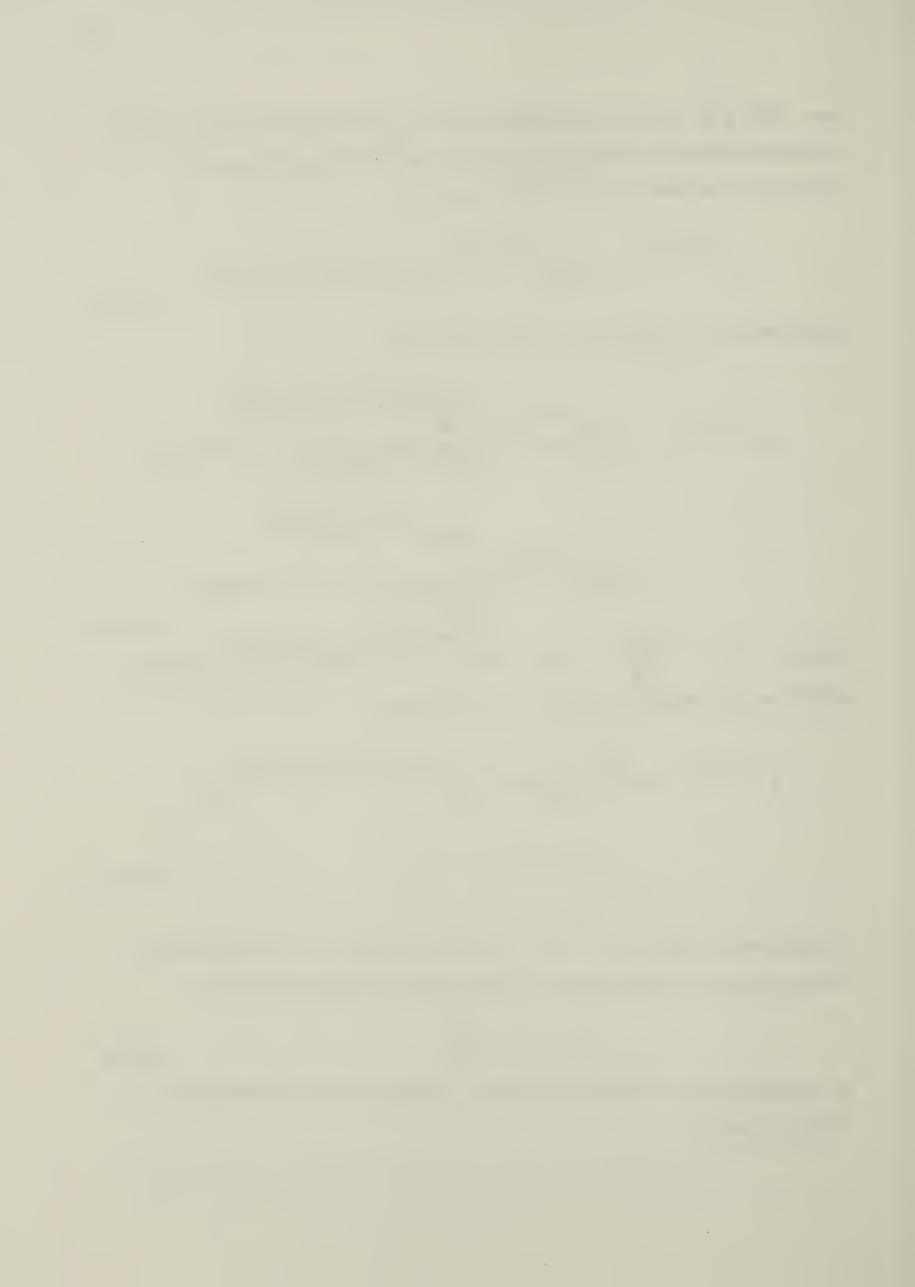
(2.4.15)

For large values of $\psi_0^2$, $< e^{i(\Phi_1 - \Phi_2)} >$ is small as long as $(1 - \rho(r'))$ is close to one. From eq. (2.4.6), the Taylor expansion of the correlation function about zero is

$$\rho(r') = 1 - \frac{r'^2}{2L^2}$$

(2.4.16)

By replacing $\rho(r')$ in eq. (2.4.15) with eq. (2.4.16), the phase factor in the integrand of $<f(\vec{x}_\perp, \vec{u}_\perp, z)>$, that is,

$$< f(\vec{x}_\perp, \vec{u}_\perp, z) > \; = \; \frac{k^2}{(2\pi)^2} \int_{-\infty}^{\infty}\int_{-\infty}^{\infty} d^2\vec{x}_\perp' \, e^{i k \vec{u}_\perp \cdot \vec{x}_\perp'} \epsilon_1(\vec{x}_\perp - \tfrac{1}{2}\vec{x}_\perp', z)$$

$$\times \; \epsilon_1^*(\vec{x}_\perp + \tfrac{1}{2}\vec{x}_\perp', z) < e^{i(\Phi_1 - \Phi_2)} > \tag{2.4.17}$$

becomes

$$< e^{i(\Phi_1 - \Phi_2)} > \; = \; e^{-r'^2 \psi_0^2 / 2L^2} \tag{2.4.18}$$

Following from this result, the distribution function at the lens plane is evaluated to be

$$< f(\vec{x}_\perp, \vec{u}_\perp, z_1) > \; = \; \frac{|E_0|^2 k^2 D^2 a_0^2}{2\pi} e^{-2r^2/a_0^2} e^{-\frac{k^2 D^2 a_0^2}{2}[(u_x + \frac{x}{f_L})^2 + (u_y + \frac{y}{f_L})^2]} \tag{2.4.19}$$

where $D = \dfrac{1}{\sqrt{1 + \psi_0^2 a_0^2 / L^2}}$

For zero values of $\psi_0$, D becomes one and perfect coherence of the beam results. On the other hand, for non-zero values of $\psi_0$, D is less than one, and phase coherence will be imperfect.

By substituting for kD by $k_{eff}$, the distribution function at the lens plane becomes

$$< f(\vec{x}_\perp, \vec{u}_\perp, z_1) > \; = \; \frac{|E_0|^2 k_{eff}^2 a_0^2}{2\pi} e^{\frac{-2r^2}{a_0^2}} e^{-\frac{k_{eff}^2 a_0^2}{2}[(u_x + \frac{x}{f_L})^2 + (u_y + \frac{y}{f_L})^2]} \tag{2.4.20}$$
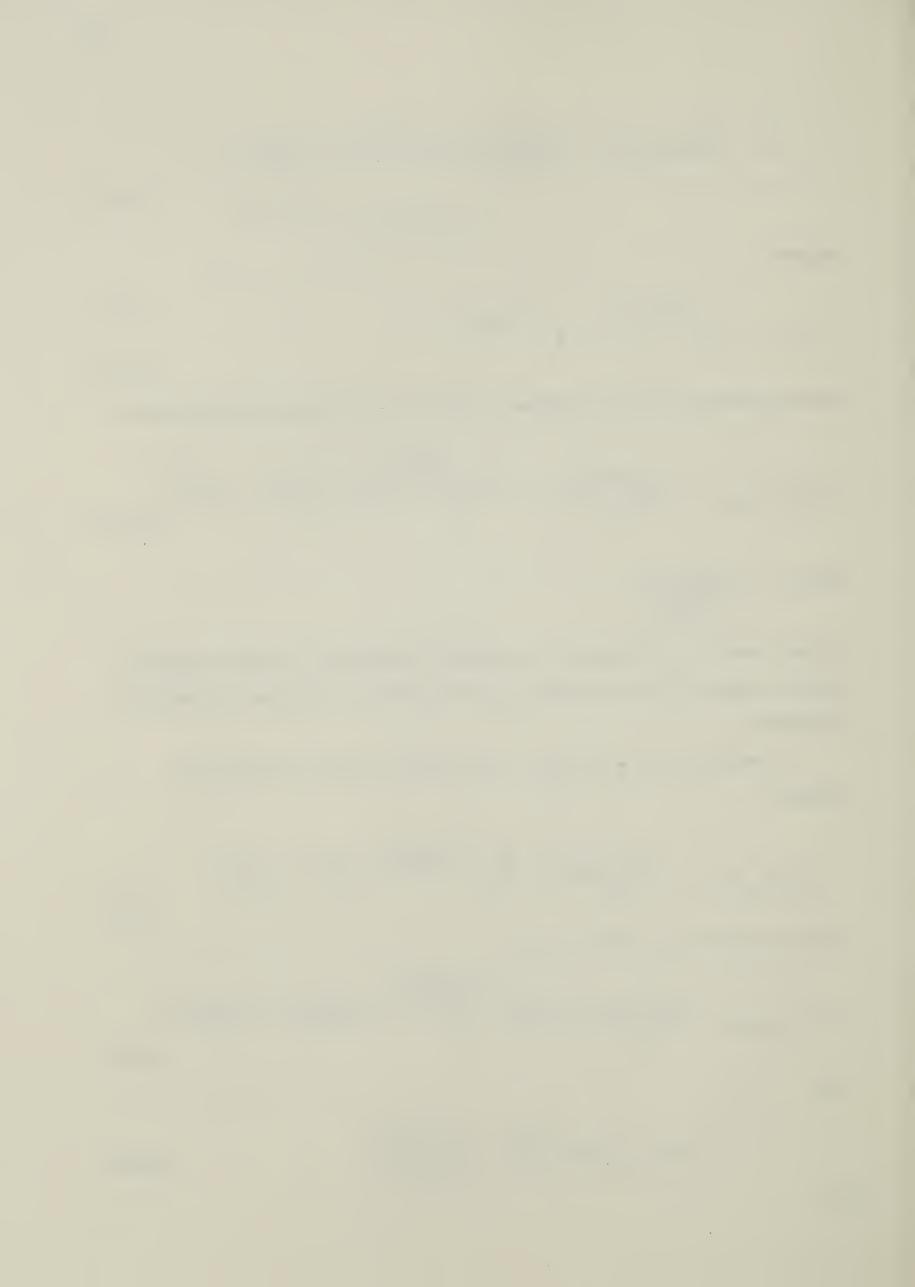
And at any z-plane, the function becomes

$$<f(\vec{x}_\perp, \vec{u}_\perp, z)> \; = \; \frac{|E_0|^2 k_{eff}^2 a_0^2}{2\pi} e^{\frac{-2r^2}{a_0^2(z)}} e^{-\frac{k_{eff}^2 a_0^2(z)}{2}[(u_x + \frac{x}{F(z)})^2 + (u_y + \frac{y}{F(z)})^2]} \tag{2.4.21}$$

where

$$a^2(z) = a_0^2\left[(1 - \frac{z - z_0}{f_L})^2 + \frac{4(z - z_0)^2}{k_{eff}^2 a_0^4}\right] \tag{2.4.22}$$

and

$$F(z) = f_L \left[ \frac{(1 - \frac{z-z_0}{f_L})^2 + \frac{4(z-z_0)^2}{k^2_{eff}a^4_0}}{1 - \frac{z-z_0}{f_L}(1 + \frac{4f^2_L}{k^2_{eff}a^4_0})} \right]$$

(2.4.23)

The introduction of phase incoherence into the electric field amplitudes at the lens plane alters the size of the beam along the path of propagation as well as the focal distance. The incoherence factor D provides a means to adjust the beam size at the focus.

In conclusion, the phase space distribution function for a radiation field allows one to allocate the field energy into various rays of which positions and directions can be defined. Moreover, by using this function, the directions of the rays are distributed in such a way that a diffraction limited focal region can be reconstructed from the rays.

# Chapter 3

## Beam propagation in a refractive medium

In this chapter, the derivation of the ray equation is carried out and solutions for this equation are given for different profiles. These profiles are used to implement the density values calculated from Milroy's laser heated solenoid model.

### 3.1 Derivation of ray equation

In this section, the general equation for the trajectories traced by energy packets (photons) is derived.

Light propagation within a refractive medium can be described in terms of the motion of quasi-particles as long as the angular frequency, $\omega$ ,of the quasi-particle varies sufficiently slowly with respect to time and space[1,2,3]. This condition ensures that the wavepackets are localized in space. Equations of motion of the wavepacket are

$$\frac{d\vec{r}}{dt} = \dot{\vec{r}} = \frac{\partial \omega(\vec{k},\vec{r},t)}{\partial \vec{k}} \tag{3.1.1}$$

$$\frac{d\vec{k}}{dt} = \dot{\vec{k}} = -\frac{\partial \omega(\vec{k},\vec{r},t)}{\partial \vec{r}} \tag{3.1.2}$$

Eq. (3.1.1) can be re-expressed as
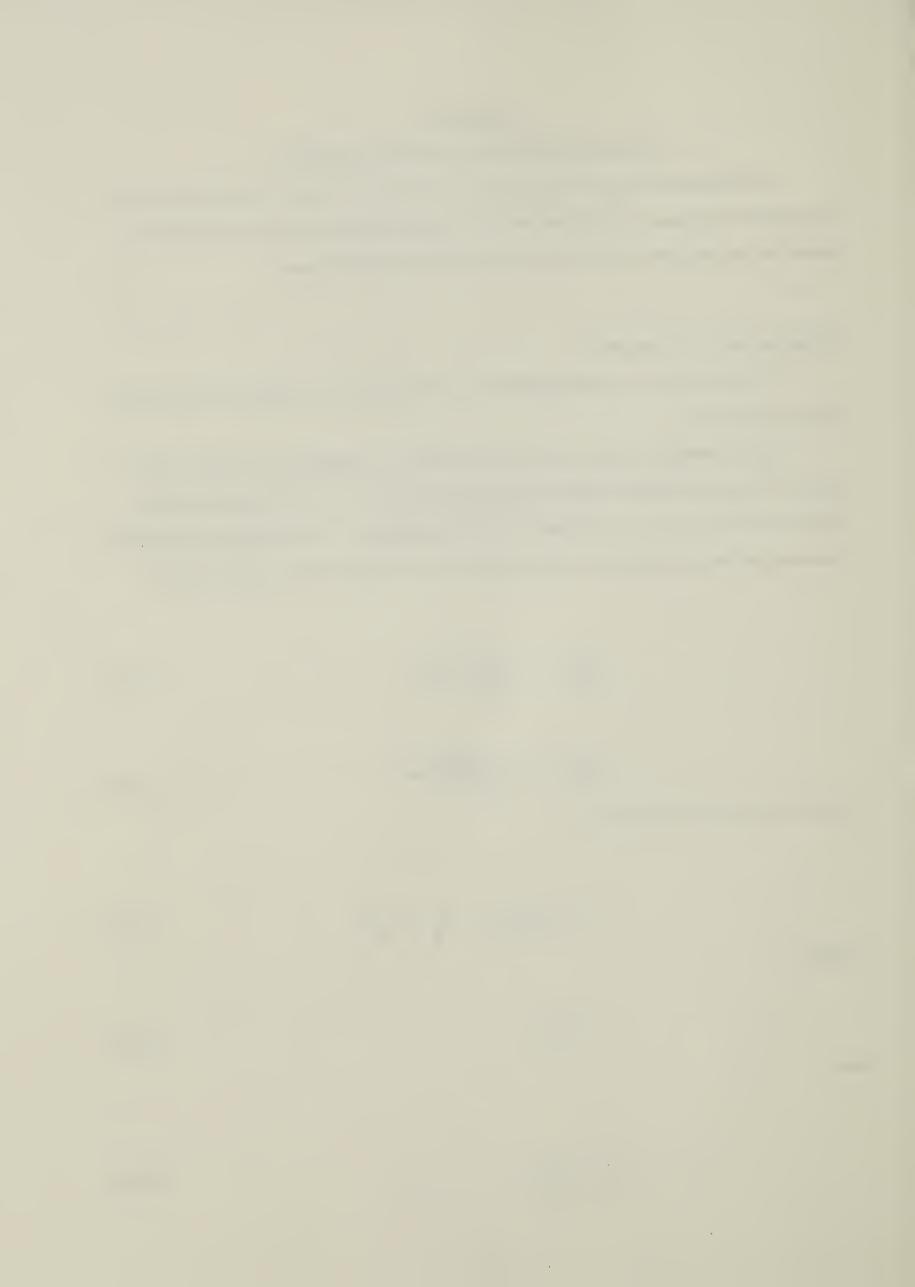
$$\dot{\vec{r}} = (\frac{\partial \omega}{\partial k})\vec{\nabla}_k k = \vec{v}_g = v_g \vec{\Omega} \tag{3.1.3}$$

where

$$\vec{\Omega} = \vec{k}/k \tag{3.1.4}$$

and

$$v_g = \frac{\partial \omega}{\partial k} \tag{3.1.5}$$

As will be shown, eq. (3.1.1) can further be expressed in terms of the refractive index of the medium[4]. To start with, eq. (3.1.4) is differentiated with respect to time, giving

$$\dot{\vec{k}} = k\dot{\vec{\Omega}} + \dot{k}\vec{\Omega}$$

(3.1.6)

By combining with eq. (3.1.2), the equation becomes

$$k\dot{\vec{\Omega}} = -\vec{\nabla}_r\omega - \dot{k}\vec{\Omega}$$

(3.1.7)

By taking the dot products of eq. (3.1.2) with $\vec{k}$,

$$\vec{k} \cdot \dot{\vec{k}} = \vec{k} \cdot \frac{\partial\omega}{\partial\vec{r}}$$

$$\dot{k} = -\vec{\Omega} \cdot \vec{\nabla}_r\omega$$

(3.1.8)

then

$$k\dot{\vec{\Omega}} = -\vec{\nabla}_r\omega + (\vec{\Omega} \cdot \vec{\nabla}_r\omega)\vec{\Omega}$$
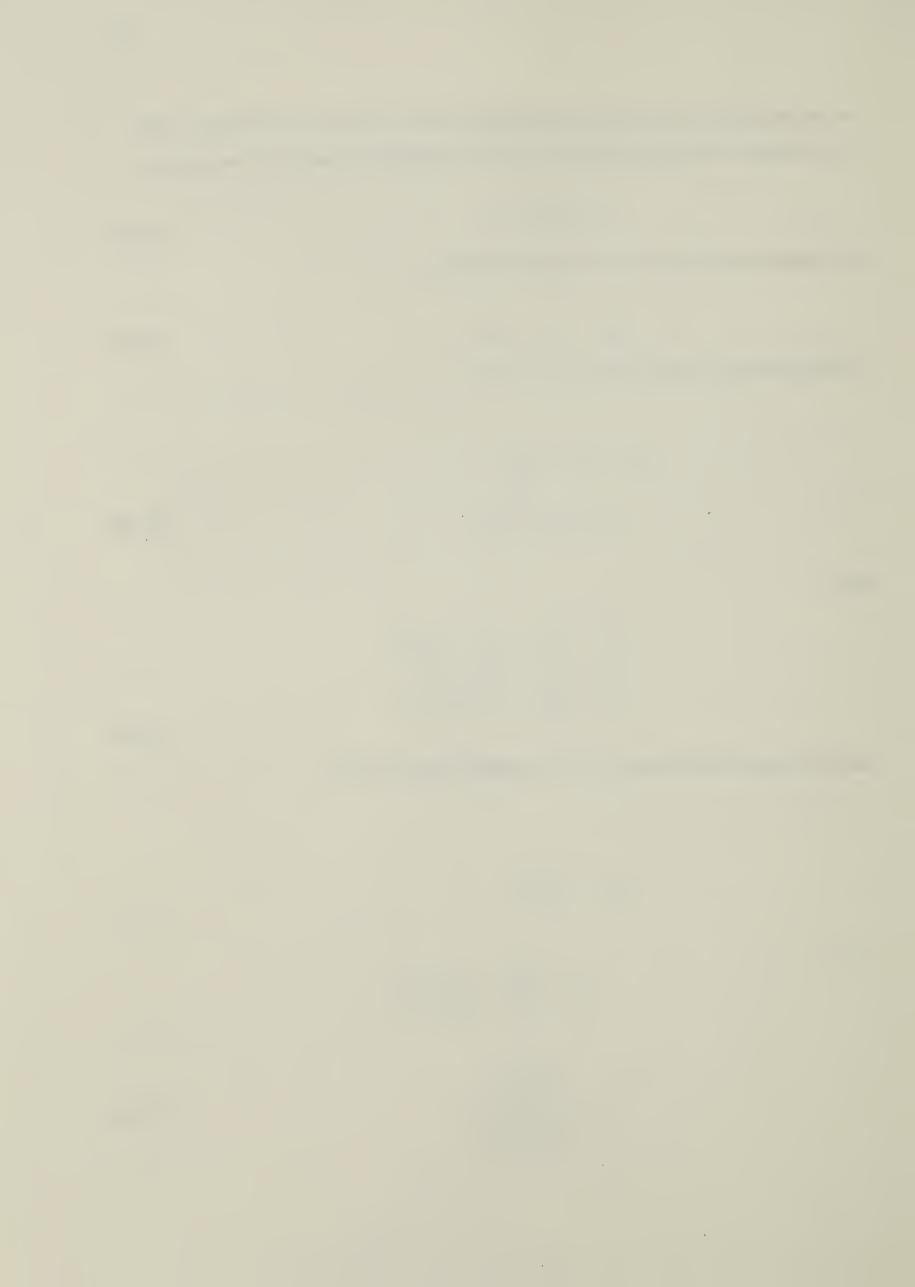
$$\dot{\vec{\Omega}} = -\frac{\vec{\nabla}_r\omega}{k} + \frac{(\vec{\Omega} \cdot \vec{\nabla}_r\omega)}{k}\vec{\Omega}$$

(3.1.9)

Let the refractive index be $\eta$ ( $\omega$ ,r,t). The spatial gradient of $\omega$ is

$$\vec{\nabla}_r\omega = \vec{\nabla}_r(\frac{ck}{\eta})$$

$$= ck[-\frac{\vec{\nabla}_r\eta}{\eta^2} - \frac{1}{\eta^2}\frac{\partial\eta}{\partial\omega}\frac{\partial\omega}{\partial r}]$$

$$= \frac{\frac{-ck\vec{\nabla}_r\eta}{\eta^2}}{(1+\frac{ck}{\eta^2}\frac{\partial\eta}{\partial\omega})}$$

(3.1.10)

Also, the gradient of $\omega$ with respect to $\vec{k}$ is

$$\frac{\partial \omega}{\partial \vec{k}} = \frac{\partial}{\partial \vec{k}} \frac{ck}{\eta(\omega,\vec{r},t)}$$

$$= \frac{c}{\eta} \hat{k} - \frac{ck}{\eta^2} \frac{\partial \eta}{\partial \omega} \frac{\partial \omega}{\partial \vec{k}}$$

$$= \frac{\frac{c}{\eta} \hat{k}}{(1 + \frac{ck}{\eta^2} \frac{\partial \eta}{\partial \omega})}$$

$$= \frac{\frac{c}{\eta} \hat{k}}{(1 + \frac{\omega \partial \eta}{\eta \partial \omega})} \tag{3.1.11}$$

where $\hat{k}$ is the unit vector of $\vec{k}$ and $\frac{ck}{\eta} = \omega$

But,

$$\left| \frac{\partial \omega}{\partial \vec{k}} \right| = |\vec{v}_g| = v_g$$

Substituting eq. (3.1.11) into eq. (3.1.10), we get

$$\vec{\nabla}_r \omega = - \frac{k v_g}{\eta} \vec{\nabla}_r \eta$$

$$\frac{\vec{\nabla}_r \omega}{k} = \frac{-v_g}{\eta} \vec{\nabla}_r \eta \tag{3.1.12}$$

Combining eq. (3.1.12) and eq. (3.1.9), gives
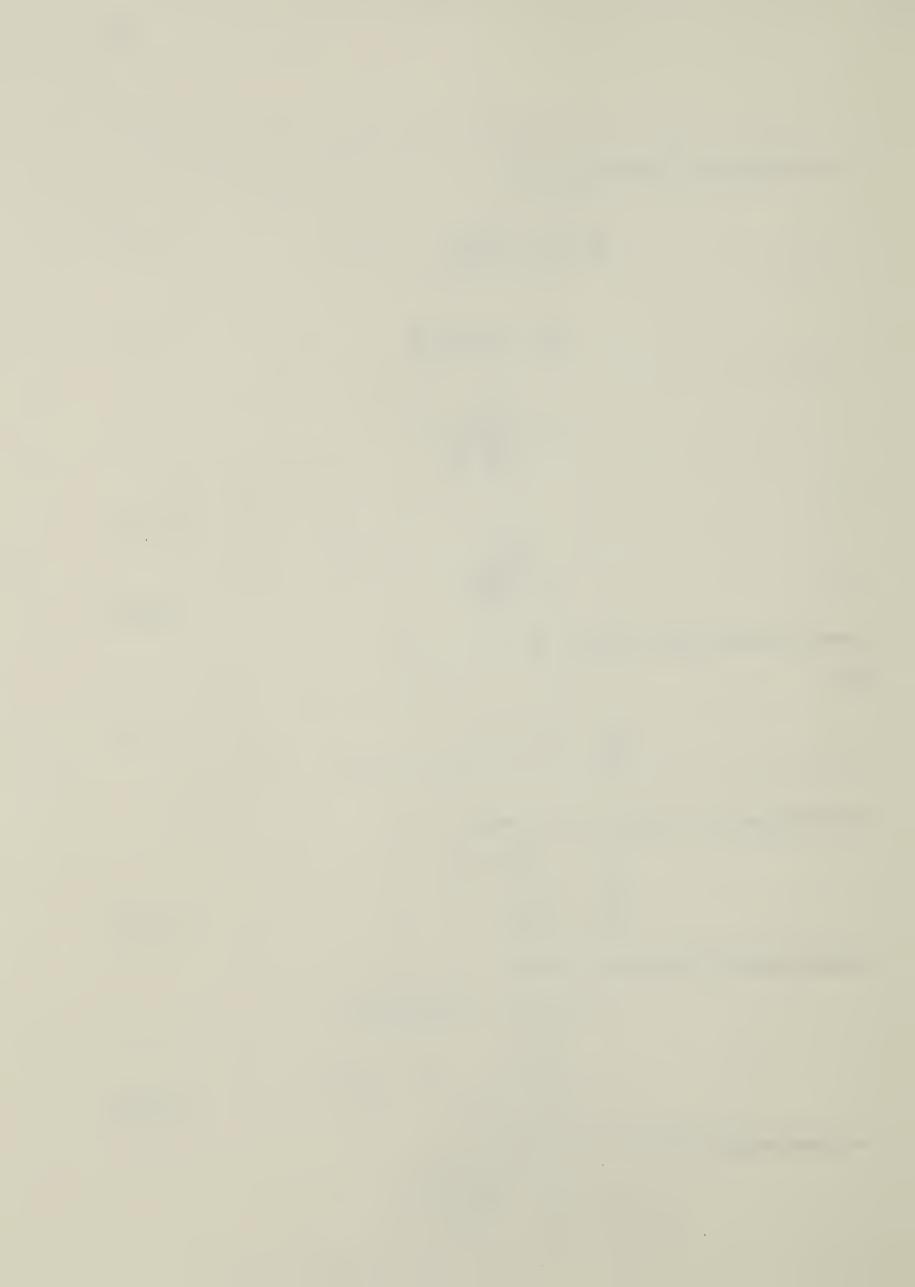
$$\dot{\vec{\Omega}} = \frac{v_g}{\eta} \vec{\nabla}_r \eta - \frac{(v_g \vec{\Omega} \cdot \vec{\nabla}_r \eta)}{\eta} \vec{\Omega}$$

$$= \frac{v_g}{\eta} [ \vec{\nabla}_r \eta - (\vec{\Omega} \cdot \vec{\nabla}_r \eta) \vec{\Omega} ] \tag{3.1.13}$$

In a plasma medium, the index of refraction is

$$\eta(\omega,\vec{r},t) = \sqrt{1 - \frac{\omega_{pe}^2(\vec{r},t)}{\omega^2}}$$

where $\omega_{pe}^2(\vec{r},t) = \dfrac{4\pi N(\vec{r},t)e^2}{m_e}$ and $N(\vec{r},t)$ is the electron density ($cm^{-3}$), $m_e$ is the electron mass. Because of the extremely short time for light to traverse the plasma medium, the plasma density does not change fast enough to give a significant change in the refractive index of the medium. The plasma refractive index can be considered as constant within the time of traversing and regarded as dependent only on space.

By substituting for $\eta$ into eq. (3.1.11), the group velocity is found to be

$$v_g = \eta(\vec{r},\omega)c \tag{3.1.14}$$

Eq. (3.1.13) thus becomes

$$\dot{\vec{\Omega}} = c\,[\,\vec{\nabla}_r\eta - (\vec{\Omega}\cdot\vec{\nabla}_r\eta)\vec{\Omega}\,] \tag{3.1.15}$$

By multiplying both sides by $\eta\,c$, which is the velocity in the medium,

$$\eta c\dot{\vec{\Omega}} = \eta c^2\vec{\nabla}_r\eta - \eta c^2(\vec{\Omega}\cdot\vec{\nabla}_r\eta)\vec{\Omega}$$

and using the expression for group velocity,

$$\dot{\vec{r}} = \vec{v}_g = v_g\vec{\Omega} = \eta c\vec{\Omega}$$

then

$$v_g\dot{\vec{\Omega}} = \eta c^2\vec{\nabla}_r\eta - (\vec{v}_g\cdot\vec{\nabla}_r v_g)\vec{\Omega}$$

But,
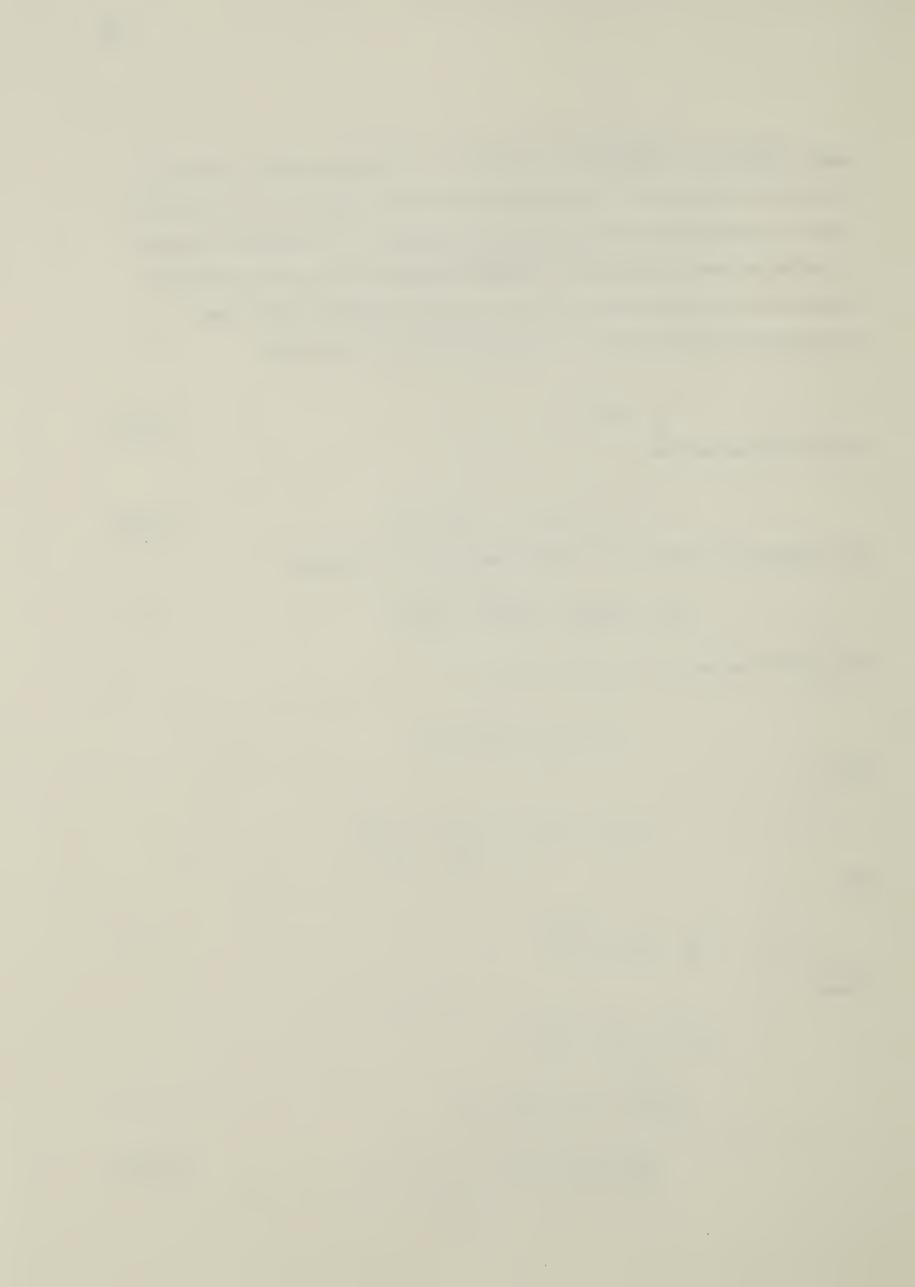
$$\vec{v}_g\cdot\vec{\nabla}_r v_g = \dfrac{dv_g}{dt}$$

Hence,

$$v_g\dot{\vec{\Omega}} + \dot{v}_g\vec{\Omega} = \eta c^2\vec{\nabla}_r\eta$$

$$\dfrac{d(v_g\vec{\Omega})}{dt} = \dfrac{c^2}{2}\vec{\nabla}_r\eta^2$$

$$\dfrac{d^2\vec{r}}{dt^2} = \dfrac{c^2}{2}\vec{\nabla}_r\eta^2 \tag{3.1.16}$$

According to the above equation, as long as the refractive index is spatially known at the instant the rays traverse the medium, ray paths can be traced.

## 3.2 Adoption of co-ordinate system

In this section, the choice of co-ordinate systems used for solving the ray equation is discussed.

The beam behaviour within a cylindrical plasma column is traced. Due to cylindrical symmetry of the column, cylindrical co-ordinate system is adopted. The ray equation can be expressed into its components as,

$$\frac{d^2 r}{dt^2} = \frac{c^2}{2} \frac{\partial \eta^2(r,z)}{\partial r} + r\dot{\theta}^2 \qquad (3.2.1)$$

$$\frac{d(r^2\dot{\theta})}{dt} = 0 \qquad (3.2.2)$$

$$\frac{d^2 z}{dt^2} = \frac{c^2}{2} \frac{\partial \eta^2(r,z)}{\partial z} \qquad (3.2.3)$$
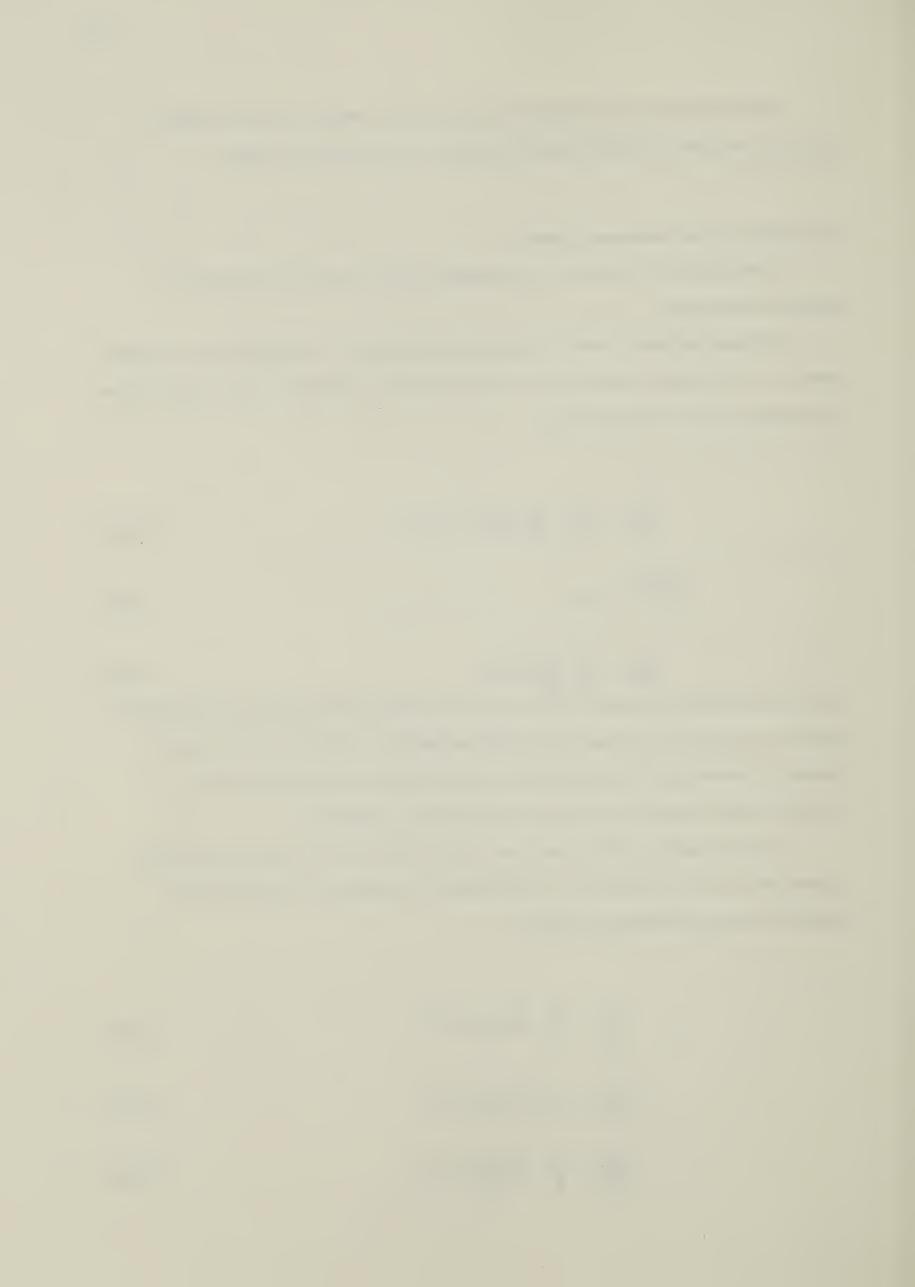
where $\dot{\theta}$ is the angular velocity of the ray. The refractive index is taken to be azimuthally independent. Eq.(3.2.2) indicates that the angular velocity component of the rays is a constant of motion due to the assumption of the azimuthal independence of the refractive index. Angular momentum of the ray is thus conserved.

In certain density profiles used later in this work, it will be more convenient to express the velocity components in the Cartesian co-ordinates for solving the ray equation. These components are given by

$$\frac{d^2 x}{dt^2} = \frac{c^2}{2} \frac{\partial \eta^2(x,y,z)}{\partial x} \qquad (3.2.4)$$

$$\frac{d^2 y}{dt^2} = \frac{c^2}{2} \frac{\partial \eta^2(x,y,z)}{\partial y} \qquad (3.2.5)$$

$$\frac{d^2 z}{dt^2} = \frac{c^2}{2} \frac{\partial \eta^2(x,y,z)}{\partial z} \qquad (3.2.6)$$

## 3.3 Choice of density profile

In this section, the ray equation is solved for different refractive indices which are determined from the density of the plasma confined in the solenoid. The behaviour of the ray is discussed accordingly.

In solving the ray equation within a plasma region, it is necessary to know the spatial variation of the refractive index in that region. The refractive index for a plasma is given as

$$\eta(\vec{r}) = \sqrt{1 - \frac{\omega_{pe}^2(\vec{r})}{\omega^2}} = \sqrt{1 - \frac{N(\vec{r})}{N_c}} \qquad (3.3.1)$$
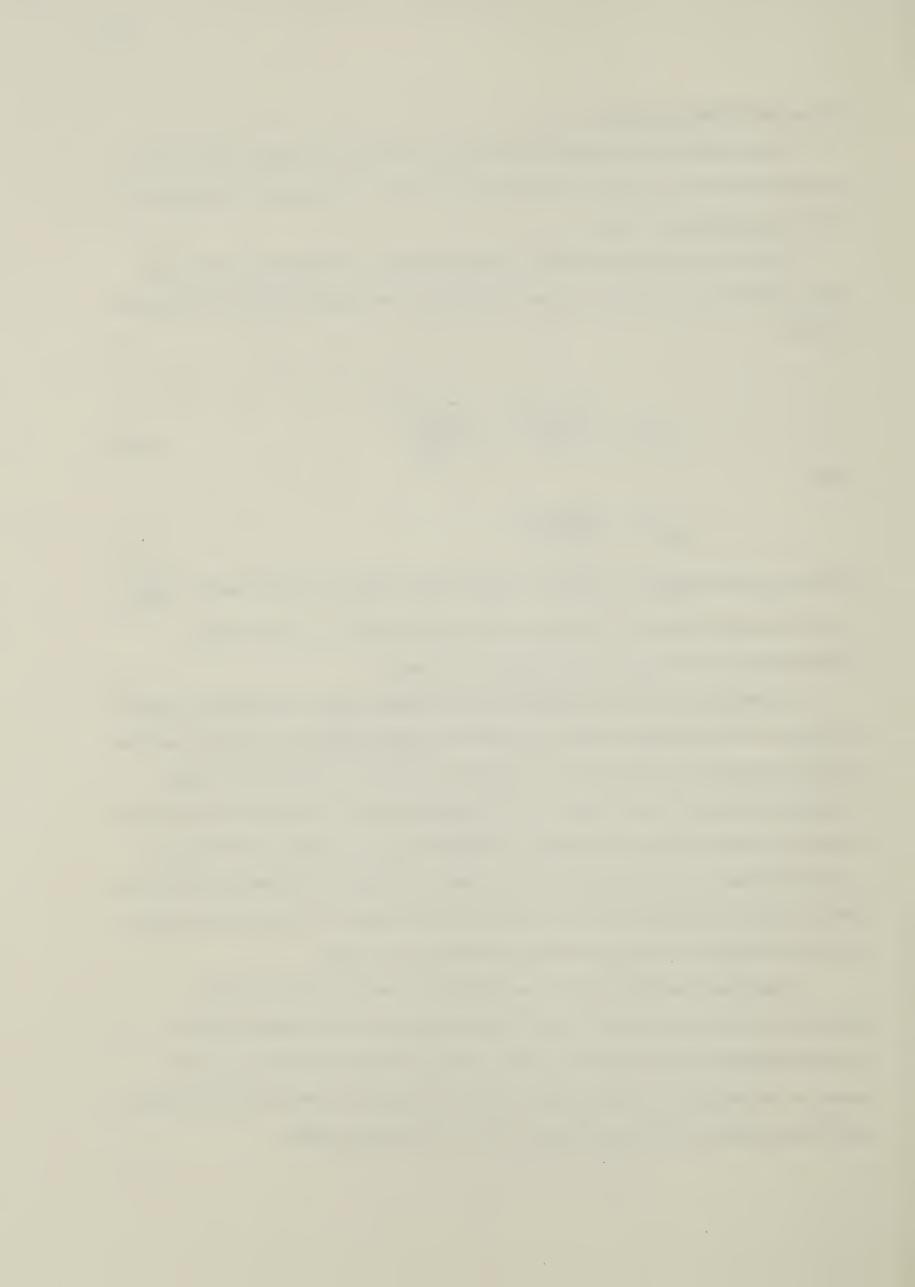
where

$$\omega_{pe}^2(\vec{r}) = \frac{4\pi N(\vec{r})e^2}{m_e}$$

$N(\vec{r})$ is the plasma density at a distance $\vec{r}$ from the origin ; $N_c$ is the critical density, $\frac{m_e \omega^2}{4\pi e^2}$ $\omega$ is the angular frequency of the laser. The refractive index at any point is thus determined directly from the plasma density at that point.

In McMullin and Milroy's simulation work, the plasma region is divided into meshes by means of a two-dimensional grid structure. The characteristics of the plasma such as energy, temperature and density are evaluated at the centre of the grid cells. These physical quantities are hence known only at discrete positions. In order to trace the beam trajectory within the plasma simulated by the MHD code, a knowledge of the density variation between any two adjacent cells is essential. Moreover, if the density variation is known to be a continuous function of position, the ray equation can be solved to give a continuous solution for the path between two adjacent grid cells.

Since plasma densities are only evaluated at the centres of the grid cells, appropriate continuous functions have to be used to describe the density variation between adjacent ones. The choice of such functions is deduced from the physical behaviour of the plasma when heated by means of a laser beam. These functions give a profile description of the plasma density in the corresponding region.

Density profiles which are functions of the square or inverse square of radial distance are used since they can give a suitable description for the density hollow created by a laser beam within the plasma column. Such a choice also enables the ray equation to be solved analytically. The density profiles are assumed to be azimuthally independent as a result of cylindrical symmetry of the plasma column.

Four different kinds of density profiles are adopted in accordance with the radial density changes at adjacent grid cells. They are as follows:

(1) $\quad \frac{dN(r)}{dr} > 0, \ \frac{d^2N(r)}{dr^2} > 0, \ N(r) = N_0(1 + \frac{r^2}{a_0^2})$ $\qquad$ (3.3.2)

(2) $\quad \frac{dN(r)}{dr} > 0, \ \frac{d^2N(r)}{dr^2} < 0, \ N(r) = N_1(1 - \frac{a_1^2}{r^2})$ $\qquad$ (3.3.3)
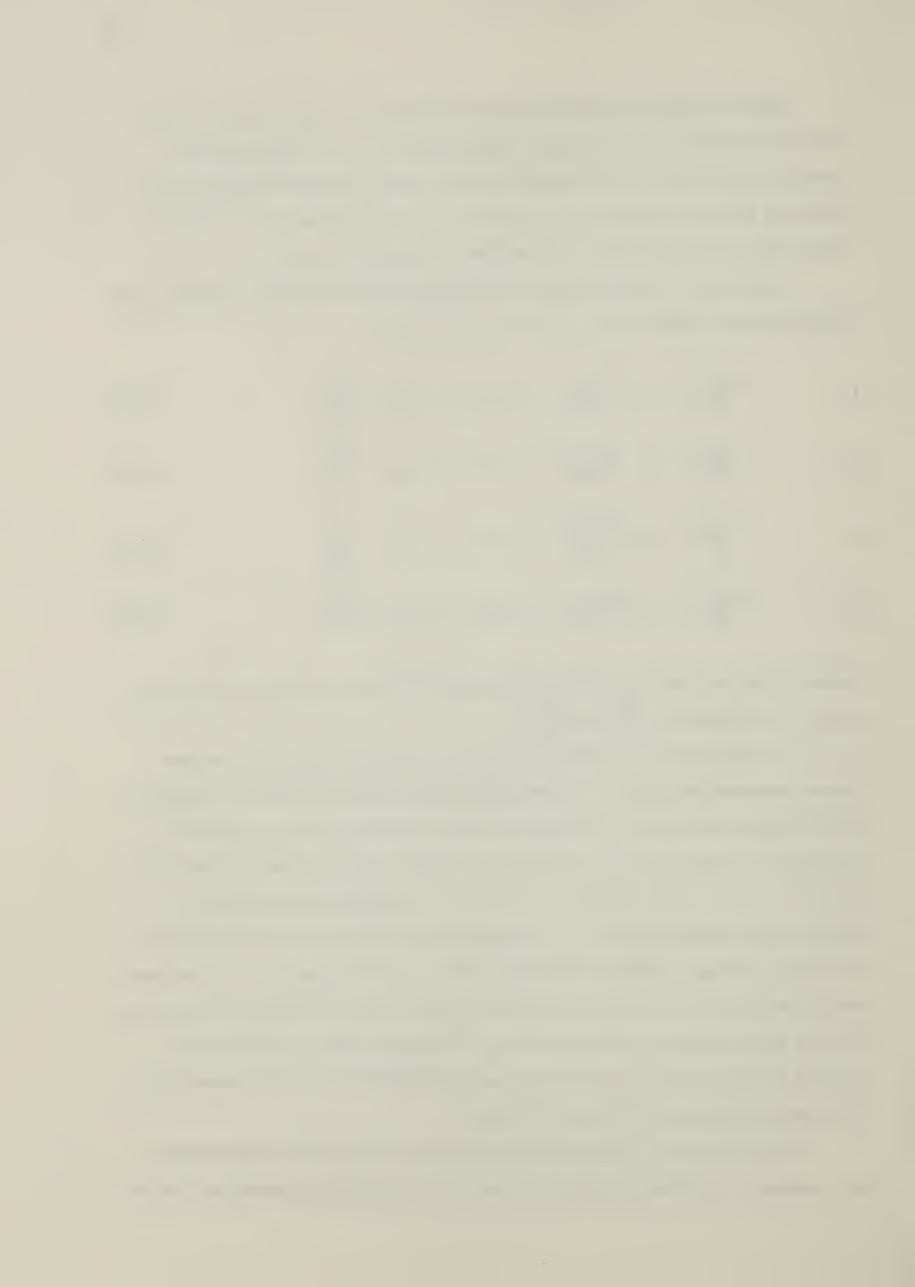
(3) $\quad \frac{dN(r)}{dr} < 0, \ \frac{d^2N(r)}{dr^2} > 0, \ N(r) = N_2(1 - \frac{r^2}{a_2^2})$ $\qquad$ (3.3.4)

(4) $\quad \frac{dN(r)}{dr} < 0, \ \frac{d^2N(r)}{dr^2} < 0, \ N(r) = N_3(1 + \frac{a_3^2}{r^2})$ $\qquad$ (3.3.5)

These profiles are fitted into corresponding regions wherever the density differences satisfy the conditions for $\frac{dN}{dr}$ and $\frac{d^2N}{dr^2}$ .

The suggested profiles are used to approximate various regions of the laser heated plasma column (fig. 3.1). The density distribution across the column can hence be approximated by segments of continuous functions. The core part of the column is described by a parabolic well corresponding to a density hollow created by laser heating (profile #1 in fig. 3.1) profile. Further from the core, the plasma density reaches a maximum due to the accumulation of plasma particles resulting from radial expansion of the plasma. The region between this density maximum and the parabolic well is simulated with profile #2 in fig. 3.1. Beyond this point, the plasma density decreases gradually. This region is approximated by profile #3 in fig. 3.1. On getting closer to the wall of the solenoid, profile #4 in fig. 3.1 is used. The density distribution across the column is thus described by segments of continuous functions.

With the refractive index given as in eq. (3.3.1), (r becomes the radial distance only, because of azimuthal and axial independence), the ray equation, as derived from eq.
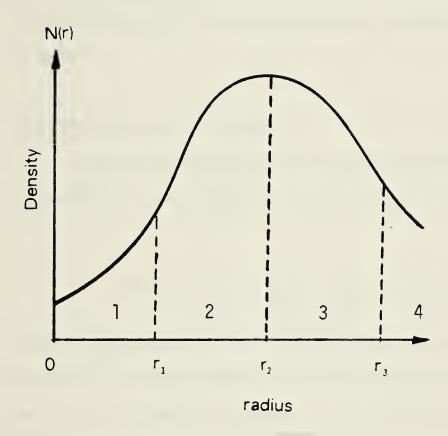
Figure 3.1 Radial density profile of the column

(3.2.1), eq. (3.2.2) and eq. (3.2.3), becomes

$$\frac{d^2r}{dt^2} = -\frac{c^2}{2N_c}\frac{dN(r)}{dr} + r\dot\theta^2$$

(3.3.6)

$$\frac{d(r^2\dot\theta)}{dt} = 0$$

(3.3.7)

$$\frac{d^2z}{dt^2} = 0$$

(3.3.8)

Eq. (3.3.7) and eq. (3.3.8) can be solved, with given initial ray conditions, for the angular velocity and the axial position. In what follows, the solutions of the differential equation for the radial position in different profiles are discussed as follow:

## (3.3.1) Parabolic radial profile

This profile is applied to the regions between two adjacent grid cells where $\frac{dN(r)}{dr}>0$ and $\frac{d^2N(r)}{dr^2}>0$(region 1 of fig. 3.1). The parabolic profile is

$$N(r) = N_0\left(1 + \frac{r^2}{a_0^2}\right) = N_0\left(1 + \frac{x^2 + y^2}{a_0^2}\right)$$

(3.3.1.1)

where $N_0, a_0$ are parameters determined from the boundary conditions of $N(r)$; and r is the radial distance. This profile applies frequently in the region near the axis of the plasma column. In Cartesian co-ordinates, the equations of motion are

$$\frac{d^2x}{dt^2} = -\frac{c^2 N_0 x}{a_0^2 N_c} = -\Omega^2 x$$

(3.3.1.2)
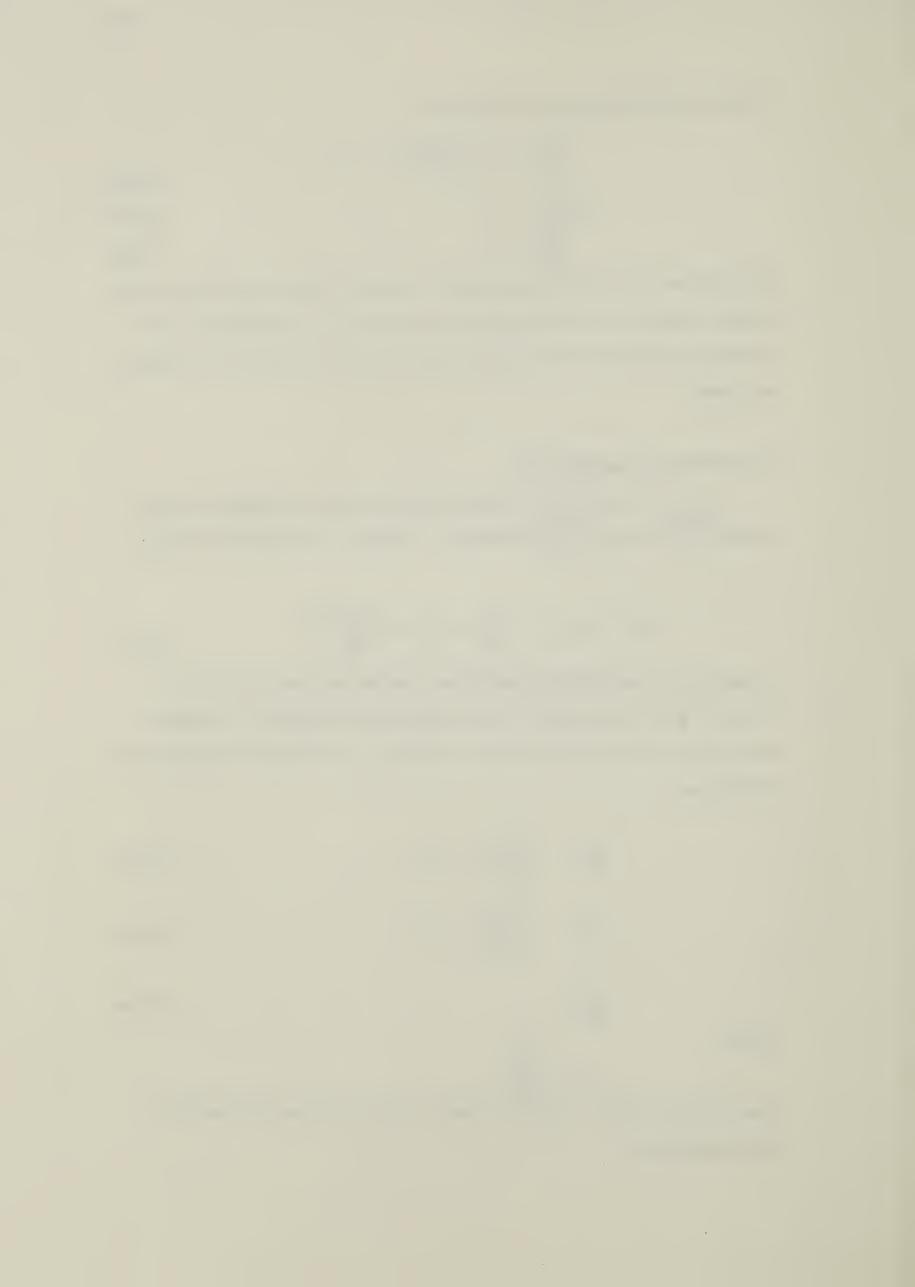
$$\frac{d^2y}{dt^2} = -\frac{c^2 N_0 y}{a_0^2 N_c} = -\Omega^2 y$$

(3.3.1.3)

$$\frac{d^2z}{dt^2} = 0$$

(3.3.1.4)

where

$$\Omega^2 = \frac{c^2 N_0}{a_0^2 N_c}$$

The solution for these equations is that of a simple harmonic motion. With initial conditions,

$t=0, x=x_0, y=y_0, \dot{x}=\dot{x}_0, \dot{y}=\dot{y}_0,$

$$x = x_0\cos(\Omega t) + \frac{\dot{x}_0}{\Omega}\sin(\Omega t) \tag{3.3.1.5}$$

$$y = y_0\cos(\Omega t) + \frac{\dot{y}_0}{\Omega}\sin(\Omega t) \tag{3.3.1.6}$$

$$\dot{x} = -\Omega x_0 \sin(\Omega t) + \dot{x}_0 \cos(\Omega t) \tag{3.3.1.7}$$

$$\dot{y} = -\Omega y_0 \sin(\Omega t) + \dot{y}_0 \cos(\Omega t) \tag{3.3.1.8}$$

$$r^2 = \frac{r_0^2}{2} + \frac{v_{0r}^2}{2\Omega^2} + B\sin(2\Omega t + \Phi) \tag{3.3.1.9}$$

where

$$\Phi = \tan^{-1}\left[\frac{\left(\frac{r_0^2}{2} - \frac{v_{0r}^2}{2\Omega^2}\right)}{\left(\frac{x_0\dot{x}_0 + y_0\dot{y}_0}{\Omega}\right)}\right]$$

$$B^2 = \left(\frac{r_0^2}{2} - \frac{v_{0r}^2}{2\Omega^2}\right)^2 + \left(\frac{x_0\dot{x}_0 + y_0\dot{y}_0}{\Omega}\right)^2$$

$$v_{0r}^2 = \dot{x}_0^2 + \dot{y}_0^2$$

$$r_0^2 = x_0^2 + y_0^2$$

The sinusoidal variation of the ray path with time indicates that the ray is trapped within the medium. A real solution for r² is guaranteed when $B<r_0^2/2+v_{0r}^2/2\Omega^2$. The last condition will depend on the initial conditions of the ray. A negative solution for r² indicates that the ray is not launched at the right position or direction and that the ray cannot go through the medium. From eq. (3.3.1.9), the maximum and minimum radial distances are given by

$$r^2 = \frac{r_0^2}{2} + \frac{v_{0r}^2}{2\Omega^2} \pm B \quad (+ \text{ for maximum}; \; - \text{ for minimum})$$

**(3.3.2) Inverse parabolic increasing profile**

This profile is used wherever the density difference between any two adjacent grid cells satisfies the conditions $\frac{dN(r)}{dr} > 0$ and $\frac{d^2N(r)}{dr^2} < 0$. The region defined within radius $r_1$, $r_2$ (region 2 of fig. 3.1) can be approximated by this profile. The profile is

$$N(r) = N_1\left(1 - \frac{a_1^2}{r^2}\right) \tag{3.3.2.1}$$

with $r \neq 0$. $N_1$, $a_1$ are constants determined from the boundary conditions of $N(r)$ in the region under consideration. On substituting for $N(r)$ from eq. (3.3.2.1) into the ray equation, the solution expressed in cylindrical co-ordinates, is

$$\frac{d^2r}{dt^2} = -\frac{c^2 N_1 a_1^2}{N_c r^3} + \frac{p^2}{r^3}$$

$$= \left(p^2 - \frac{c^2 N_1 a_1^2}{N_c}\right)\frac{1}{r^3} \tag{3.3.2.2}$$
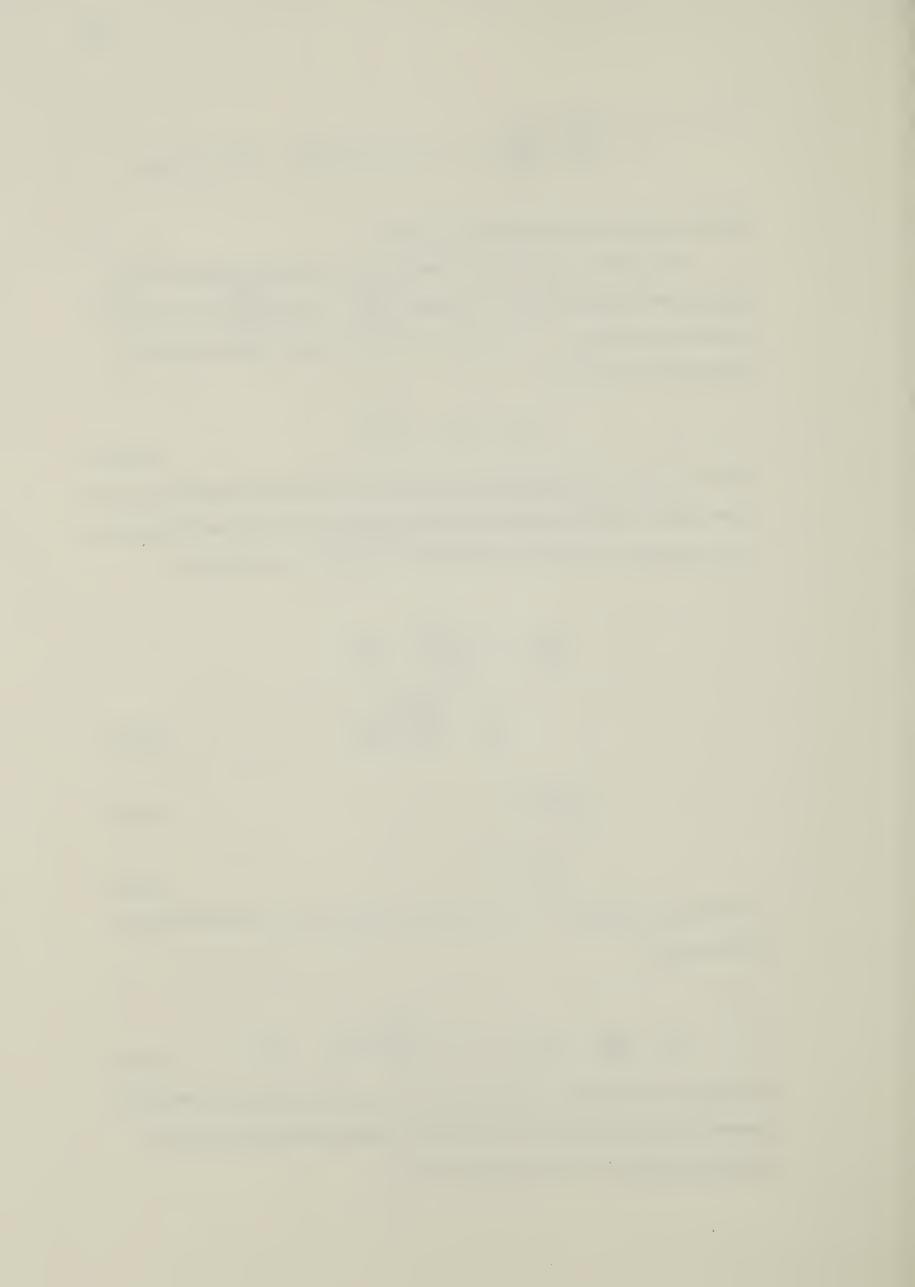
$$\frac{d(r^2\dot{\theta})}{dt} = 0 \tag{3.3.2.3}$$

$$\frac{d^2z}{dt^2} = 0 \tag{3.3.2.4}$$

With the initial conditions, $t=0$, $r=r_0$, $\dot{\theta}=\dot{\theta}_0$, $p=r_0^2\dot{\theta}_0$, $v_r=v_{0r}$, the radial velocity is found to be

$$\dot{r}^2 = \left(\frac{dr}{dt}\right)^2 = v_{0r}^2 + \left(p^2 - \frac{c^2 a_1^2 N_1}{N_c}\right)\left(\frac{1}{r_0^2} - \frac{1}{r^2}\right) \tag{3.3.2.5}$$

By integrating this equation with respect to time, the expression for the radial position can be obtained. Cases for outward radial acceleration and inward radial acceleration are considered as follows:

(i) For the case of outward radial acceleration, the quantity

$$p^2 - \frac{c^2 a_1^2 N_1}{N_c}$$ is positive. The corresponding solution for the equation

is

$$t = \frac{r_0}{r_0^2 v_{0r}^2 + (p^2 - \frac{c^2 a_1^2 N_1}{N_c})} [\pm \sqrt{r^2(r_0^2 v_{0r}^2 + (p^2 - \frac{c^2 a_1^2 N_1}{N_c})) - r_0(p^2 - \frac{c^2 a_1^2 N_1}{N_c})}]$$

$$- \frac{r_0^2 v_{0r}}{r_0^2 v_{0r}^2 + (p^2 - \frac{c^2 a_1^2 N_1}{N_c})}$$

(3.3.2.6)

for $v_{0r} > 0$, t takes the positive root; for $v_{0r} < 0$, t takes the negative root. The radial distance is given by

$$r = \frac{1}{\sqrt{(r_0^2 v_{0r}^2 + p^2 - \frac{c^2 a_1^2 N_1}{N_c})}} [(p^2 - \frac{c^2 a_1^2 N_1}{N_c}) r_0^2 + \frac{1}{r_0^2}(r_0^2 v_{0r}^2 + p^2 - \frac{c^2 a_1^2 N_1}{N_c})^2$$

$$\times (t \pm \frac{r_0^3 v_{0r}}{r_0^2 v_{0r}^2 + p^2 - \frac{c^2 a_1^2 N_1}{N_c}})^2]^{\frac{1}{2}}$$
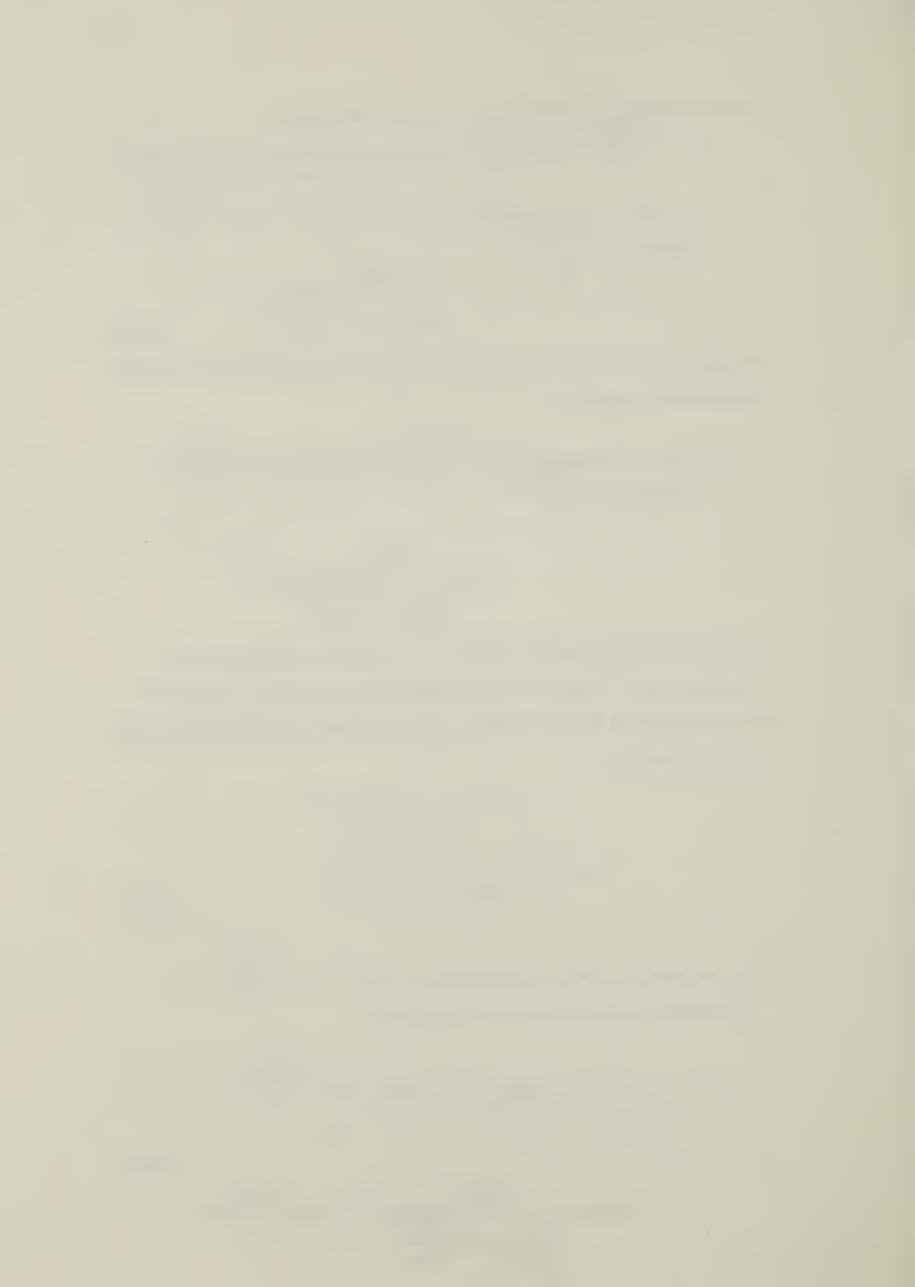
With an initial inward radial velocity, the ray will move towards the axis of propagation until it reaches a minimum radial position where it is refracted away from the axis. From eq. (3.3.2.5), one can deduce that the minimum radial position of the ray is

$$r_{min} = \sqrt{[\frac{r_0^2(p^2 - \frac{c^2 a_1^2 N_1}{N_c})}{(r_0^2 v_{0r}^2 + p^2 - \frac{c^2 a_1^2 N_1}{N_c})^{\frac{1}{2}}}]}$$

(3.3.2.7)

(ii) For the case of inward radial acceleration, that is $p^2 - \frac{c^2 a_1^2 N_1}{N_c} < 0$,

the square of radial position will be given by

$$r^2 = \frac{1}{r_0^2 v_{0r}^2 - |p^2 - \frac{c^2 a_1^2 N_1}{N_c}|} [\frac{1}{r_0^2}(r_0^2 v_{0r}^2 - |p^2 - \frac{c^2 a_1^2 N_1}{N_c}|)^2$$

(3.3.2.8)

$$\times (t \pm \frac{r_0^3 v_{0r}}{r_0^2 v_{0r}^2 - |p^2 - \frac{c^2 a_1^2 N_1}{N_c}|})^2 - r_0^2 |p^2 - \frac{c^2 a_1^2 N_1}{N_c}|]$$

When $r_0^2 v_{0r}^2 - |p^2 - \dfrac{c^2 a_1^2 N_1}{N_c}| > 0$ and $v_{0r}$ is < 0, the solution of r is imaginary. This implies that rays of which the initial locations and directions satisfy these conditions, cannot penetrate this region.

**(3.3.3) Parabolic decreasing radial profile**

This approximation is used in regions where the spatial density variation follows the relations $dN(r)/dr < 0$ and $d^2N(r)/dr^2 > 0$ (region 3 of fig. 3.1). A possible region in the density well is beyond where the plasma density reaches its maximum (region bounded by the radii $r_2$ and $r_3$ in fig. 3.1). The density profile is expressed as

$$N(r) = N_2\left(1 - \frac{r^2}{a_2^2}\right) \tag{3.3.3.1}$$

Solution for the ray path expressed in Cartesian co-ordinates, is

$$x = \frac{\dot{x}_0}{\Omega} \sinh(\Omega t) + x_0 \cosh(\Omega t) \tag{3.3.3.2}$$

$$y = \frac{\dot{y}_0}{\Omega} \sinh(\Omega t) + y_0 \cosh(\Omega t) \tag{3.3.3.3}$$
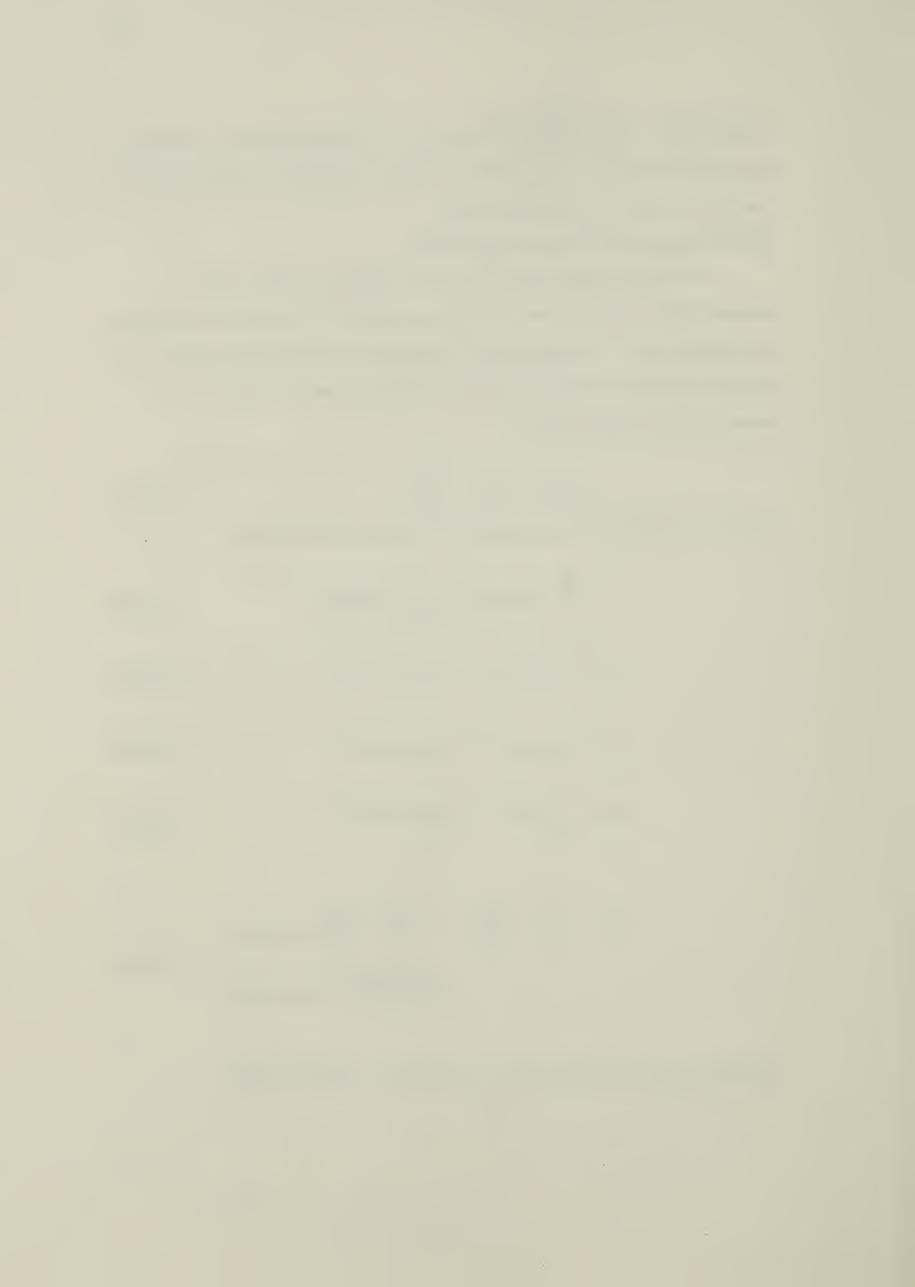
$$\dot{x} = \dot{x}_0 \cosh(\Omega t) + \Omega x_0 \sinh(\Omega t) \tag{3.3.3.4}$$

$$\dot{y} = \dot{y}_0 \cosh(\Omega t) + \Omega y_0 \sinh(\Omega t) \tag{3.3.3.5}$$

$$r^2 = \left(\frac{r_0^2}{2} - \frac{v_{0r}^2}{2\Omega^2}\right) + \left(\frac{r_0^2}{2} + \frac{v_{0r}^2}{2\Omega^2}\right)\cosh(2\Omega t) + \left(\frac{x_0\dot{x}_0 + y_0\dot{y}_0}{\Omega}\right)\sinh(2\Omega t) \tag{3.3.3.6}$$

where $x_0, y_0$ are the initial positions of the ray; $r_0^2 = x_0^2 + y_0^2, v^2 = \dot{x}_0^2 + \dot{y}_0^2$

$$\Omega^2 = \frac{c^2 N_2}{N_c a_2^2} ; \dot{x}_0, \dot{y}_0 \text{ are the initial velocities.}$$

Depending on the initial conditions of the ray, the ray will traverse in this region radially inward or radially outward. If all terms in eq. (3.3.3.6) are positive, the radial distance will increase directly with t. The ray will leave the region gradually and will not be trapped. $r^2$ will become negative according to the initial ray conditions. A negative value for $r^2$ indicates that the ray may launch into the plasma region such that it is reflected off. When the ray goes radially inward, the minimum radial distance that the ray will approach is,

$$r_{min}^2 = ( \frac{r_0^2}{2} - \frac{v_{0r}^2}{2\Omega^2}) + \sqrt{( \frac{r_0^2}{2} + \frac{v_{0r}^2}{2\Omega^2})^2 - ( \frac{x_0\dot{x}_0 + y_0\dot{y}_0}{\Omega})^2} \qquad (3.3.3.7)$$

which can be seen to be dependent on the initial position and velocity of the ray.

## (3.3.4) Non-parabolic decreasing radial profile

This profile fits into the region where the relations $\frac{dN(r)}{dr} < 0$ and $\frac{d^2N(r)}{dr^2} < 0$ hold(region 4 of fig. 3.1). The density profile in the region is given as

$$N(r) = N_3( 1 + \frac{a_3^2}{r^2}) \qquad (3.3.4.1)$$

with $r \neq 0$. By using cylindrical co-ordinates and initial conditions $v_{0r}, r_0$, the radial location of the ray trajectory is given by

$$r = \frac{1}{(r_0^2 v_{0r}^2 + p^2 + \frac{c^2 a_3^2 N_3}{N_c})^{\frac{1}{2}}} [ r_0^2(p^2 + \frac{c^2 a_3^2 N_3}{N_c}) + \frac{1}{r_0^2}(r_0^2 v_{0r}^2 + p^2 + \frac{c^2 a_3^2 N_3}{N_c})^2$$

$$\times (t \pm \frac{r_0^3 v_{0r}}{r_0^2 v_{0r}^2 + p^2 + \frac{c^2 a_3^2 N_3}{N_c}})^2]^{\frac{1}{2}} \qquad (3.3.4.2)$$

Through comparing the two expressions for r given by eq. (3.3.4.2) and eq. (3.3.2.6), it can be noted that only the term $(p^2+c^2a_3^2N_3/N_c)$ is changed. Similar results can thus be concluded for the inward radial velocity case. The ray will approach its minimum radial distance, according to the relation,

$$r_{min}^2 = \frac{r_0^2(p^2+\dfrac{c^2a_3^2N_3}{N_c})}{r_0^2v_{0r}^2+p^2+\dfrac{c^2a_3^2N_3}{N_c}}$$

(3.3.4.3)

The adoption of the four profiles for describing the plasma density in the column is initiated from the density well shown in fig. 3.1. Regions within the plasma column are matched to the corresponding density profiles according to the sign of the density gradient and the derivative of the density gradient within that region. The density gradient conditions $\dfrac{dN(r)}{dr} > 0$ or $< 0$ and the derivative of the density gradient $\dfrac{d^2N(r)}{dr^2} > 0$ or $< 0$ determine the type of density profiles to be used in computing the ray trajectories. In previous work[5, 6, 7], only parabolic profiles were assumed within the column. The corresponding ray path is sinusoidal as was discussed in section (3.1). However, in McMullin and Milroy's MHD code, the plasma density profile is arbitrary and determined only through a self-consistent set of fluid equations. Both parabolic and non-parabolic profiles are used for simulating the density distribution. Such choice eliminates the use of numerical methods to solve the ray equation. However, corresponding parameters for various profiles are needed to be evaluated for each set of density values calculated from the MHD code. The axial density variation is assumed to be slow so that there is no significant change over one axial grid distance. This assumption is valid as long as there is no abrupt axial density change encountered, otherwise axial density variation has to be included.

## Chapter 4

### Laser power absorption and ponderomotive forces

The deposition of laser energy within the plasma medium is discussed in this chapter. The ponderomotive force due to high laser intensity is considered as well. In section 4.1, the distribution of power among rays is discussed. and in section 4.2 an account of the absorption mechanism involved in the energy transfer process is given. Moreover, the ponderomotive force due to inhomogeneous laser intensity distribution is considered in section 4.3.

### 4.1 Power carried by individual rays

In this section, methods of distributing the radiation power among the rays are briefly discussed.

In a cylindrical co-ordinate system, the radial power of a Gaussian beam at a radial distance r, can be obtained by integrating the intensity distribution I(r) over the cross sectional area with radius r. From eq. (2.2.2), the amplitude of the Gaussian beam across a transverse cross section at the lens plane is

$$|\epsilon(r, z_0)| = \sqrt{\frac{2}{\pi}} \frac{1}{\omega(z_0)} e^{\frac{-r^2}{\omega^2(z_0)}}$$

(4.1.1)

The intensity of the beam transmitted through an area of radius r is
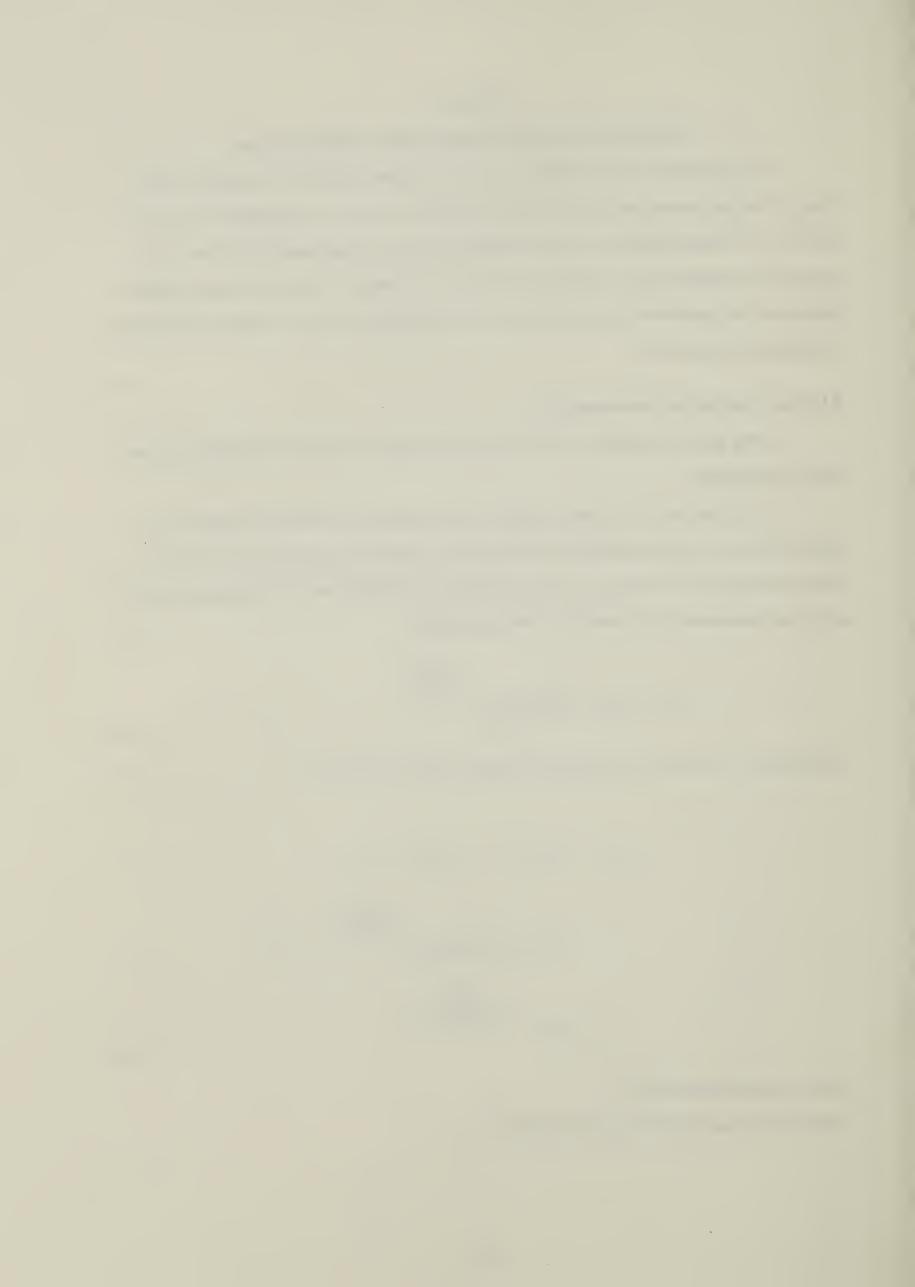
$$I(r) = 2\pi \int_0^r |\epsilon(r', z_0)|^2 r' dr' I_0$$

$$= 2\pi \int_0^r I_0 \frac{2}{\pi} \frac{1}{\omega^2(z_0)} e^{\frac{-2r'^2}{\omega^2(z_0)}} r' dr'$$

$$= I_0 (1 - e^{\frac{-2r^2}{\omega^2(z_0)}})$$

(4.1.2)

where $I_0$ is the total intensity.

The power transmitted through this area is

$$P(r) = \frac{cI(r)}{8\pi}$$

$$= \frac{cI_0}{8\pi} (1 - e^{\frac{-2r^2}{\omega^2(z_0)}} ) \tag{4.1.3}$$

This power can be distributed among the rays simulating the beam by using the distribution function derived for an incoherent Gaussian beam (eq. 2.4.19), namely,

$$< f(x,y,u_x,y_y,z) > = \frac{|E_0|^2 k^2 D^2 a_0^2}{2\pi} e^{\frac{-2(x^2+y^2)}{a_0^2}}$$

$$\times e^{\frac{-k^2 D^2 a_0^2}{2}[(u_x+\frac{x}{F(z)})^2+(u_y+\frac{y}{F(z)})^2]} \tag{4.1.4}$$
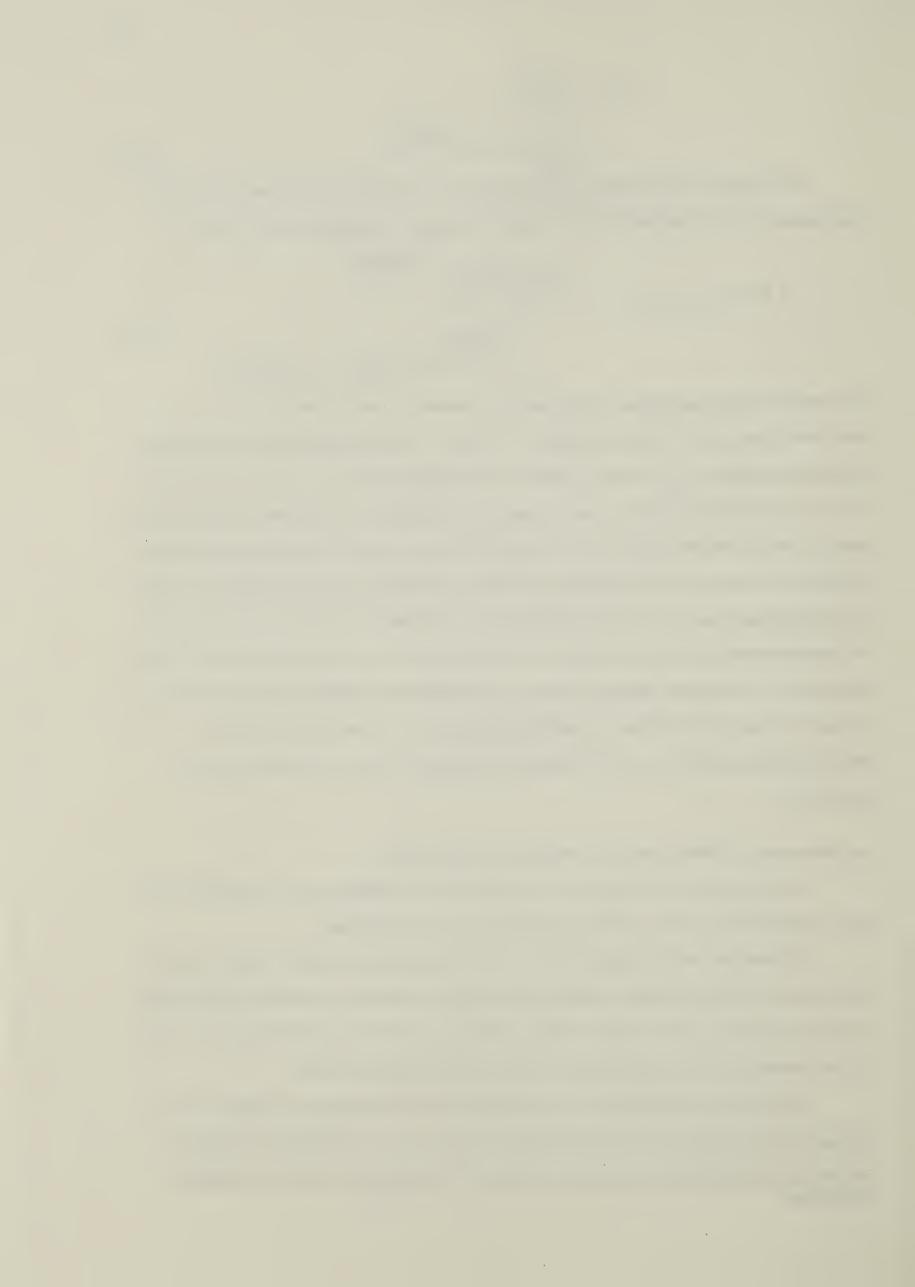
The energy density associated with a ray at a location (x,y) and a direction $(u_x,u_y)$ is evaluated from eq. (4.1.4) and is given by $\int <f> du_\perp$ . Power transmitted along the axial direction is given by $\frac{c}{8\pi} \int <f> du_\perp$, where c is the speed of light. The power carried by a ray can be determined directly once its position and direction are known. The set of rays used for describing the beam can be determined in two ways. Firstly, the positions and directions of the rays can be preset so that the ray density is constant across the beam. The associated power carried by each ray is then evaluated from eq. (4.1.3) in terms of its predetermined position and direction. Alternatively, the rays can be assumed to carry equal power. The power density within a certain beam area is determined by counting the number of rays within the area. Locations and directions of the the rays can be determined according to a random Gaussian distribution which will be discussed in section 5.1.

## 4.2 Derivation of the absorption coefficient along a ray

In this section, the coefficient of absorption in a plasma along unit length of the rays is derived. The power absorbed along a ray is then evaluated.

For the case of laser heated solenoid, the plasma absorbs laser energy through the process of inverse Bremsstrahlung. This process dominates over other laser heating mechanisms(see footnote) because laser intensity is in the order of less than $10^{11}-10^{12}$ W/cm² which is not strong enough to initiate other heating processes.

From Johnston and Dawson[1],the absorption coefficient per unit length for this process for an incident monochromatic beam wave with a wavelength of 10.6 $\mu$m, is

--------------------
Anomalous ion and electron heating resulting from parametric excitation of plasma instabilities

$$K_a = \frac{8.67 \times 10^{-30} \; Ze^2 n\lambda^2 \ln\Lambda}{T_e^{\frac{3}{2}}(1 - \frac{\omega_{pe}^2}{\omega^2})} \quad cm^{-1}$$

(4.2.1)

where

$$\Lambda = \min \; [\frac{2.19 \times 10^3 \times T_e^{\frac{3}{2}} \lambda \, (cm)}{Z} \; , \; 1.14\lambda_{cm} T_e \; ]$$

The absorption coefficients along ray paths can be found by considering absorption on small segments of the trajectory. This is explained as follows. For a ray segment of length ds, the associated absorption coefficient within a grid cell(see footnote) is

$$dK = K_a ds$$

(4.2.2)

Also ds is the length of the trajectory travelled by a photon in a time dt, at a velocity n(r)c (n(r) is the refractive index of the medium). The equation can thus be written as
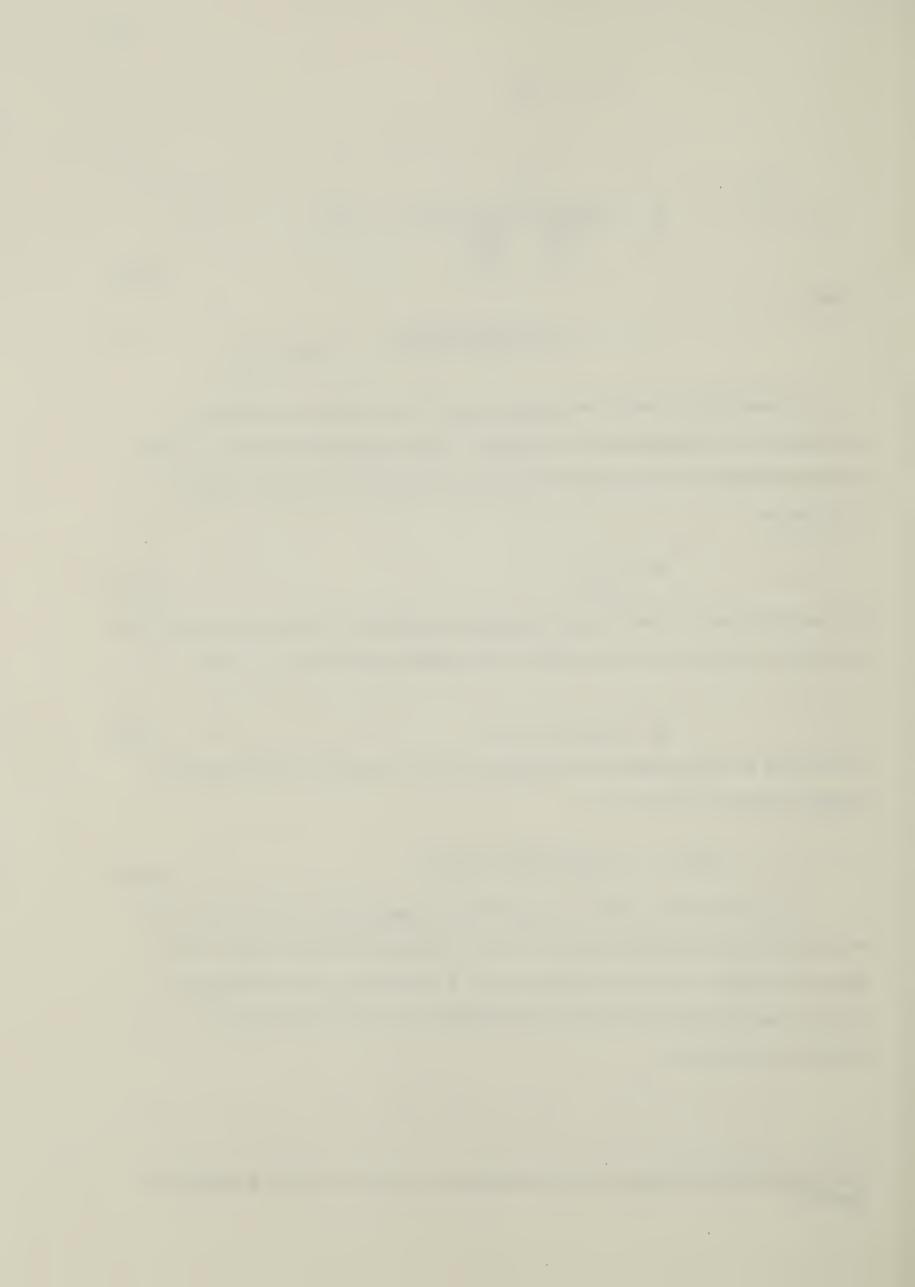
$$dK = K_a n(r(t))c \; dt$$

(4.2.3)

where r(t) is the radial position of the photon at time t. The power transferred to the medium within this segment ds is

$$dP(r,t) = -K_a n(r(t))cP(r,t)dt$$

(4.2.4)

Since the time interval(dt) for the beam to propagate along a distance ds within the plasma column is relatively short ($10^{-8}$ sec. ) compared to the pulse width of the laser(in the order of $10^{-6}$ sec.), the beam power from the laser can be regarded as constant over the time (dt) for traversing the distance ds. The amount of power left,$P_f$,after a time dt is

------------------------

The plasma column is divided into tiny volumes by a mesh. Each volume is termed as a grid cell.

$$\int_{P_i}^{P_f} \frac{dP(r,t_0)}{P(r,t_0)} = -\int_0^{dt} K_a n(r(t'))c\,dt' \qquad (4.2.5)$$

$$P_f(r_0+dr,t+dt) = P_i(r_0,t_0)e^{-\int_0^{dt} K_a n(r(t'))c\,dt'} \qquad (4.2.6)$$

where $P_i(r_0,t_0)$ is the beam power at time $t_0$ and location $r_0$. Within the time interval $dt$, the input beam power is assumed to be constant with time and has the value $P_i(r_0,t_0)$. The amount of absorbed power is

$$P_{abs} = P_i(r_0,t_0) - P_f(r_0+dr,t_0+dt)$$

$$= P_i(r_0,t_0)[\; 1 - e^{-\int_0^{dt} K_a n(r(t'))c\,dt'}\;]$$

$$(4.2.7)$$

The beam loses $\Delta P_{abs}$ watts for each traverse of the distance $ds$.

## 4.3 Calculation of ponderomotive forces

In this section, the ponderomotive force is derived according to Chen's analysis[2].

As a laser beam is focused onto a plasma medium, the intensity at the focal region is extremely high. The electromagnetic field which is proportional to intensity rises significantly. The consequent effect is that the field imposes a strong Lorentz force on the particles leading to a charge separation which bundles up electrons and ions into discrete regions. This force acting on an electron ,with mass $m_e$, located at r is
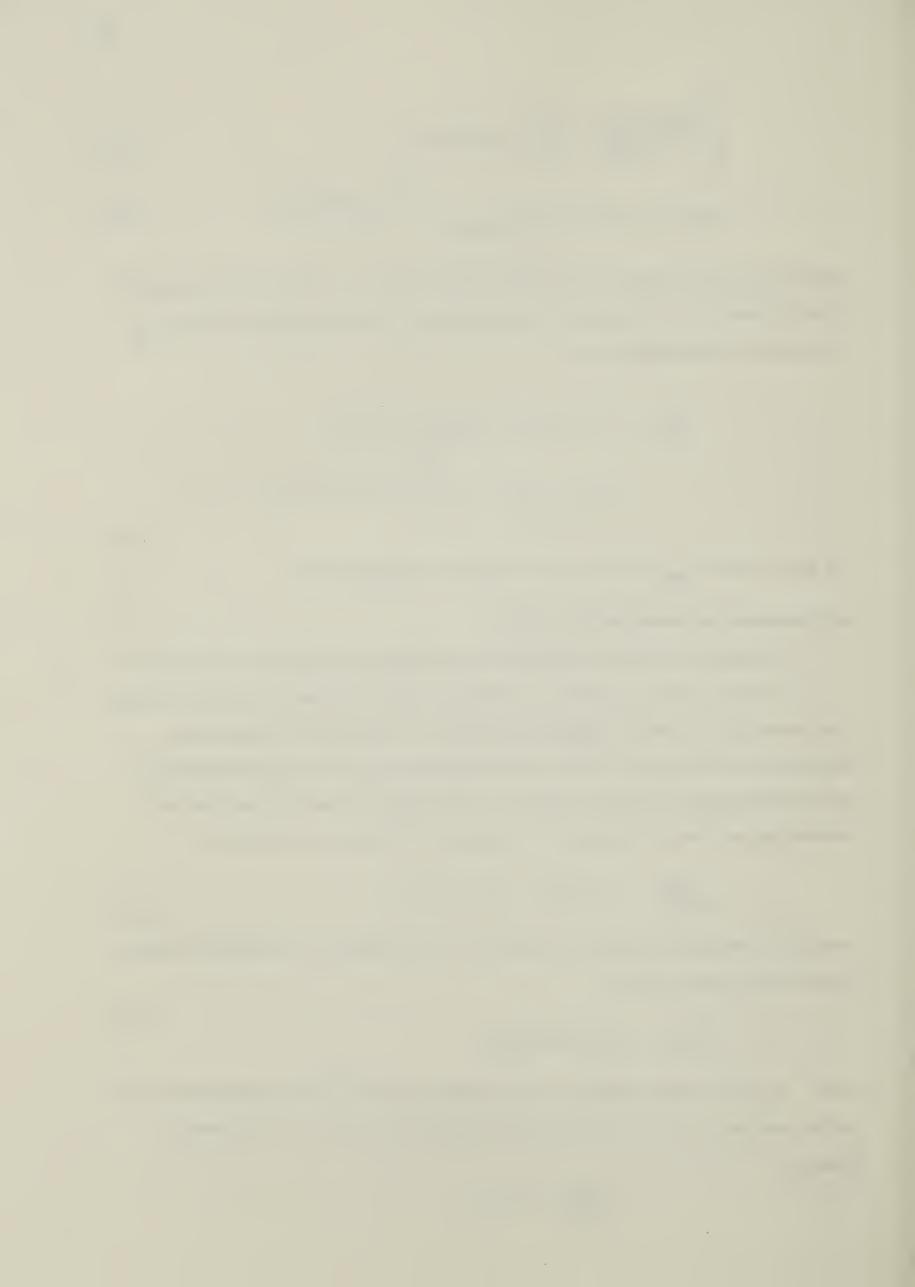
$$m_e\left(\frac{d\vec{v}}{dt}\right) = -e[\; \vec{E}(\vec{r}) + \frac{1}{c}\vec{v} \times \vec{B}(\vec{r})\; ] \qquad (4.3.1)$$

where $\vec{E}(\vec{r})$ is the electric field of the radiation ; $\vec{v}$ is the velocity of the electrons. With an incident electric field given as

$$(4.3.2)$$

$$\vec{E}(\vec{r},t) = \vec{E}_s(\vec{r})\cos(\omega_0 t)$$

where $\omega_0$ is the angular frequency of the incident wave. $\vec{E}_s(\vec{r})$ is the electric field with spatial dependence only. The corresponding magnetic field is found from Maxwell's equation

$$\frac{1}{c}\frac{\partial \vec{B}}{\partial t} = -\vec{\nabla} \times \vec{E}$$

$$\vec{B}(\vec{r}) = -\frac{c}{\omega_0} \vec{\nabla} \times \vec{E}_s(\vec{r})\sin(\omega_0 t)$$

(4.3.3)

To the first order, the force on an electron at location $\vec{r}$ can be evaluated by taking $\vec{E}$ at the initial position $\vec{r}$, and neglecting the term $\vec{v} \times \vec{B}$ since it is smaller than $\vec{E}$ by a factor of $v/c$. The force is

$$m_e\left(\frac{d\vec{v}}{dt}\right) = -e\vec{E}(\vec{r}_0)$$

(4.3.4)

On integrating, and using the initial conditions that the electron has a zero velocity and locates at the maximum amplitude of oscillation, the first order velocity perturbation is

$$\vec{v}^{(1)} = \frac{-e}{m_e\omega_0}\vec{E}_s(\vec{r})\sin(\omega_0 t)$$

(4.3.5)

and upon further integration, the first order displacement perturbation of the electron from the position $r_0$ is,

$$\delta\vec{r}^{(1)} = \int\vec{v}^{(1)} \, dt = \frac{e}{m_e\omega_0^2}\vec{E}_s(\vec{r})\cos(\omega_0 t)$$

(4.3.5a)
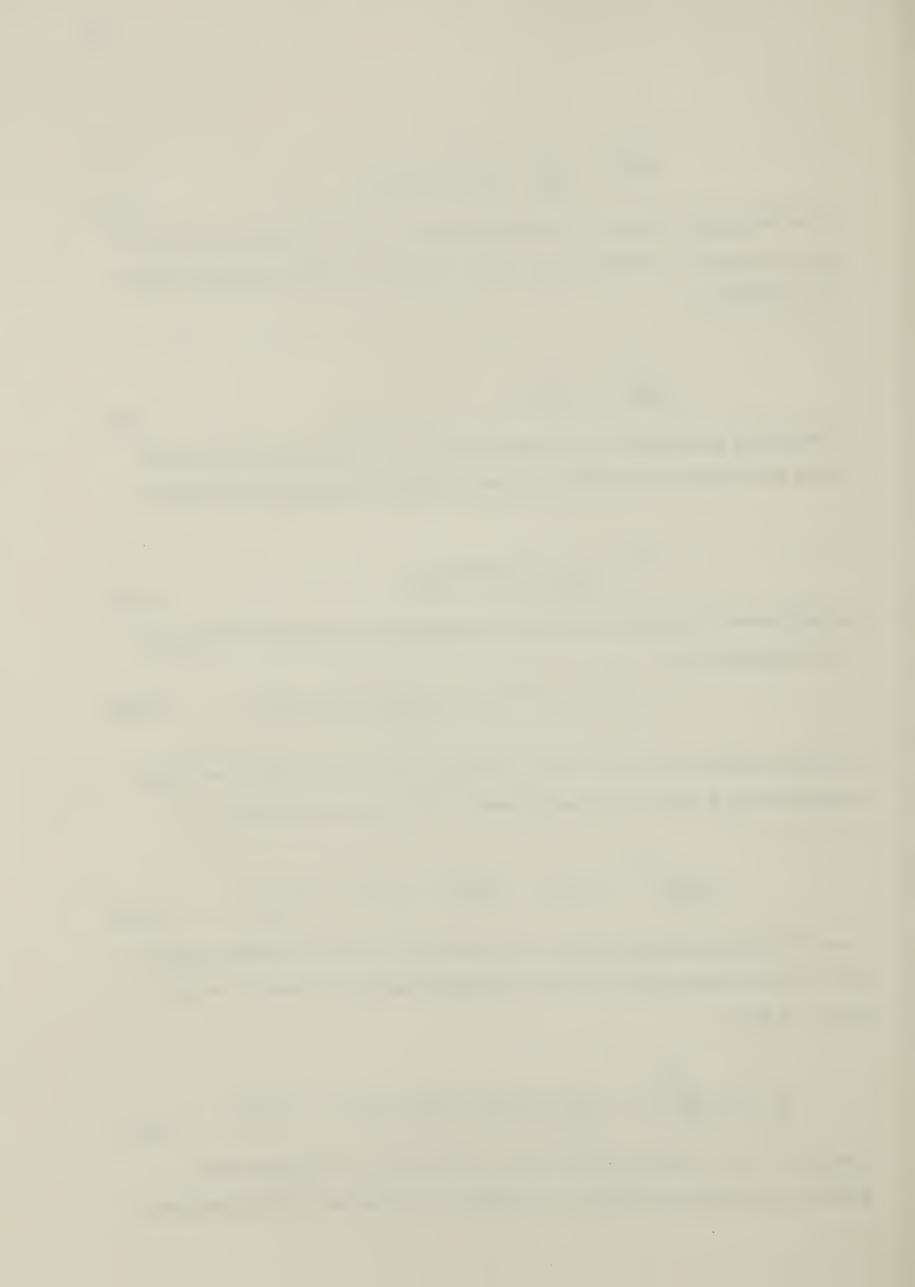
By using the velocity, and a first order expansion of $\vec{E}(\vec{r})$ in eq. (4.3.1) about the electron initial position $\vec{r}_0$, a second order approximation of the force is found to be

$$m_e\left(\frac{d\vec{v}}{dt}\right)^{(2)} = -e\left[(\delta\vec{r} \cdot \vec{\nabla})\vec{E}(\vec{r}_0) + \frac{1}{c}\vec{v}^{(1)} \times \vec{B}(\vec{r}_0)\right]$$

(4.3.6)

where $\vec{v}^2$ is a second order correction term to velocity $\vec{v}$. By taking the time average of eq. (4.3.6), and using eq. (4.3.3), (4.3.5),and (4.3.5a),the average non-linear force on an electron is thus

$$\vec{f}_{NL} = m_e\left<\frac{d\vec{v}^{(2)}}{dt}\right> = -\frac{e^2}{m_e\omega_0^2}\frac{1}{2}\left[(\vec{E}_s \cdot \vec{\nabla})\vec{E}_s + \vec{E}_s \times \vec{\nabla} \times \vec{E}_s\right]$$

(4.3.7)

The $\vec{E}_s \times \vec{\nabla} \times \vec{E}_s$ force component (which is equal to $\vec{E}_s \times \vec{k} \times \vec{E}_s$ upon Fourier transform) acts along the direction of propagation and causes both electrons and ions to

move along the direction of propagation, while the $(\vec{E}_s \cdot \vec{\nabla})\vec{E}_s$ denotes the force

component acting along the direction of the electric field vector. This force pushes the

plasma to bundle up in a direction perpendicular to the direction of propagation. As a

result, the formation of a low density region along the column is enhanced.(see footnote)

This causes a change in the refractive index which will cause the beam to be focused and

defocused as it propagates within the medium. Using the vector identity,

$$\frac{1}{2}\vec{E}_s = (\vec{E}_s \cdot \vec{\nabla})\vec{E}_s + \vec{E}_s \times \vec{\nabla} \times \vec{E}_s$$

the ponderomotive force per unit volume is given by Chen,

$$\vec{F}_{NL} = \frac{-\omega_{pe}^2}{\omega_0^2} \vec{\nabla}\left(\frac{E_s^2(\vec{r})}{16}\right) \tag{4.3.8}$$

where $\omega_{pe}^2 = \dfrac{4\pi N_0 e^2}{m_e}$ ; $m_e$ is the electron mass, $N_0$ is the plasma density. However,

the intensity of the radiation field is also given by

$$I = \frac{\eta c |E_A(\vec{r}_0)|^2}{8\pi} \tag{4.3.9}$$

where $\eta$ is the index of refraction of the medium.
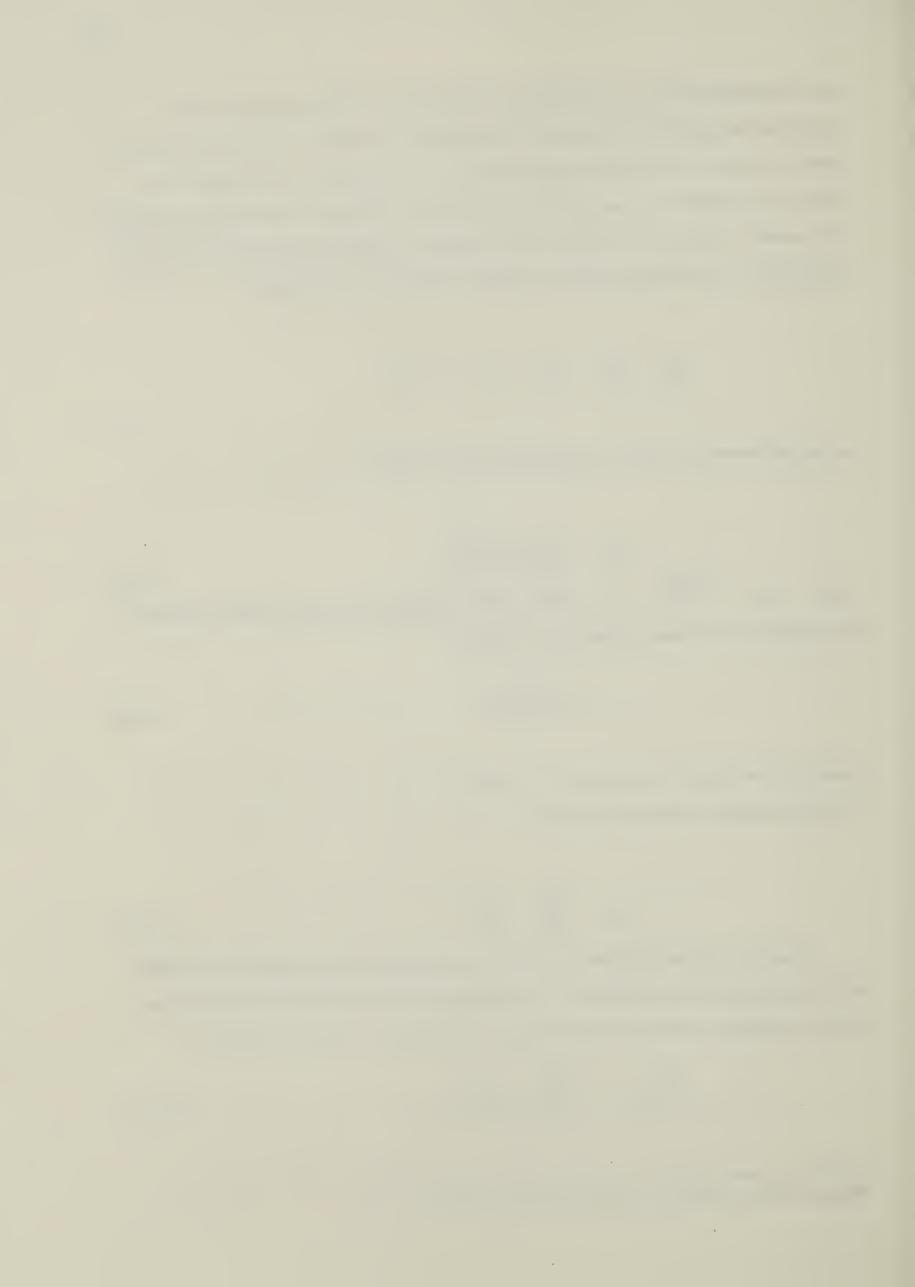
The ponderomotive force thus becomes

$$\vec{F}_{NL} = -\frac{\omega_{pe}^2}{2\omega_0^2} \vec{\nabla}\left(\frac{I}{nc}\right) \tag{4.3.10}$$

Due to cylindrical symmetry, there is no azimuthal intensity gradient for the beam

within the plasma. So only radial and axial components of the ponderomotive force have

to be considered. The relevant components, in cylindrical co-ordinate system, are

$$(\vec{F}_{NL})_r = -\frac{\omega_{pe}^2}{2\omega_0^2} \frac{\partial}{\partial r}\left(\frac{I}{nc}\right)\hat{r} \tag{4.3.11}$$

-------------------------

Plasma heating is the major factor for this formation.

$$(\vec{F}_{NL})_z = -\frac{\omega_{pe}^2}{2\omega_0^2} \frac{\partial}{\partial z}\left(\frac{I}{nc}\right)\hat{z}$$

(4.3.12)

where $\hat{r}$, $\hat{z}$ are unit vectors in radial and axial direction respectively. These force

components can be known once the spatial variation in the beam intensity is known.

# Chapter 5

## Computational method

Numerical treatment of the analytical results in chapters three and four are dealt with in this chapter. Program packages are designed for computing ray distributions, density gradients, ray paths within plasma medium, power absorption along the paths and ponderomotive forces. These packages are designed to replace the laser profile routine used in the magnetic flux shell code.

### 5.1 Ray distribution package

In this section, the distribution of locations and directions of the rays is deduced from the distribution function for a coherent gaussian beam. Ray locations and directions are distributed according to a Gaussian distribution function.

Beam propagation is simulated in terms of bundles of rays. From the discussion in section (4.1), rays can be either chosen to carry power which varies according to a Gaussian distribution or to carry equal power. For rays carrying different power,the locations and directions must be predetermined. However, for rays carrying equal power,the locations and directions are so chosen that the number of rays varies according to a Gaussian distribution function. This scheme is explained as follows.
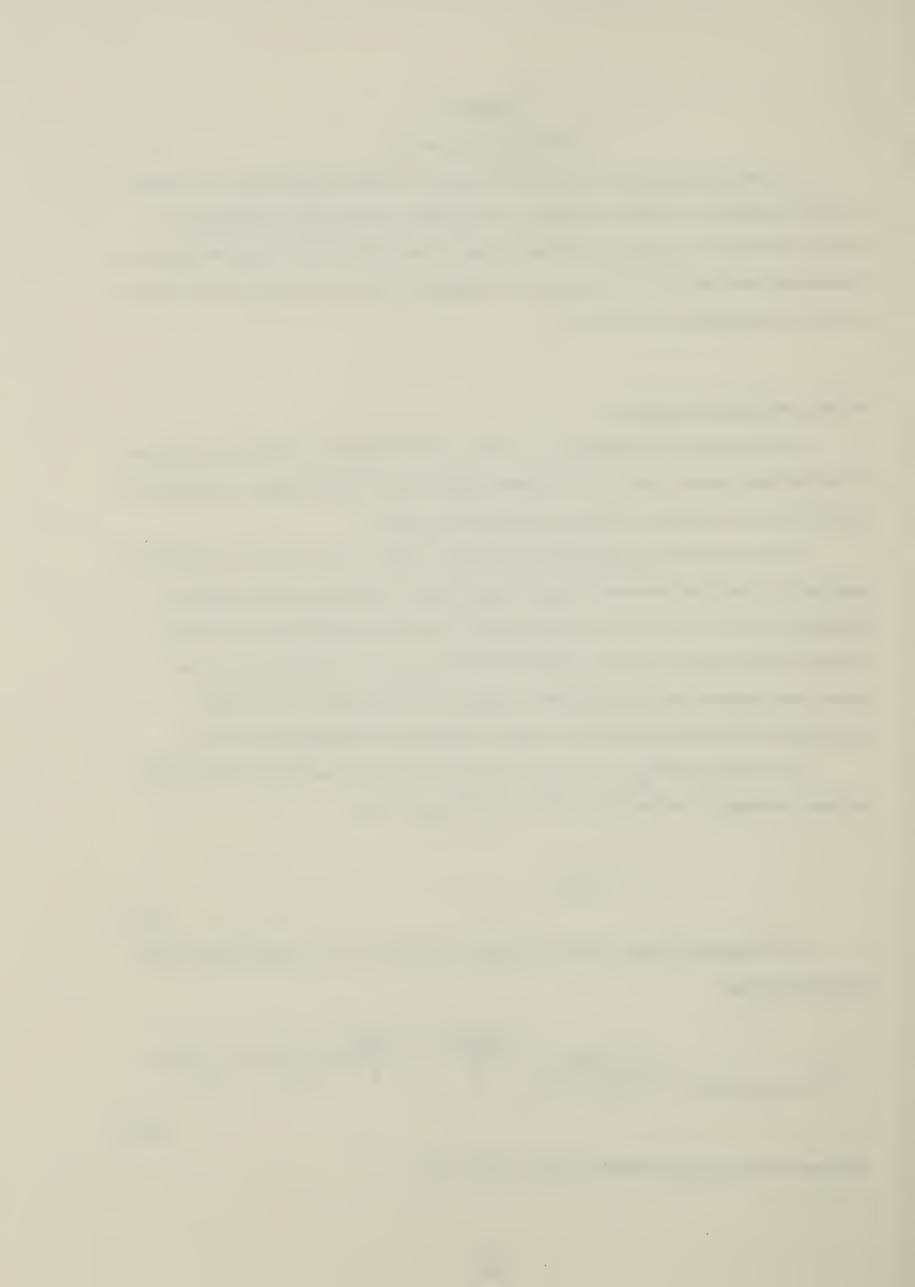
The initial power($P_{avg}$ ) for each ray is just the beam power($P_0$) at the lens plane at time t averaged over the total number of rays ($N_0$ ).That is,

$$P_0 = P_{avg}N_0$$

(5.1.1)

From Tappert's phase-space distribution function for an incoherent beam at the lens plane,namely,

$$f(x,y,u_x,u_y,z_1) = \frac{|E_0|^2 k^2 a_0^2 D^2}{2\pi} e^{\frac{-2(x^2+y^2)}{a_0^2}} e^{\frac{-k^2 a_0^2 D^2}{2}[(u_x+\frac{x}{f_L})^2+(u_y+\frac{y}{f_L})^2]}$$

(5.1.2)

the beam power density evaluated at the point (x,y) is

$$P(x,y) = \frac{c}{8\pi}\int_{-1}^{1}\int_{-1}^{1}\frac{|E_0|^2 k^2 D^2 a_0^2}{2\pi} e^{\frac{-2(x^2+y^2)}{a_0^2}} e^{\frac{-k^2 a_0^2 D^2}{2}[(u_x + \frac{x}{f_L})^2 + (u_y + \frac{y}{f_L})^2]} du_x du_y$$

(5.1.3)

If there are $N(x,y)dxdy$ rays passing through an infinitesimal area $dxdy$ at location $(x,y,z_1)$, the beam power can be expressed as

$$P(x,y)dxdy = P_{avg}N(x,y)dxdy$$

(5.1.4)

By comparing eqs.(5.1.3) and (5.1.4), the number density of rays passing through the point can be seen to be given by

$$N(x,y) = \frac{c|E_0|^2 k^2 D^2 a_0^2}{8\pi P_{avg}} e^{\frac{-2(x^2+y^2)}{a_0^2}} \int_{-1}^{1}\int_{-1}^{1} e^{\frac{-k^2 a_0^2 D^2}{2}[(u_x + \frac{x}{f_L})^2 + (u_y + \frac{y}{f_L})^2]} du_x du_y dxdy$$
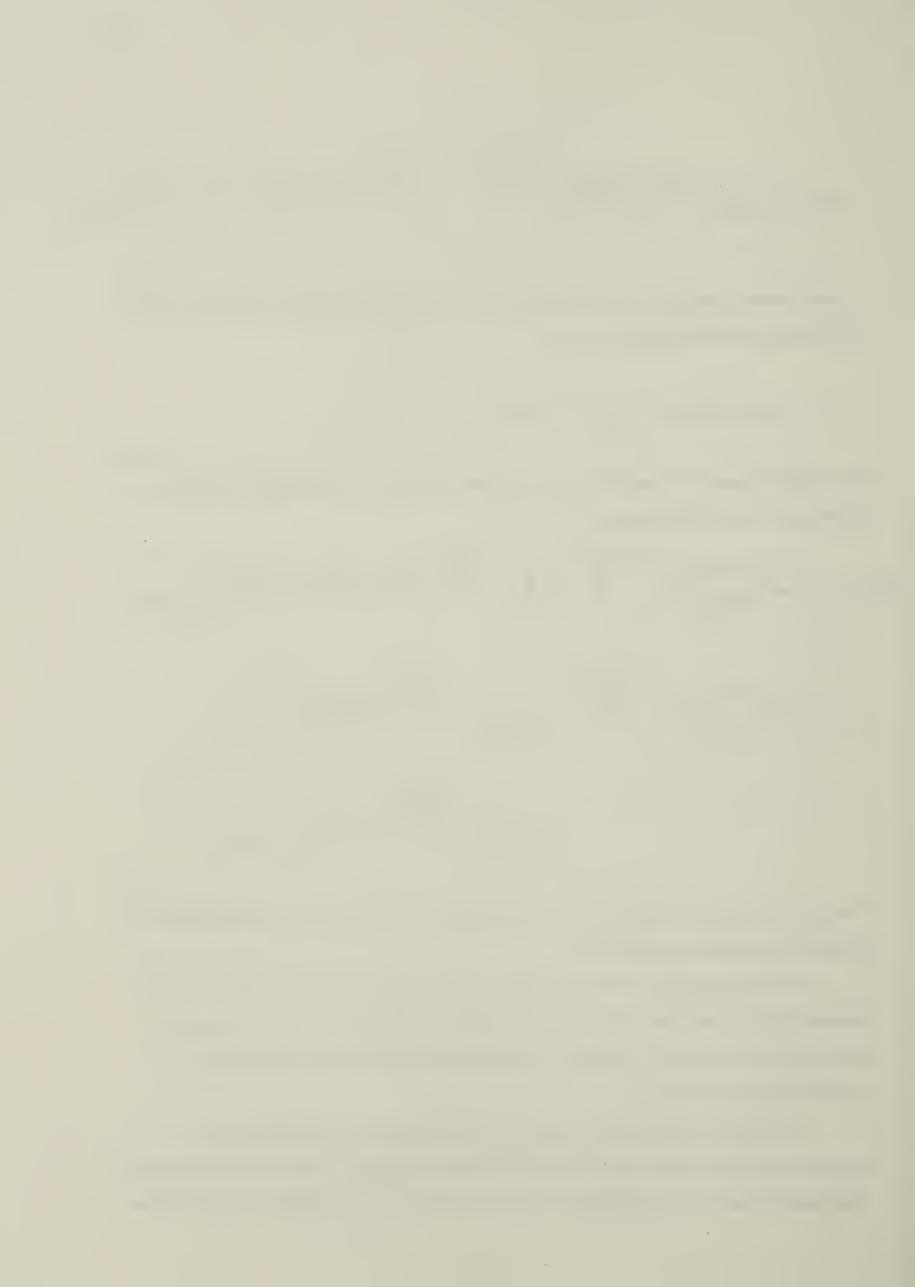
$$= \frac{c|E_0|^2 k^2 D^2 a_0^2}{8\pi P_{avg}} e^{\frac{-2(x^2+y^2)}{a_0^2}} [\int_{-1}^{1}\frac{1}{\sqrt{2\pi}} e^{\frac{-k^2 D^2 a_0^2}{2}(u_x + \frac{x}{f_L})^2} du_x$$

$$\times \int_{-1}^{1}\frac{1}{\sqrt{2\pi}} e^{\frac{-k^2 D^2 a_0^2}{2}(u_y + \frac{y}{f_L})^2} du_y] \, dx \, dy$$

(5.1.5)

The expression shows that the total number density of rays is distributed gaussianly with respect to locations and directions.

In actual simulation of the laser beam, a set of rays is chosen such that they are gaussianly distributed over the lens plane. Moreover, the directions of the rays are so selected that the number of rays will be gaussianly distributed about the direction pointing towards the focus.

Such choice is achieved by using a normal random deviate generator. The generator will generate numbers which are normally distributed. A set of such numbers is designated to each of the locations x, y and directions $u_x$, $u_y$. For the x, y locations, the

generated numbers are scaled according to the laser beam width to give actual spatial ray locations. For the directions, $u_x$, $u_y$, the generated numbers $n_x$, $n_y$ are transformed to the real ray directions through the relations

$$n_x = (u_x + \frac{x}{f_L})ka_0D$$

(5.1.6)

$$n_y = (u_y + \frac{y}{f_L})ka_0D$$

(5.1.7)

These relations are deduced from the cumulative normal distribution function used in the number generator, namely, (fig. 5.1)

$$P_R(t) = \int_{-\infty}^{t}\sqrt{\frac{1}{2\pi}}\ e^{\frac{-T^2}{2}}\ dT$$

(5.1.8)

From eq. (5.1.5), the range of values for $u_x$, $u_y$ in the integrands is between $(-1,1)$. A comparison of this function with the integrands over $u_x$, $u_y$ in eq. (5.1.5), shows that as long as the value of t is within the interval $(\pm 1 + \frac{x}{f_L})ka_0D$ (or $P_R(t)$ assumes values between A and B ), eqs. (5.1.6), (5.1.7) are valid.

Under this scheme, much flexibility is provided for the choice of rays. Since only a finite number of rays are used, a variable ray distribution will prevent a localization of heated regions within the plasma.

## 5.2 Solenoid grid package

In this section, the choice of grid structure used for defining ray positions is discussed.

In the plasma column, cylindrical symmetry is assumed. A two dimensional numerical grid in radial and axial direction is used. Since this package is designed for implementation in the shell MHD code, the chosen grid structure is the same as that used in that code. In the MHD code, the radial grid layers are made up of coaxial magnetic shells(Fig. 5.2).In this package, the radii of the shells are taken to be the same as the radii

$$F_R(T) = \frac{1}{\sqrt{2\pi}} \; e^{\frac{-T^2}{2}}$$

$$P_R(t) = \int_{-\infty}^{t} \frac{1}{\sqrt{2\pi}} \; e^{\frac{-T^2}{2}} \; dT$$

Area under the curve is A

Area under the curve is B
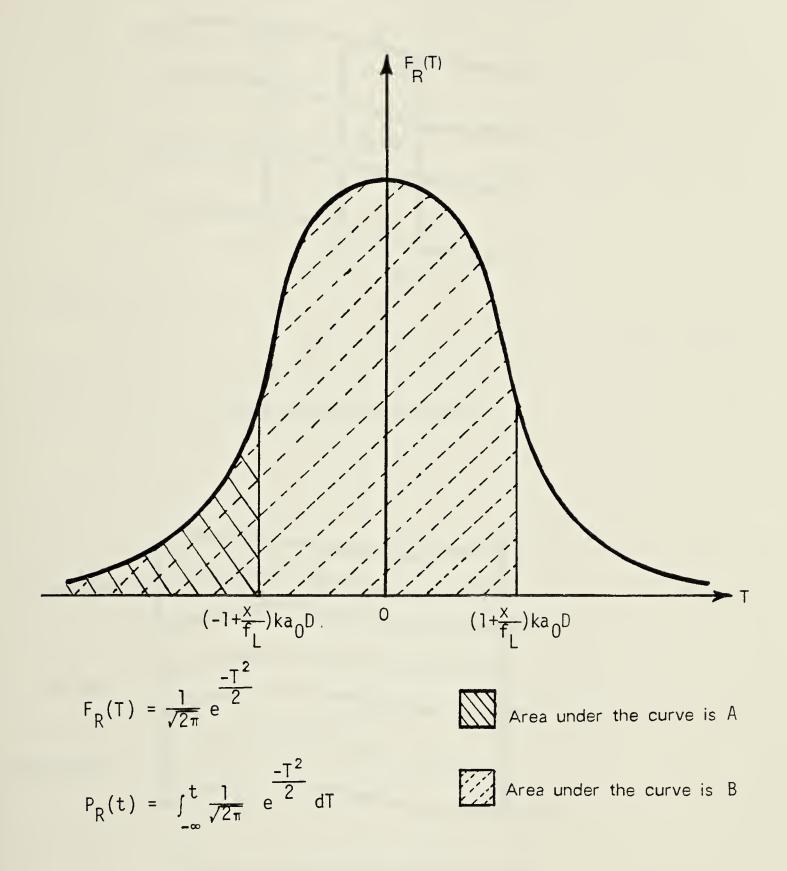
Figure 5.1 Cumulative gaussian distribution function.
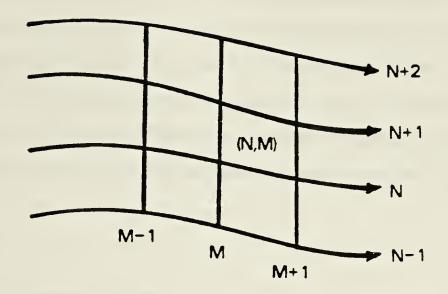
Figure 5.2 Spatial grid structure.
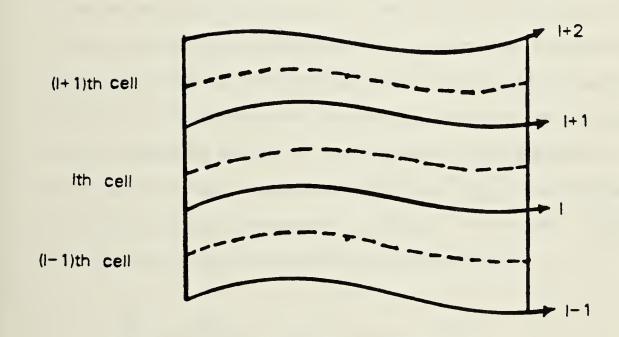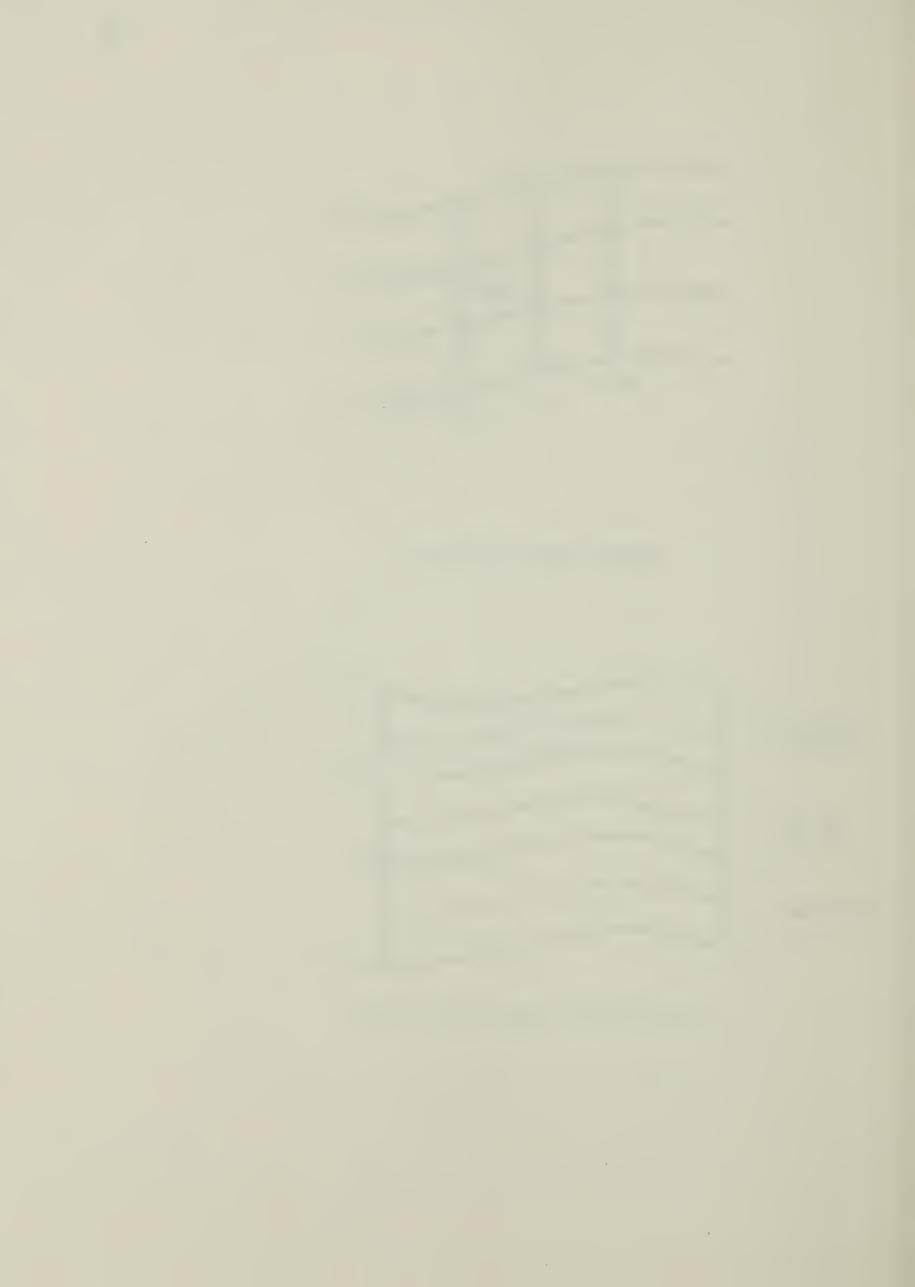


Figure 5.3 Density gradient between shells.

of the magnetic flux shells for the purpose of matching the plasma parameters in the MHD code. Each shell is divided into two subshells so that density gradients can be evaluated in each half of the shell. In the $I^{TH}$ shell, the density gradient in the outer half shell is different from that in the inner half shell due to different values for calculating the gradient. The density gradient in the outer half shell is determined by the difference in densities in the $I^{TH}$ and $(I+1)^{TH}$ shell layer, while the density gradient within the inner half shell is obtained from the difference between densities in the $I^{TH}$ and $(I-1)^{TH}$ shell (fig. 5.3).

## 5.3 Density gradient package

In this section, the fitting of density profiles between any two adjacent grid cells is discussed. By calculating the density gradient changes between grid cells which are radially adjacent to each other, the appropriate profiles can be chosen correspondingly.

From the MHD code, values of plasma density are obtained for the center of each grid cell(see footnote). The radial density gradient between two adjacent cells located at radial distances $r_1$, $r_2$ from the axis is determined from the plasma densities $N_1$, $N_2$ in these two cells. Once the density gradient of the plasma in a certain region is known, the appropriate density profile can be chosen correspondingly, the solution of the ray equation for this chosen profile can be used to describe the propagation of a ray. In order to determine the proper density profile, the first and second derivative of the density with respect to radial distance, $\frac{dN(r)}{dr}$, $\frac{d^2N(r)}{dr^2}$ are calculated since the choice of profiles is based on the conditions $\frac{dN(r)}{dr} > 0$ or $< 0$ and $\frac{d^2N(r)}{dr^2} > 0$ or $< 0$. The corresponding profiles are listed as follows:(see fig.3.1)

(1)     $\frac{dN}{dr} > 0, \quad \frac{d^2N}{dr^2} > 0, \quad N(r) = N_0(1 + \frac{r^2}{a_0^2})$

(2)     $\frac{dN}{dr} > 0, \quad \frac{d^2N}{dr^2} < 0, \quad N(r) = N_1(1 - \frac{a_1^2}{r^2})$

---------------------

A cell is bounded by two radial and two axial magnetic shell boundaries.

(3) $\qquad \dfrac{dN}{dr} < 0, \quad \dfrac{d^2 N}{dr^2} > 0, \quad N(r) = N_2 \left(1 - \dfrac{r^2}{a_2^2}\right)$

(4) $\qquad \dfrac{dN}{dr} < 0, \quad \dfrac{d^2 N}{dr^2} < 0, \quad N(r) = N_3 \left(1 + \dfrac{a_3^2}{r^2}\right)$

The parameters $N_i$, $a_i$ , i=0,1,2,3,can be evaluated by knowing the densities in any two radially adjacent cells(with known radii).

The density curve fitting method, however, does not give a good approximation for the density values at regions where there is a transition from one density profile to another. As shown in figure 5.4, the kind of curve used to approximate the density variation between $r_1$,$r_2$ can be $N_0(1+r^2/a_0^2)$ or $N_0(1-a_0^2/r^2)$;similarly in regions between radii $r_3$ and $r_4$,profiles $N_2(1-r^2/a_2^2)$ or $N_3(1+a_3^2/r^2)$ can be used. For these regions, profiles used in the shell lying next to this region (in the first case, shell with radius less than $r_1$ , in the second case, shell with radius less than $r_2$) are chosen as the fitting profiles.
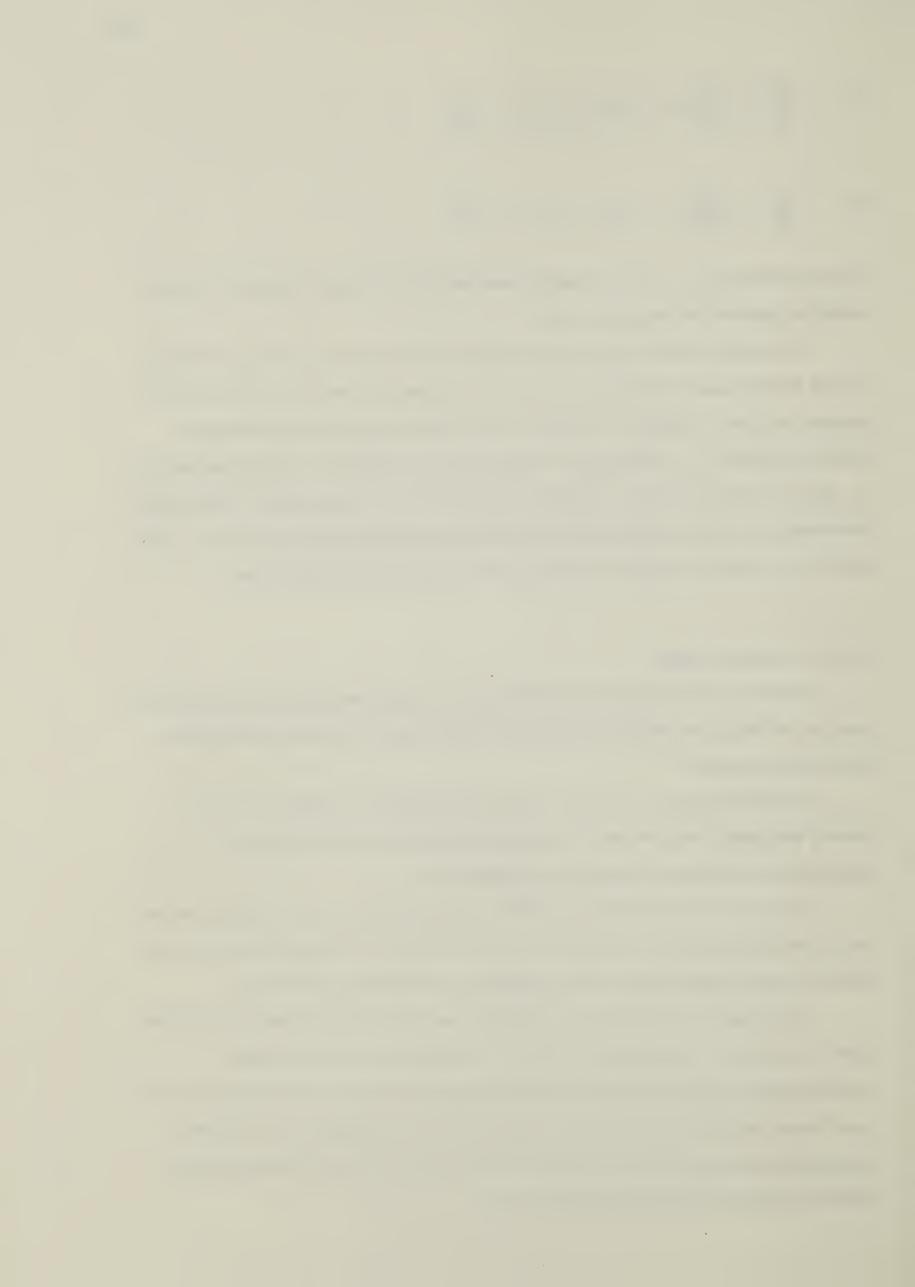
## 5.4 Ray tracing package

In this section, methods of tracing the rays through the plasma are discussed. Ray locations at the grid boundaries are computed. Rays staying in the innermost shell are specifically discussed.

This package gives a routine of tracing rays through the plasma column by locating the points which the rays intersect with the cell boundaries. Moreover, absorption coefficient are calculated within each cell.

As soon as the rays reach the column, their radial locations are tracked down to the corresponding grid cell. Knowing which cell the ray hits, its subsequent path can be traced through the application of the ray equation as discussed in section 3.1.

Within each cell, the density is assumed to vary according to one of the profiles given in section 3.1. The subsequent ray path will be governed by the solution corresponding to that particular profile. Ray locations are evaluated at the points where rays intersect with the cell boundaries. At each such intersecting point, the velocity components are evaluated so as to give the initial conditions for the ray entering into another region with a different refractive index.
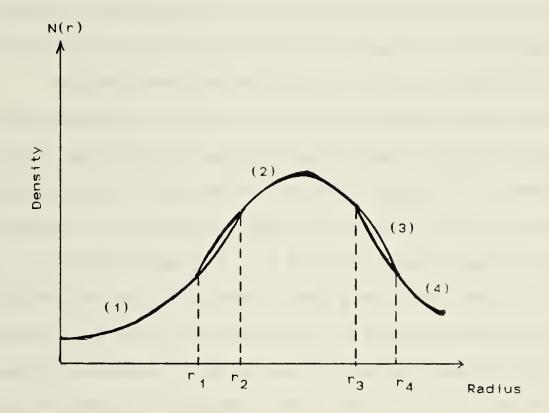
Figure 5.4 Density profile approximation used in various region.

As the initial and final locations of a ray within a cell are known, the associated absorption coefficient can be found from eq. (4.2.2),

$$\int_0^{\Delta s} dK = \int_0^{\Delta s} K_a ds = \int_0^{\Delta t} K_a n(r(t))cdt$$

(5.4.1)

where $K_a$ is the absorption coefficient per unit length; $\Delta t$ is the time for the ray to traverse from the initial position to the final position(or a distance of $\Delta s$).
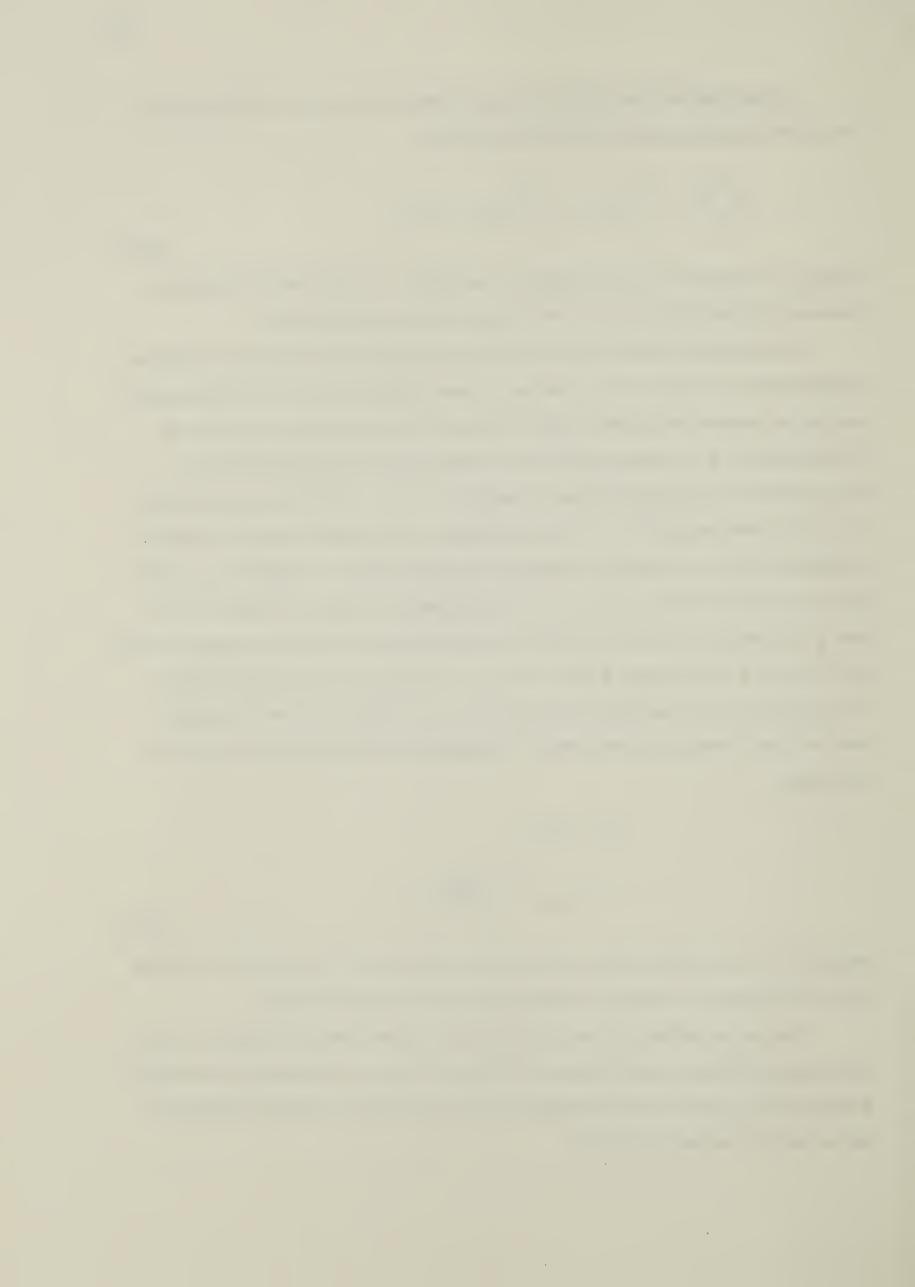
As can be seen from the solutions of the ray equation for different profiles, the radial positions of a ray is a direct function of time. Knowing the time of traverse over a cell, the ray location can be determined. In order to find the traversing time, the final radial position of a ray is taken to be the cell radius(fig. 5.5). Corresponding time is calculated from the equations derived in section 3.1. The ray advances an axial distance of $v_z \Delta t$ in a time interval of $\Delta t$. If this axial distance is less than an axial grid interval, it indicates that the ray will cross the radial grid boundary before it crosses the axial grid boundary (fig. 5.4). On the other hand, if the calculated axial distance is larger than the axial grid separation, the ray will cross the axial grid boundary before it crosses the radial one. The time is then changed to that for the ray to travel over one axial grid distance. The radial distance corresponding to this time can be evaluated from the ray solution. Axial and radial distances are thus known. The angular position can also be found from the equation

$$r^2 \dot{\theta} = r_0^2 \dot{\theta}_0$$

$$\theta = \theta_0 + \int_0^{\Delta t} \frac{r_0^2 \dot{\theta}_0}{r^2} dt$$

(5.4.2)

where $r_0, \dot{\theta}_0$ are the initial radial ray location and angular velocity respectively. The three spatial co-ordinates of a point on a trajectory can be completely defined.

When a ray reaches the inner most shell, the ray path remains straight since there is no change in refractive index within the core and the ray is not refracted. Ray locations at the boundary points and at the closest point to the axis have to be found differently. The ray path is illustrated in fig. 5.6.
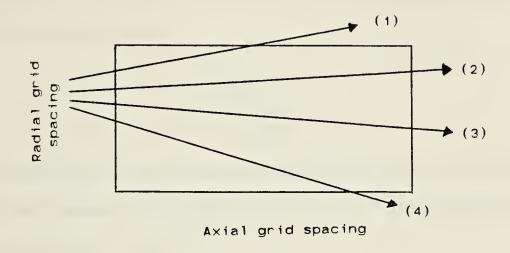
Figure 5.5 Intersection points of rays with cell boundaries.
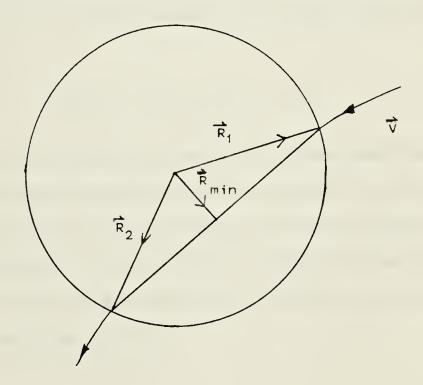


Figure 5.6 Ray path in the central core of the plasma column.

It should also be noticed that the radial velocity component is taken to be negative if the ray travels towards the axis, otherwise positive. The absorption path for calculating the absorption coefficient is the magnitude of the ray segment between the initial and final ray locations within a cell. The time taken for a ray to traverse from one side of the core boundary to another side is

$$t = \frac{-2\vec{R}_1 \cdot \vec{v}}{|\vec{v}|^2}$$

(5.4.3)

where $\vec{R}_1$ is the radial position of the ray at the shell boundary; $\vec{v}$ is the velocity within the core and at the boundary. The time taken for a ray to traverse from the boundary to a point which is closest to the axis is

$$t_{min.dist.} = \frac{-\vec{R}_1 \cdot \vec{v}}{|v|^2}$$

(5.4.4)

With this time and the velocity at the boundary of the core, locations of the closest point can be determined as

$$\vec{R}_{min} = \vec{v} \, t_{min.dist.} + \vec{R}_1$$

(5.4.5)

Depending on the velocity components of a ray, there are three types of rays. Rays with a non-zero angular velocity will spiral in a trajectory forming a helix around the axis of propagation and approach a position close to the axis but never through it because of the finite angular momentum of the ray. Rays without an angular velocity component, will go through the axis. Finally, rays that have only a non zero axial velocity component will propagate along the axis.

## 5.5 Absorption package

This package calculates the power absorption along a ray. Power exchanges are only encountered in those cells through which rays pass.

Power absorption in the $I^{TH}$ cell can be calculated from eq. (4.2.7), namely,

$$\Delta P_{abs} = P_i(r_0, t_0)[\, 1 - e^{-\int_0^{\Delta t_i} K_a n(r(t))cdt}\, ] \tag{5.5.1}$$

where $P_i(r_0, t_0)$ denotes the power carried by the ray before it traverses the $I^{TH}$ cell; $t_0$ is the time at which the ray advances to the $I^{TH}$ cell; $r_0(t_0)$ is the radial position of the ray before it enters the $I^{TH}$ cell; $\Delta t_i$ is the time taken to traverse through the cell.
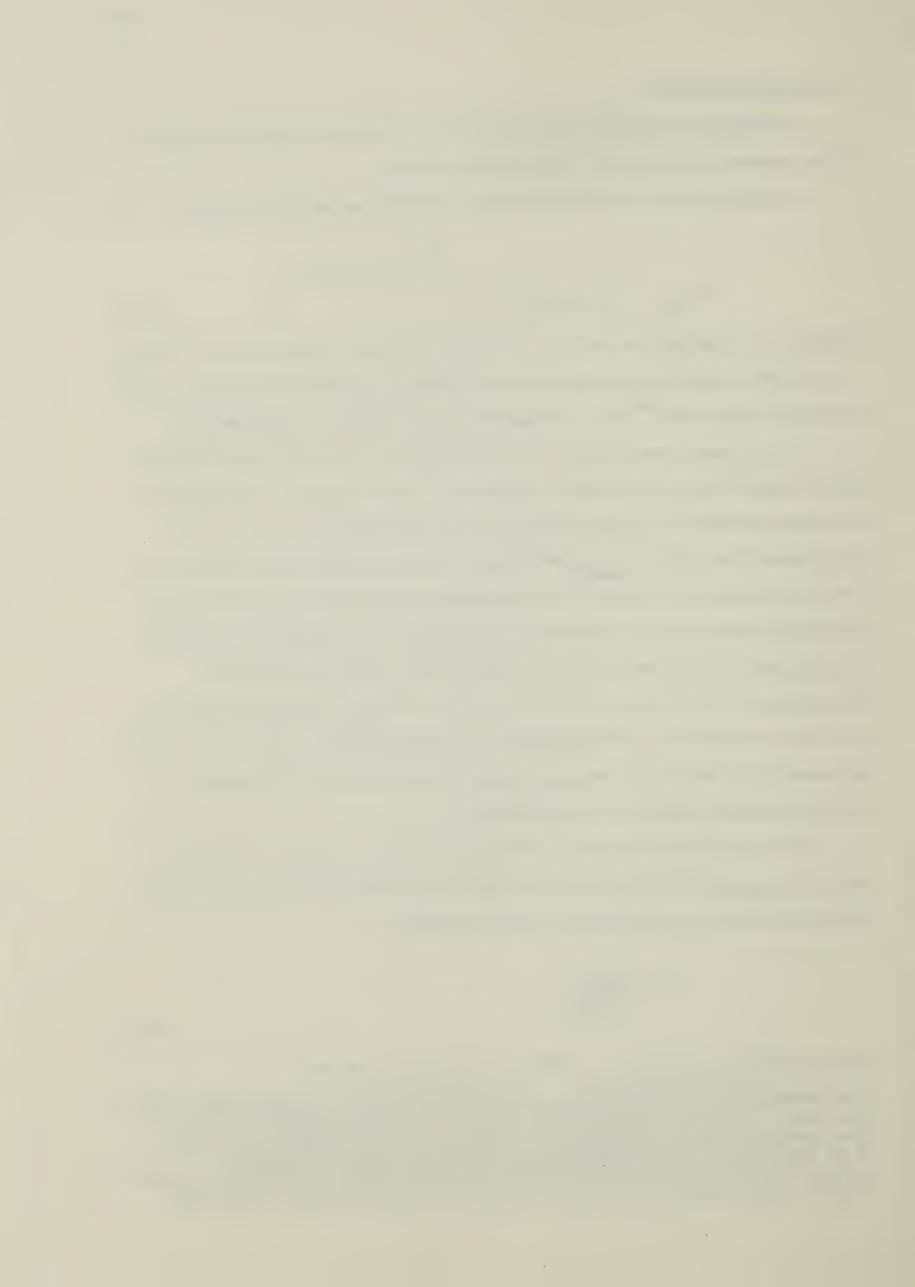
The temporal power profile of the laser beam follows the one used in the MHD code. It is approximated as straight line segments as shown in fig. 5.7. In the MHD code, the temporal change of the plasma behaviour is calculated at discrete time values(or hydrodynamic time steps, $\Delta t_{MHD}$)(see footnote). Power is assumed to remain constant within a hydrodynamic time step. It is only changed when the hydrodynamic time steps are altered. This assumption is valid as long as the size of a time step is much less than the pulse width. For the case of a short solenoid (5cm in length,ion and electron temperature of 1eV), the step size is in the order of $10^{-3}$ sec. and the pulse width is in the order of $10^{-6}$ sec. Thus, the assumption is a reasonable approximation. As the plasma becomes hotter, the step size even gets smaller since the particles become more energetic and their velocities thus become higher.

The advancement of the beam is simulated in terms of a number of beam time steps, $\Delta t_{LASER}$ which is the time for the beam to propagate over one cell. Within one hydrodynamic time step, the number of beam time steps is

$$M = \frac{\Delta t_{MHD}}{\Delta t_{LASER}} \tag{5.5.2}$$

The beam advances over one cell spacing for every beam time step.

--------------------

The hydrodynamic time step($\Delta t_{MHD}$) is the time interval within which the plasma is taken to be stable. This time is bounded by the time for the plasma fluid element to traverse over a grid cell radially or axially. Namely, $\Delta t_{MHD}= \Delta R/v_{ma}$ or $\Delta t_{MHD}= \Delta x/v_s$ where $\Delta R, \Delta x$ are the radial and axial grid size; $v_{ma}$ is the magneto-acoustic velocity, $(v_s^2+v_A^2)/(1+v_A^2/c^2)$; $v_A$ is the Alfven velocity, $B^2/\sqrt{4\pi N_{ion} m_{ion}}$ ; $v_s$ is the sound velocity, $\sqrt{T_e/m_e}$. In actual runs, the time step is adjusted to be less than 50% of these limits.
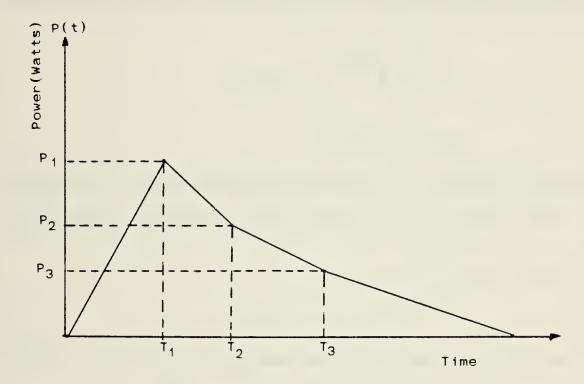
Figure 5.7 Temporal power profile of the laser beam.

The absorbed energy in a cell can be calculated as follows. The initial energy carried by a ray in any hydrodynamic time step is

$$E_{MHD} = \Delta t_{MHD} \times P_{MHD}$$

(5.5.3)

where $P_{MHD}$ is the laser power of the ray in a particular MHD step. Having this energy divided among the M beam time steps, the initial energy which the ray carries is

$$E_{LASER} = \frac{\Delta t_{MHD} \times P_{MHD}}{M}$$

$$= \Delta t_{LASER} \times P_{MHD}$$

(5.5.4)

This amount of energy will be the input energy for each laser time step. The energy deposited in an individual cell will be governed by an equation similar to eq. (5.5.1), that is,

$$E_{abs} = E_i [ 1 - e^{-\int_0^{\Delta t} K_a n(r(t)) c dt} ]$$

(5.5.5)

where $E_i$ is the energy associated with the ray before it enters into the $i^{TH}$ cell and is equal to $E_{i-1} e^{-\int_0^{\Delta t} K_a n(r(t)) c dt}$. The total amount of energy absorbed in a cell will be the sum of all the absorbed energy contributed from each ray passing through the cell.
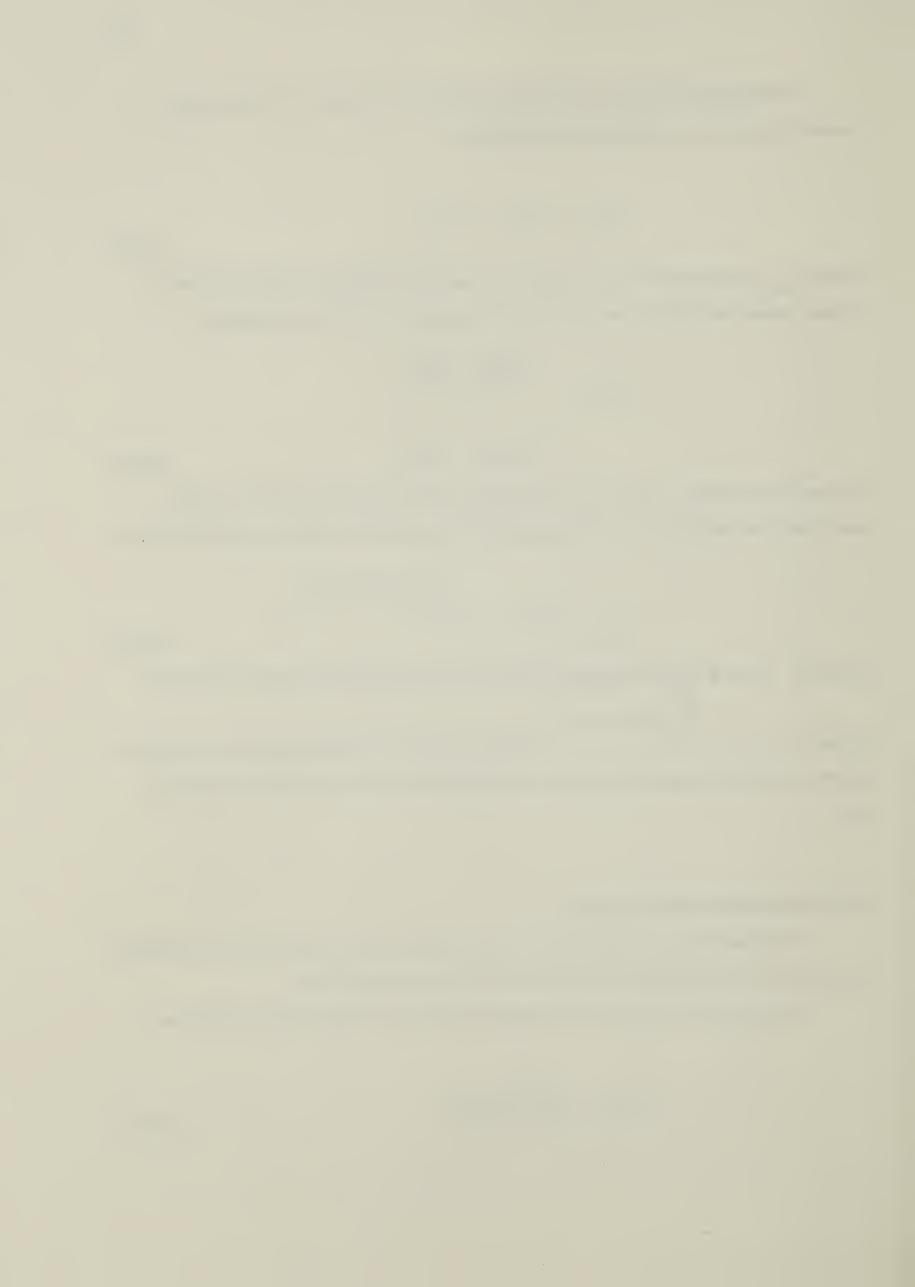
## 5.6 Ponderomotive force package

In this section, the ponderomotive force in each cell through which the ray passes is computed from the energy intensity gradient across the grid cells.

From eq. (4.3.11), (4.3.12), the radial and axial force components are given as

$$(F_{NL})_r = \frac{-\omega_{pe}^2}{2\omega_0^2} \frac{\partial}{\partial r}(\frac{I}{nc})$$

(4.3.11)

$$(F_{NL})_z = \frac{-\omega_{pe}^2}{2\omega_0^2} \frac{\partial}{\partial z}(\frac{I}{nc})$$

(4.3.12)

Through using finite difference scheme, the force components in the cell labelled with grid co-ordinates (N,M) are

$$(F_{NL})_r = \frac{-\omega_{pe}^2}{2\omega_0^2} \frac{I_{Upper} - I_{Low}}{R_{N+1} - R_N} \frac{1}{\eta_{N,M}c}$$

(5.6.1)

$$(F_{NL})_z = \frac{-\omega_{pe}^2}{2\omega_0^2} \frac{I_{Right} - I_{Left}}{Z_{M+1} - Z_M} \frac{1}{\eta_{N,M}c}$$

(5.6.2)

where $I_{UPPER}, I_{LOW}, I_{RIGHT}, I_{LEFT}$ are radiation intensities at the cell boundaries located at radial distances $R_{N+1}, R_N$, and axial distances $Z_{M+1}, Z_M$, respectively; $\eta_{N,M}$ is the refractive index in cell located at grid position (N,M) (fig. 5.1).

The intensities at the cell boundaries are taken to be the averages of the cell centre values of two adjacent cells. Thus, for cases of $I_{UPPER}$ and $I_{LOW}$, they are given as

$$I_{Upper} = \frac{1}{2} ( I_{N+1,M} + I_{N,M})$$

$$I_{Left} = \frac{1}{2} ( I_{N,M} + I_{N,M+1})$$

(5.6.3)

where N,M are subscripts referred to the corresponding grid cell.

For cells located at the plasma boundary, they are not completely surrounded by other cells. At the outermost radial boundaries, the intensities are taken as half the value at the centre. At both ends of the column, the intensities at the outermost boundary are taken to be that of the beam.

# Chapter 6

## Computational results
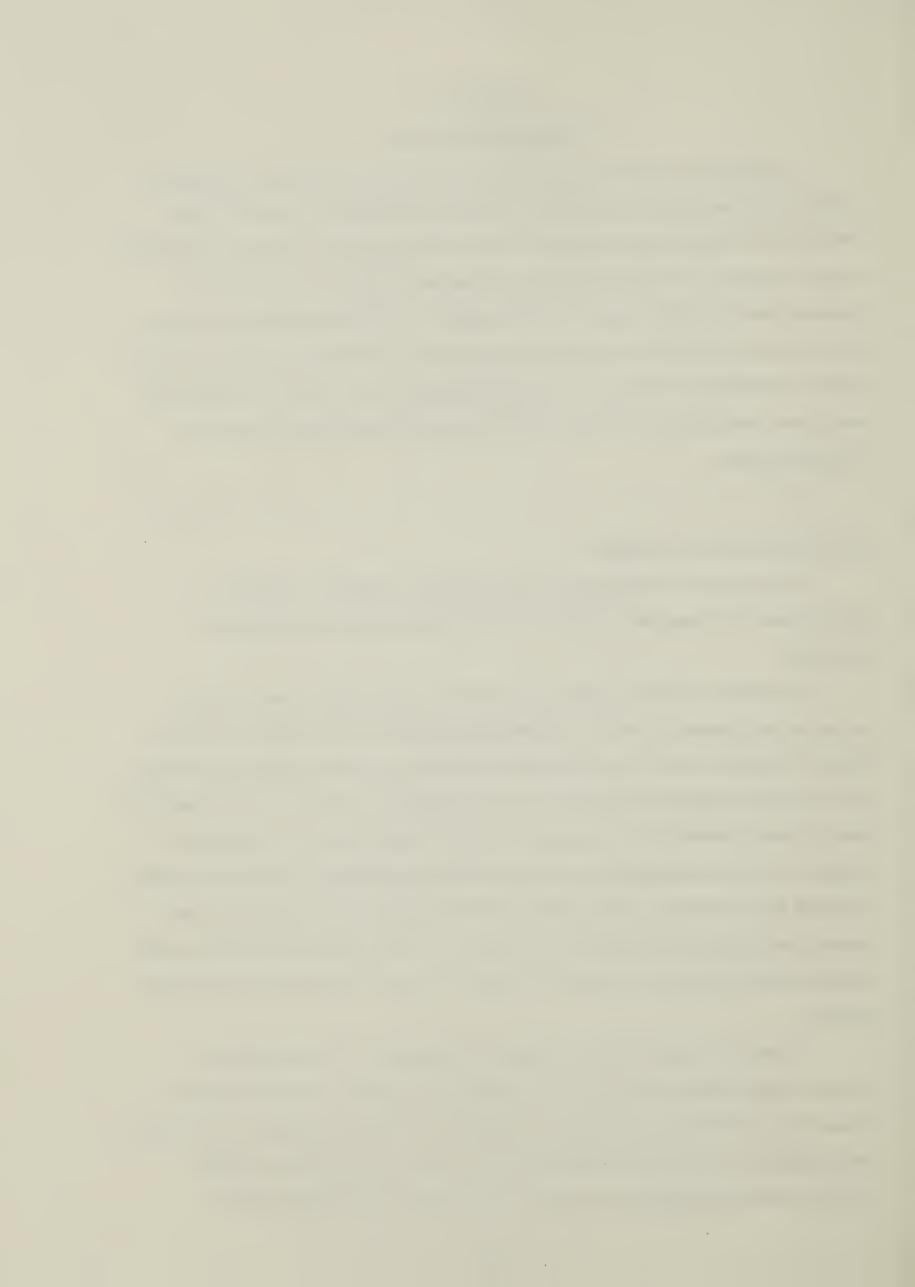
In section 6.1, plots for ray trajectories in a vacuum, and plots for the spatial distribution of ray locations and energy are given and discussed. In section 6.2, the simulation of a typical plasma density profile from the data obtained from the shell MHD code is discussed. Ray trajectories are computed within a plasma column for the assumed density profile in section 6.3. The behaviour of the rays within the medium is also discussed. In section 6.4, the energy distribution in the plasma is presented in terms of the ray distribution at various axial positions along the column. Finally, the absorbed energy and ponderomotive forces within the plasma are illustrated with the three dimensional plots.

### 6.1 Ray propagation in vacuum

In this section, trajectories of rays propagating in vacuum , the spatial distributions of the rays and the radial variation of beam power are plotted and discussed.

A sample of 100 rays is used to simulate the beam. Beam power is divided equally among the rays. A lens of 5cm(radius) aperture and a focal length of 150cm is chosen. Transverse locations and directions of the rays at the lens plane are determined from a random Gaussian distribution function as explained in section 5.1. The locations of the rays along the direction of propagation are determined from eq. (2.1.26) given in chapter two. The ray trajectories in vacuum are shown graphically in fig. 6.1 from which it is clear that the density of rays is higher in the axial region. Such a ray distribution results from a Gaussian choice of the intensity profile for the beam. The nonzero radial position of the rays at the focus(shown in Fig. 6.1) is due to the inclusion of diffraction effects.

A plot of the square of the average radial distance of all rays is given as a function of axial distance in fig. 6.2. The trajectory shows axial symmetry about the focus. In fig. 6.3, there is a minimum for the square of the half power beam radius at the focal distance. The half power beam radius at the focus is calculated to be $4.88 \times 10^{-3}$cm. This finite beam size is a result of the inclusion of diffraction effects.
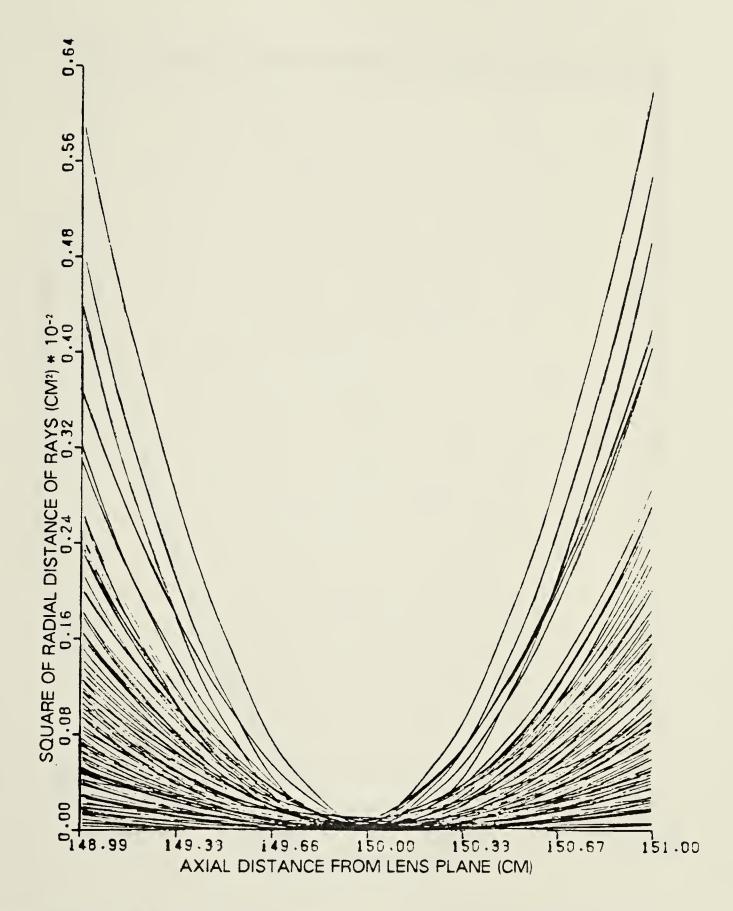
Figure 6.1 Variation of the square of radial position of the trajectories along the axis of propagation.
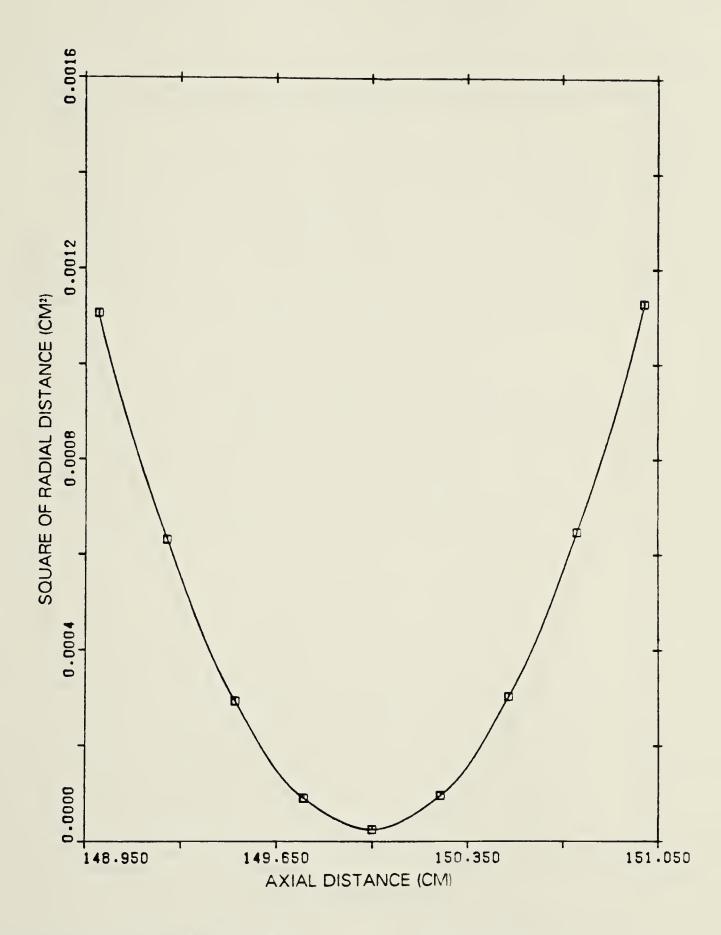
Figure 6.2 Square of the average radial ray position with incoherence factor=0.5.
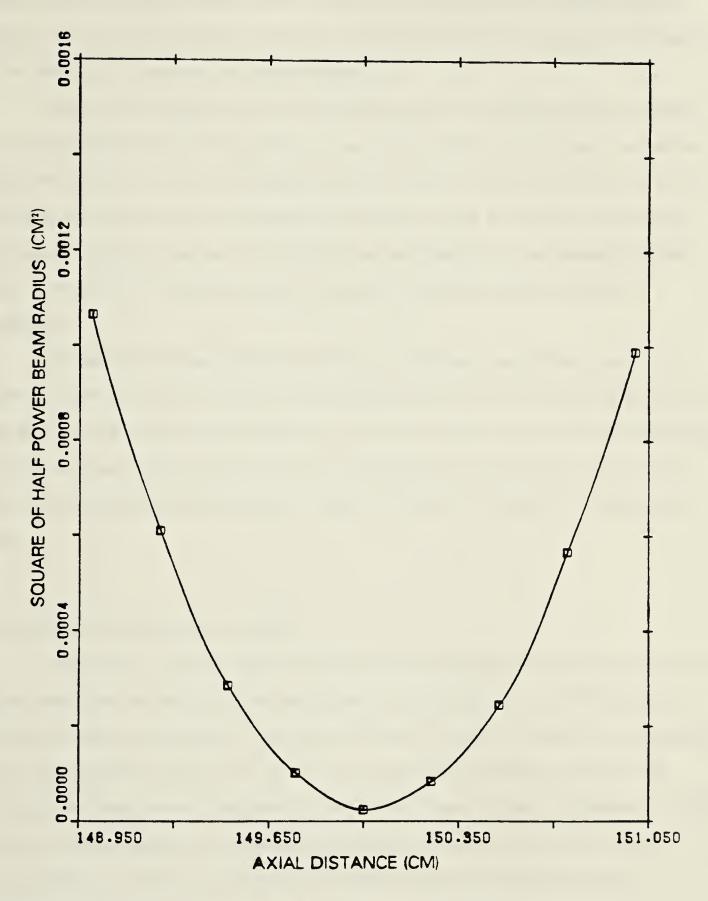
Figure 6.3 Square of the half power radial ray position around focal spot with incoherence factor=1.0.
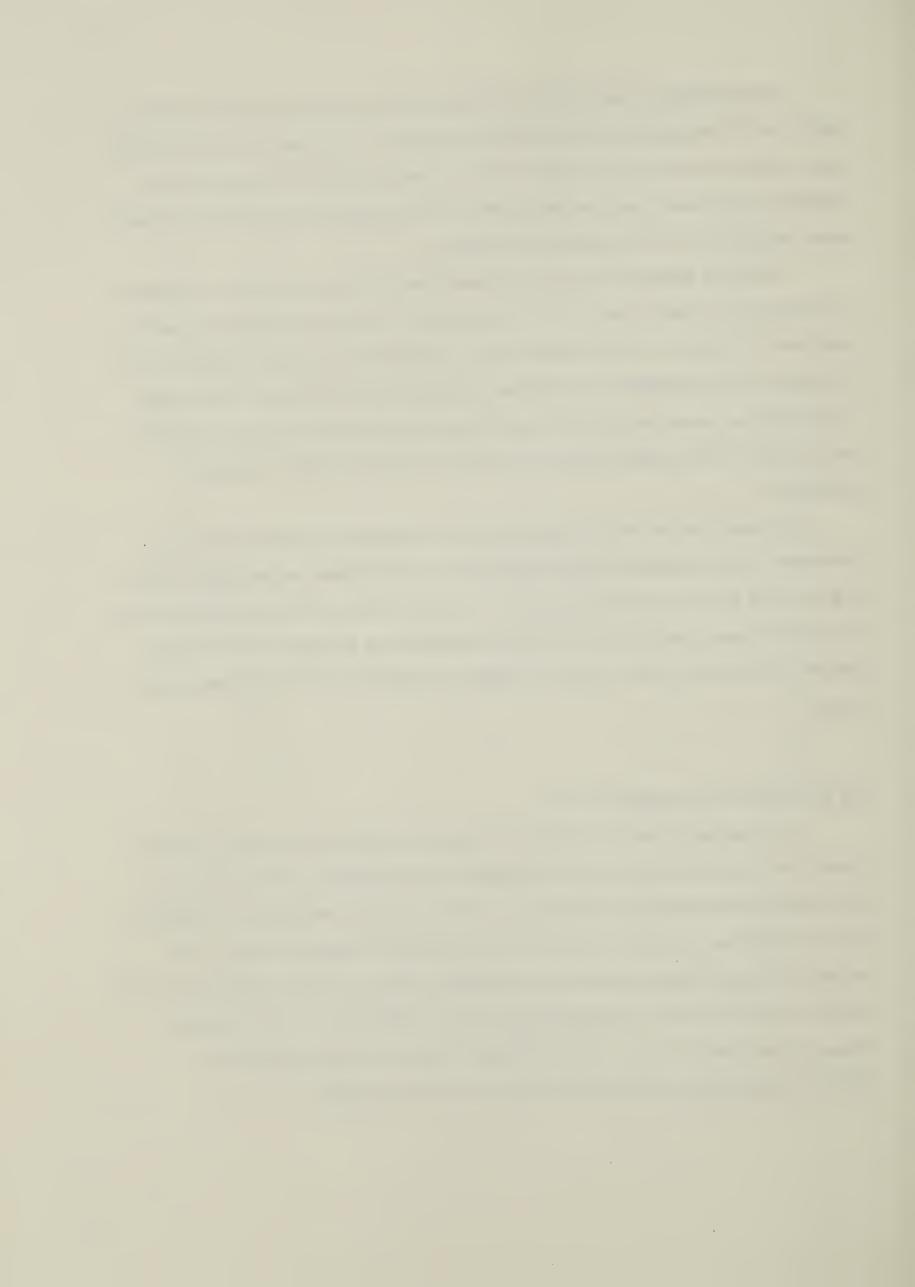
The distribution of ray locations at the lens plane and the focal plane are shown in figs. 6.4 and 6.5 respectively. According to the diagrams, the spread of rays at the focal plane is shown to have a similar pattern as that at the lens plane. This implies that the locations of rays have a Gaussian distribution at the focal plane. An analysis on the radial power distribution confirms the above conclusion.

The power distribution profile at the lens plane and the focal plane are obtained by counting the number of rays within a circular area of radius r. Since each ray carries equal units of power, the total number of rays represent the total units of power within the region. This is presented as cumulative histograms in figs. 6.6 and 6.7. The average deviation of the power values from those calculated directly from a Gaussian intensity profile is about 0.3%, indicating that the rays at the focal plane follow a Gaussian distribution.

The square of the average radial distance of the rays around the focus for an incoherent beam (incoherence factor=0.5) is shown in fig. 6.8 and the half power radius is given in fig. 6.9. The spotsize (radius 9.77 x $10^{-3}$cm.) is about twice as much as that for the coherent beam case. A plot of the power distribution is also given in fig. 6.10. The degree of incoherence can be used as a means for altering the size of the beam at the focus.

## 6.2 Simulation of the density profile

In this section, a plasma density profile used for testing the ray tracing routine is constructed from the density values computed from McMullin et. al.'s MHD code for a short laser heated solenoid(5cm. in length and 1.5cm. in radius). The plasma is assumed to have an initial density of 2.0 x $10^{18}$ cm$^{-3}$ and is confined by a magnetic field of 100 kilogauss. The laser power is assumed to rise linearly from 0 at t=0 to 100MW at t=10ns and then remains constant. A typical density profile is constructed from the density values computed at time 1.2 x $10^{-7}$sec. The density values at an axial distance of 0.917cm. from the laser entry end are listed in the following table:
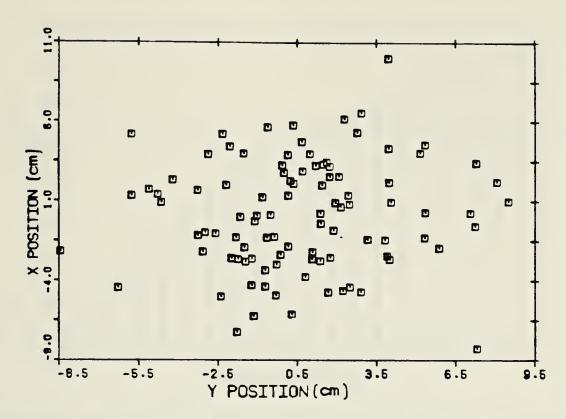
Figure 6.4 Distribution of rays at the lens plane (100 rays)
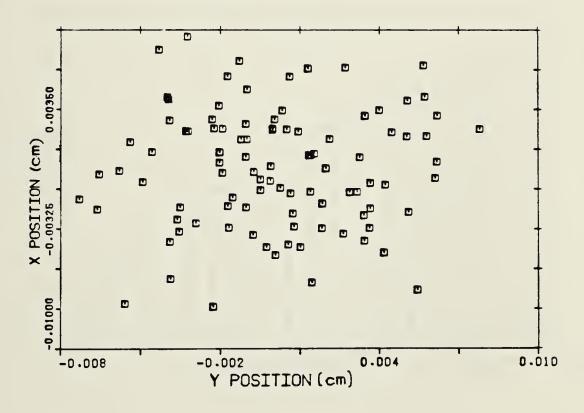


Figure 6.5 Distribution of rays at the focal plane (100 rays).
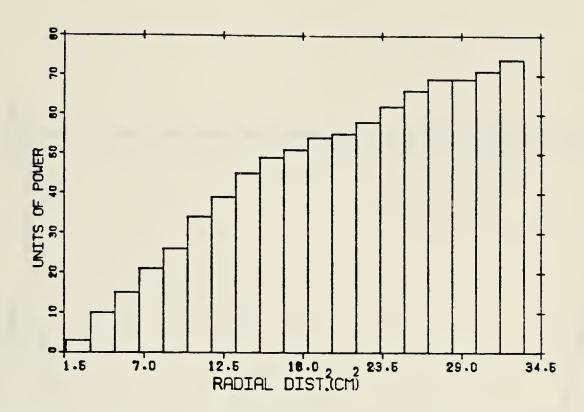
Figure 6.6 Power distribution for beam with incoherence factor=1.0 at the lens plane
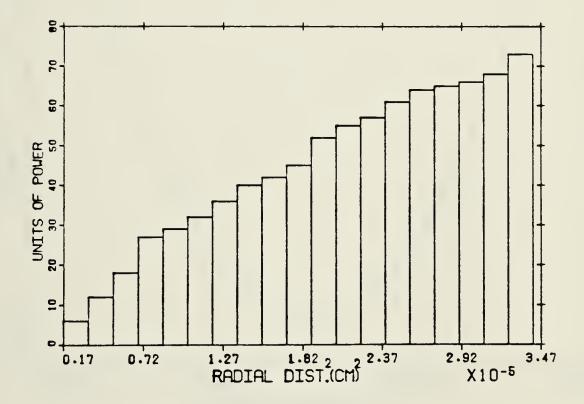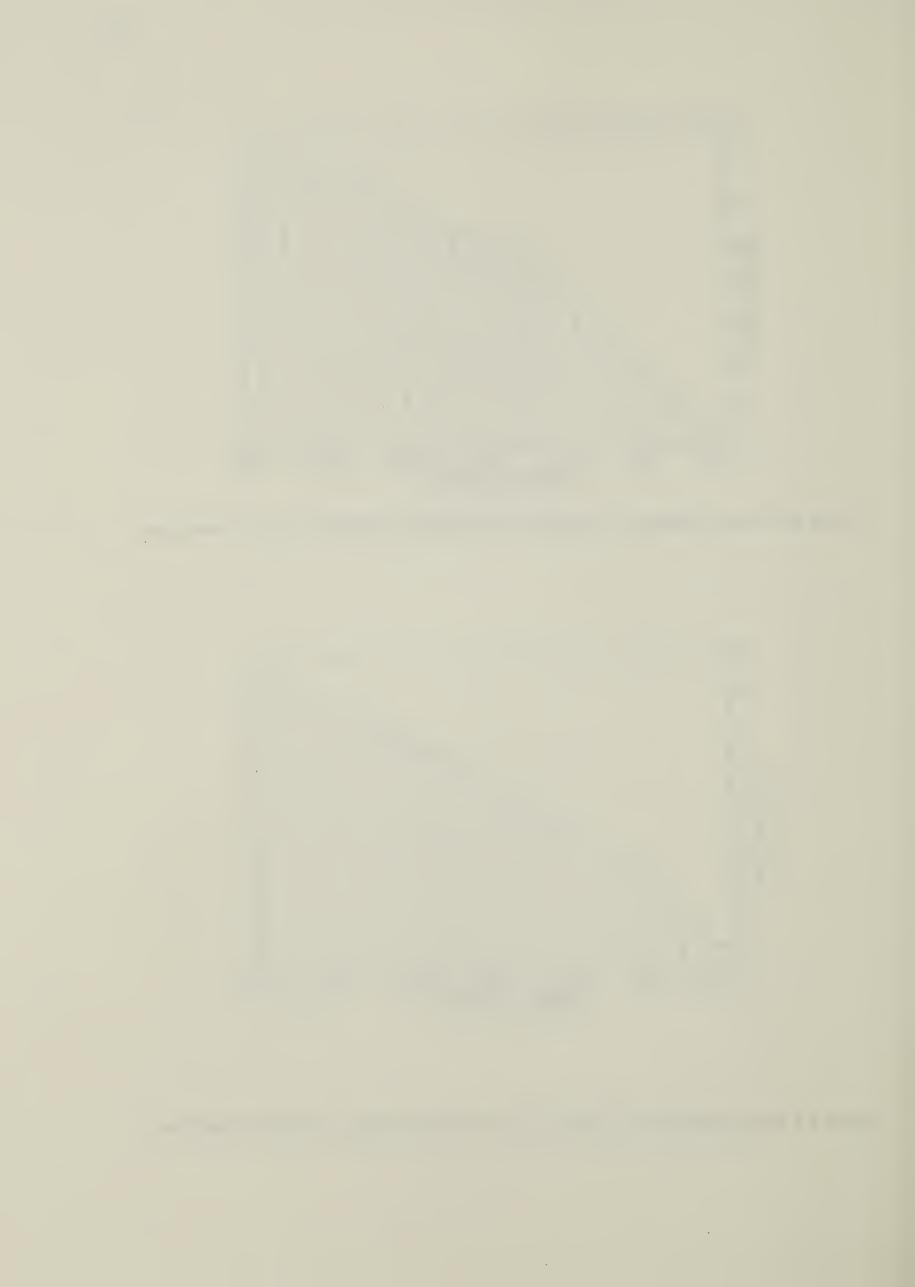


Figure 6.7 Power distribution for beam with incoherence factor=1.0 at the focal plane.
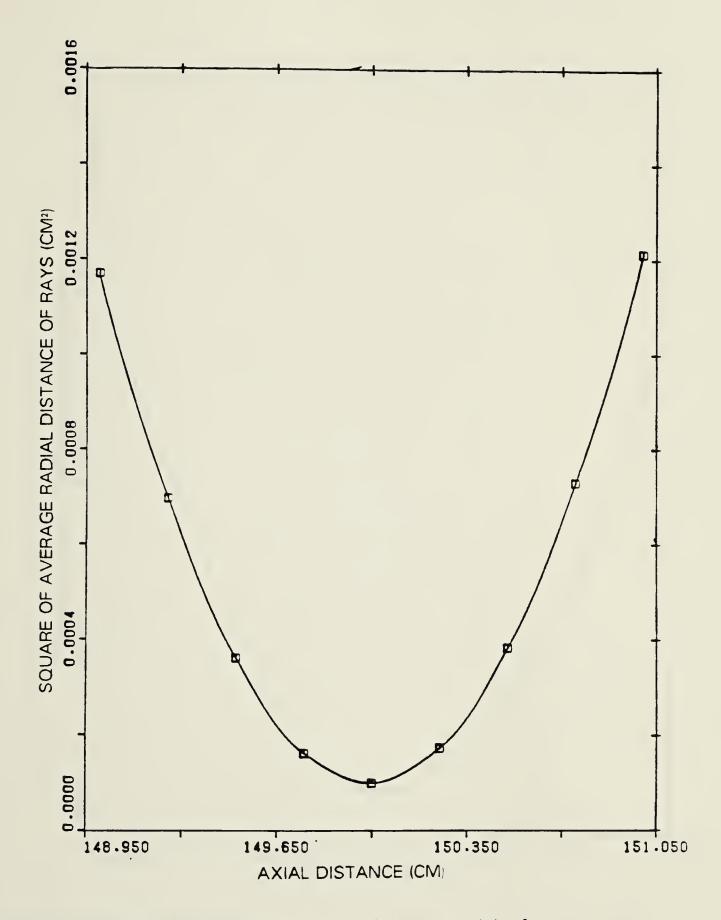
Figure 6.8 Square of average radial distance of rays around the focus.
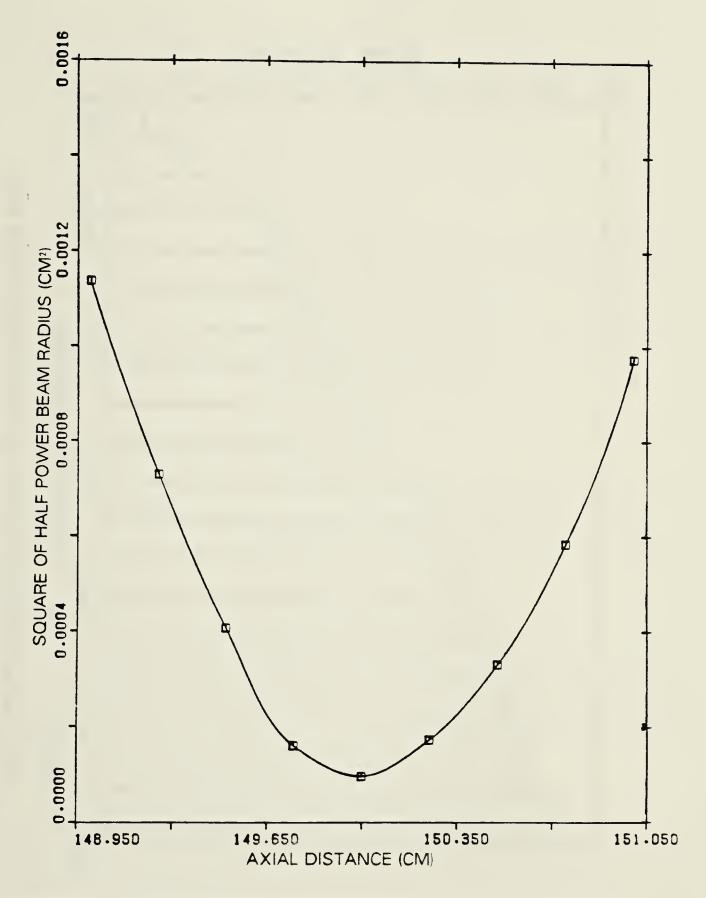
Figure 6.9 Square of half power beam radius with the incoherence factor=0.5.

Figure 6.10 Power distribution for beam with the incoherence factor=0.5.
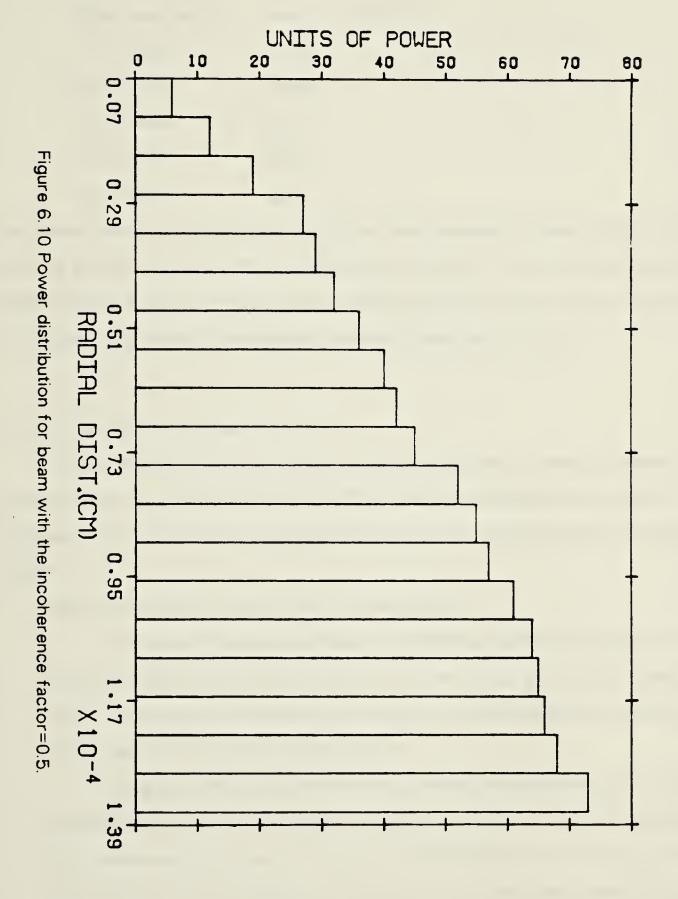
Table 1

| Radial position(cm) | Density( x $10^{18}$/cm$^3$) |
|---|---|
| (1)  0.1330 | 1.152 |
| (2)  0.2745 | 1.656 |
| (3)  0.4200 | 2.46 |
| (4)  0.6720 | 2.26 |
| (5)  0.9740 | 2.0 |

The density variation between the first and second locations is fitted with the profile $N_0$ $(1+r^2/a_0^2)$. For the second and third locations, the profile, $N_1(1-a_1^2/r^2)$ is used. Following the same procedure, the rest of the data are fitted with the corresponding profiles $N_2$ $(1-r^2/a_2^2)$ and $N_3(1+a_3^3/r^2)$. This simulated profile is illustrated in fig. 6.11.
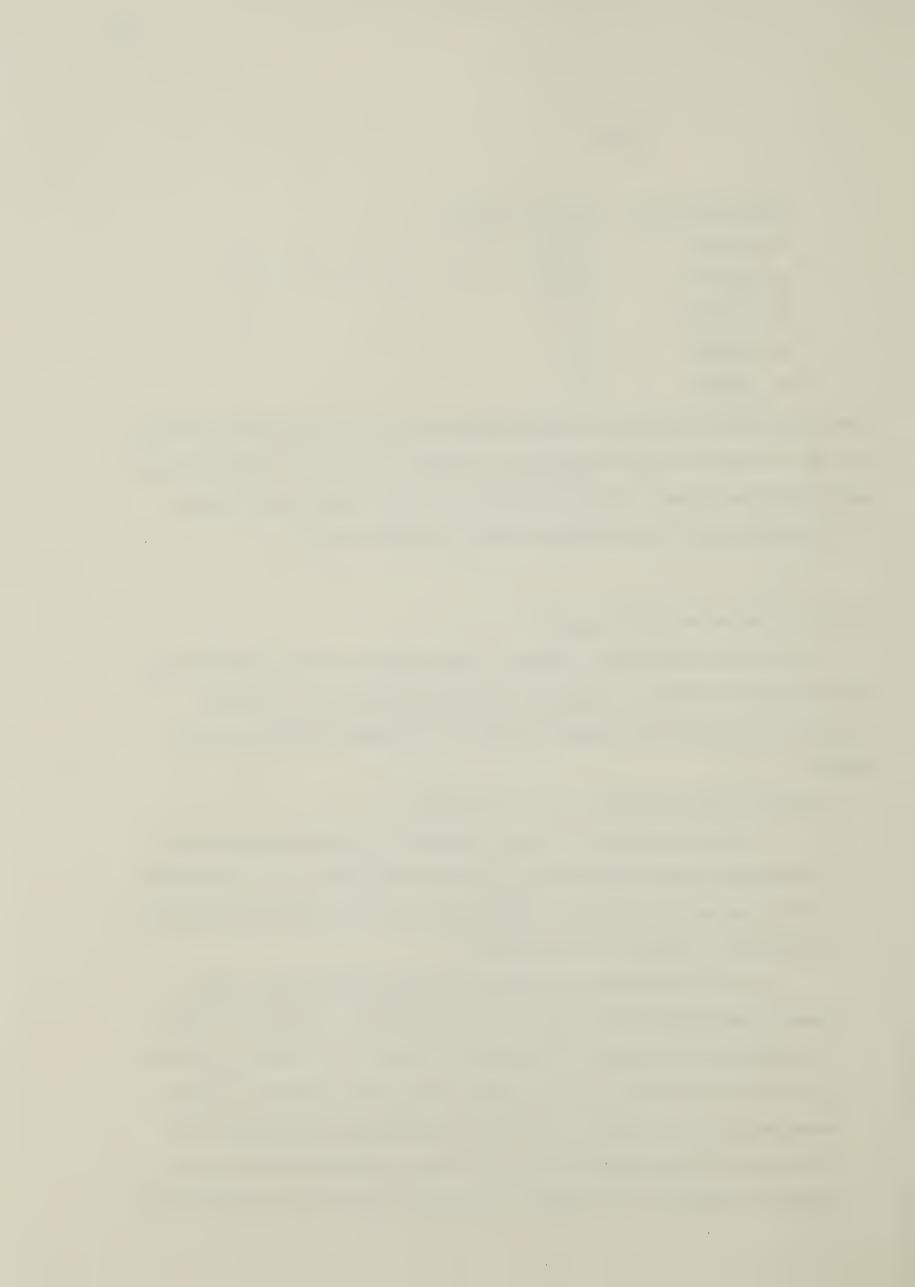
## 6.3 Ray Tracing in the plasma column

In this section, the radial locations of rays propagating in various regions of the plasma column are plotted and discussed. The radial components of the rays are calculated according to the ray equation solutions for the density profiles in various regions.

1. *Rays with radially outward velocity components*

The radial components of the ray trajectories within the plasma for rays having an initial radial outward velocity are shown in figs. 6.12 to 6.17. The plasma column is assumed to be placed 10cm behind the focus to ensure that the rays will diverge before they enter into the medium.

In fig. 6.12, the radial component of the ray trajectory within a radial parabolic density profile(see region 1 in fig. 6.11) is shown. The initial transverse co-ordinates and directions of the ray are x=0.219cm, y=-0.114cm, $u_x$=0.0147, $u_y$=-0.715 x $10^{-2}$. The sinusoidal fluctuation of the radial component of the ray along the plasma column shows that the ray is trapped within the region. A full illustration of the ray propagating along the column is given in fig. 6.13. The ray gyrates around the axis of propagation and traces a helix with an oscillating radius.
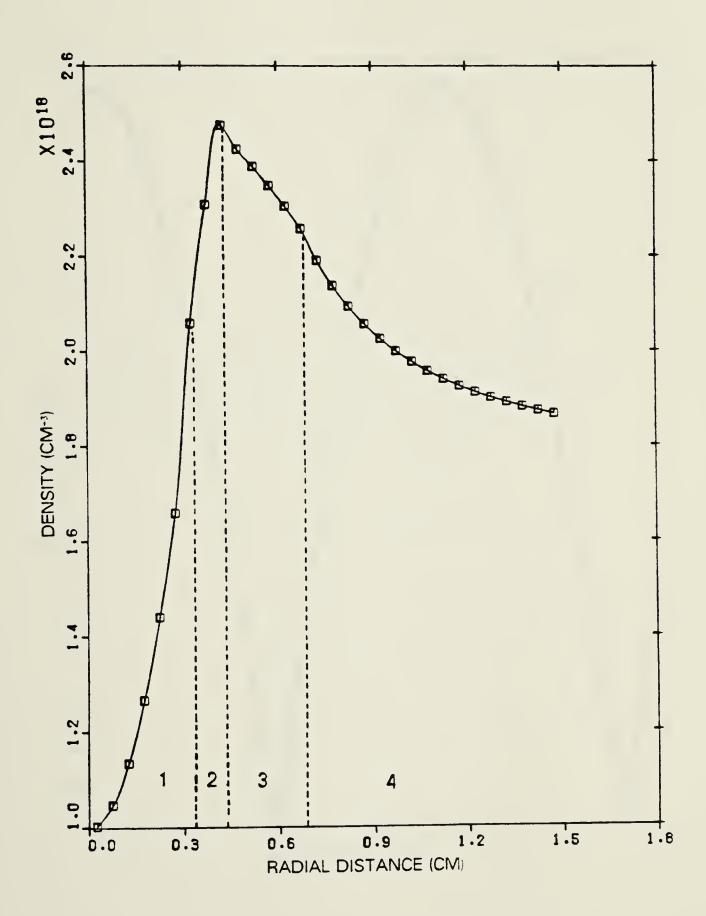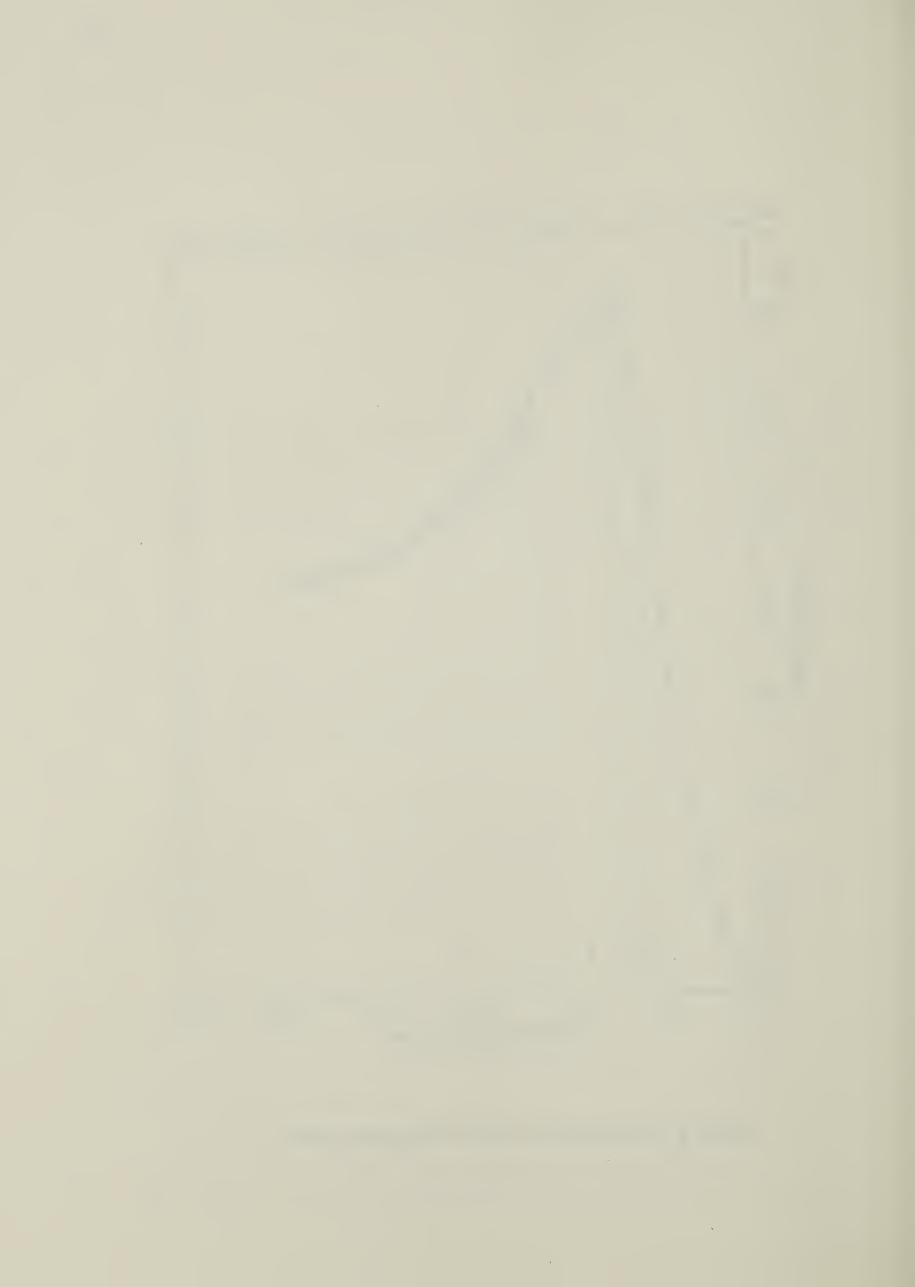
Figure 6.11 Radial density profile of the plasma column.
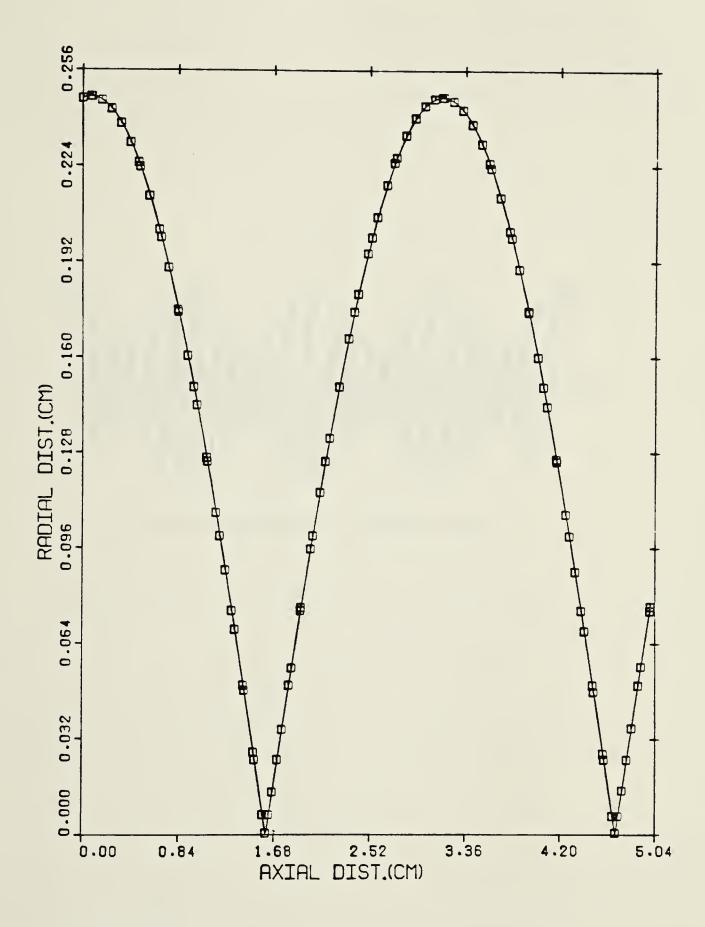
Figure 6.12 Ray path within region 1 (with initial outward radial velocity)
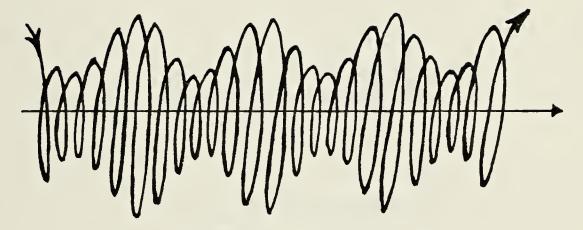
Figure 6.13 Ray trajectory in plasma column

This gyrating ray trajectory shows that beam focusing and defocusing takes place in the parabolic density region.

In the following, the result obtained by the ray tracing technique is compared with those obtained from the normal mode analysis developed by McMullin, Capjack, and James. From the normal mode analysis, the axial period of beam intensities within a parabolic density profile is

$$K = \left. \frac{\omega_{pe}(r,z)}{k(z)c_0 a_0(z)} \right|_{z=0, r=0}$$

(6.3.1)

where

$$\left. \omega_{pe}^2(r,z) \right|_{\substack{r=0 \\ z=0}} = \frac{4\pi e^2 N_e(0,0)}{m_e}$$

$$\left. k(z) \right|_{\substack{r=0 \\ z=0}} = \frac{2\pi}{\lambda} [1 - \frac{\omega^2}{\omega_{pe}^2(0,0)}]^{\frac{1}{2}}$$

$c_0$ is the speed of light in vacuum.

$a_0(z)$ is the coefficient used in the following density profile
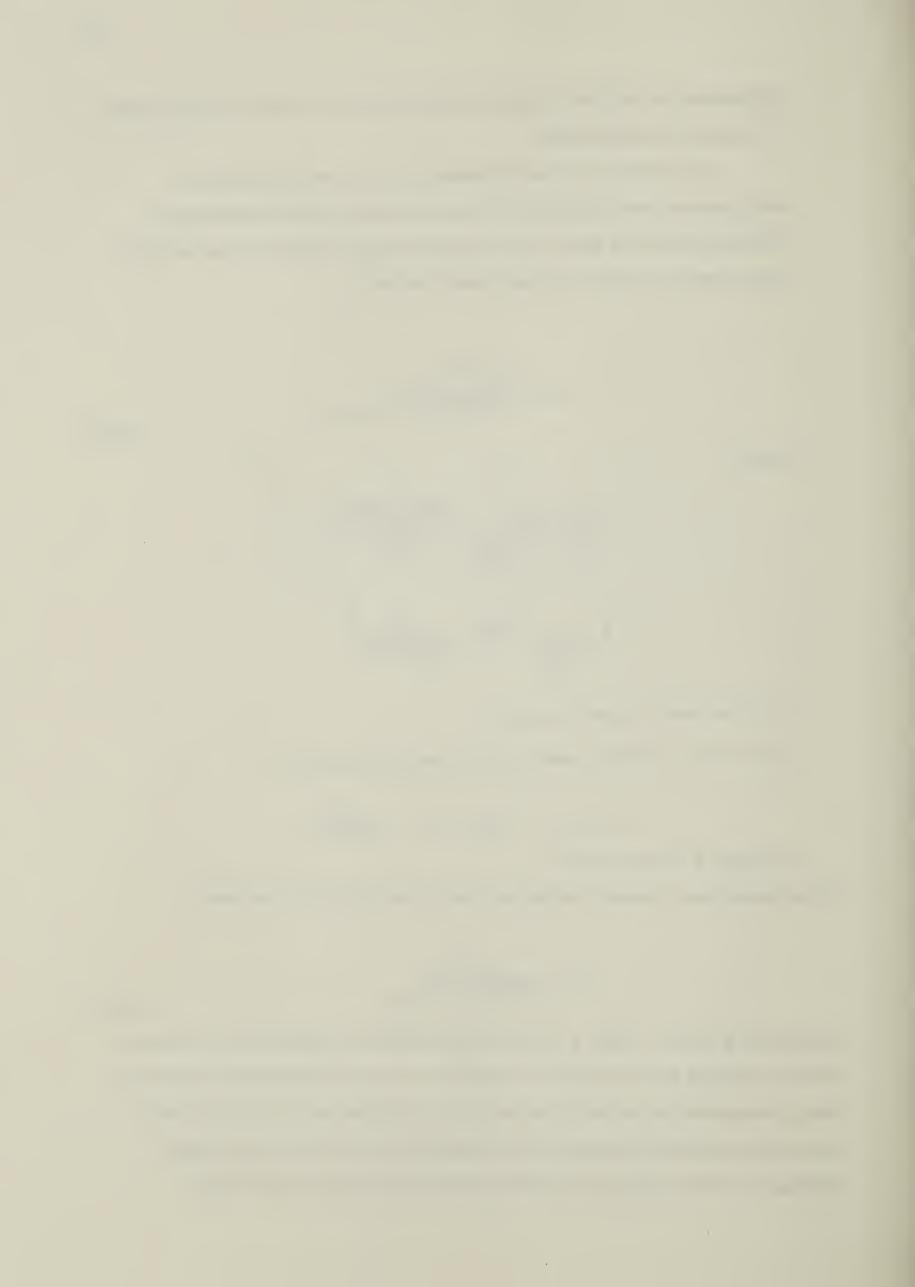
$$N_e(r,z) = N_0(0,z) [1 + \frac{r^2}{a_0^2(z)}]$$

and $N_e(0,z)$ is the axial density.

For the special case of axially independent plasma density, eq.(6.3.1) becomes

$$K = \left. \frac{\omega_{pe}(r)}{k(0)c_0 a_0(0)} \right|_{r=0}$$

(6.3.2)

By substituting for $N_0 = 0.997 \times 10^{18}/cm^{-3}$, $a_0(0)=0.338$ and $\omega_{pe}(0)=5.63 \times 10^{13} sec^{-1}$ in the above equation, the axial period of oscillation is found to be 6.028cm. From the ray tracing computation, the period is calculated to be 6.1678cm which is within 2% error with the value calculated from eq. (6.3.2). The period obtained from the ray tracing technique is further compared with that derived by Mani . Results show a small

discrepancy of 2.5%. Thus, this ray tracing method gives consistent description of the beam propagating in a medium with a parabolic density profile.

In fig. 6.14 and fig. 6.15, the radial variations of two rays propagating in the region where the plasma density varies according to the relation $N_1(1-a_1^2/r^2)$ (see region 2 in fig. 6.11) are shown. The case in which the ray penetrates into a region where the plasma density is close to the peak value is displayed in fig. 6.14. The initial locations and directions of the ray are x=−0.396cm, y=0.149cm, $u_x$=−0.0265, $u_y$=0.0103. The plasma density in this region is too high for the ray to be trapped. As a result, the ray propagates radially outward and enters into another region with a radially decreasing plasma density, where the ray is further refracted off the column.

In fig. 6.15, the ray propagates close to region 1(see fig. 6.11). The initial locations and directions are x=0.091cm, y=0.295cm, $u_x$=0.646 x $10^{-2}$, $u_y$=0.199 x $10^{-1}$. The plasma density is high enough to cause total reflection of the ray. Consequently, the ray penetrates into the parabolic density region where it is trapped.
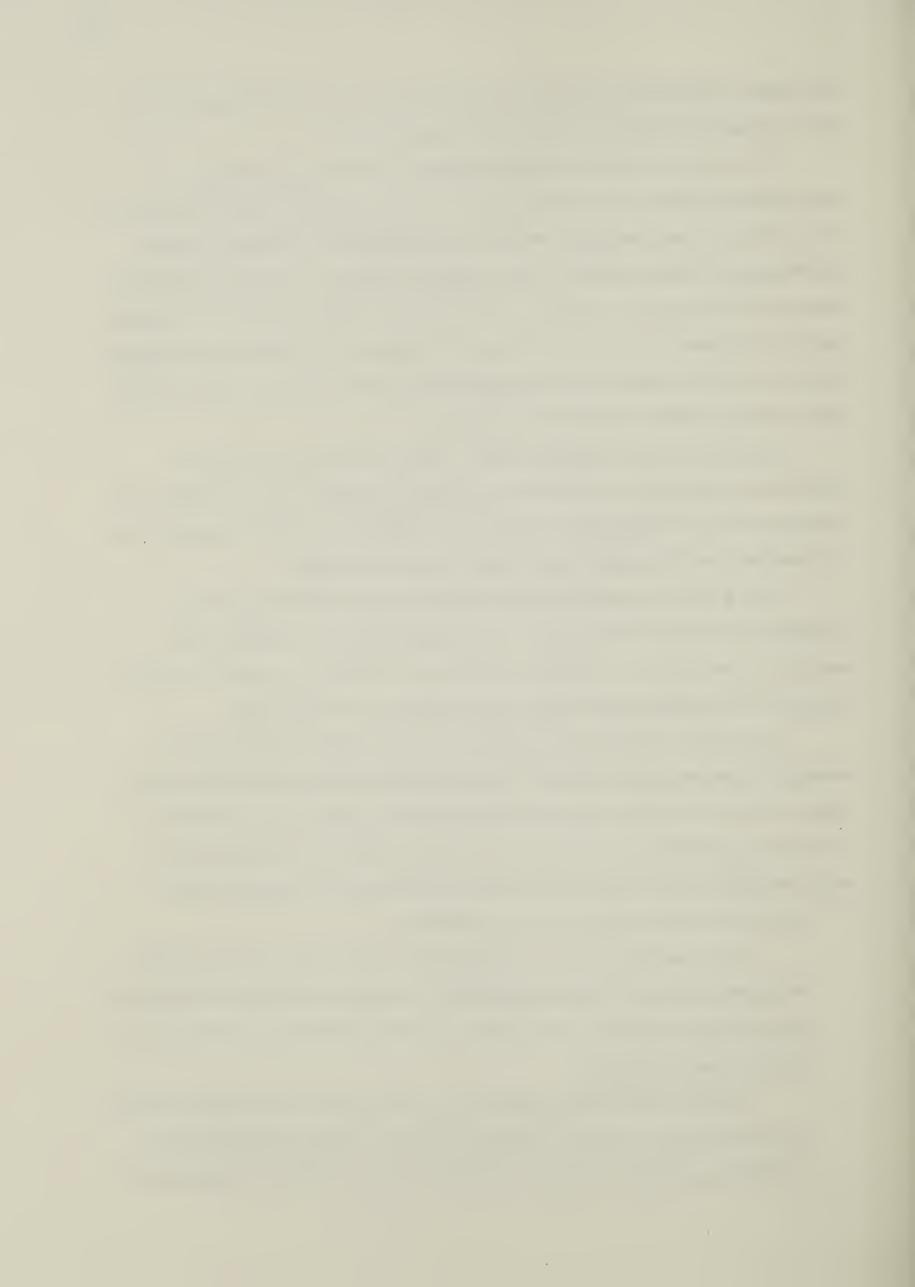
In fig. 6.16, the radial component of the ray is seen to increase as the ray propagates within region 3 (see fig. 6.11). The initial transverse co-ordinates and directions of the ray are x=−0.22cm, y=−0.4cm, $u_x$=−0.0145, $u_y$=−0.0265. The ray is refracted off the plasma column due to a decrease in the refractive index.

The variation of the radial component illustrated in fig. 6.17 gives how a ray propagates along the plasma column if it initially lies close to the plasma periphery (see region 4 in fig. 6.11). The ray locations and directions are chosen to be x=0.822cm, y=−0.731cm, $u_x$=0.0551, $u_y$=−0.0487. The plot shows that the ray propagates only within the outside core of the column and cannot penetrate into the plasma column.

2.    *Rays with radially inward velocity components*

In this section, rays with an initial radially inward velocity are traced along the plasma column in various density regions. The plasma column is assumed to be placed 10cm in front of the focus. Rays are thus ensured to be converging by the time they reach the column.

In fig. 6.18, the radial component of the ray location in the parabolic density region (see region 1 in fig.6.11) is shown. The initial locations and directions are x=0.287cm, y=0.69 x $10^{-1}$cm., $u_x$=−0.192 x $10^{-1}$, $u_y$=−0.465 x $10^{-2}$. The period of
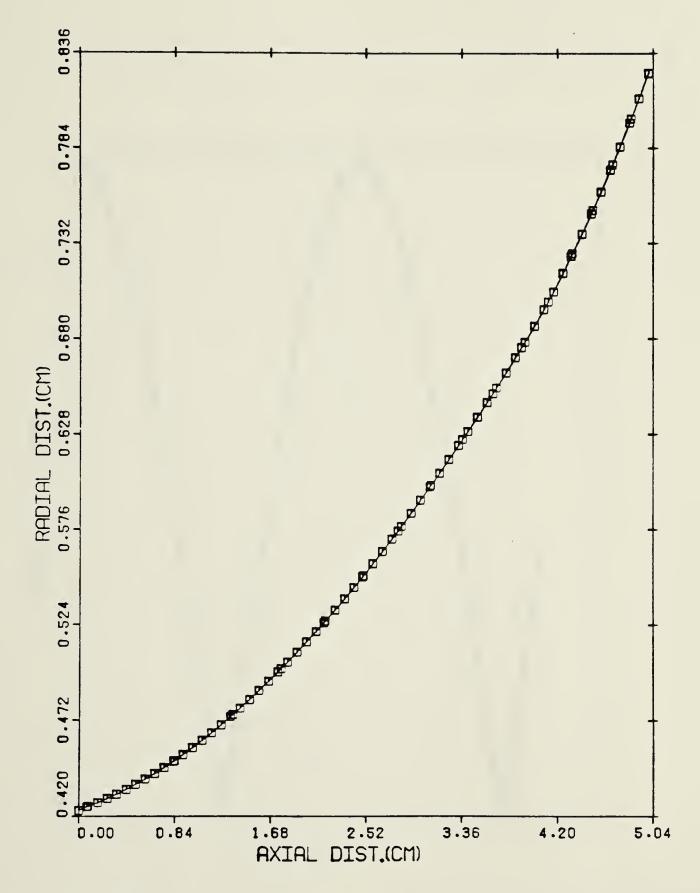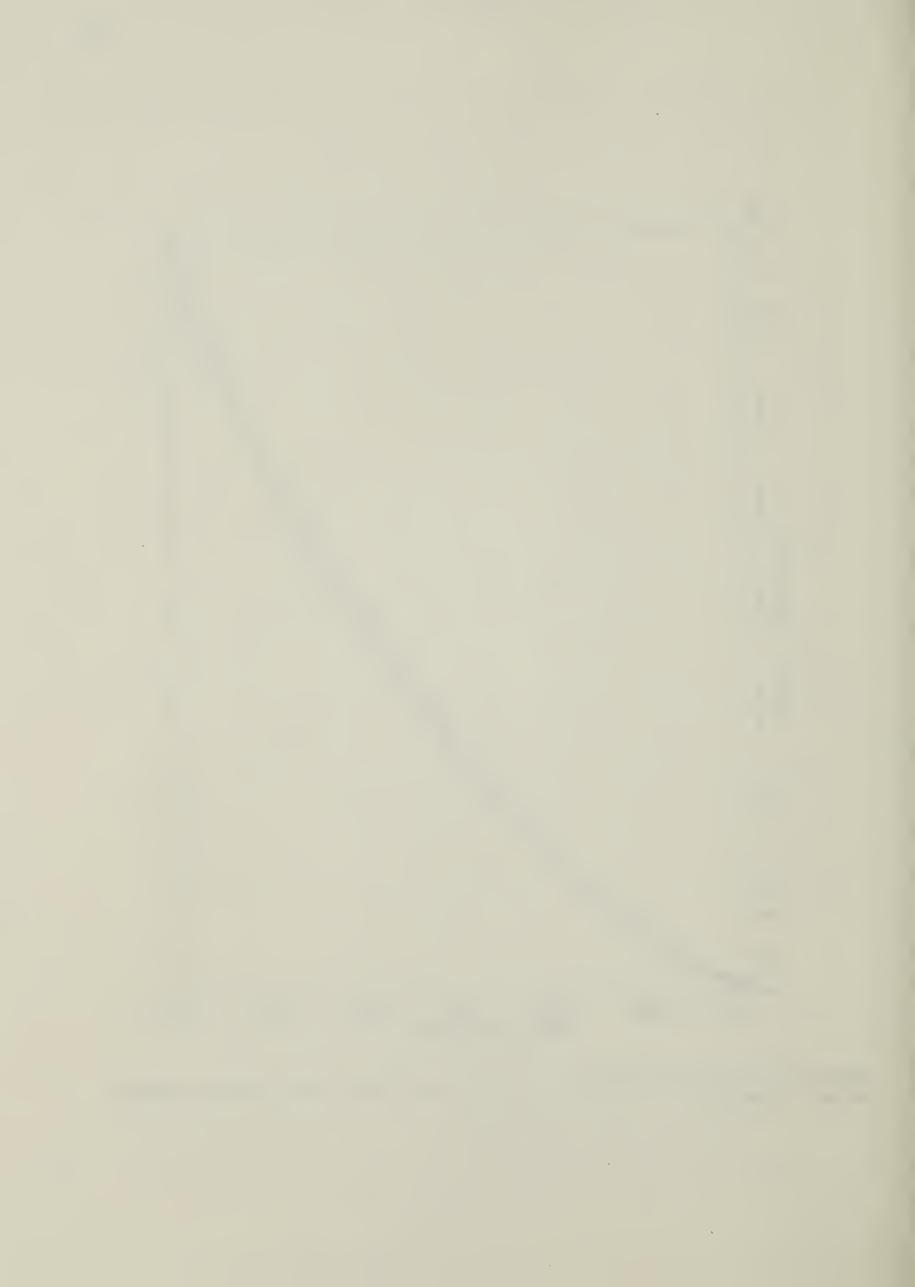
Figure 6.14 Ray path within region 2 (with initial outward radial velocity and initial position close to region 3).
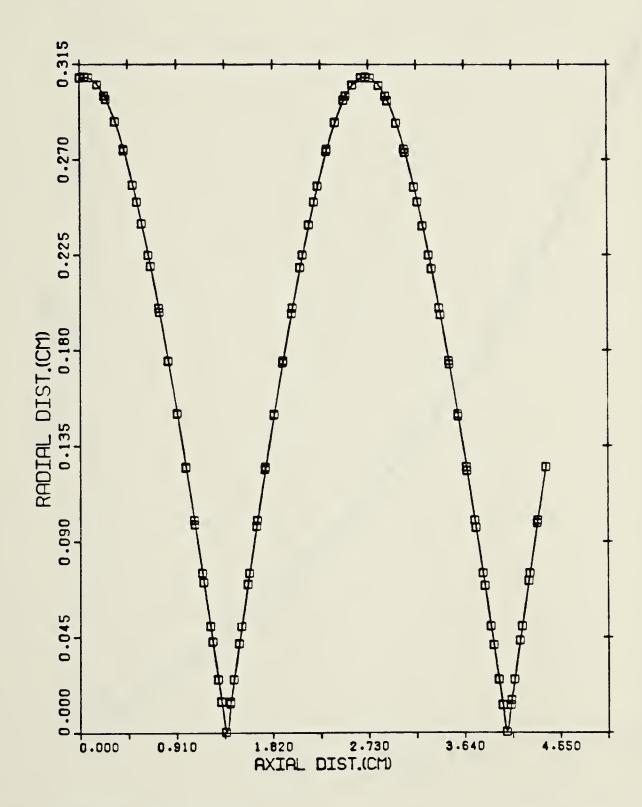
Figure 6.15 Ray path within region 2 (with initial outward radial velocity and initial position close to region 1).
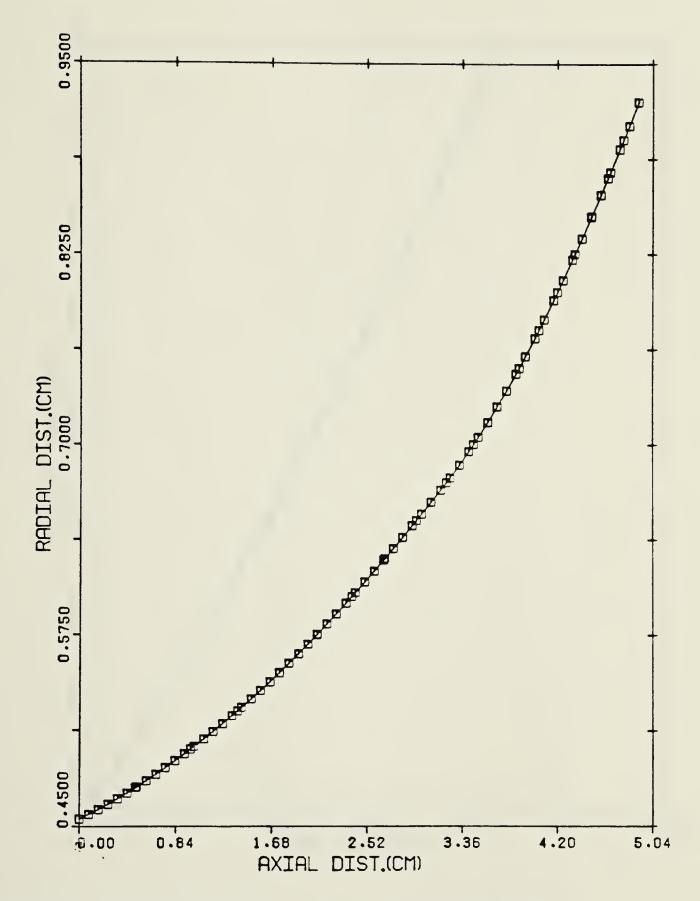
Figure 6.16 Ray path within region 3 (with initial outward radial velocity).
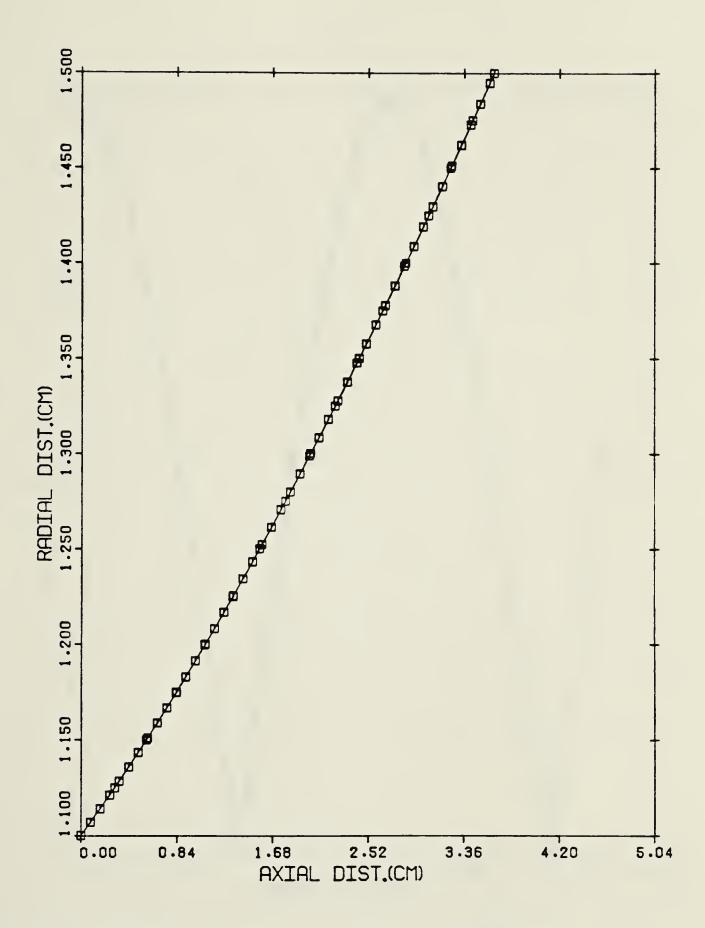
Figure 6.17 Ray path within region 4 (with initial outward radial velocity).
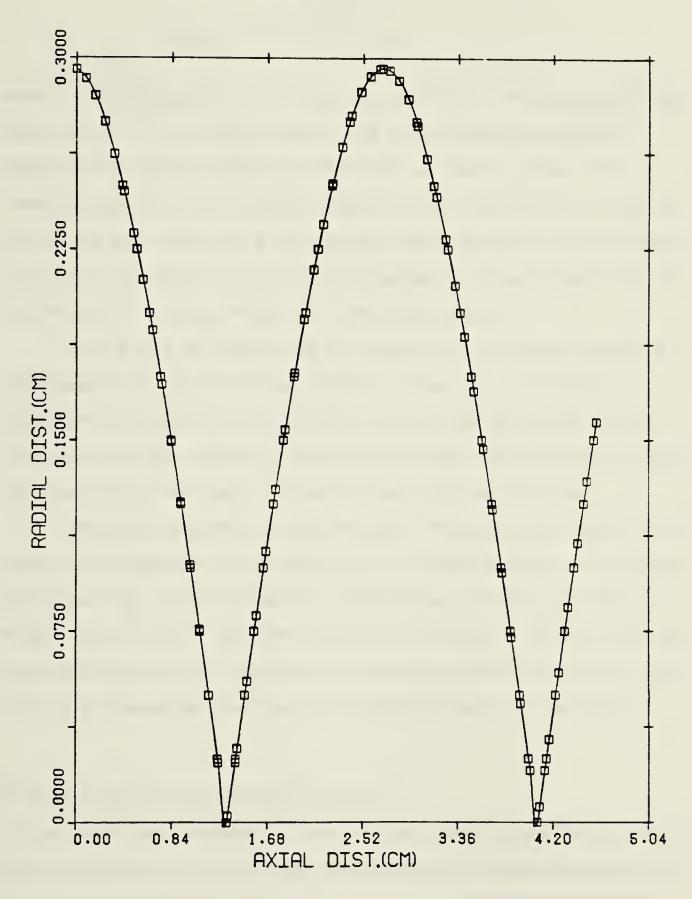
Figure 6.18 Ray path within region 1 (with initial inward radial velocity).

oscillation is found to be 5.48cm. A comparison to the period derived from eq.
(3.3.1.2), namely,

$$z_{period} = \frac{2\pi}{\lambda} \sqrt{1 - \frac{N_0}{N_c}} \; v_z$$

where $\Omega$ is $\sqrt{\frac{c^2 N_0}{a_0^2 N_c}}$; $v_z$ is $2.9 \times 10^{10}$cm/sec.; $N_0$ is $0.997 \times 10^{11}$/cm³; $a_0$ is $0.337$; $N_c$ is $9.94 \times 10^{11}$/cm³ ( for $\lambda = 10.6\mu$m ) and c is the speed of light, shows a 13%

difference. This deviation arises from the choice of density profiles in the

corresponding region. In this case, the plasma density in the region into which the

ray enters is approximated by a non-parabolic increasing density profile. However,

the density is assumed to vary according to a parabolic increasing density profile.

This mismatch of density profile leads to the above deviation.
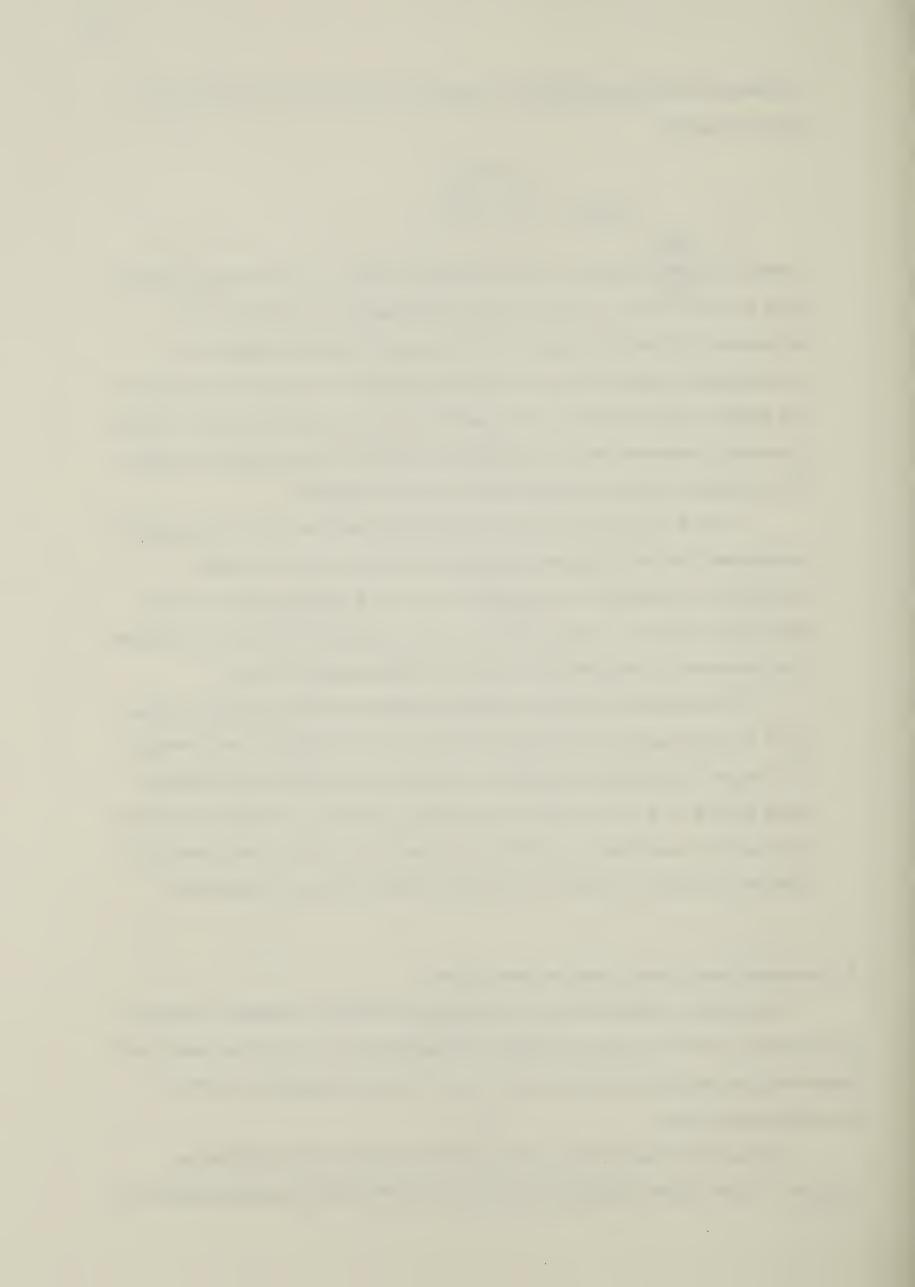
In fig. 6.19, a ray which enters the plasma core from region 2(see fig. 6.11)

is displayed. The initial locations and directions of the ray are x=-0.43cm,

$\dot{y}=-0.13$cm, $u_x=0.2868 \times 10^{-1}$, $u_y=0.8241 \times 10^{-2}$. The ray approaches the inner

core region gradually , reaches a minimum radial position and then exits the column.

This phenomenon is indicated by a change in radial distance of the ray.

The behaviour of the rays when they enter into region 3 and region 4 (see

fig. 6.11) are revealed in fig. 6.20 and fig. 6.21. The initial locations and directions

for the ray in fig. 6.20 are x=0.404cm, y=0.513cm, $u_x=-0.027$, $u_y=-0.034$ and

those in fig. 6.21 are x=-0.831cm, y=0.731cm, $u_x=0.055$, $u_y=-0.049$. As the rays

approach the column axis, they enter into a medium of which the refractive index

gradually decreases. Eventually, the rays are totally reflected off the column.

## 6.4 Absorbed energy and ponderomotive forces

In this section, the distribution of rays along the column is presented in terms of

their locations at various transverse planes. The magnitudes of the absorbed energy and

ponderomotive forces for a beam simulated with 10 rays are presented in terms of

three dimensional plots.

Distributions of rays in the transverse planes located at the axial distances,

z=0.0cm, 1.25cm, 2.5cm, 3.75cm and 5.0cm from the left end of the plasma column are
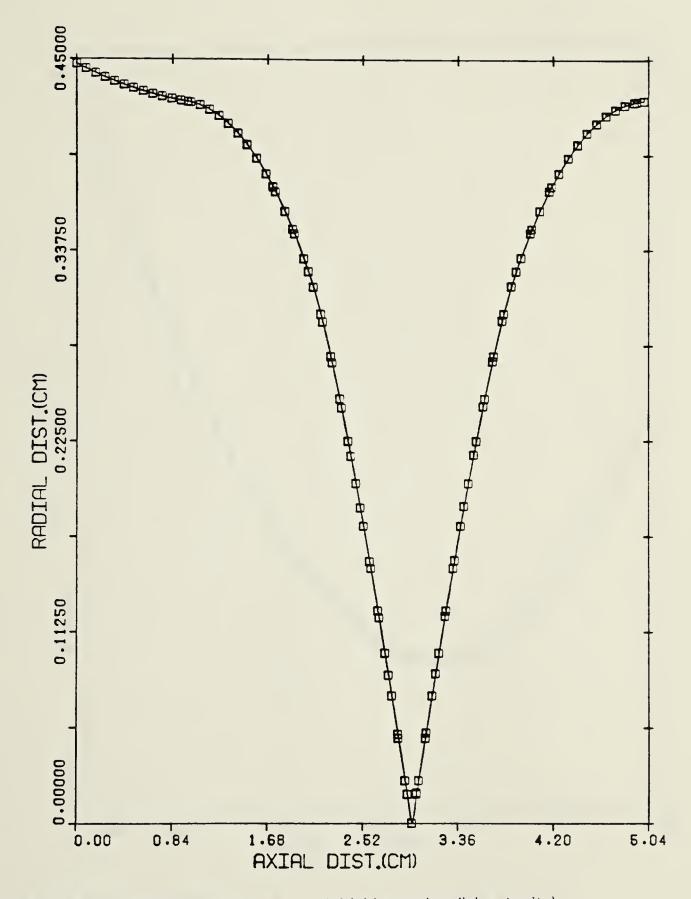
Figure 6.19 Ray path within region 2 (with initial inward radial velocity).
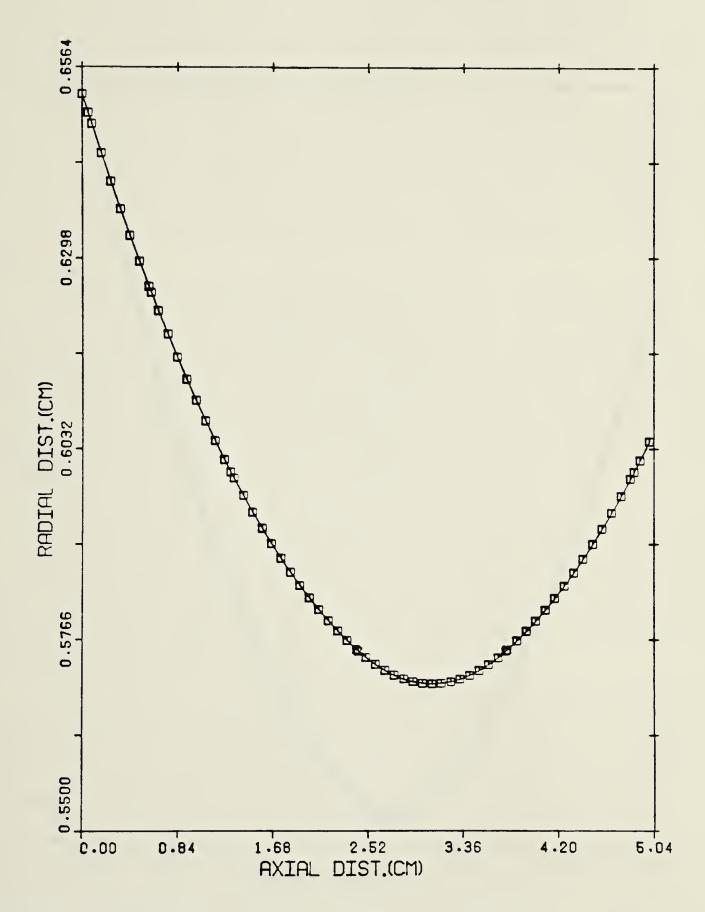
Figure 6.20 Ray path within region 3 (with initial inward radial velocity).
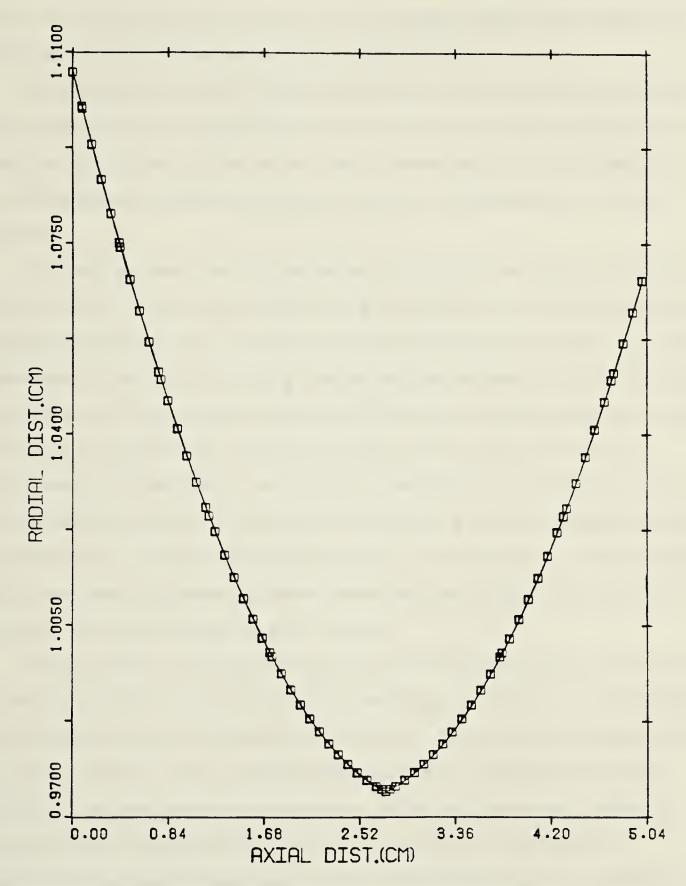
Figure 6.21 Ray path within region 4 (with initial inward radial velocity).

shown in figs. 6.22 to 6.26. Cases for converging rays (figs. 6.22a–6.26a) and diverging rays (fig. 6.22b–6.26b) are compared. From figs. 6.22a to 6.26a, the distribution of ray locations indicates that the rays are focused and defocused as they propagate along the column. At z=1.25cm and 5.0cm, almost all rays propagate within the first shell in the column, showing that the beam is focused at these locations.

From figs. 6.22b to 6.26b, the behaviour of the rays is seen to be very similar to the set of rays displayed in figs. 6.22a to 6.26a. However, more rays are also seen to spread over the periphery of the column. This is a consequence of the divergence of the rays which implies that a higher proportion of the rays is distributed away from the column axis.

The absorbed energy and ponderomotive forces associated with rays focused at the centre of the column are illustrated in figs. 6.27 to 6.29. In fig. 6.27, the absorbed energy per grid cell peaks at z=1.25cm and z=4.4cm. This maximum absorption is only a consequence of the rays concentrating at those locations and does not imply that strong absorption occurs in those regions. Moreover, the amount of absorbed energy in a cell at z=1.25cm is just slightly higher than that at z=4.4cm. This is due to the small and approximately equal magnitude of the absorption coefficients at both locations. When the beam reaches the location at z=1.25cm, the beam power is not strongly absorbed and most of the power is transmitted down the column. At z=4.4cm, the input beam power does not decrease significantly. Moreover, due to the approximately equal absorption coefficient, the absorbed power is about the same.

Plots of radial and axial ponderomotive forces along the column are shown in fig. 6.28 and fig. 6.29. Both forces have maximum magnitudes at the region with the highest radiation intensity. Negative amplitudes imply that the forces and radial displacement are in opposite directions. With an input laser intensity of $1.0 \times 10^8$watts, the maximum magnitude of the radial and axial ponderomotive forces are found to be $0.198 \times 10^4$ (dynes/cm$^3$) and the axial ponderomotive force to be $0.54 \times 10^3$ (dynes/cm$^3$) respectively. By comparing these values to the hydrodynamic force(for T=100eV,dN /dr=$8.8 \times 10^{17}$ /cm$^4$,over a scale length of 0.05cm, k=$1.6 \times 10^{-12}$erg/eV,dP/dr=kT(dN /dr)=$1.41 \times 10^9$ dynes/cm$^3$), the ponderomotive forces are far smaller than the hydrodynamic ones. These force components will become significant when the laser

intensity becomes much higher.

Z=0.0CM
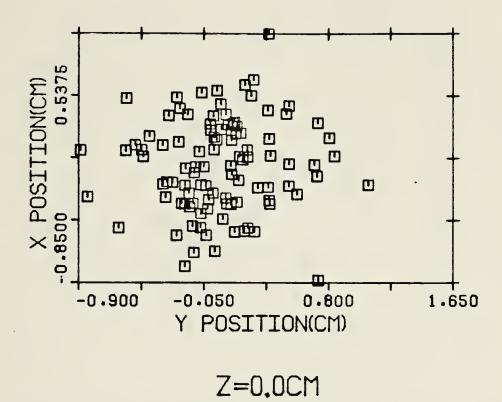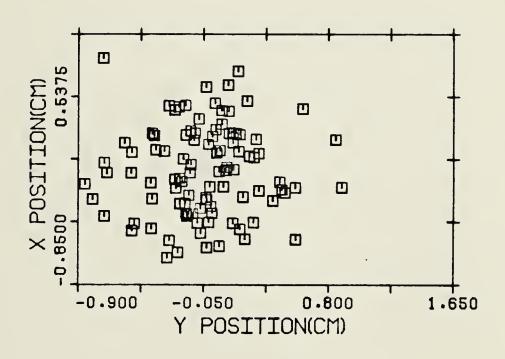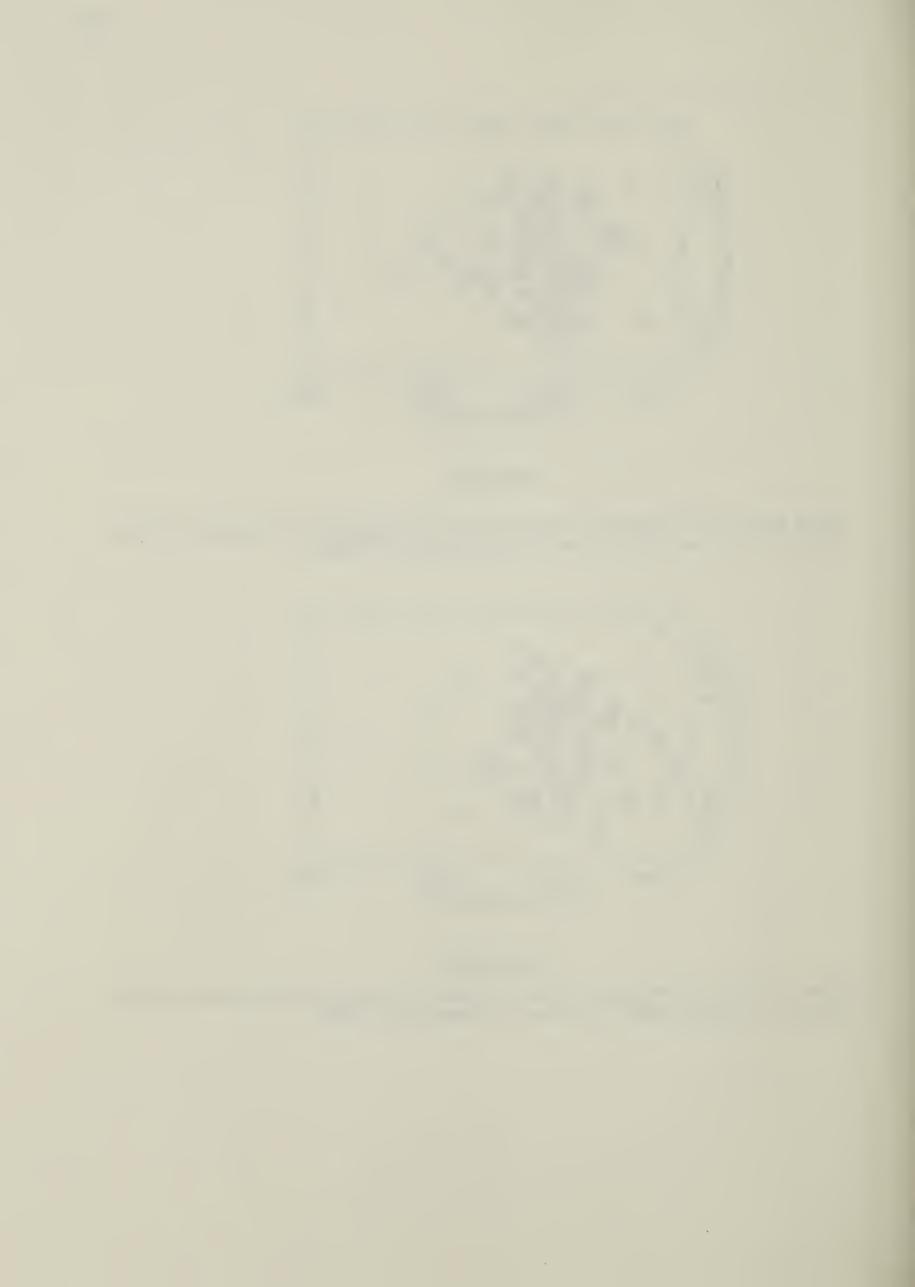
Figure 6.22 a Ray distribution with the front end of the plasma column placed at 135cm from lens. The focal length of the lens is assumed to be 150cm.



Z=0.00CM

Figure 6.22 b Ray distribution with the front end of the plasma column placed at 165cm from lens. The focal length of the lens is assumed to be 150cm.

Z=1.25CM
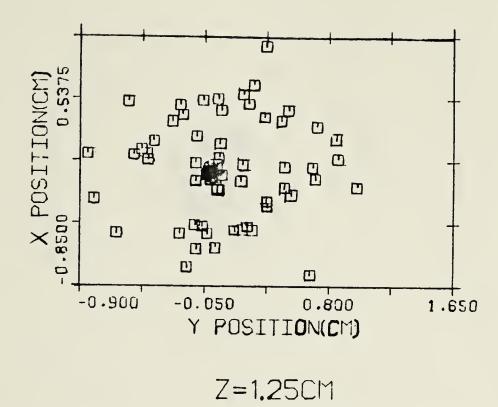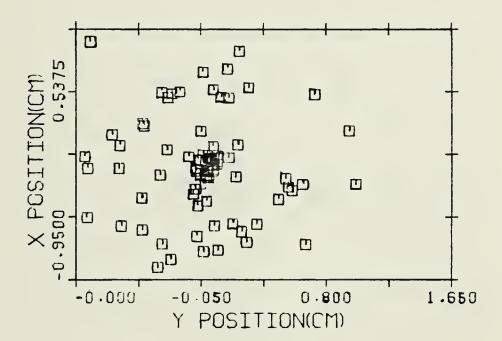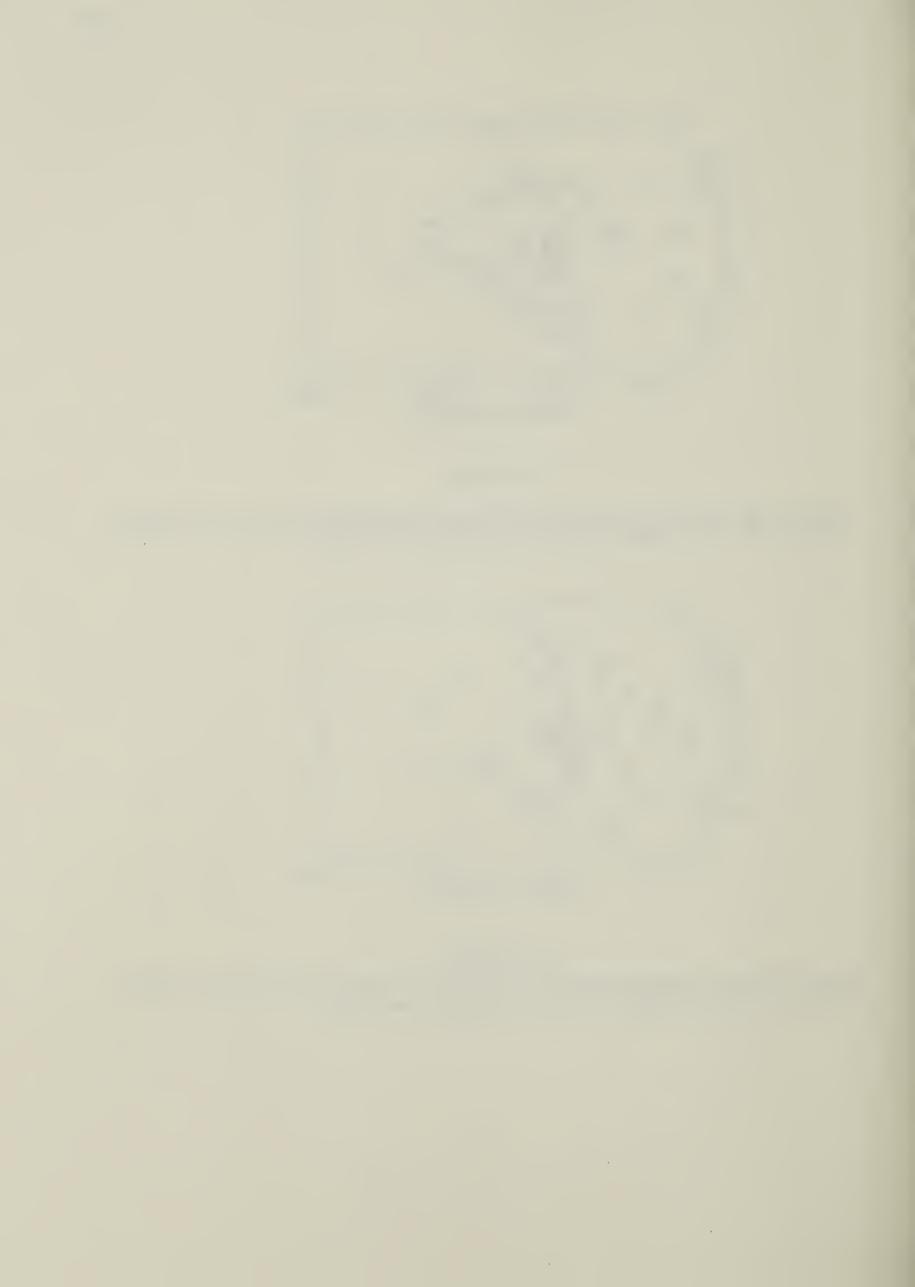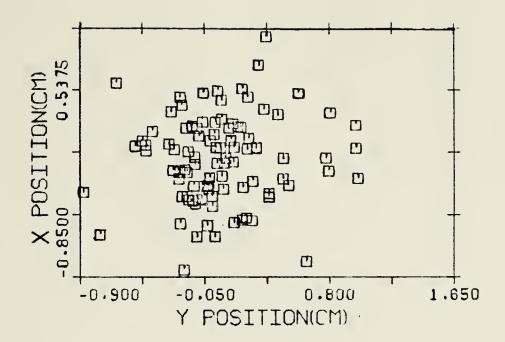
Figure 6.23a  Ray distribution with the front end of the plasma column placed at 135cm from lens. The focal length of the lens is assumed to be 150cm.



Z=1.25CM
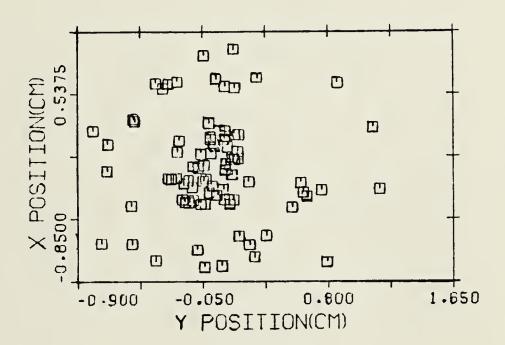
Figure 6.23b  Ray distribution with the front end of the plasma column placed at 165cm from lens. The focal length of the lens is assumed to be 150cm.
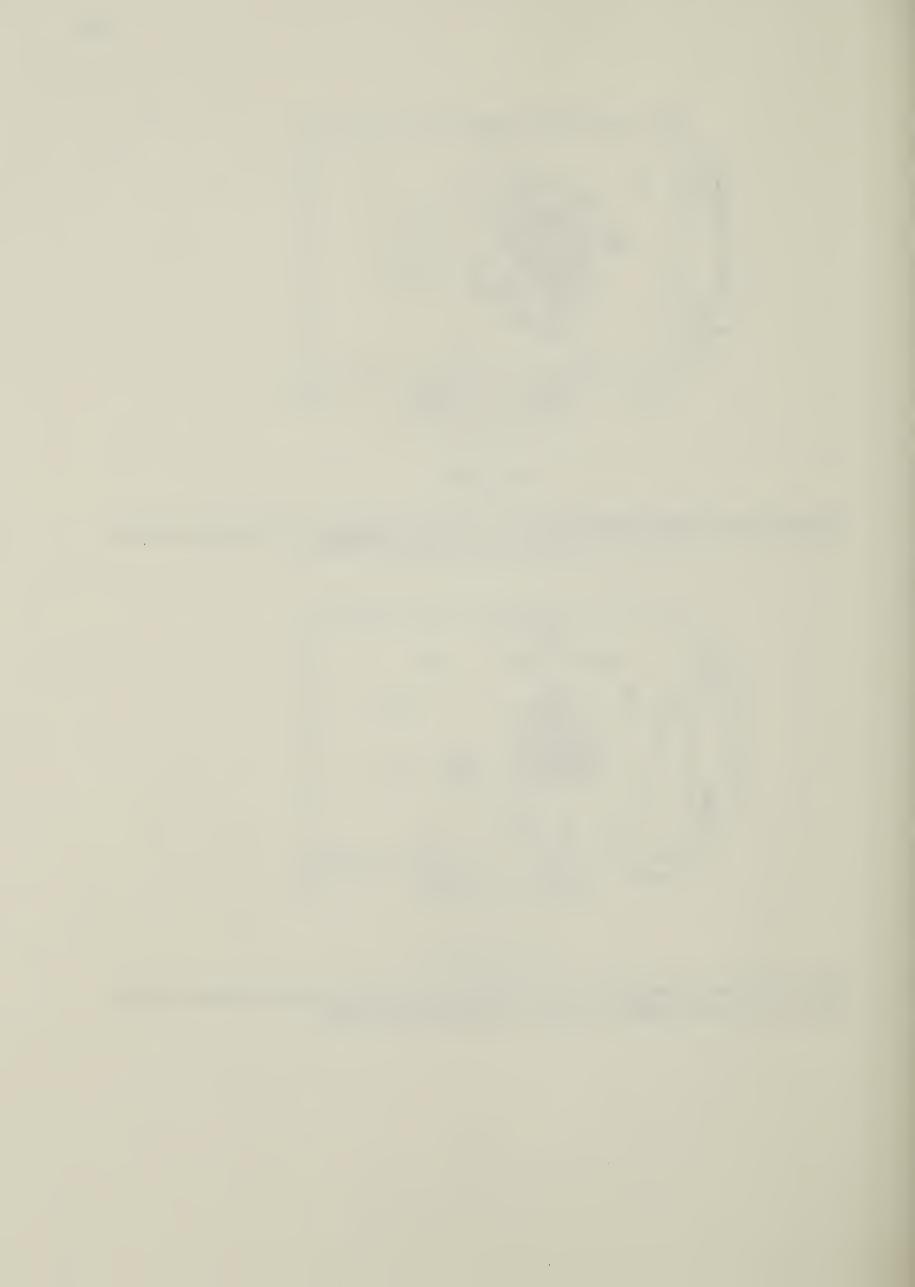
Z=2.5CM
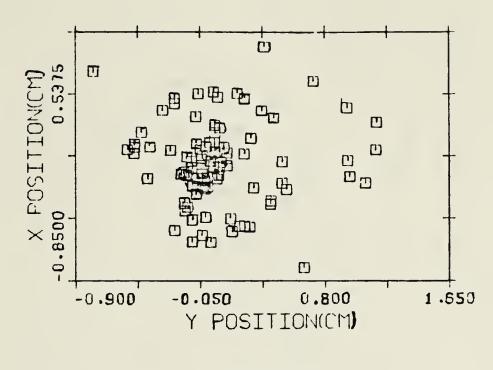
Figure 6.24a Ray distribution with the front end of the plasma column placed at 135cm from lens. The focal length of the lens is assumed to be 150cm.



Z=2.5 CM
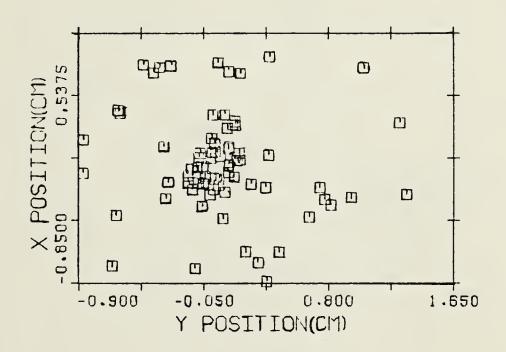
Figure 6.24b Ray distribution with the front end of the plasma column placed at 165cm from lens. The focal length of the lens is assumed to be 150cm.
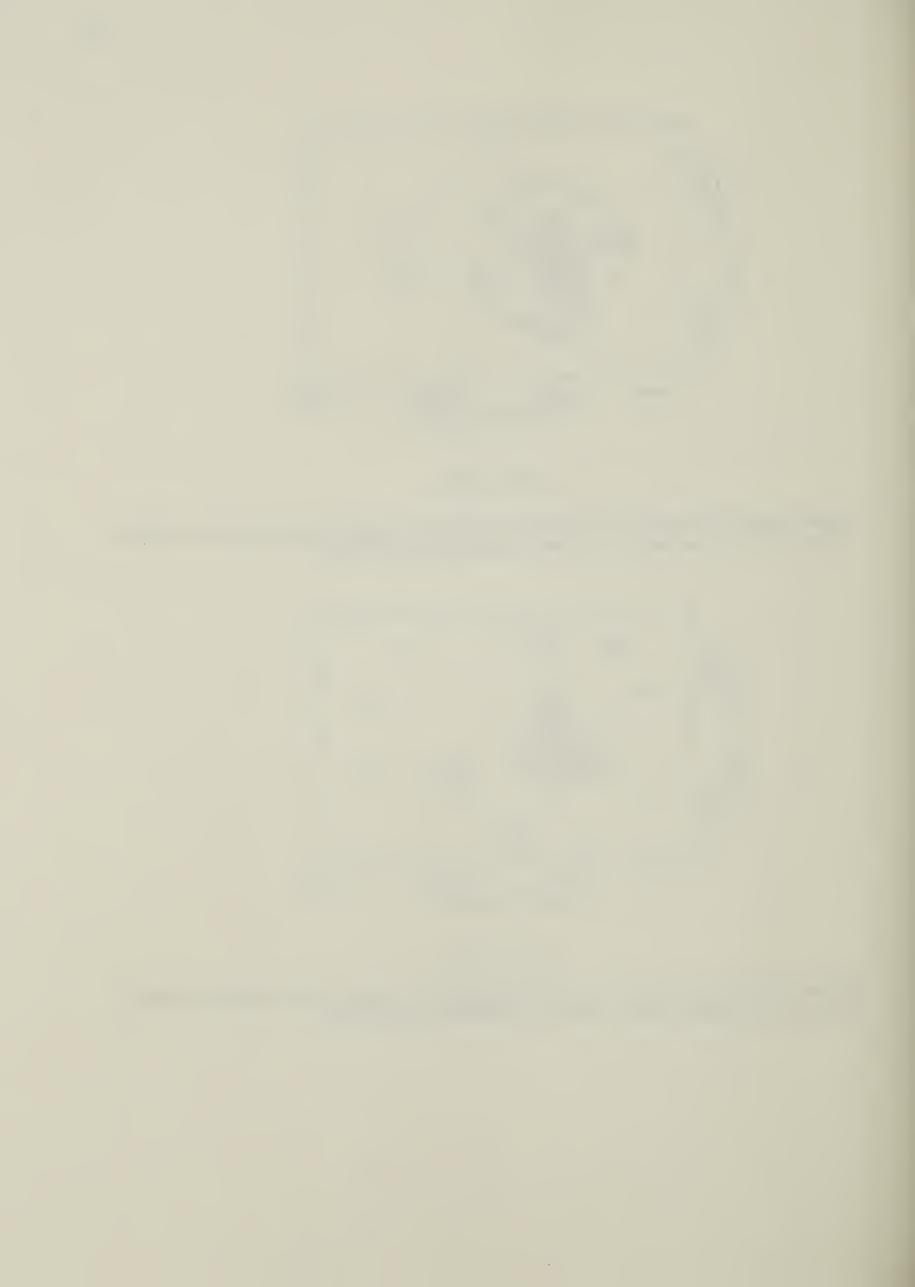
Z=3.75CM
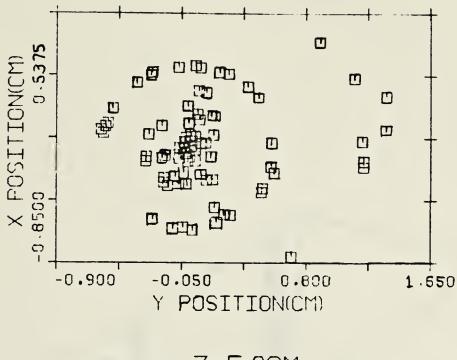
Figure 6.2 5a Ray distribution with the front end of the plasma column placed at 135cm from lens. The focal length of the lens is assumed to be 150cm.



Z=3.75CM
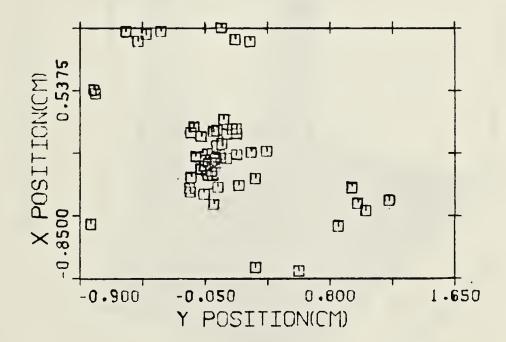
Figure 6.2 5b Ray distribution with the front end of the plasma column placed at 165cm from lens. The focal length of the lens is assumed to be 150cm.
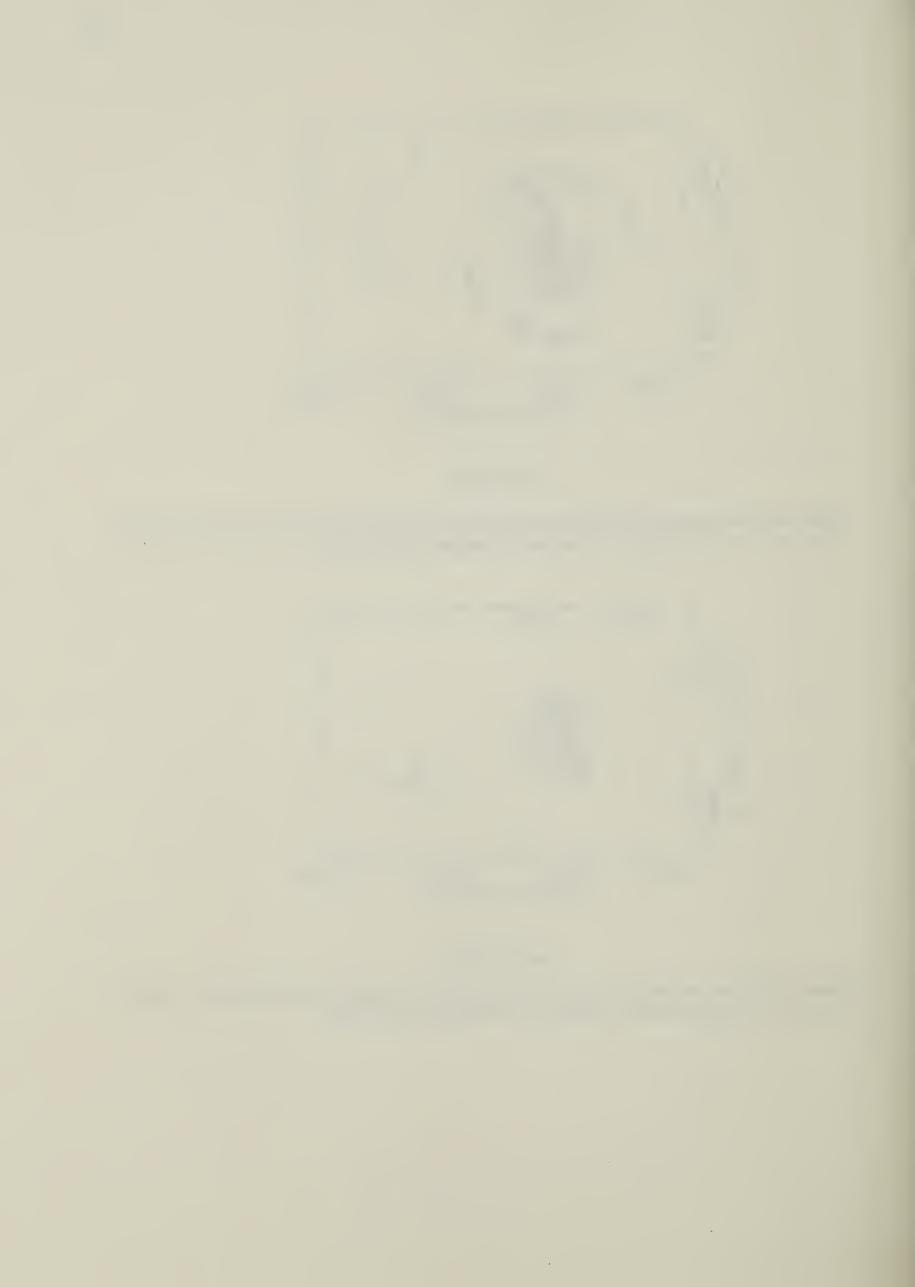
Z=5.0CM

Figure 6.26 a Ray distribution with the front end of the plasma column placed at 135cm from lens. The focal length of the lens is assumed to be 150cm.



Z=5.00CM

Figure 6.26 b Ray distribution with the front end of the plasma column placed at 165cm from lens. The focal length of the lens is assumed to be 150cm.
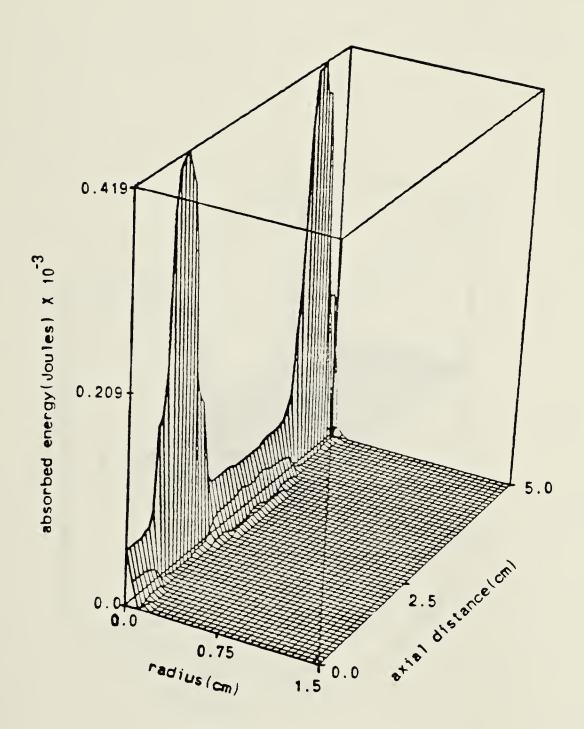
Figure 6.27 Distribution of absorbed energy within plasma column (with beam focused at the middle of the column).
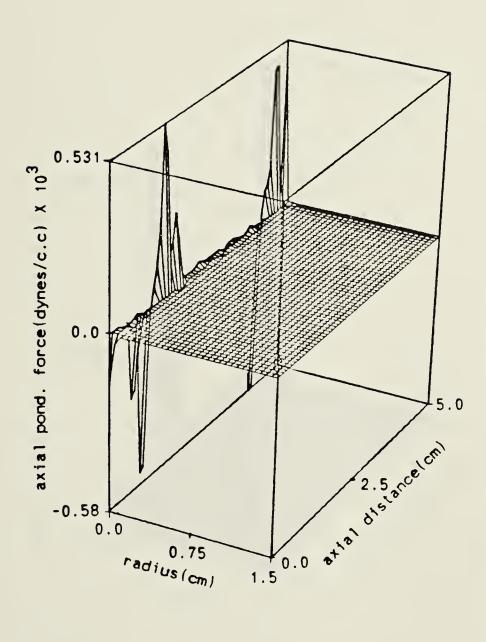
Figure 6.28 Distribution of axial ponderomotive force within the column.
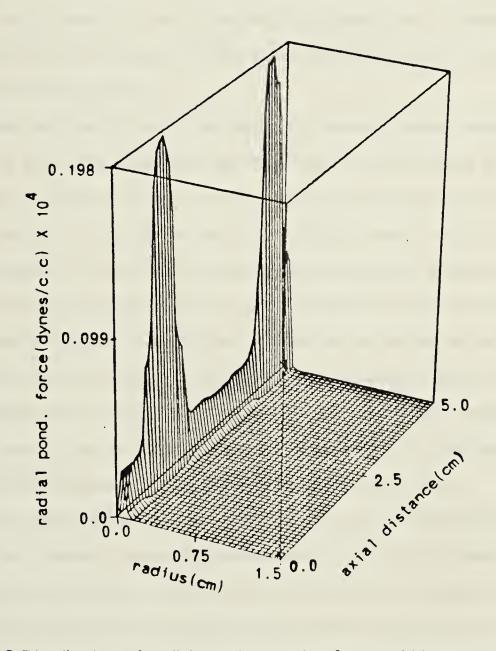
Figure 6.29 Distribution of radial ponderomotive force within the column.

## Conclusion

The propagation of a focused laser beam in a vacuum and in a plasma medium is investigated by using a ray tracing technique which accounts for the diffraction effects of the beam. The effect is introduced by means of a phase-space distribution function which was suggested by Tappert. The distribution function provides a range of values for the ray directions so that rays are not focused at one point, but are spread out at the focal region. If the laser beam intensity assumes a Gaussian profile at the lens plane, rays will be then distributed across the focal plane in a Gaussian manner. Results show that this method can generate rays which give the diffraction limited focal spot size. Optical defects such as aberration, are modelled by introducing an incoherence factor into the distribution function. By means of this factor, the focal spot size can be adjusted to meet experimental measurements.

Rays are traced through the plasma by means of analytic methods. The ray equation is solved for different kinds of refractive index profiles. Ray trajectories within the medium are traced in terms of these solutions. Since the plasma density is spatially non-homogeneous, appropriate density profiles are used to describe the density in various regions. Corresponding ray path solutions are used. A testing density profile with an on-axis minimum obtained from an MHD simulation of a laser heated plasma confined by a solenoidal magnetic field is used as a sample run for the ray tracing package. Results indicate that rays are trapped within regions with a parabolic radial density variation; rays are reflected off axis when they propagate in regions having a radially decreasing density profile. Focusing and defocusing effects of the beam within the predefined profile are shown by the distribution of ray locations at various axial planes.

The plasma density profile used in the simulation is assumed to be axially independent. However, in actual plasma density distribution evaluated by the shell code, the density varies axially as well. In the ray tracing routine, this axial density change is taken into account by the appropriate fitting of density profiles over the grid cells. Since the choice of density profiles is determined by the density values in the grid cells, any variations in density values will give different choices for the density profile.
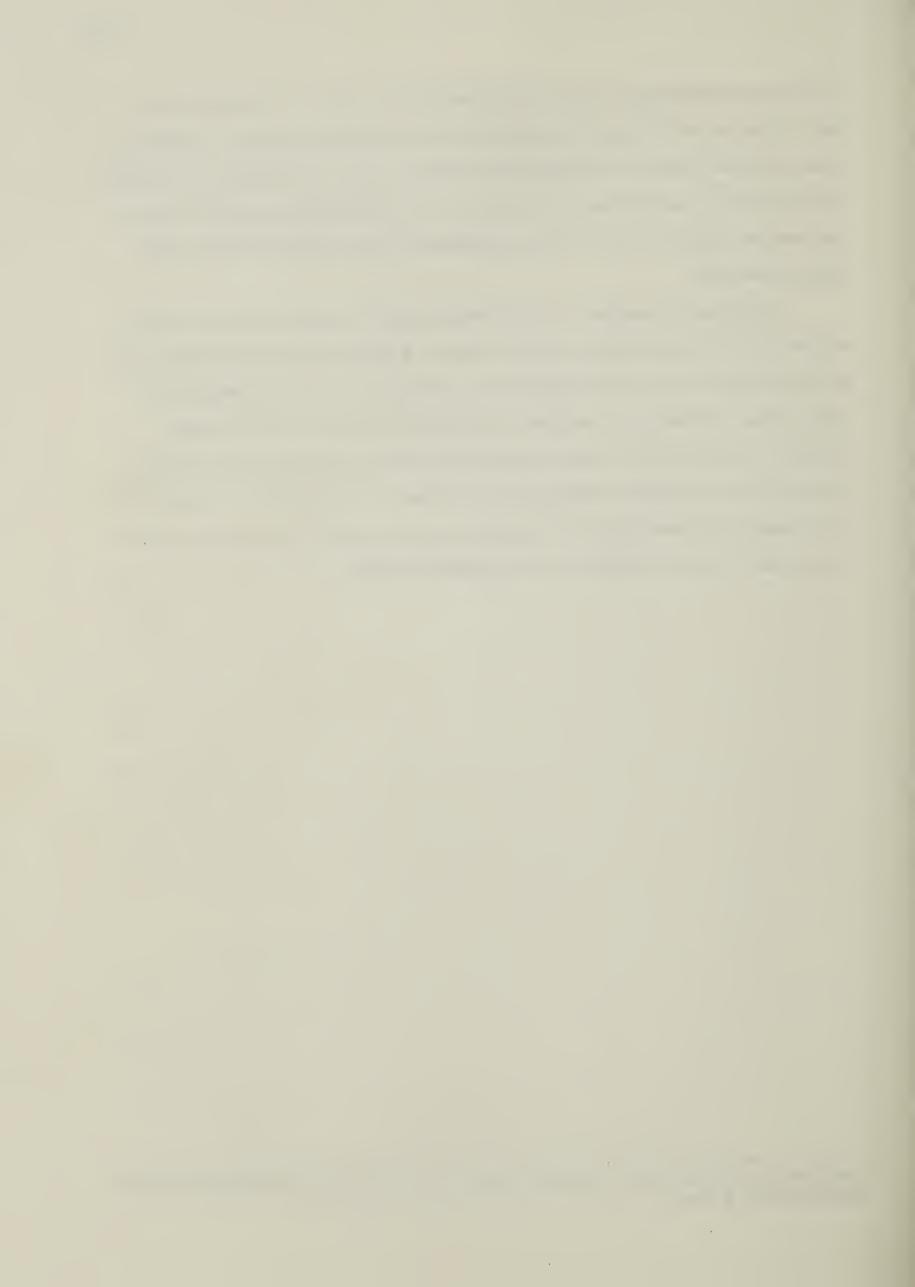
An extension of the ray tracing technique to gas target experiments will be of interest and use for future research. For the gas targets, there are no magnetic fields

confining the plasma and as a result, the plasma expands freely in all directions upon heating. The rays will intersect the plasma boundary at different locations in subsequent times. Moreover, because of the high plasma density, rays can be scattered as they reach the region with critical densities. The problems of a moving plasma boundary and beam scattering are significant factors to be considered in the ray tracing program for gas target experiments.

Throughout the analysis, the spatial distribution of the laser beam is assumed to be composed of the fundamental Gaussian mode. In a real situation, the beam may have a different mode structure mixed together(see footnote) and cylindrical symmetry no longer holds. The intensity of the beam is expected to vary with angular and radial positions. Thus, the choice of ray locations and directions are determined by the radial and azimuthal co-ordinates. Consequently, the number of rays required for simulation will be increased significantly and will increase the operating cost of the simulation program considerably. Further investigation on this problem is needed.

-------------------

Diagrams of different mode structure are given in fig. 4.12 in 'An introduction to optical electronics' by A. Yariv
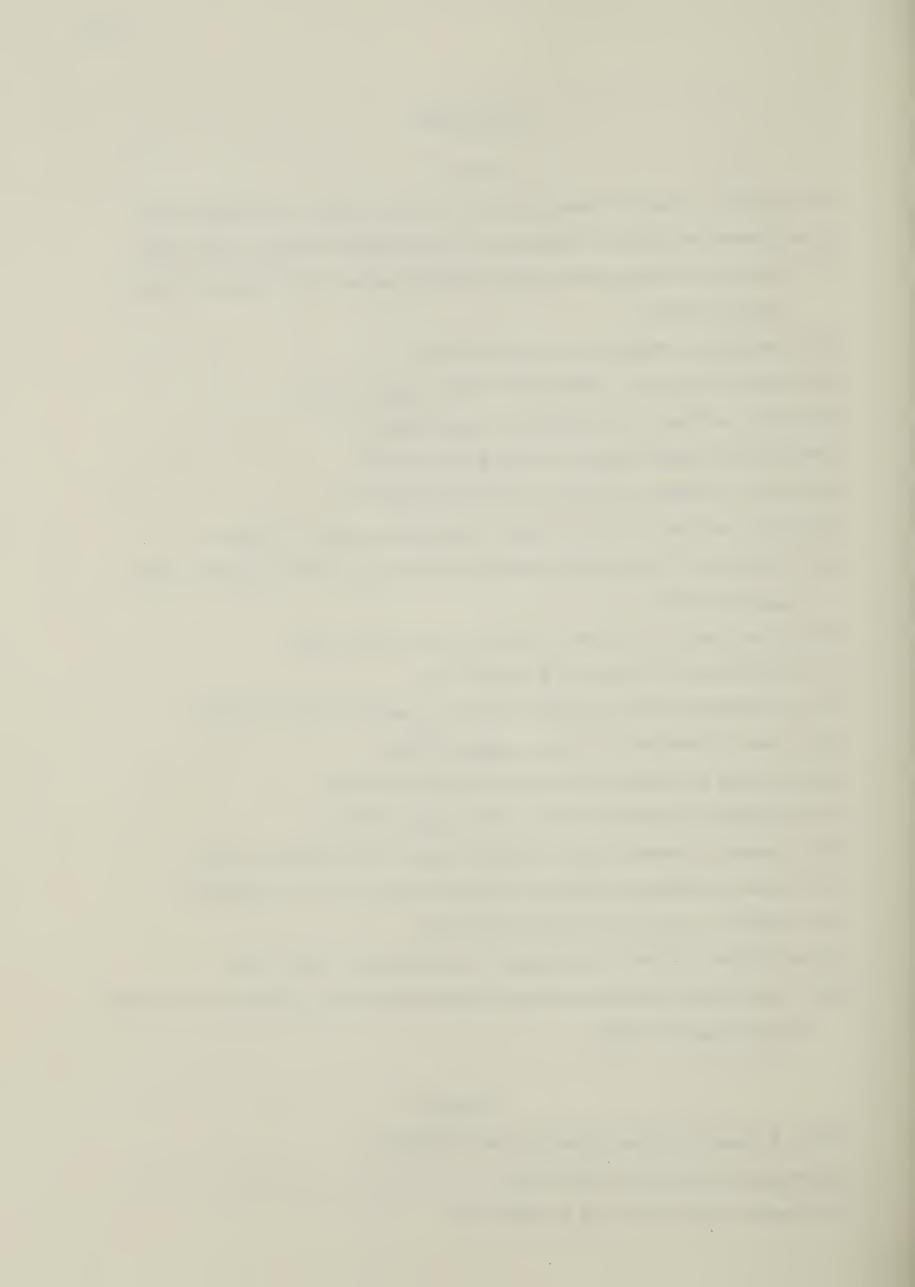
# Bibliography

## Chapter 1

(1) J. Nuckolls, L. Wood, A. Thiessen, and G. Zimmerman, Nature, 2 3 9 (Sep. 1972).

(2) J.M. Dawson, R.E. Kidder, A. Hertzberg, G.C. Vlases and H.G. Ahlstrom, IAEA Fourth
    Conference on Plasma Physics and Controlled Nuclear Fusion Research, Madison,
    Wisconsin (1971).

(3) S. Humphries, Jr., Plasma Phys. 1 6, (1974) 623.

(4) S.A. Mani, J.E. Eninger, J. Wallace, Nucl. Fusion 1 5 (1975) 371.

(5) M.D. Feit, J.A. Fleck, Jr., Appl. Phys. Lett., 2 8 (1976) 121.

(6) M.D. Feit, D.E. Maiden, Appl. Phys. Lett 2 8 (1976) 331.

(7) M.D. Feit, J.A. Fleck, Jr., Appl. Phys. Lett., 2 9 (1976) 234.

(8) M.D. Feit, J.A. Fleck, Jr., and J.R. Morris, J. Appl. Phys., 4 8 (1977) 3301.

(9) J.N. McMullin, C.E. Capjack, C.R. James, Phys. Fluids 2 1 (1978) 1828; Phys. Fluids
    2 2 (1979) 953.

(10) L.C. Steinhauer, H.G. Ahlstrom, Phys. Fluids 1 4 (1971) 1109.

(11) L.C. Steinhauer, Phys. Fluids 1 9 (1976) 1740.

(12) A.A. Offenberger, M.R. Cervenan, P.R. Smy, J. Appl. Phys. 4 7 (1976) 494.

(13) C. Cohn, W. Halverson, Phys. Lett., 4 9 A (1974) 95.

(14) G.C. Vlases, N.A. Amherd, Appl. Phys. Lett 2 4 (1974) 93.

(15) H.D. Dudder, D.B. Henderson, Phys. Comm. 1 0 (1975) 155.

(16) M. Hubbard, A. Montes, Culham Laboratory Report, CLM-R189 (Jul. 1978).

(17) G. Rinker, G. Bohannon, IEEE Trans. on Plasma Science P S - 8 (1980) 55.

(18) F. Tappert, J. Opt. Soc. Am. 6 6 (1976) 1368.

(19) J.N. McMullin, R.D. Milroy, C.E. Capjack, Phys. Fluids 2 2 (1979) 1913.

(20) F. Chen,in Laser Interaction and Related Plasma Phenomena 3 A (Schwartz, Hora, Eds)
    Plenum Press (1971) 291.

## Chapter 2

(1) Born, Principle of Optics, Pergamon Press (1980) 435.

(2) E. Wigner, Phy. Rev. 4 0 (1932) 479.

(3) A. Papoulis,J. Opt. Soc. Am. 6 4 (1974) 779.

(4) F. Tappert, J.Opt.Soc.Am. 6 6 (1976) 1368.

(5) Siegman, Introduction to Lasers and Masers, Ch. 8, McGraw-Hill (1971).

(6) Papoulis, Probability, Random Variables and Stochastic Processes, McGraw-Hill
    (1965).

(7) H.D. Dudder, D.B. Henderson, Phys. Comm. 1 0 (1975) 155.

(8) Y.W. Lee, Statistical Theory of Communication, Ch.7, John Wiley & Sons., Inc. (1960)


## Chapter 3

(1) E.G. Harris, Phy. Rev. 1 3 8 (1965) B479.

(2) S. Weinberg, Phy. Rev. 1 2 6 (1962) 1899.

(3) Stix, The Theory of Plasma Waves, McGraw-Hill (1962) 56.

(4) G.C. Pomraning, "High temperature radiative transfer and hydrodynamics", in Progress
    in High Temperature Physics and Chemistry, 4 (C.A. Rouse, Eds) Pergamon Press,
    New York (1971) 39.

(5) J. Nuckolls, L. Wood, A. Thiessen, and G. Zimmerman, Nature 2 3 9 (1972) 239.

(6) S.A. Mani, J.E. Eninger, J. Wallace, Nucl. Fusion 1 5 (1975) 371.

(7) L.C. Steinhauer, H.G. Ahlstrom, Phys. Fluids 1 4 (1971) 1109.


## Chapter 4

(1) Johnston and Dawson, Phys. Fluids 1 6 (1973) 722.

(2) F. Chen in Laser Interaction and Related Plasma Phenomena 3 A (Schwartz, Hora, Eds)
    Plenum Press (1971) 291.

## Appendix 1

### 1.1 Derivation of Poynting vector in eq.(2.1.8)

Assume that the electric field vector $\vec{E}$ has components $\vec{E}_x, \vec{E}_z$ where $|\vec{E}_z| << |\vec{E}_x|$

$$\vec{E} = E_x \hat{x} + E_z \hat{z}$$

From Maxwell's equation,

$$\vec{\nabla} \cdot \vec{E} = 0$$

we get

$$\frac{\partial E_x}{\partial x} + \frac{\partial E_z}{\partial z} = 0 \tag{1}$$

$$\frac{\partial E_x}{\partial x} = \frac{-\partial E_z}{\partial z}$$

Let

$$E_x = \varepsilon(x,y,z)e^{i(kz-\omega t)} \tag{2}$$

Therefore, equation(1) becomes

$$\frac{\partial E_z}{\partial z} = -\frac{\partial \varepsilon}{\partial x} e^{i(kz-\omega t)}$$

$$E_z \doteq \frac{i}{k} \frac{\partial \varepsilon}{\partial x} e^{i(kz-\omega t)} \tag{3}$$

Again from Maxwell's equation,

$$\vec{\nabla} \times \vec{E} = -\frac{1}{c} \frac{\partial \vec{B}}{\partial t}$$

With

$$\vec{B} = \vec{B}(x,y,z)e^{i(kz-\omega t)}$$

$$\vec{B} = \frac{-ic}{\omega}\vec{\nabla} \times \vec{E}$$

Substituting $\vec{E}$ with eq.(2) and (3),

$$\vec{B} = \frac{-ic}{\omega}[\frac{\partial E_z}{\partial y}\hat{x} + (\frac{\partial E_x}{\partial z} - \frac{\partial E_z}{\partial x})\hat{y} - \frac{\partial E_x}{\partial y}\hat{z}]$$

$$\doteq \frac{-ic}{\omega}[\frac{i}{k}\frac{\partial^2 \epsilon}{\partial x \partial y}\hat{x} + (ik\epsilon + \frac{\partial \epsilon}{\partial z} - \frac{i}{k}\frac{\partial^2 \epsilon}{\partial x^2})\hat{y} - \frac{\partial \epsilon}{\partial y}\hat{z}]e^{i(kz-\omega t)}$$

Dropping the second order derivative of $\epsilon$,

$$\vec{B} = \frac{-ic}{\omega}[(ik\epsilon + \frac{\partial \epsilon}{\partial z})\hat{y} - \frac{\partial \epsilon}{\partial y}\hat{z}]e^{i(kz-\omega t)}$$
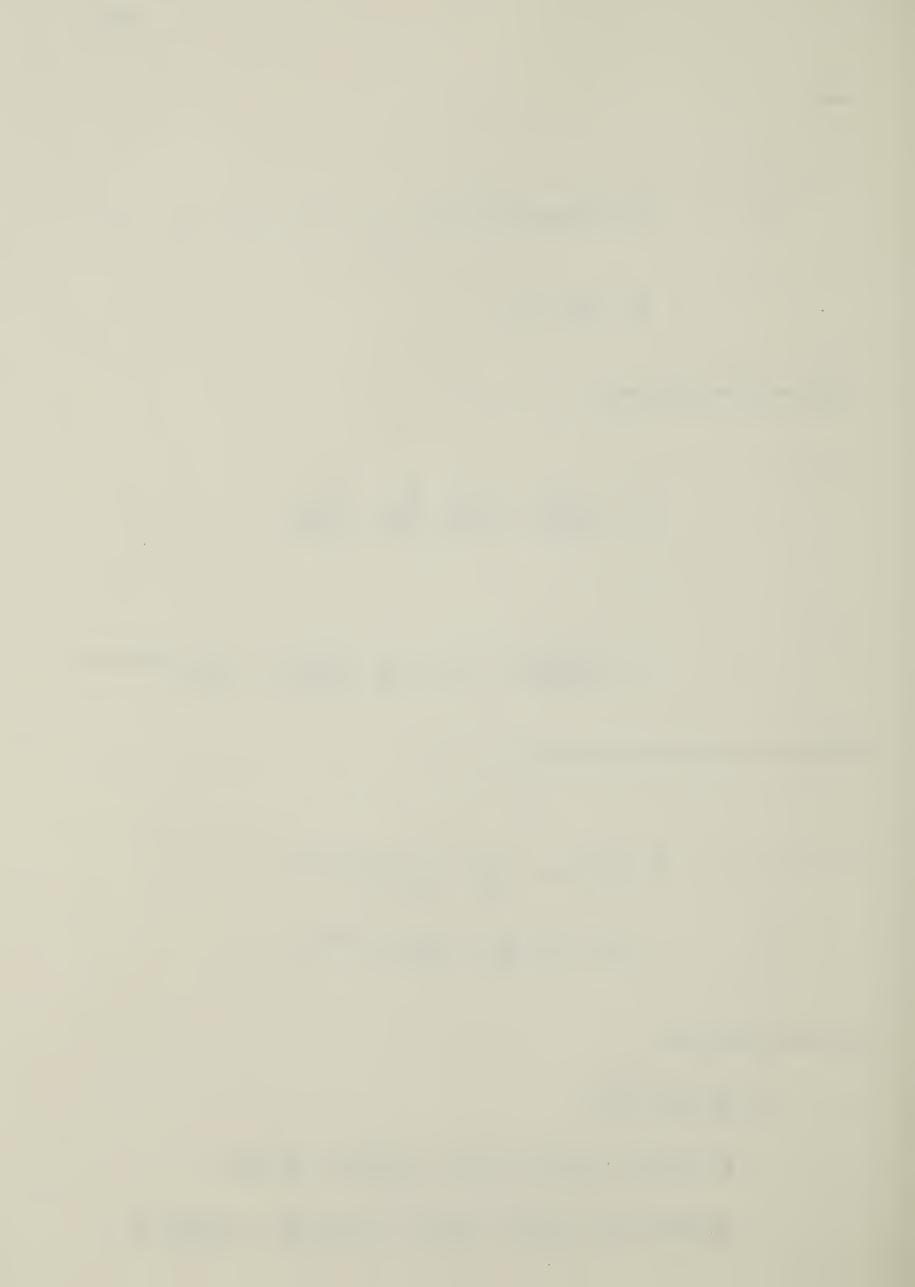
$$= [\epsilon\hat{y} + \frac{ic}{\omega}(-\frac{\partial \epsilon}{\partial z}\hat{y} + \frac{\partial \epsilon}{\partial y}\hat{z})]e^{i(kz-\omega t)}$$

The Poynting vector $\vec{S}$ is

$$\vec{S} = \frac{c}{8\pi} Re[\vec{E} \times \vec{B}^*]$$

$$= \frac{c}{8\pi} Re[(\epsilon\hat{x} + \frac{i}{k}\frac{\partial \epsilon}{\partial x}\hat{z}) \times [\epsilon^*\hat{y} - \frac{ic}{\omega}(\frac{-\partial \epsilon^*}{\partial z}\hat{y} + \frac{\partial \epsilon^*}{\partial y}\hat{z})]]$$

$$= \frac{c}{8\pi} Re[|\epsilon|^2\hat{z} - \frac{i}{k}\epsilon^*\frac{\partial \epsilon}{\partial x}\hat{x} + \frac{ic}{\omega}\epsilon\frac{\partial \epsilon^*}{\partial z}\hat{z} + \frac{ic}{k\omega}\frac{\partial \epsilon}{\partial x}\frac{\partial \epsilon^*}{\partial z}\hat{x} + \frac{ic}{\omega}\epsilon\frac{\partial \epsilon^*}{\partial y}\hat{y}]$$

Assume

$$|\epsilon|^2 \gg |\frac{1}{k}\epsilon\frac{\partial\epsilon^*}{\partial z}| \qquad\qquad |\epsilon^*\frac{\partial\epsilon}{\partial x}| \gg \frac{1}{k}|\frac{\partial\epsilon}{\partial x}||\frac{\partial\epsilon^*}{\partial z}|$$

Then,

$$\vec{S} = \frac{c}{8\pi} \text{Re}[|\epsilon|^2\ \hat{z} - \frac{i}{k}\epsilon^*\frac{\partial\epsilon}{\partial x}\ \hat{x} + \frac{ic}{\omega}\epsilon\frac{\partial\epsilon^*}{\partial y}\ \hat{y}]$$

$$= \frac{c}{8\pi}\ [|\epsilon|^2\hat{z} + \frac{i}{2k}[(\epsilon\frac{\partial\epsilon^*}{\partial x} - \epsilon^*\frac{\partial\epsilon}{\partial x})\ \hat{x} + (\epsilon\frac{\partial\epsilon^*}{\partial y} - \epsilon^*\frac{\partial\epsilon}{\partial y})\ \hat{y}]$$

$$= \frac{c}{8\pi}\ [|\epsilon|^2\hat{z} + \frac{i}{2k}[\epsilon\frac{\partial\epsilon^*}{\partial x}\ \hat{x} + \epsilon\frac{\partial\epsilon^*}{\partial y}\ \hat{y} - (\epsilon^*\frac{\partial\epsilon}{\partial x}\ \hat{x} + \epsilon^*\frac{\partial\epsilon}{\partial y}\ \hat{y})]]$$

$$= \frac{c}{8\pi}\ [|\epsilon|^2\hat{z} + \frac{i}{2k}(\epsilon\vec{\nabla}_\perp\epsilon^* - \epsilon^*\vec{\nabla}_\perp\epsilon)]$$

$$= \frac{c}{8\pi}\ [|\epsilon|^2\hat{z} - \frac{i}{2k}(\epsilon^*\vec{\nabla}_\perp\epsilon - \epsilon\vec{\nabla}_\perp\epsilon^*)]$$

## Appendix 2

### 2.1 Derivation of the electric field after the lens plane

The far field approximation of the electric field of a laser beam at a distance of z from the source is given as[5]

$$u(r,z) = \sqrt{\frac{2}{\pi}} \frac{1}{w(z)} e^{i(kz-\Phi(z))} e^{-\frac{r^2}{w^2(z)}} e^{-\frac{ikr^2}{2R(z)}}$$

(1)

where

$$\Phi = \tan^{-1}\left(\frac{\lambda z}{\pi w_0^2}\right)$$

$$R(z) = z\left[1 + \left(\frac{\pi w_0^2}{\lambda z}\right)^2\right]$$
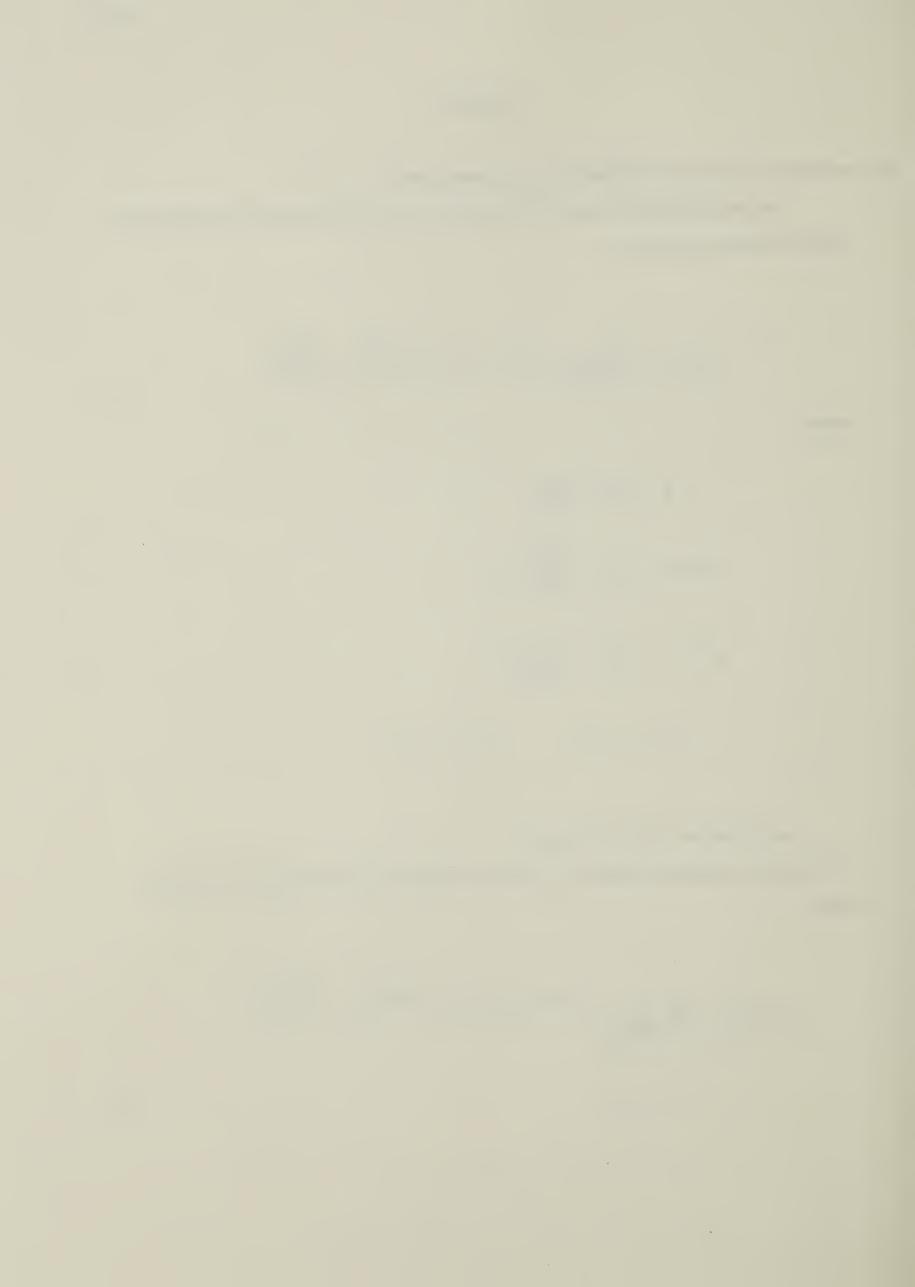
$$w^2(z) = w_0^2\left[1 + \left(\frac{\lambda z}{\pi w_0^2}\right)^2\right]$$

$$r^2 = x^2 + y^2 \qquad \text{and} \quad r \ll R$$

$w_0$ is the beam waist of the laser.

If a thin lens is placed at a distance $z_0$ from the origin, the field amplitude of the light beam is

$$u(r,z_0) = \sqrt{\frac{2}{\pi}} \frac{1}{w(z_0)} e^{-i(kz_0-\Phi(z_0))} e^{-\frac{r^2}{w^2(z_0)}} e^{-\frac{ikr^2}{2R(z_0)}}$$

(2)

On passing through the lens, the field amplitude becomes

$$u(r,z_1) = \sqrt{\frac{2}{\pi}} \frac{1}{w(z_1)} e^{-i(kz_1 - \phi(z_1))} e^{-\frac{r^2}{w^2(z_1)}} e^{\frac{ikr^2}{2R(z_1)}}$$

(3)

where $R(z_1)$ is negative (by convention) since the beam converges. But the radius of curvature of the wavefront is related to the focal length of a thin lens by

$$\frac{1}{R(z_1)} = [\frac{1}{R(z_0)} - \frac{1}{f_L}]$$

(4)

The field becomes

$$u(r,z_1) = \sqrt{\frac{2}{\pi}} \frac{1}{w(z_1)} e^{-i(kz_1 - \phi(z_1))} e^{-r^2[\frac{1}{w^2(z_1)} - \frac{ik}{2R(z_0)} + \frac{ik}{2f_L}]}$$

(5)

Since the lens is assumed to be thin, the axial distance and spotsize are approximated as
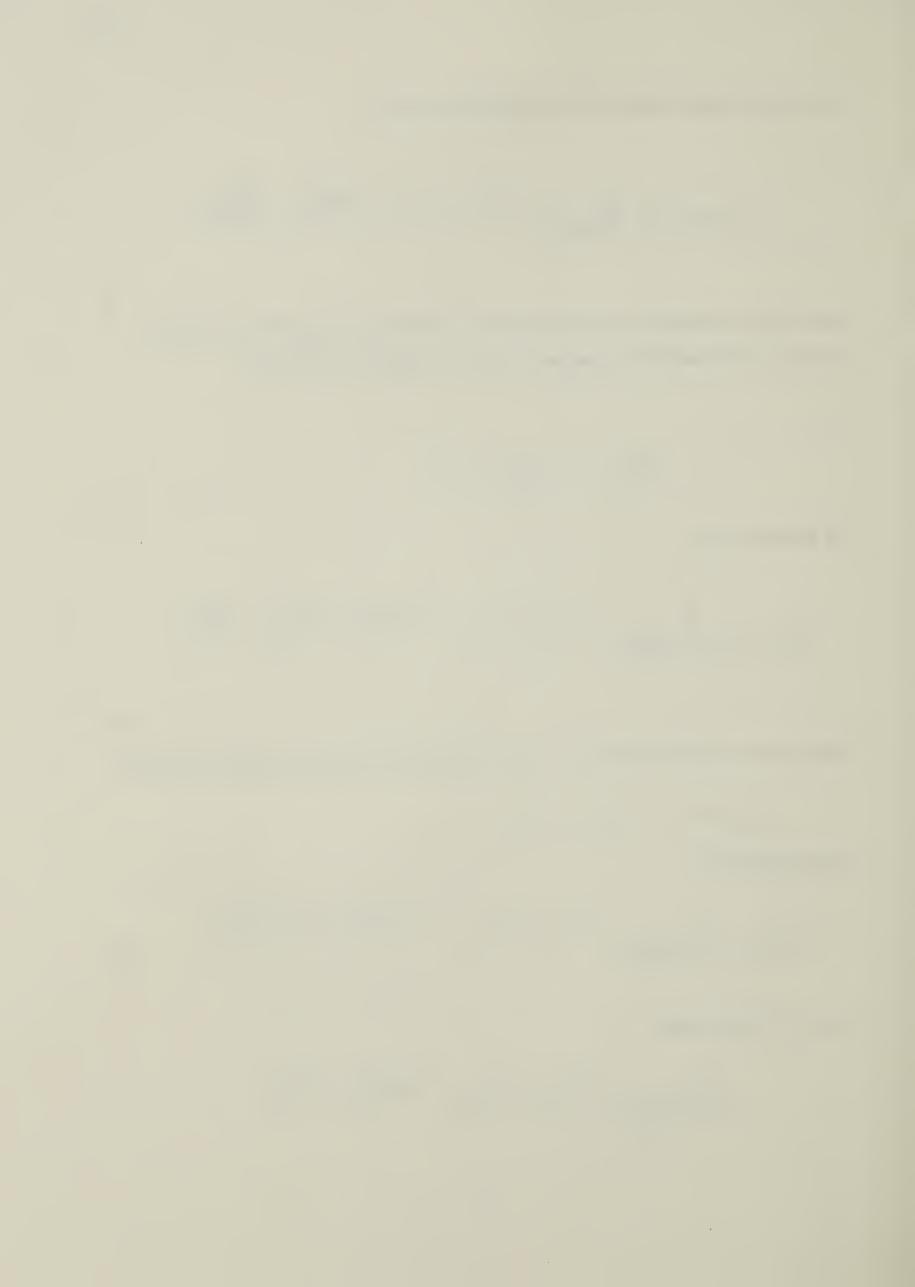
$$z_0 = z_1, \qquad w(z_0) = w(z_1)$$

The field becomes

$$u(r,z_1) = \sqrt{\frac{2}{\pi}} \frac{1}{w(z_0)} e^{-i(kz_0 - \phi(z_0))} e^{-r^2[\frac{1}{w^2(z_0)} + \frac{ik}{2f_L} - \frac{ik}{2z_0}]}$$

(6)

As $z_0 >> 1$ for far field,

$$= \sqrt{\frac{2}{\pi}} \frac{1}{w(z_0)} e^{-i(kz_0 - \phi(z_0))} e^{-r^2[\frac{1}{w^2(z_0)} + \frac{ik}{2f_L}]}$$

Let

$$E_0 = \sqrt{\frac{2}{\pi}} \frac{1}{w(z_0)} e^{-i(kz_0 - \Phi(z_0))}$$

the electric field becomes

$$u(r, z_1) = E_0 e^{\frac{-r^2}{w^2(z_0)}} e^{\frac{-ikr}{2f_L}}$$

(7)
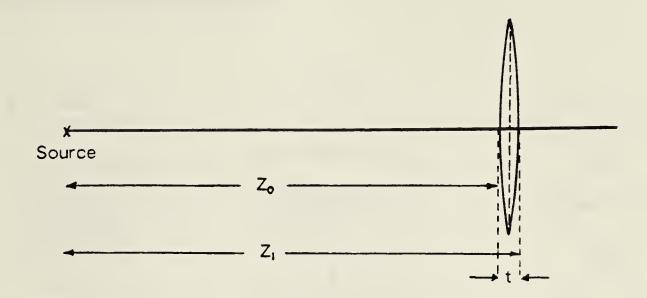
Fig. 2.1 Optical system described in Appendix 2

# Appendix 3

## 3.1 Program listings and flowcharts
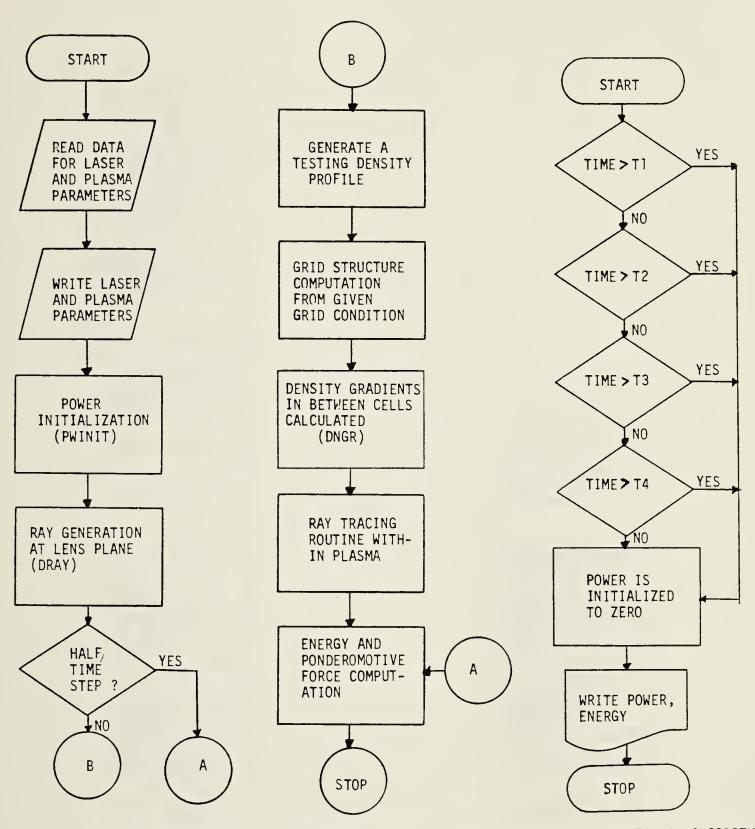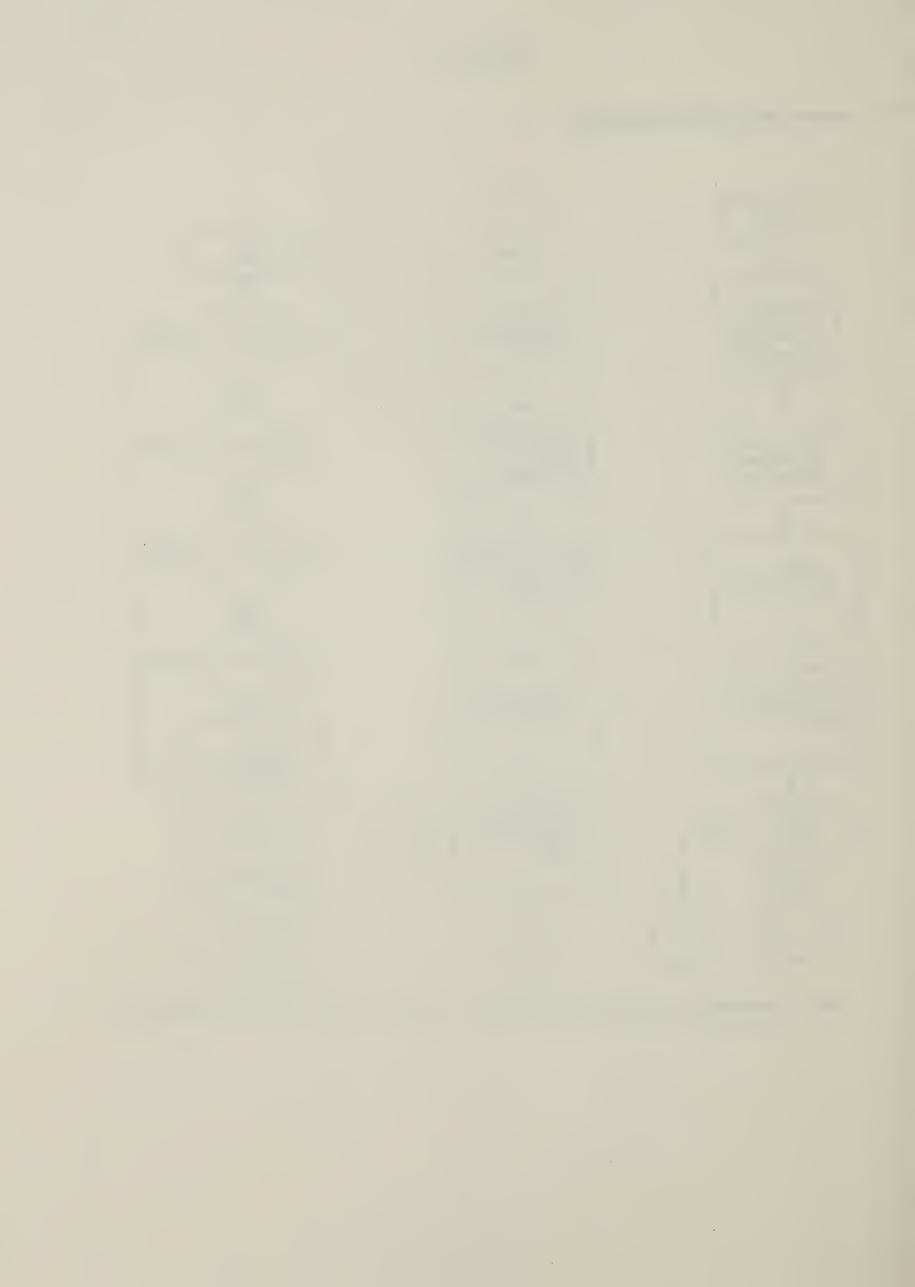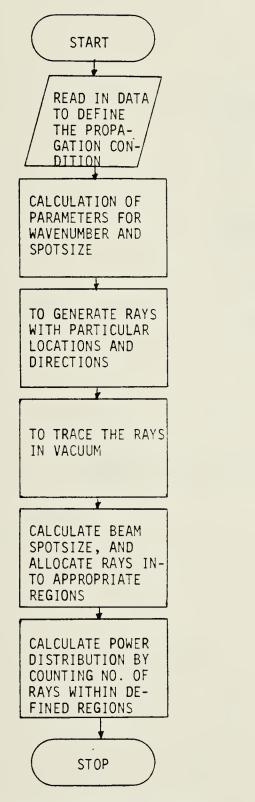


CHART I. PROGRAM FOR TESTING SUBROUTINE PACKAGES     CHART 2. POWER INITIALIZATION ALGORITHM

```
        ┌─────────────┐
        │    START    │
        └─────────────┘
               │
               ▼
       ╱──────────────╱
      ╱ READ IN DATA ╱
     ╱  TO DEFINE   ╱
    ╱   THE PROPA-  ╱
   ╱    GATION CON-╱
  ╱      DITION    ╱
  ────────────────
               │
               ▼
       ┌──────────────┐
       │CALCULATION OF│
       │PARAMETERS FOR│
       │WAVENUMBER AND│
       │SPOTSIZE      │
       └──────────────┘
               │
               ▼
       ┌──────────────┐
       │TO GENERATE RAYS│
       │WITH PARTICULAR │
       │LOCATIONS AND   │
       │DIRECTIONS      │
       └──────────────┘
               │
               ▼
       ┌──────────────┐
       │TO TRACE THE RAYS│
       │IN VACUUM        │
       └──────────────┘
               │
               ▼
       ┌──────────────┐
       │CALCULATE BEAM │
       │SPOTSIZE, AND  │
       │ALLOCATE RAYS IN-│
       │TO APPROPRIATE │
       │REGIONS        │
       └──────────────┘
               │
               ▼
       ┌──────────────┐
       │CALCULATE POWER│
       │DISTRIBUTION BY│
       │COUNTING NO. OF│
       │RAYS WITHIN DE-│
       │FINED REGIONS  │
       └──────────────┘
               │
               ▼
        ┌─────────────┐
        │    STOP     │
        └─────────────┘
```
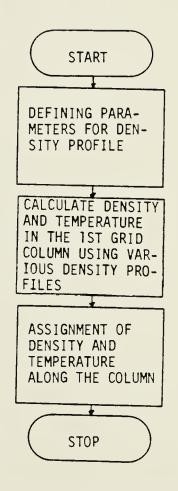
CHART 3. RAY GENERATION ALGORITHM

```
        ┌─────────────┐
        │    START    │
        └─────────────┘
               │
               ▼
       ┌──────────────┐
       │DEFINING PARA-│
       │METERS FOR DEN-│
       │SITY PROFILE  │
       └──────────────┘
               │
               ▼
       ┌──────────────┐
       │CALCULATE DENSITY│
       │AND TEMPERATURE │
       │IN THE 1ST GRID │
       │COLUMN USING VAR-│
       │IOUS DENSITY PRO-│
       │FILES           │
       └──────────────┘
               │
               ▼
       ┌──────────────┐
       │ASSIGNMENT OF │
       │DENSITY AND   │
       │TEMPERATURE   │
       │ALONG THE COLUMN│
       └──────────────┘
               │
               ▼
        ┌─────────────┐
        │    STOP     │
        └─────────────┘
```

CHART 4. DENSITY AND TEMPERATURE PROFILE ALGORITHM
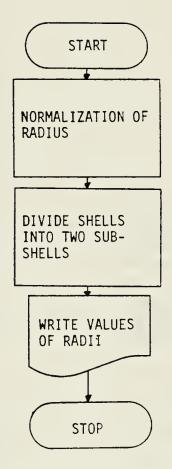
CHART 5. FINE GRID STRUCTURE ALGORITHM
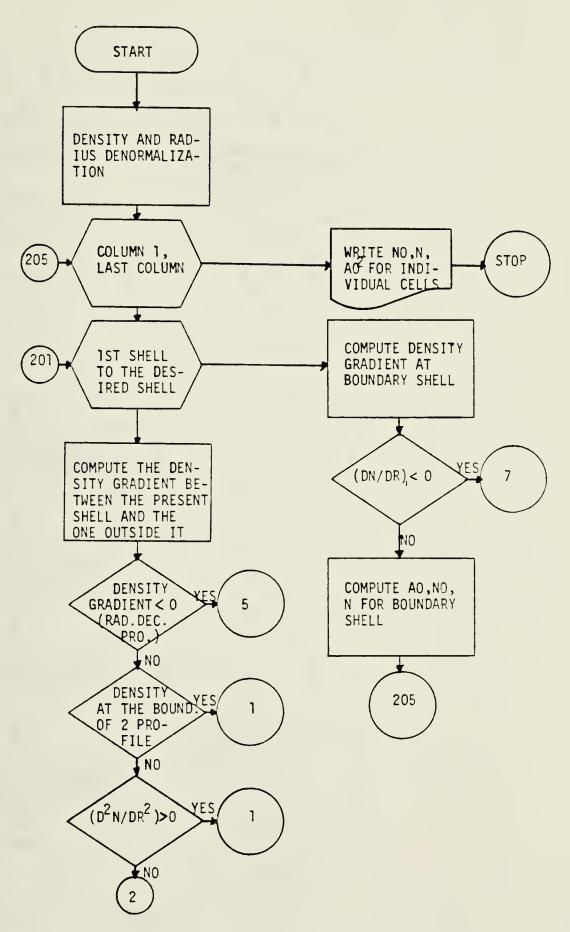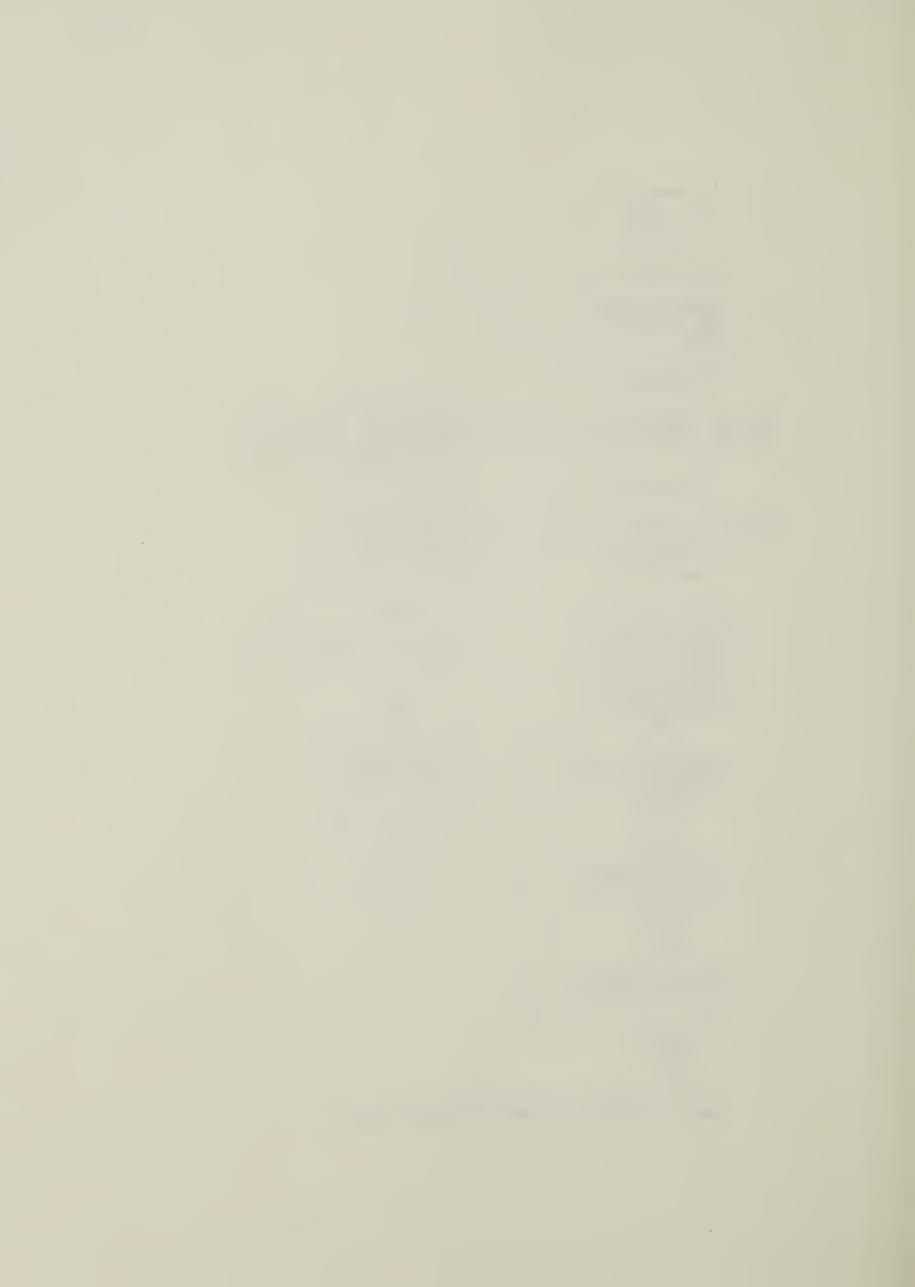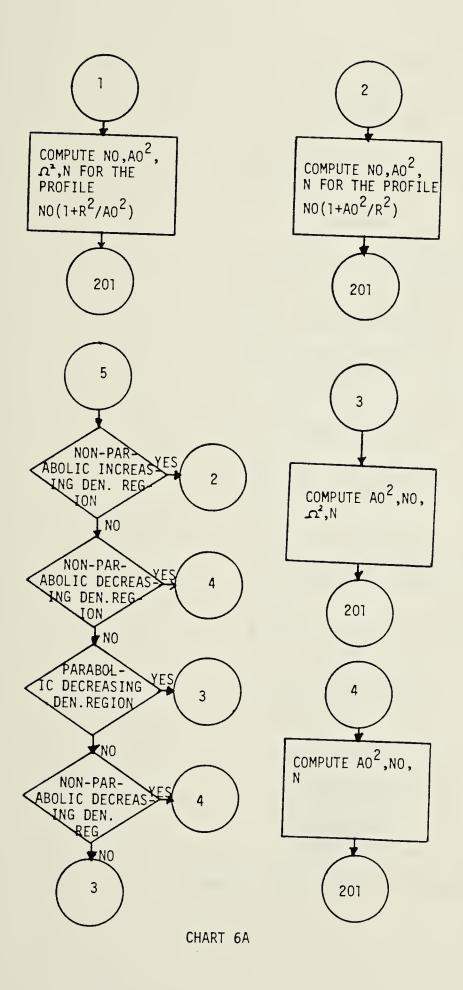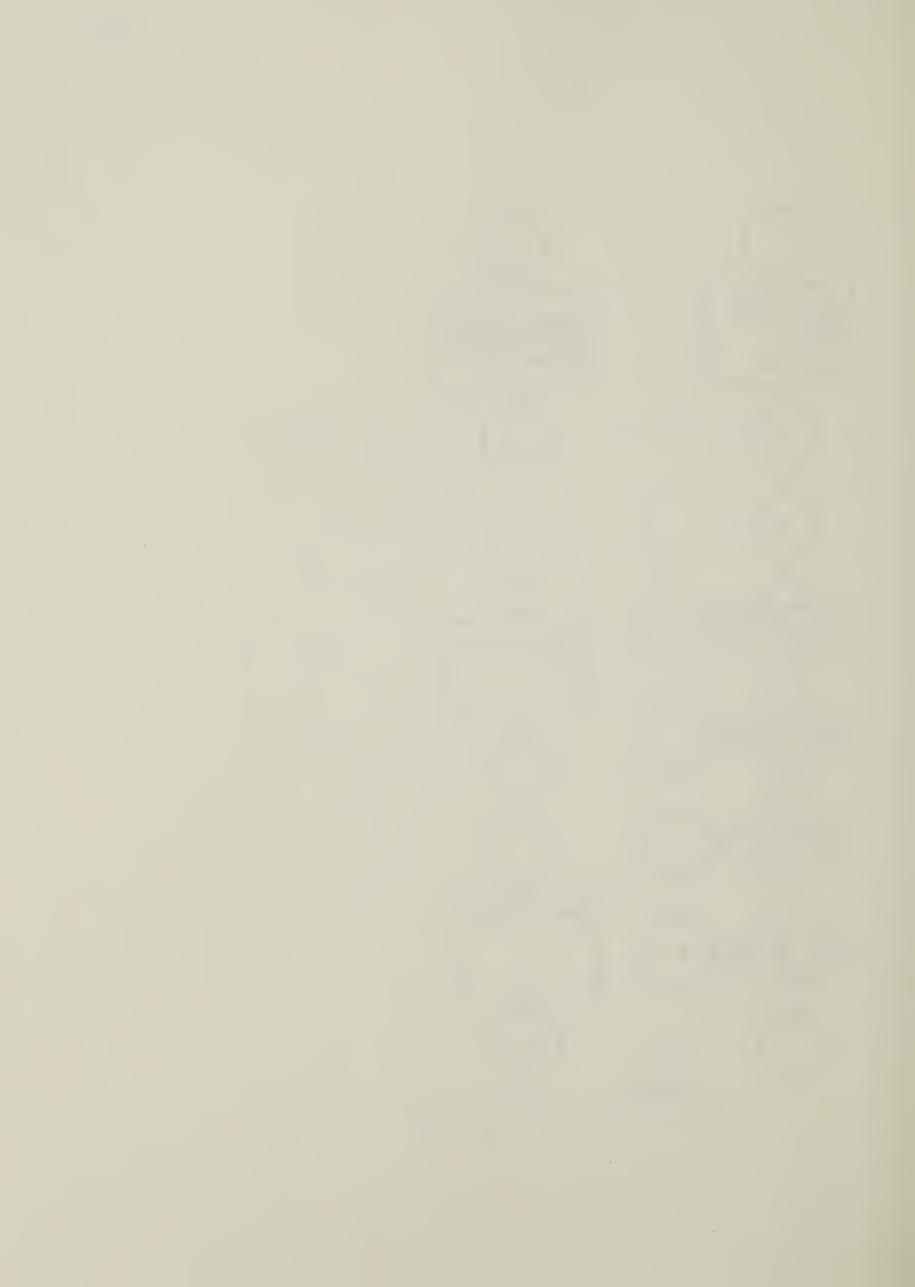
CHART 6. ALGORITHM FOR COMPUTING DENSITY GRADIENT

COMPUTE NO,$AO^2$, $\Omega^2$,N FOR THE PROFILE $NO(1+R^2/AO^2)$

201

5

NON-PARABOLIC INCREASING DEN. REGION — YES → 2

NO

NON-PARABOLIC DECREASING DEN.REGION — YES → 4

NO

PARABOLIC DECREASING DEN.REGION — YES → 3

NO

NON-PARABOLIC DECREASING DEN. REG — YES → 4

NO

3

COMPUTE NO,$AO^2$, N FOR THE PROFILE $NO(1+AO^2/R^2)$

201

3

COMPUTE $AO^2$,NO, $\Omega^2$,N

201

4

COMPUTE $AO^2$,NO, N

201

CHART 6A
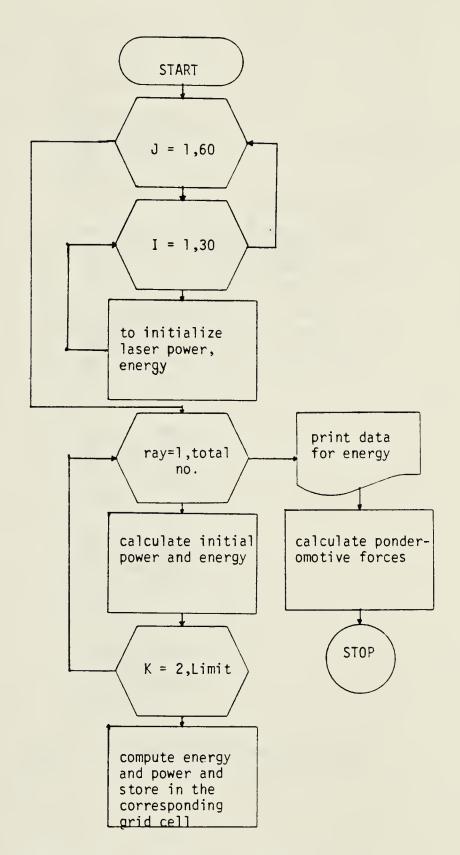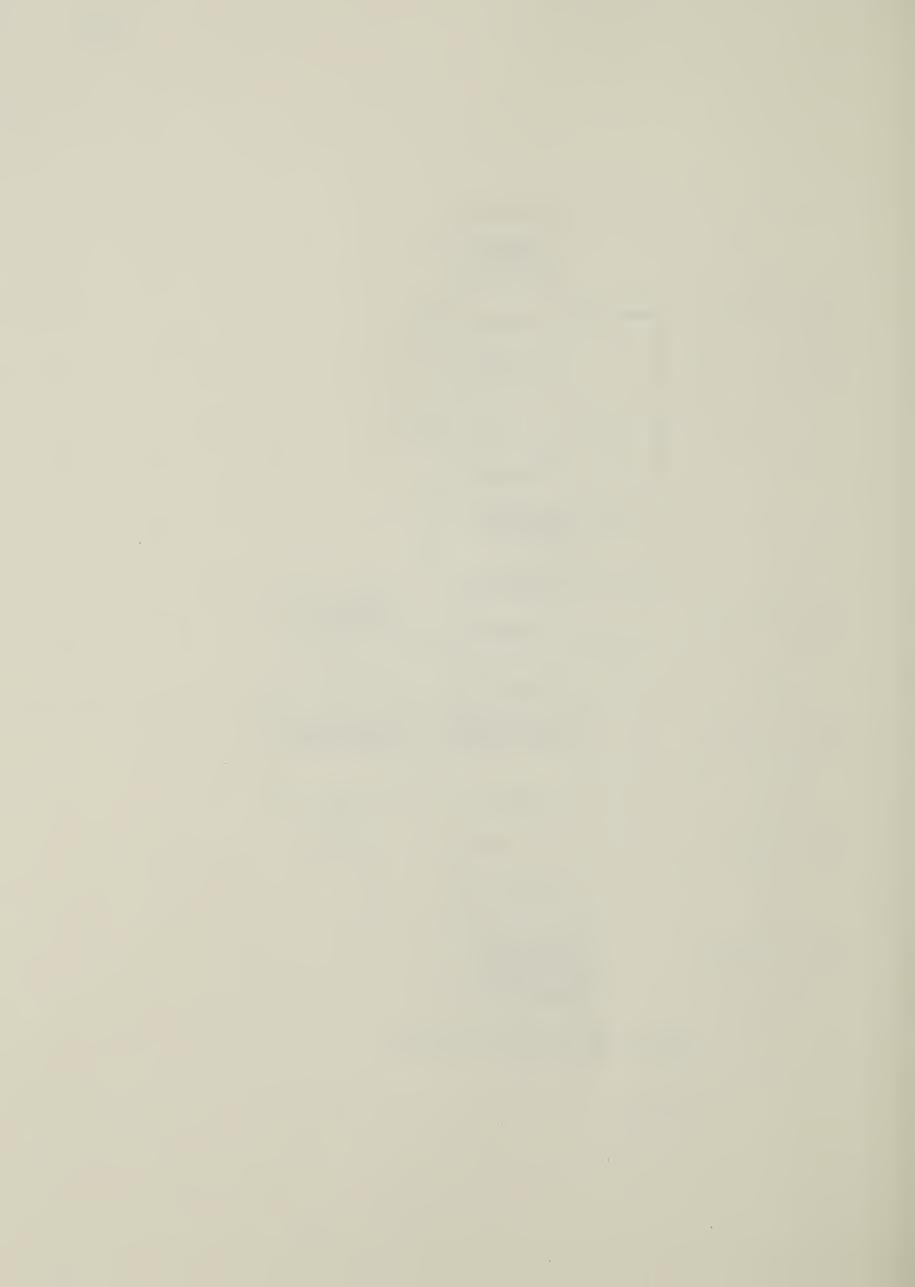
CHART 7. ENERGY ABSORPTION ALGORITHM

START

CALCULATE AVE-
RAGE BEAM INTEN-
SITY IN EACH
CELL

2ND SHELL LAY-
ER TO 29TH
LAYER

PRINT PONDER-
OMOTIVE
FORCES

CALCULATE POWER,
VELOCITIES IN
UPPER,LOWER,LEFT,
AND RIGHT CELLS;
INTENSITY GRAD...

STOP

CALCULATE RADIAL
AND AXIAL POND-
EROMOTIVE FORCE
AT THE INNERMOST
LAYER

CALCULATE RADIAL
AND AXIAL POND-
EROMOTIVE FORCE
AT THE OUTERMOST
LAYER

CALCULATE FORCES
AT COLUMN 1,
LAST COLUMN AND
CORNER CELLS

CHART 8. ALGORITHM FOR PONDEROMOTIVE FORCE
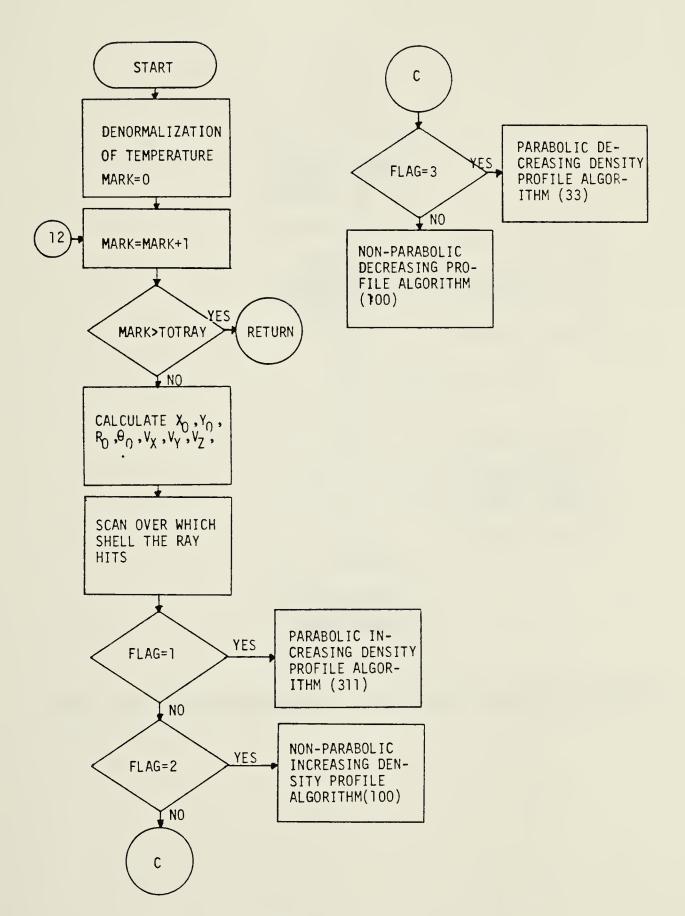
CHART 9. RAY TRACING PROGRAM ROUTINE
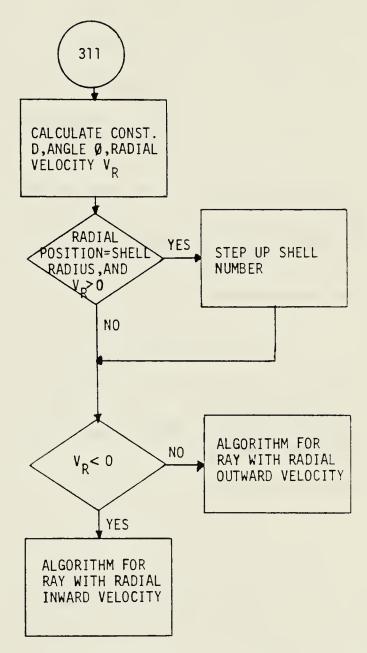
CHART 10. ALGORITHM FOR LOCATING RAY IN THE REGION WITH DENSITY $N_0(1+R^2/A0^2)$
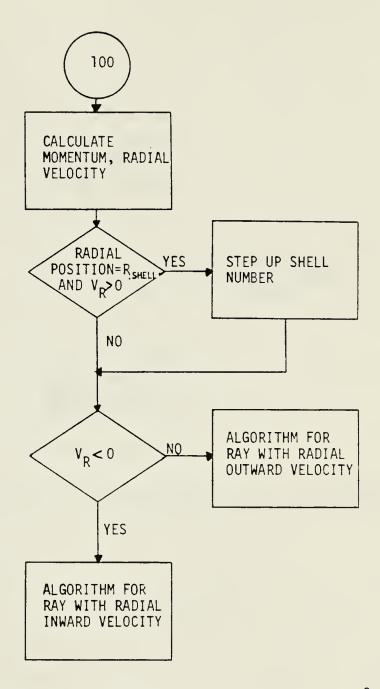
CHART 11. ALGORITHM FOR LOCATING RAY IN THE REGION WITH DENSITY $N_0(1+A0^2/R^2)$

$$\boxed{33}$$

EVALUATE CONSTS.
$\frac{R^2}{2} + \frac{V^2}{2\Omega^2}$, $\frac{XV_X + YV_Y}{\Omega}$,
IN EQN.(3.3.3.6)

$\frac{XV_X + YV_Y}{\Omega} < 0$

YES → ALGORITHM FOR RADIAL INWARD VELOCITY

NO ↓

ALGORITHM FOR RADIAL OUTWARD VELOCITY
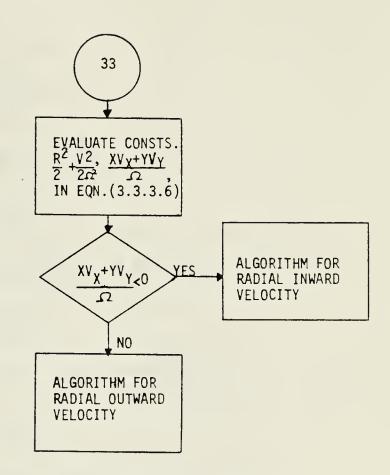
CHART 12. ALGORITHM LOCATING RAYS IN THE REGION WITH DENSITY $N_0(1-R^2/AO^2)$
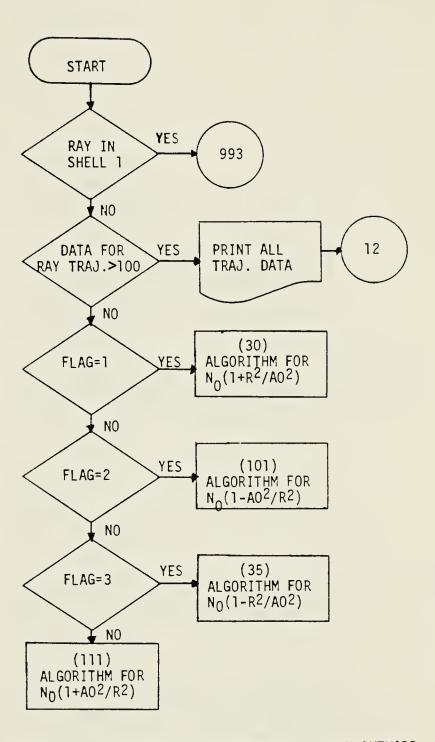
CHART 13. ALGORITHM FOR RAYS GOING RADIALLY OUTWARD
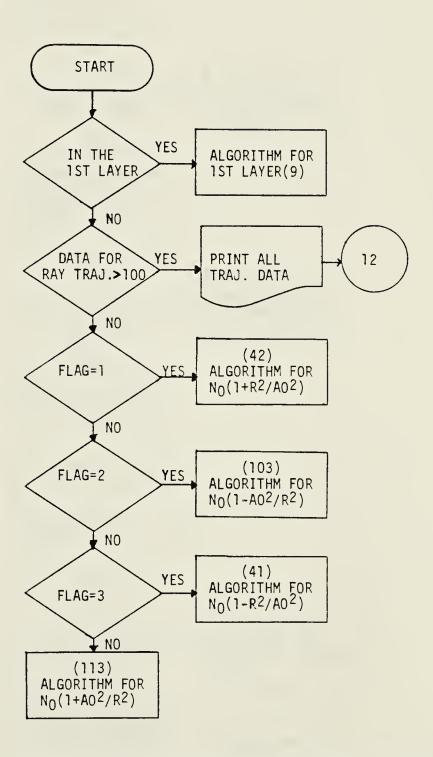
CHART 14. ALGORITHM FOR RAYS GOING RADIALLY OUTWARD
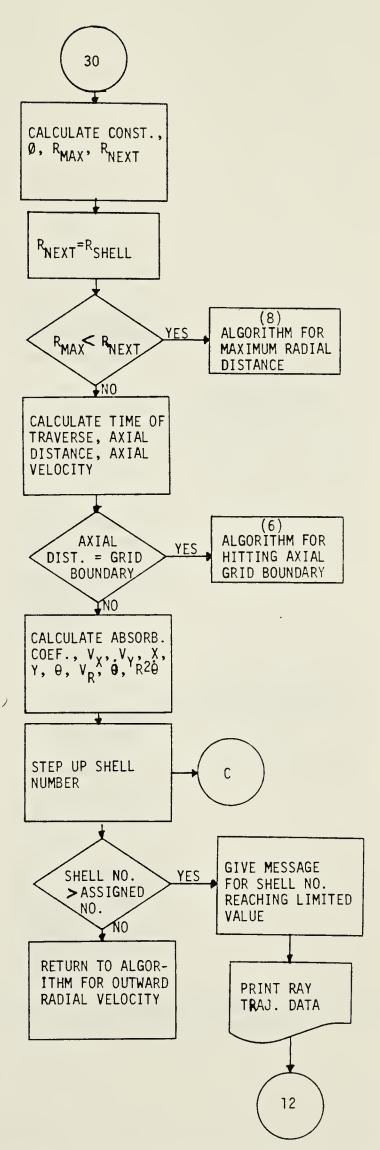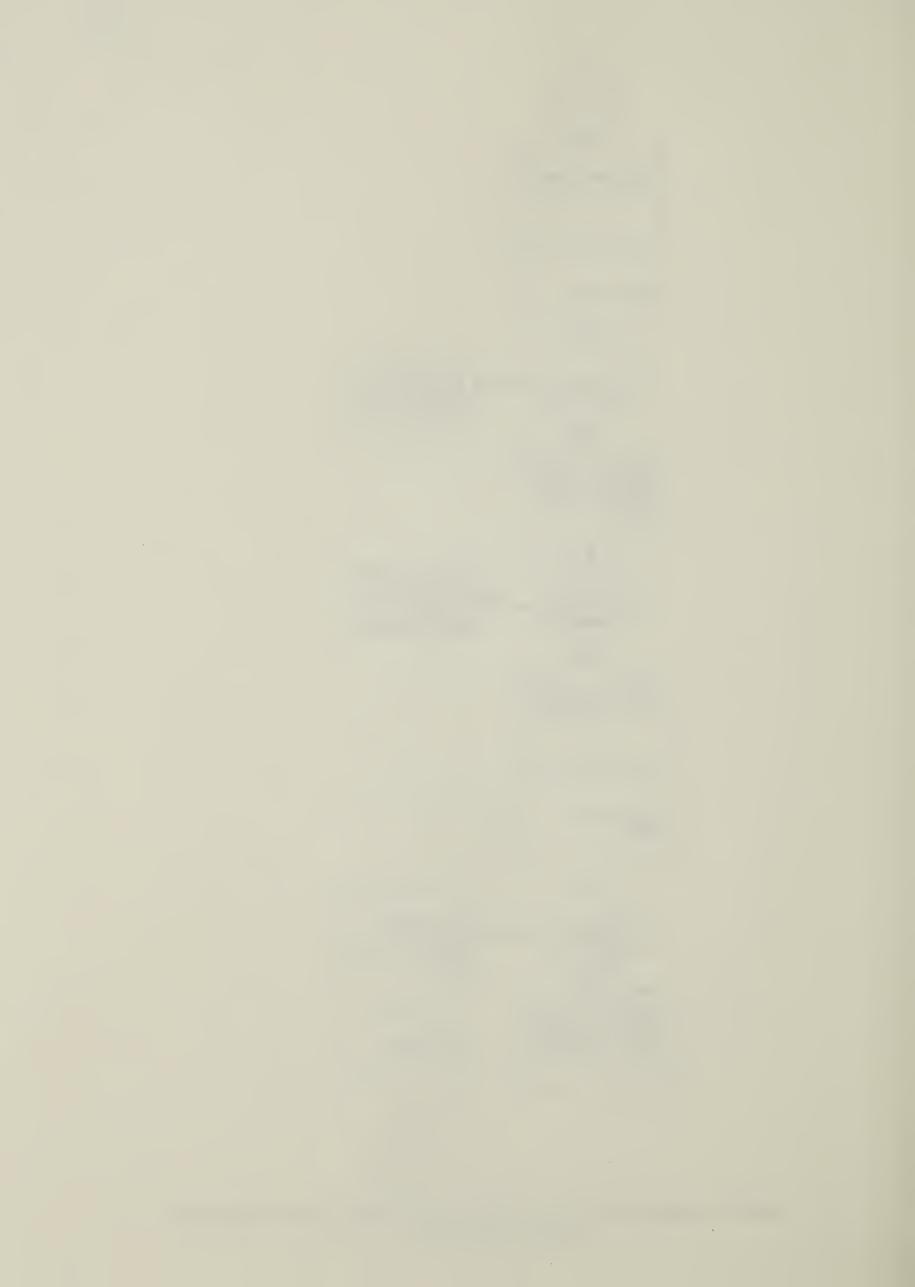
CHART 15. ALGORITHM FOR RAYS WITH RADIAL OUTWARD VELOCITY IN THE REGION WITH DENSITY $N_0(1+R^2/A0^2)$

```
        ┌──────┐
        │ 101  │
        └──┬───┘
           ▼
  ┌─────────────────────┐
  │ CALCULATE CONST.    │
  │ R4θ²-C²N0A0²/Nc      │
  └──────────┬──────────┘
             ▼
        ╱─────────╲                    ┌─────────────────────┐
       ╱           ╲      YES           │ ALGORITHM FOR       │
      ╱  CONST. < 0  ╲──────────────────│ NEGATIVE CONST.     │
       ╲           ╱                    │ (105)               │
        ╲─────────╱                     └─────────────────────┘
             │ NO
             ▼
  ┌─────────────────────┐
  │                     │
  │ R_NEXT = R_SHELL    │
  │                     │
  └──────────┬──────────┘
             ▼
  ┌─────────────────────┐
  │ CALCULATE TIME OF   │
  │ TRAVERSE,AXIAL      │
  │ VELOCITY,AXIAL      │
  │ DISTANCE            │
  └──────────┬──────────┘
             ▼
        ╱─────────╲                    ┌─────────────────────┐
       ╱  AXIAL    ╲     YES            │ ALGORITHM FOR       │
      ╱ DIST.= AXIAL ╲──────────────────│ AXIAL GRID BOUND.   │
       ╲ GRID BOUND.╱                   │ (102)               │
        ╲─────────╱                     └─────────────────────┘
             │ NO
             ▼
  ┌─────────────────────┐
  │ CALCULATE ABS.      │
  │ COEF.,θ,V_R,V_X,    │
  │ V_Y, X, Y           │
  └──────────┬──────────┘
             ▼
  ┌─────────────────────┐
  │ STEP UP SHELL       │
  │ NUMBER AND          │
  │ RETURN TO ALG.      │
  │ FOR OUTWARD RAD.    │
  │ VELOCITY            │
  └─────────────────────┘
```
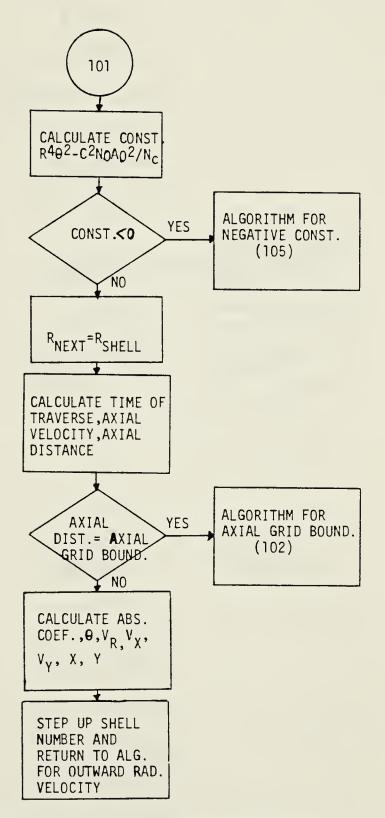
CHART 16. ALGORITHM FOR RAYS WITH RADIALLY OUTWARD VELOCITY IN THE REGION WITH DENSITY PROFILE $N_0(1+A0^2/R^2)$
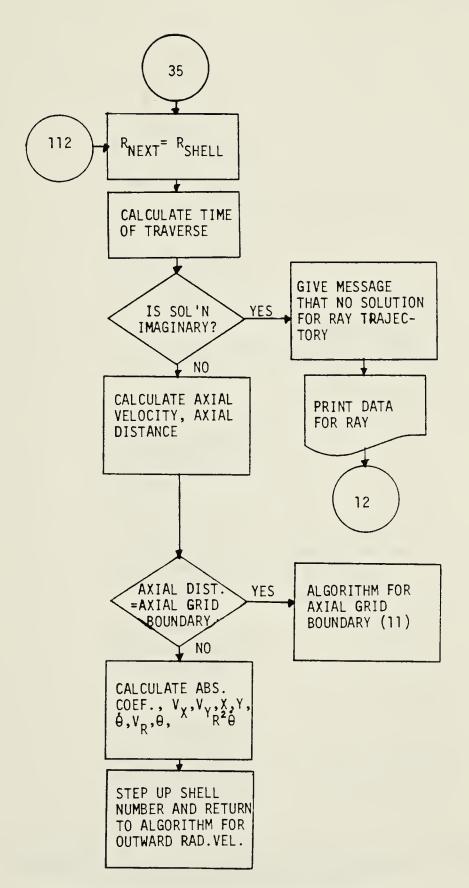
CHART 17. ALGORITHM FOR RAYS WITH RADIALLY OUTWARD VELOCITY IN THE REGION WITH DENSITY PROFILE $N_0(1-R^2/A0^2)$
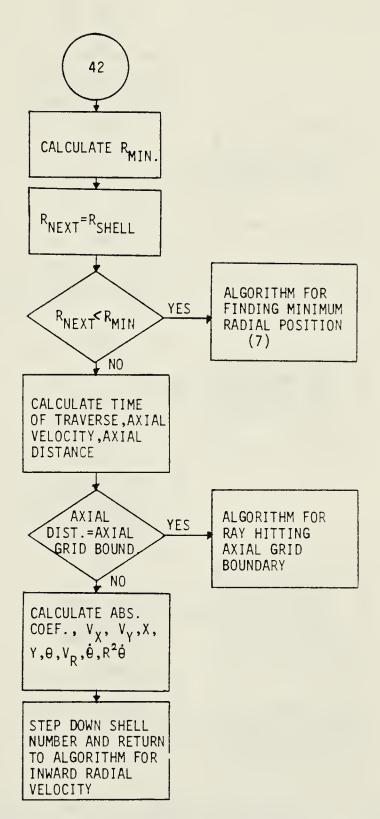
CHART 18. ALGORITHM FOR RAYS WITH RADIALLY OUTWARD VELOCITY IN THE REGION WITH DENSITY PROFILE $N_0(1+R^2/A0^2)$

( 103 )

EVALUATE CONST.
$R^4\theta^2 - c^2 A_0^2 N_0/N_c$

CONST. < 0 — YES → ALGORITHM FOR NEGATIVE CONST. (107)

NO

( 104 ) → CALCULATE $R_{MIN}$
$R_{NEXT} = R_{SHELL}$

$R_{NEXT} < R_{MIN}$ — YES → ALGORITHM FOR COMPUTING MIN. RADIUS (106)

NO

CALCULATE TIME OF TRAVERSE, AXIAL VELOCITY, AXIAL DISTANCE

AXIAL DIST. =AXIAL GRID BOUNDARY — YES → ALGORITHM FOR RAYS HITTING THE AXIAL GRID BOUNDARY (1021)

NO

CALCULATE ABS. COEF., $V_R$, $V_T$, $V_X$, $V_Y$, X, Y → STEP DOWN SHELL NUMBER AND RETURN TO ALGORITHM FOR INWARD RAD. VEL.
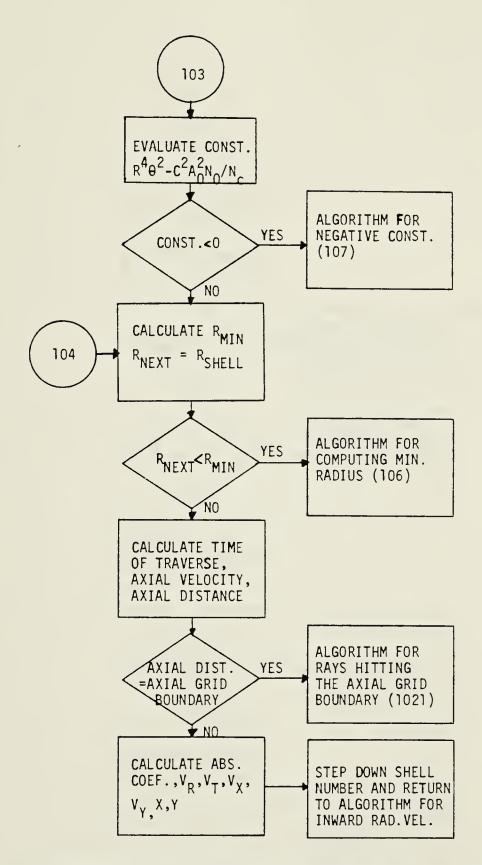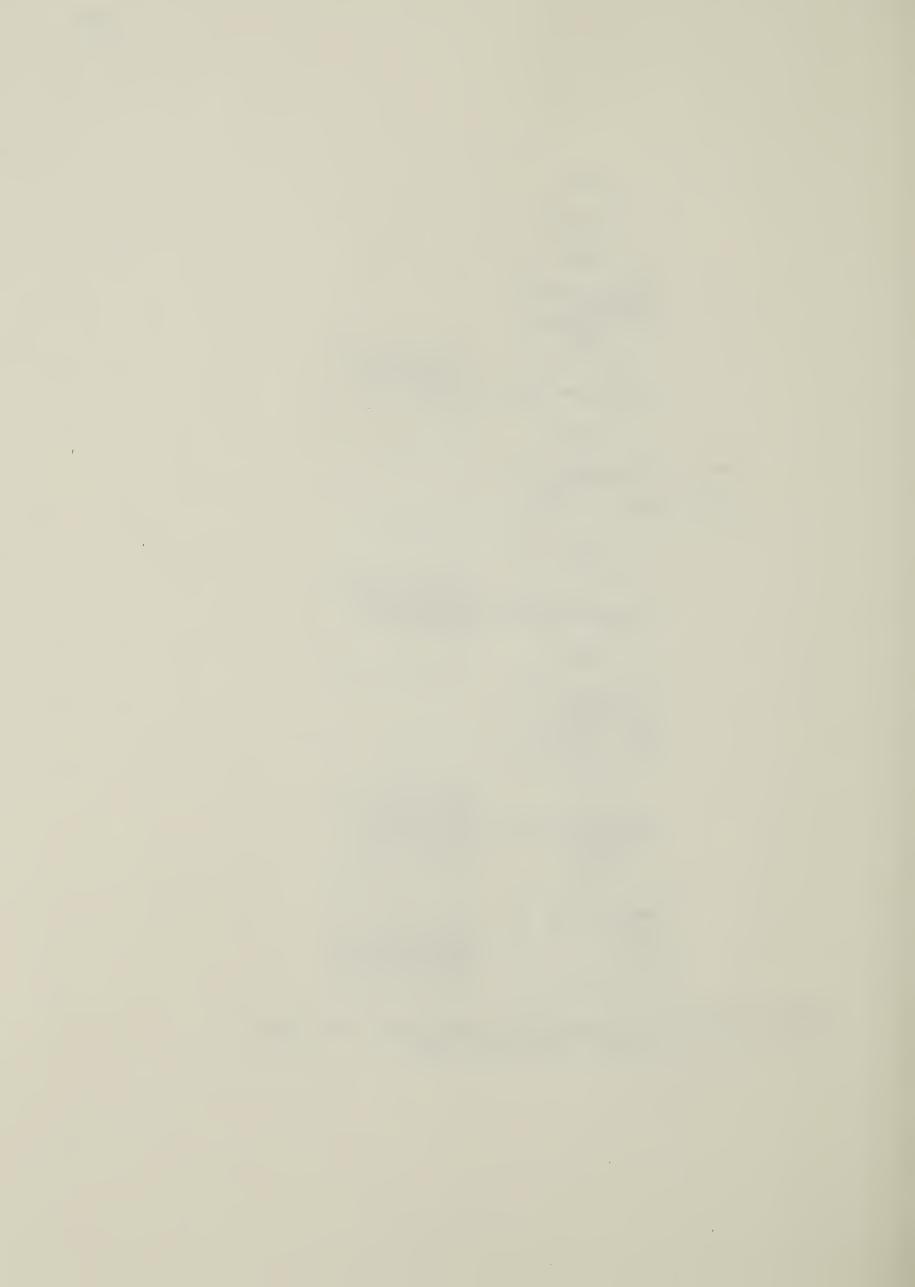
CHART 19. ALGORITHM FOR RAYS WITH RADIALLY INWARD VELOCITY IN THE REGION WITH DENSITY PROFILE $N_0(1-AO^2/R^2)$

**41**

$R_{NEXT} = R_{SHELL}$

CALCULATE $R_{MIN}$

$R_{MIN} < 0$ — YES → WRITE MESSAGE AND PRINT DATA FOR RAYS → **12**

NO

$R_{NEXT} < R_{MIN}$ — YES → ALGORITHM FOR FINDING MINIMUM RADIAL POSITION (43)

NO

CALCULATE TIME OF TRAVERSE, AXIAL VELOCITY, AXIAL DISTANCE

AXIAL DIST.=AXIAL GRID BOUND. — YES → ALGORITHM FOR RAYS HITTING THE AXIAL GRID BOUNDARY (11)

NO

CALCULATE ABS. COEF., $V_X, V_Y, V_R, X, Y, \theta, R^2\dot{\theta}, \dot{\theta}$ → STEP DOWN SHELL NUMBER AND RETURN TO ALGORITHM FOR INWARD RADIAL VELOCITY
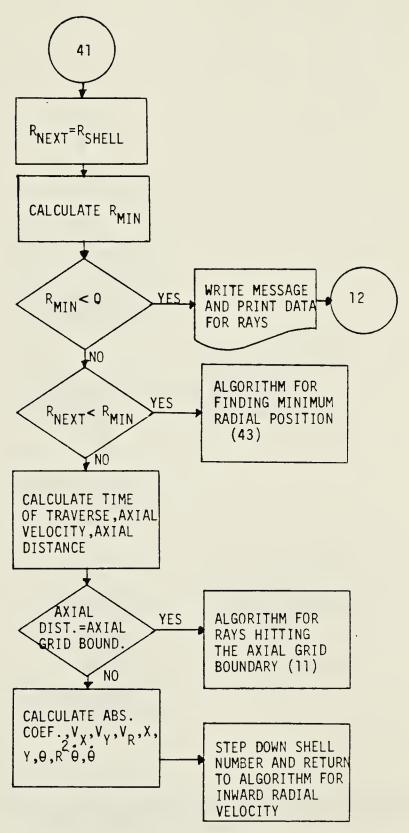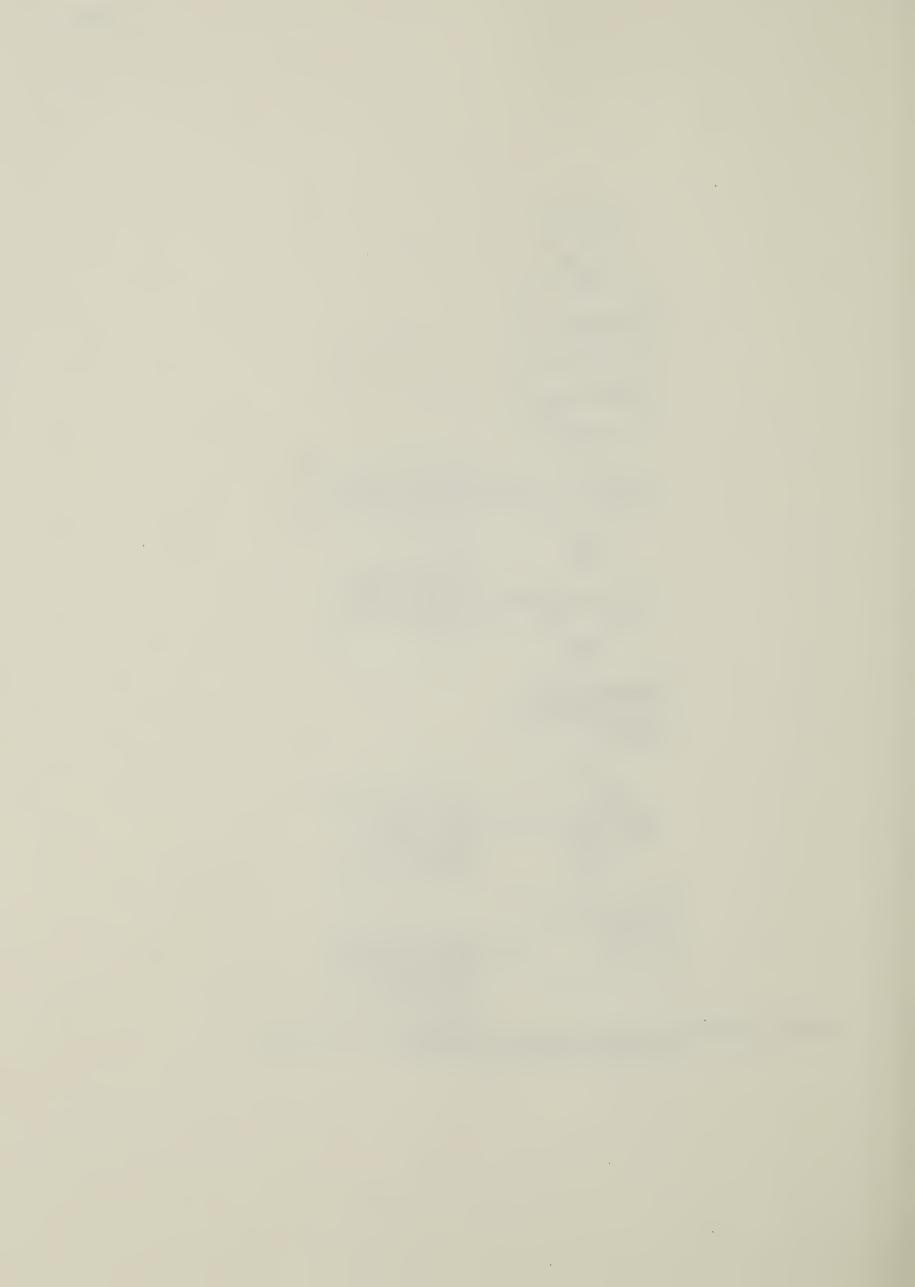
CHART 20. ALGORITHM FOR RAYS WITH RADIALLY INWARD VELOCITY IN THE REGION WITH DENSITY PROFILE $N_o(1-R^2/AO^2)$
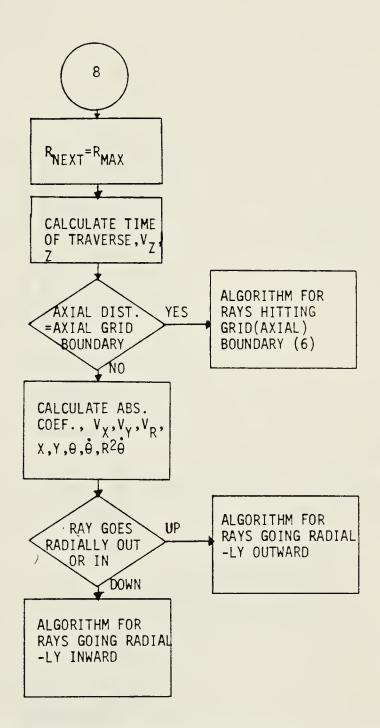
CHART 21. ALGORITHM FOR FINDING MAXIMUM RADIAL POSITION IN THE REGION WITH DENSITY PROFILE $N_0(1+R^2/A0^2)$
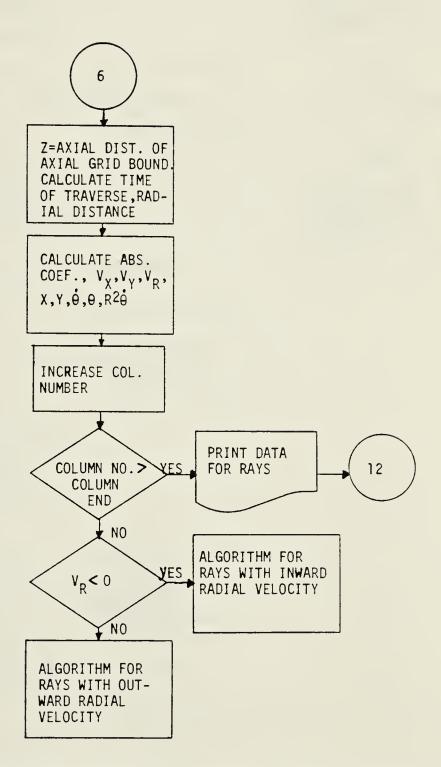
CHART 22. ALGORITHM FOR RAYS HITTING AT AXIAL GRID BOUNDARY
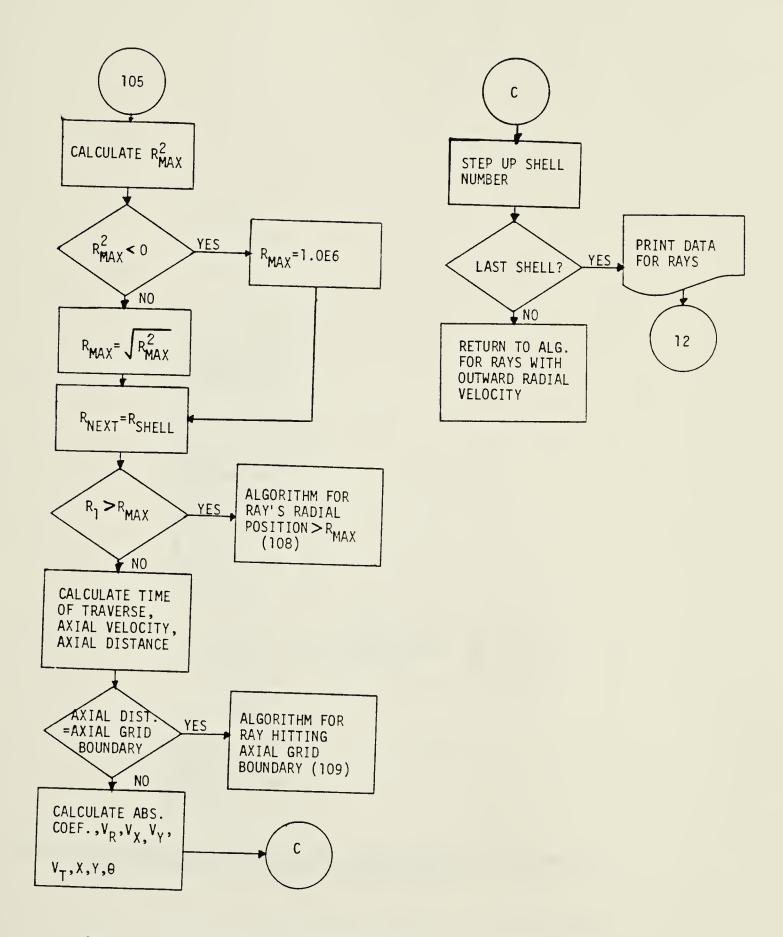
CHART 23. ALGORITHM FOR RAYS PROPAGATING IN THE REGION WITH DENSITY
PROFILE $NO(1-AO^2/R^2)$   [CONSTANT < 0, $V_R$ > 0]
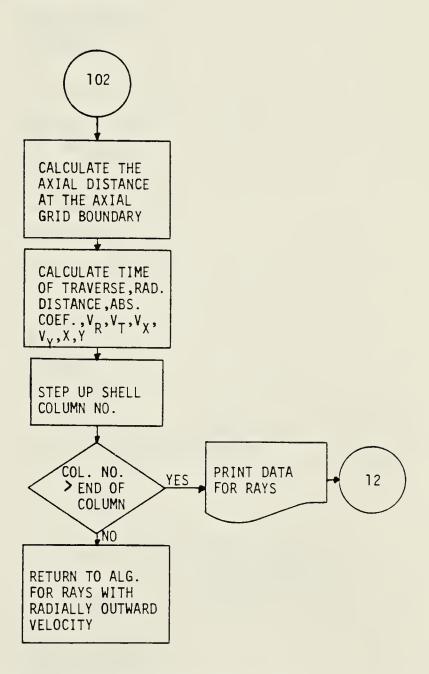
CHART 24. ALGORITHM FOR RAY HITTING AXIAL GRID BOUNDARY IN THE REGION WITH
DENSITY PROFILE $N0(1-A0^2/R^2)$ [CONST > 0, $V_R$ > 0]
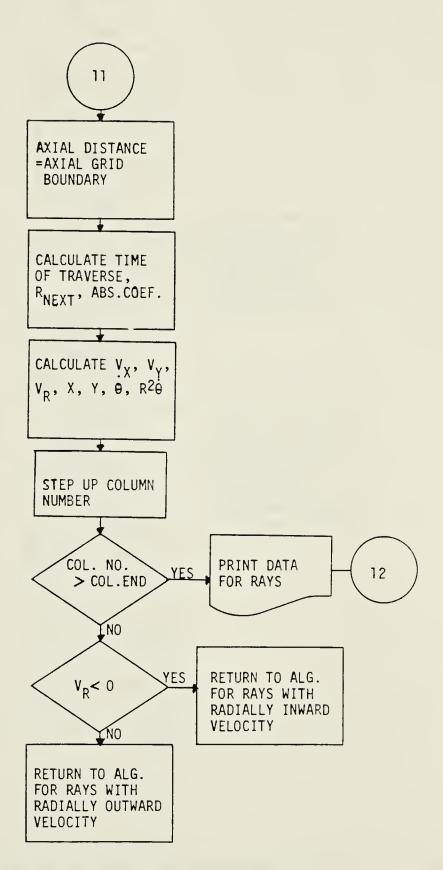
CHART 25. ALGORITHM FOR RAY HITTING AXIAL GRID BOUNDARY IN THE REGION WITH DENSITY PROFILE $NO(1-R^2/AO^2)$
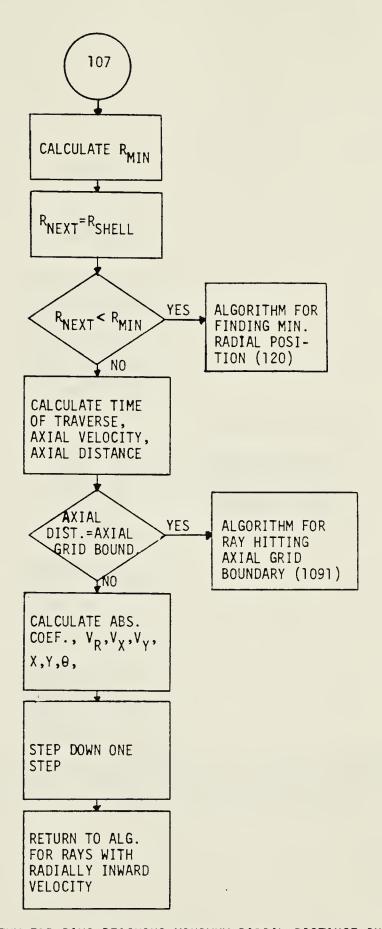
CHART 26. ALGORITHM FOR RAYS REACHING MINIMUM RADIAL DISTANCE IN THE REGION
WITH DENSITY PROFILE $N0(1-A0^2/R^2)$ [CONSTANT $<0$ ]
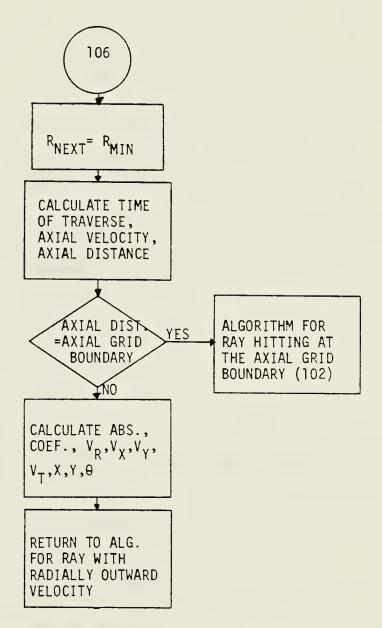
CHART 27. ALGORITHM FOR FINDING MINIMUM RADIAL DISTANCE IN THE REGION WITH
DENSITY PROFILE $NO(1-AO^2/R^2)$  [CONSTANT $> 0$, $V_R < 0$]
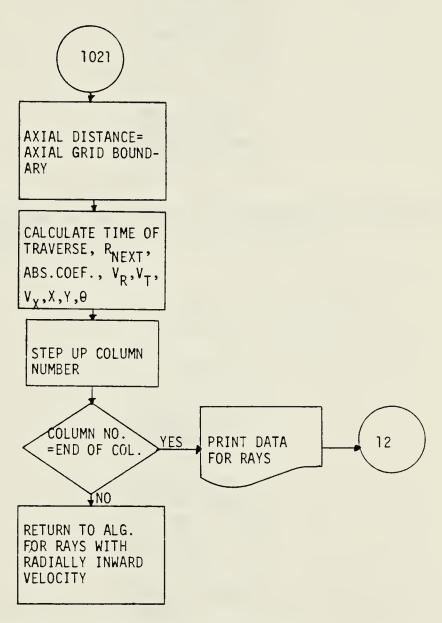
CHART 28. ALGORITHM FOR RAYS HITTING AXIAL GRID BOUNDARY IN THE REGION WITH
DENSITY PROFILE $NO(1-AO^2/R^2)$  [CONSTANT > 0, $V_R$ < 0]
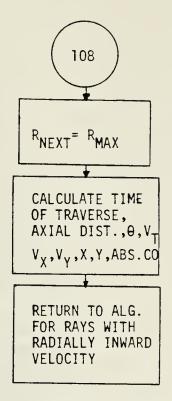
CHART 29. ALGORITHM FOR RAYS ATTAINING THE MAXIMUM RADIAL DISTANCE IN
THE REGION WITH DENSITY PROFILE $NO(1-AO^2/R^2)$
[CONSTANT $<0$, $V_R>0$]
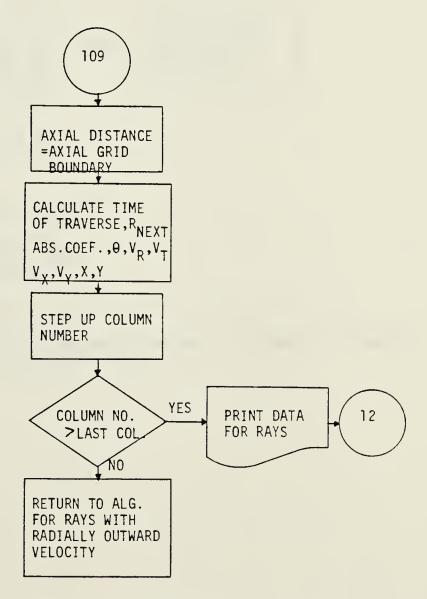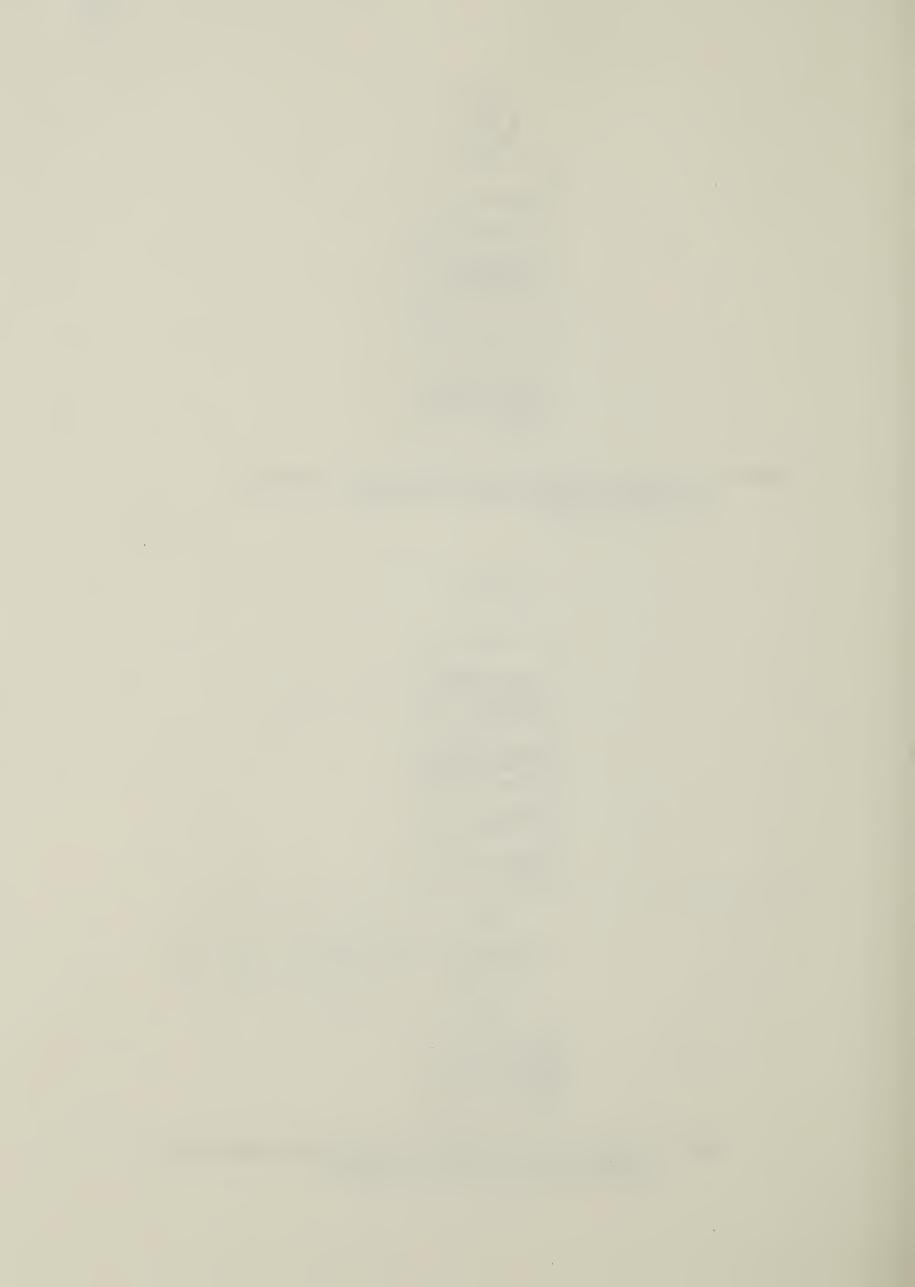


CHART 30. ALGORITHM FOR RAYS HITTING AT THE AXIAL GRID BOUNDARY IN THE
REGION WITH DENSITY PROFILE $NO(1-AO^2/R^2)$
[CONSTANT$< 0$, $V_R> 0$]
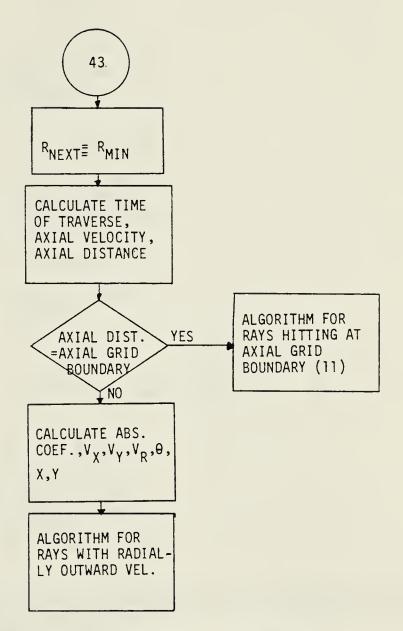
CHART 31. ALGORITHM FOR RAY ATTAINING MINIMUM RADIAL DISTANCE IN THE REGION WITH DENSITY PROFILE $NO(1-R^2/AO^2)$
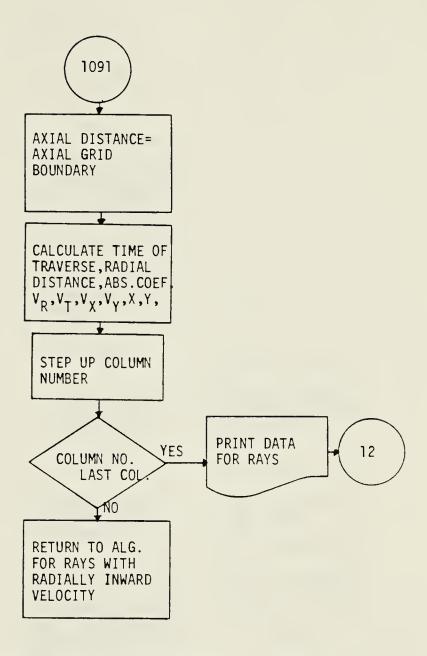
CHART 32. ALGORITHM FOR RAYS HITTING THE AXIAL GRID BOUNDARY IN THE REGION
WITH DENSITY PROFILE $NO(1-AO^2/R^2)$
[ CONSTANT $< 0$, $V_R < 0$]
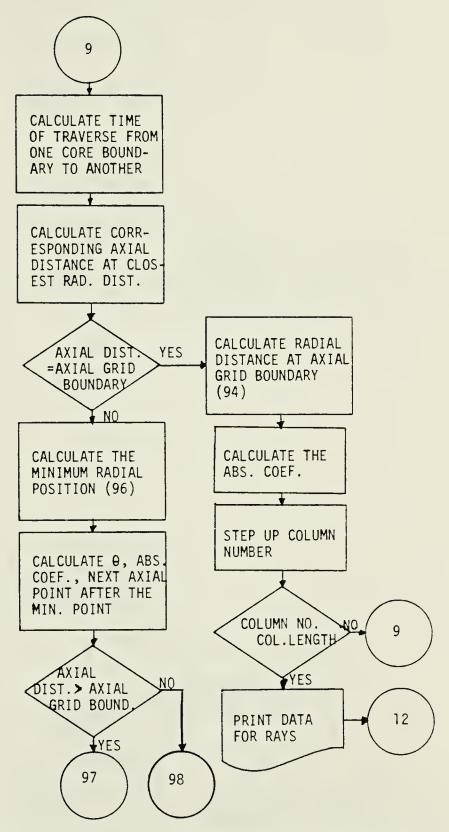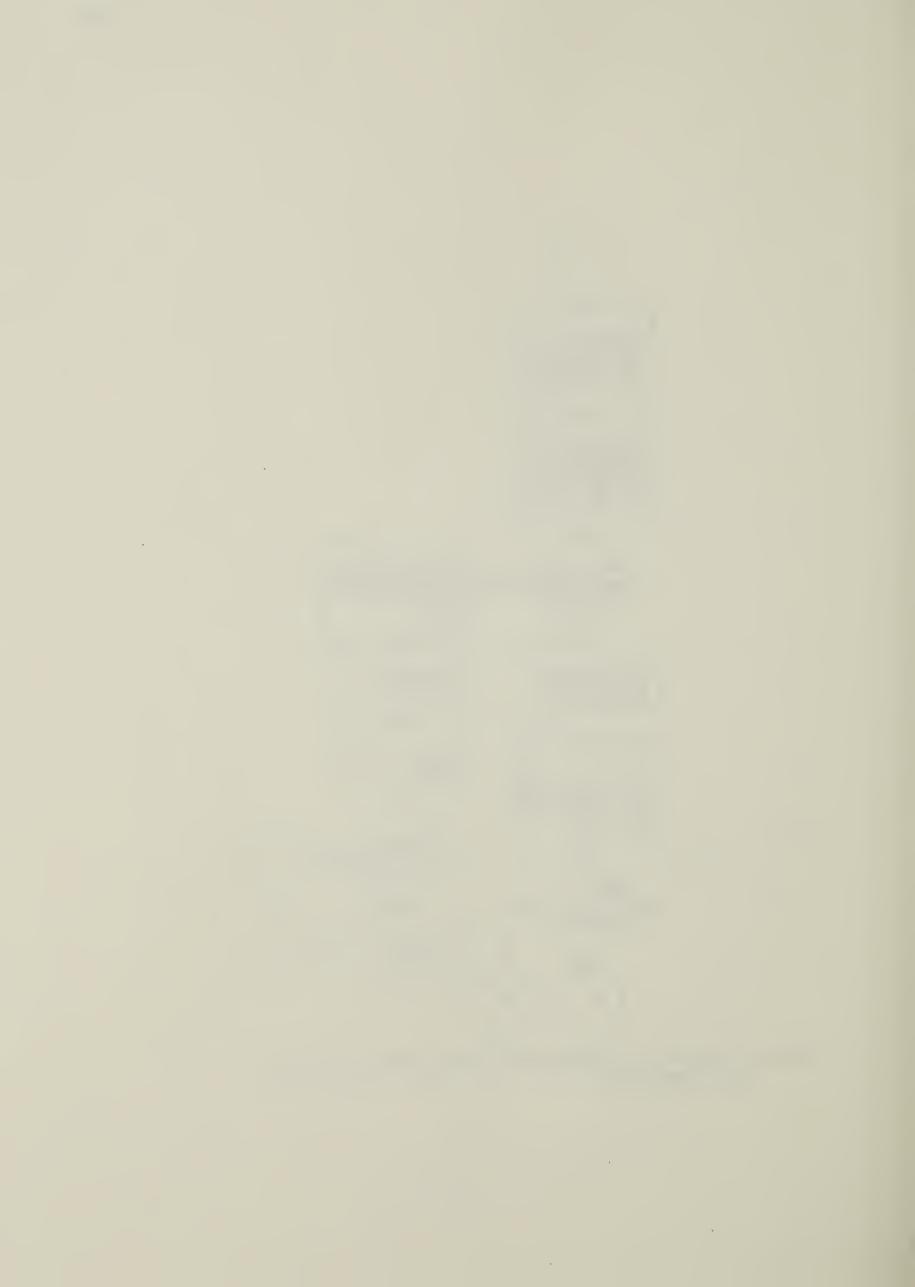
CHART 33. ALGORITHM FOR DETERMINING RAY LOCATIONS WHEN THE RAYS REACH
THE INNERMOST CORE

```
        ( 97 )
           │
           ▼
┌──────────────────┐
│ AXIAL DISTANCE=  │
│ AXIAL GRID       │
│ BOUNDARY VALUE   │
└──────────────────┘
           │
           ▼
┌──────────────────┐
│ CALCULATE θ,     │
│ ABSORPTION COEF. │
└──────────────────┘
           │
           ▼
┌──────────────────┐
│ STEP UP COLUMN   │
│ NUMBER           │
└──────────────────┘
           │
           ▼
      ◇─────────◇                    ┌──────────────┐
     │COLUMN NO. │   YES             │ PRINT DATA   │      ( 12 )
     │ >LAST COL.│──────────────────▶│ FOR RAYS     │─────▶
      ◇─────────◇                    └──────────────┘
           │ NO
           ▼
        ( 994 )
```

CHART 33A

```
        ( 98 )
           │
           ▼
┌──────────────────┐
│ CALCULATE RADIAL │
│ DISTANCE, θ,     │
│ ABSORPTION COEF. │
└──────────────────┘
           │
           ▼
      ◇─────────◇        ┌──────────────────┐
     │ RAY HITS  │  NO   │ CALCULATE THE    │
     │ 1ST SHELL │──────▶│ AXIAL DISTANCE OF│
     │ BOUND.    │       │ THE RAY (995)    │
      ◇─────────◇        └──────────────────┘
           │ YES                 │
           ▼                     ▼
┌──────────────────┐        ◇─────────◇
│ STEP UP SHELL    │       │ RAY HITS  │  NO
│ NUMBER           │       │ AXIAL GRID│──────▶ ( 992 )
└──────────────────┘       │ BOUNDARY? │
           │                ◇─────────◇
           ▼                     │ YES
┌──────────────────┐             ▼
│ RETURN TO ALG.   │          ( 991 )
│ FOR RAYS WITH    │
│ RADIALLY OUTWARD │
│ VELOCITY         │
└──────────────────┘
```

CHART 33B

CHART 33C



CHART 33D
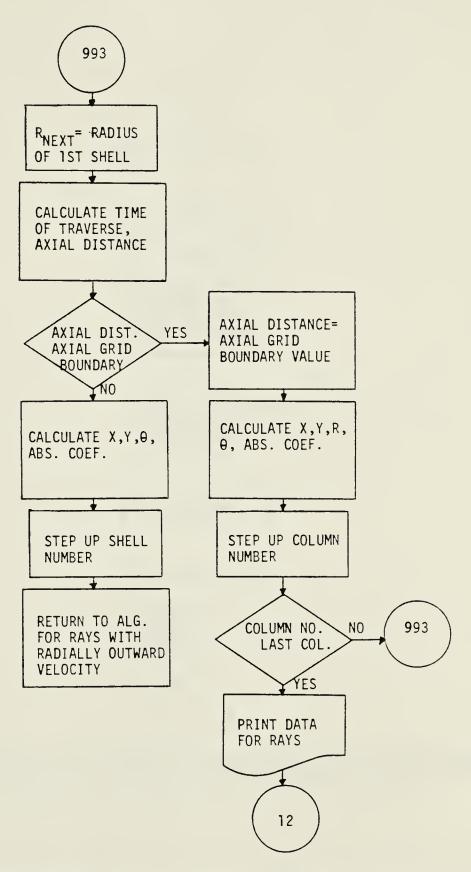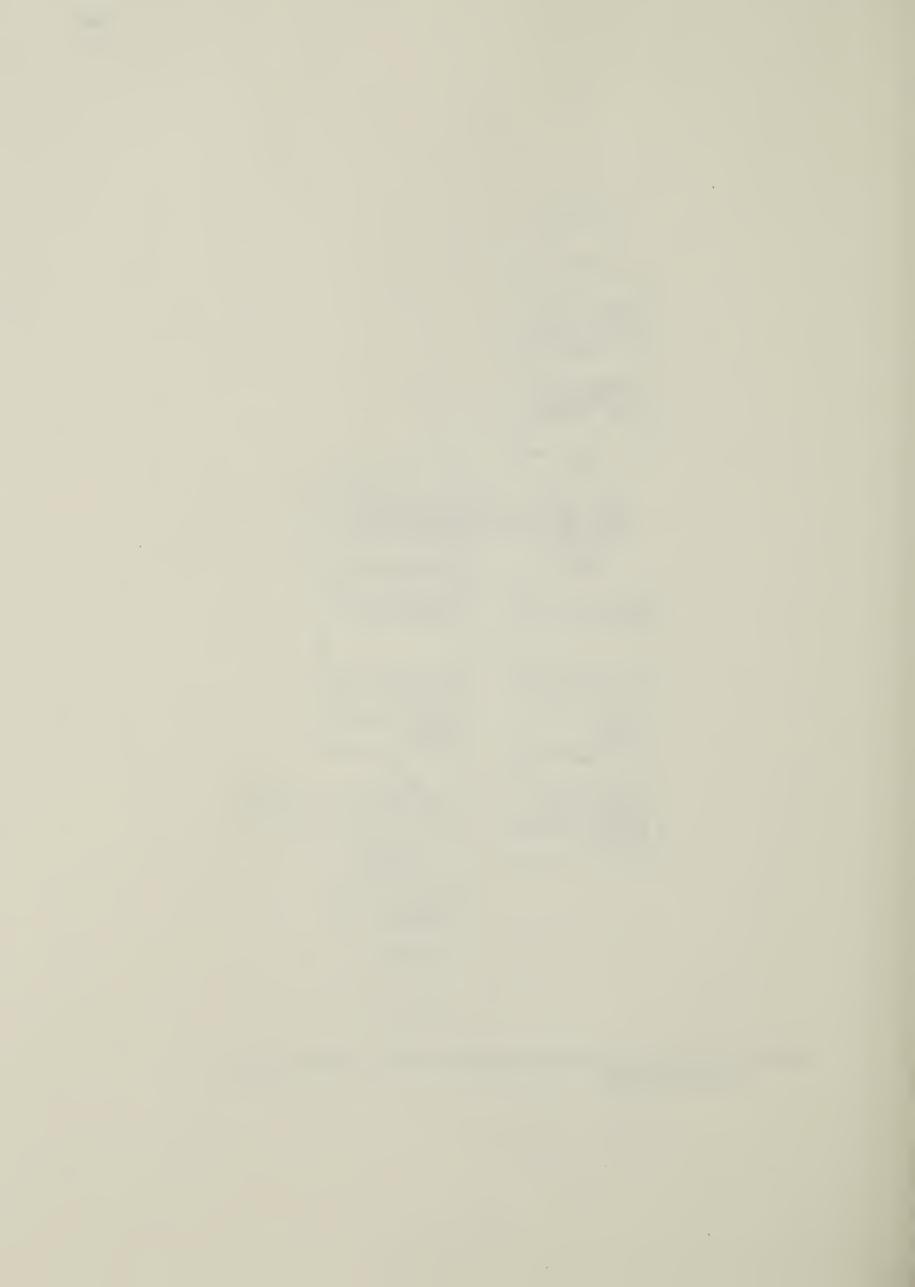
CHART 34. ALGORITHM FOR COMPUTING RAY TRAJECTORY WHEN RAY LOCATES INITIALLY
IN THE INNER CORE
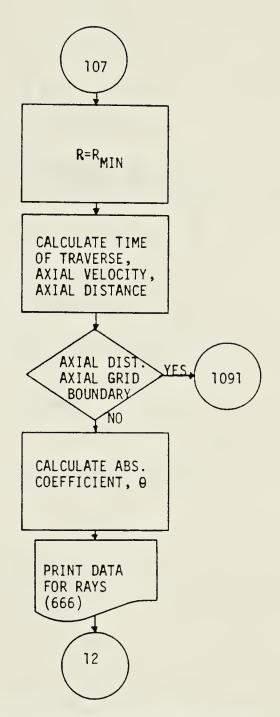
CHART 35. ALGORITHM FOR RAY REACHING MINIMUM RADIAL DISTANCE IN THE REGION WITH DENSITY PROFILE $NO(1-AO^2/R^2)$  [CONSTANT $<0$, $V_R<0$]
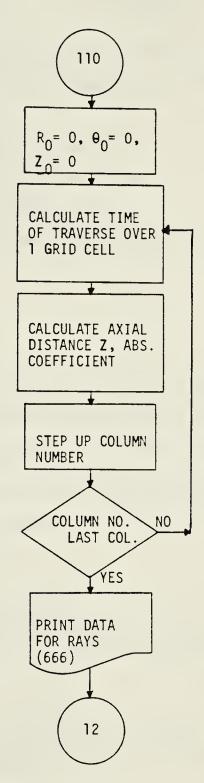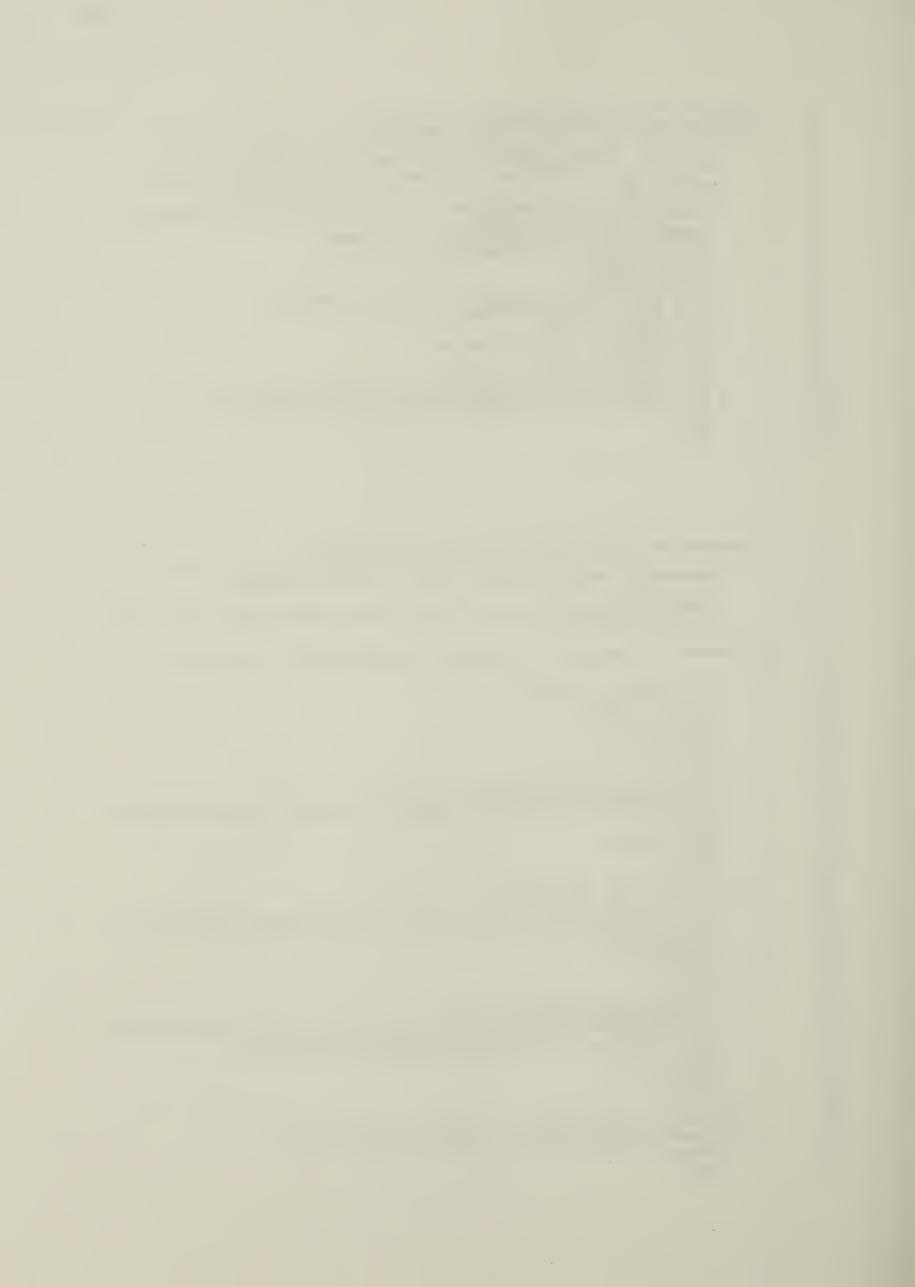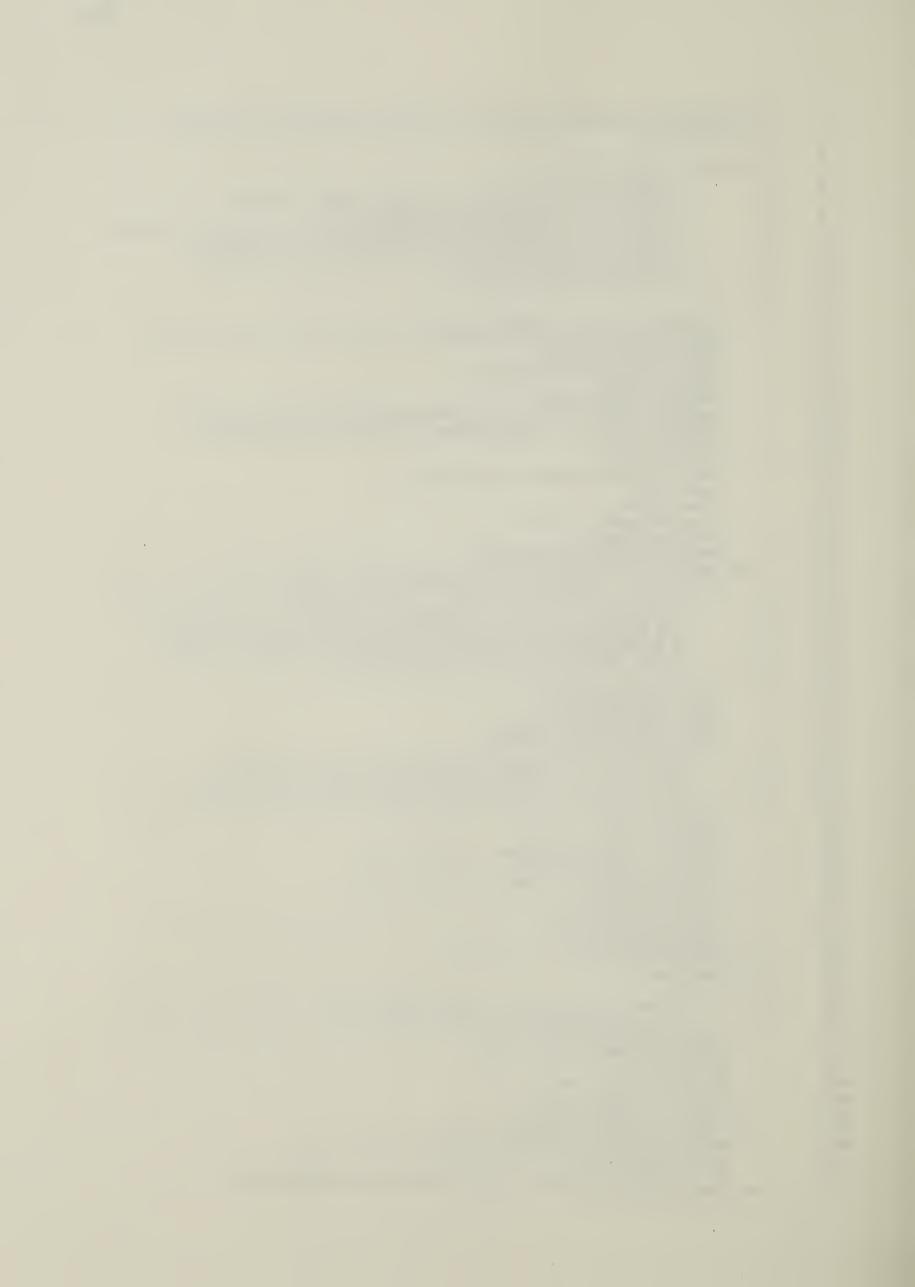
CHART 36. ALGORITHM FOR RAYS TRAVELLING ALONG THE AXIS OF PROPAGATION
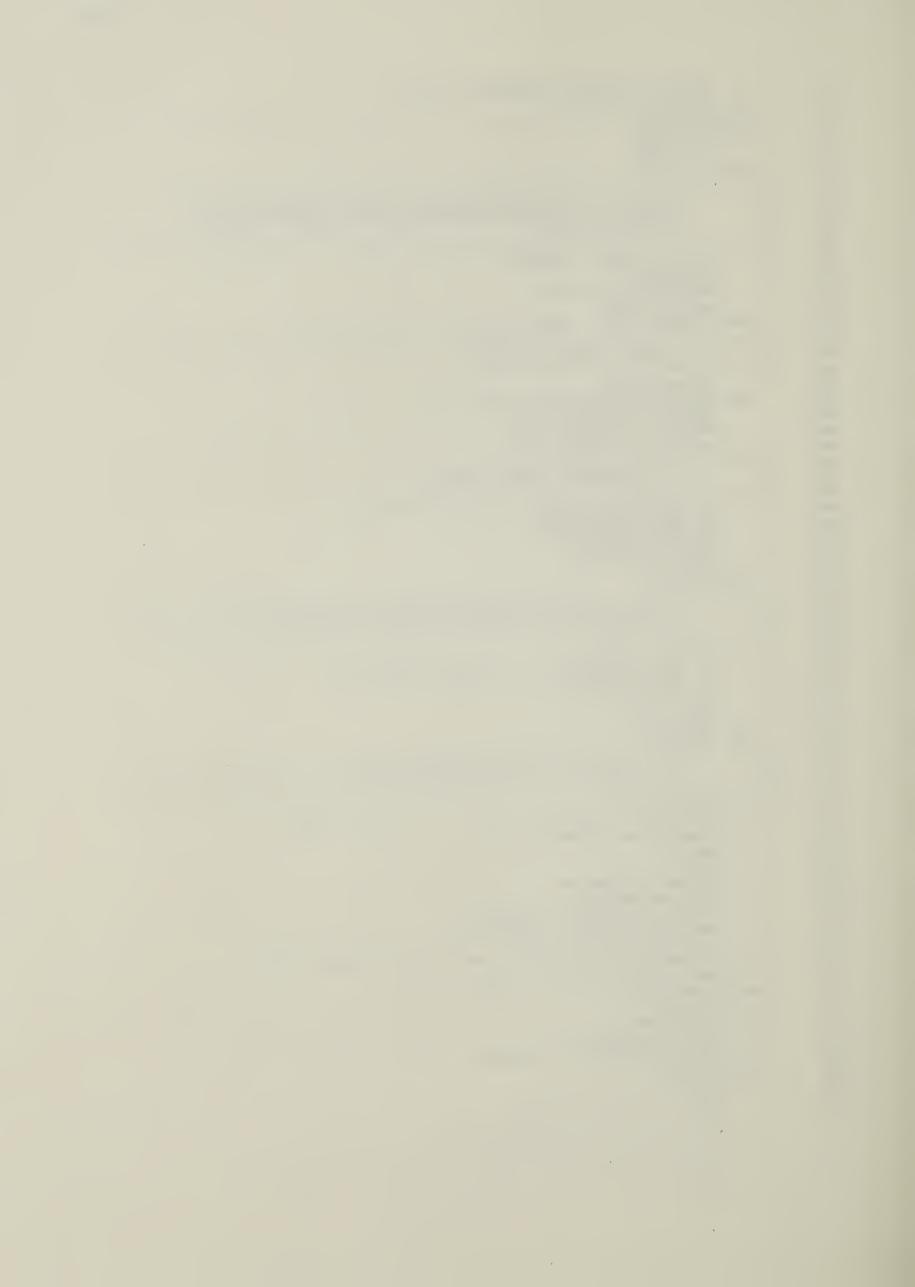
```
1      C -------------------------------------------------------------------
2      C TESTING PROGRAM FOR THE RELATED SUBROUTINES
3      C -------------------------------------------------------------------
4            NAMELIST /MAIDAT/TIME,STEP,NBOUND,PWR1,PWR2,PWR3,T1,T2,T3,T4,
5           *NX,M,Z,RO,TO,LO,NO,VLAS,XMIN,LAMDA,DTL,MRMAX,XLAS,DX,TL,F,AO,
6           *TOTRAY,EN1
7            REAL LAMDA,LO,NO,R(30,60),N(30,60),TE(30,60),EP(30,60),PWR(30,60)
8            INTEGER STEP,XMIN,Z,TOTRAY
9            COMMON /LASP/L3,RLO,BMS,NCRIT,TL,DTL,MRMAX
10           DATA PWR/1800*0.0/,EP/1800*0.0/
11           READ(5,MAIDAT)
12           WRITE(6,MAIDAT)
13           CALL PWINIT(PWR1,PWR2,PWR3,T1,T2,T3,T4,TIME,EN1)
14           CALL DRAY(F,LAMDA,AO,TOTRAY)
15           IF (STEP.EQ.1) GOTO 1
16           CALL MHDDEN(R,N,TE,NO,RO,NX,M)
17           CALL GRID(R,NX,RO)
18           CALL DNGR(R,N,LAMDA,NX,RO,NO)
19           CALL RAYABS(M,NX,TE,TO,LAMDA,LO,Z,XLAS,VLAS,TIME,DX,XMIN)
20         1 CALL ENERGY(TIME,STEP,XMIN,NX,XLAS,VLAS,DX,EP,PWR,N)
21           STOP
22           END
```

```
1      C -----------------------------------------------------------------
2      C PROGRAM FOR INITIALIZING THE INCIDENT BEAM POWER
3      C -----------------------------------------------------------------
4            SUBROUTINE PWINIT(PWR1,PWR2,PWR3,T1,T2,T3,T4,TIME,EN1)
5            REAL INDEX
6            COMMON /DRAYP/XO(100),YO(100),THETAX(100),THETAY(100),P(100),TOTRA
7           *Y,ENIN,P1,EN(100)
8      C
9      C TEMPORAL BEAM PROFILE IS SECTIONED INTO FOUR PARTS--T1,T2,T3,T4
11     C
12           IF (TIME.GT.T1) GOTO 15
13           P1=PWR1*TIME/T1
14           ENO=P1*0.5*TIME
15           ENIN=ENO-EN1
16           EN1=ENO
17           GOTO 1
18        15 IF (TIME.GT.T2) GOTO 16
19           P1=PWR1+(PWR2-PWR1)*(TIME-T1)/(T2-T1)
20           ENO=(TIME+TIME-T1)*0.5*PWR1+((PWR2-PWR1)*(TIME-T1)/(T2-T1))*0.5*(T
21          *IME-T1)
22           ENIN=ENO-EN1
23           EN1=ENO
24           GOTO 1
25        16 IF (TIME .GT. T3) GOTO 17
26           P1=PWR2+(PWR3-PWR2)*(TIME-T2)/(T3-T2)
27           ENO=(TIME+TIME-T1)*0.5*PWR1+(TIME-T1+TIME-T2)*(PWR2-PWR1)*0.5+0.5*
28          *(TIME-T2)*(P1-PWR2)
29           ENIN=ENO-EN1
30           EN1=ENO
31           GOTO 1
32        17 IF (TIME.GT.T4) GOTO 18
33           P1=PWR3-PWR3*(TIME-T3)/(T4-T3)
34           ENO=(TIME+TIME-T1)*PWR1*0.5+(TIME-T1+TIME-T2)*0.5*(PWR2-PWR1)+(TIM
35          *E-T2+TIME-T3)*0.5*(PWR3-PWR2)-(P1-PWR2)*0.5*(TIME-T3)
36           ENIN=ENO-EN1
37           EN1=ENO
38           GOTO 1
39        18 P1=0.0
40         1 WRITE(6,601)P1,ENIN
41       601 FORMAT(/'POWER=',E10.3,/,'INITIAL ENERGY=',E10.3)
42           RETURN
43           END
```
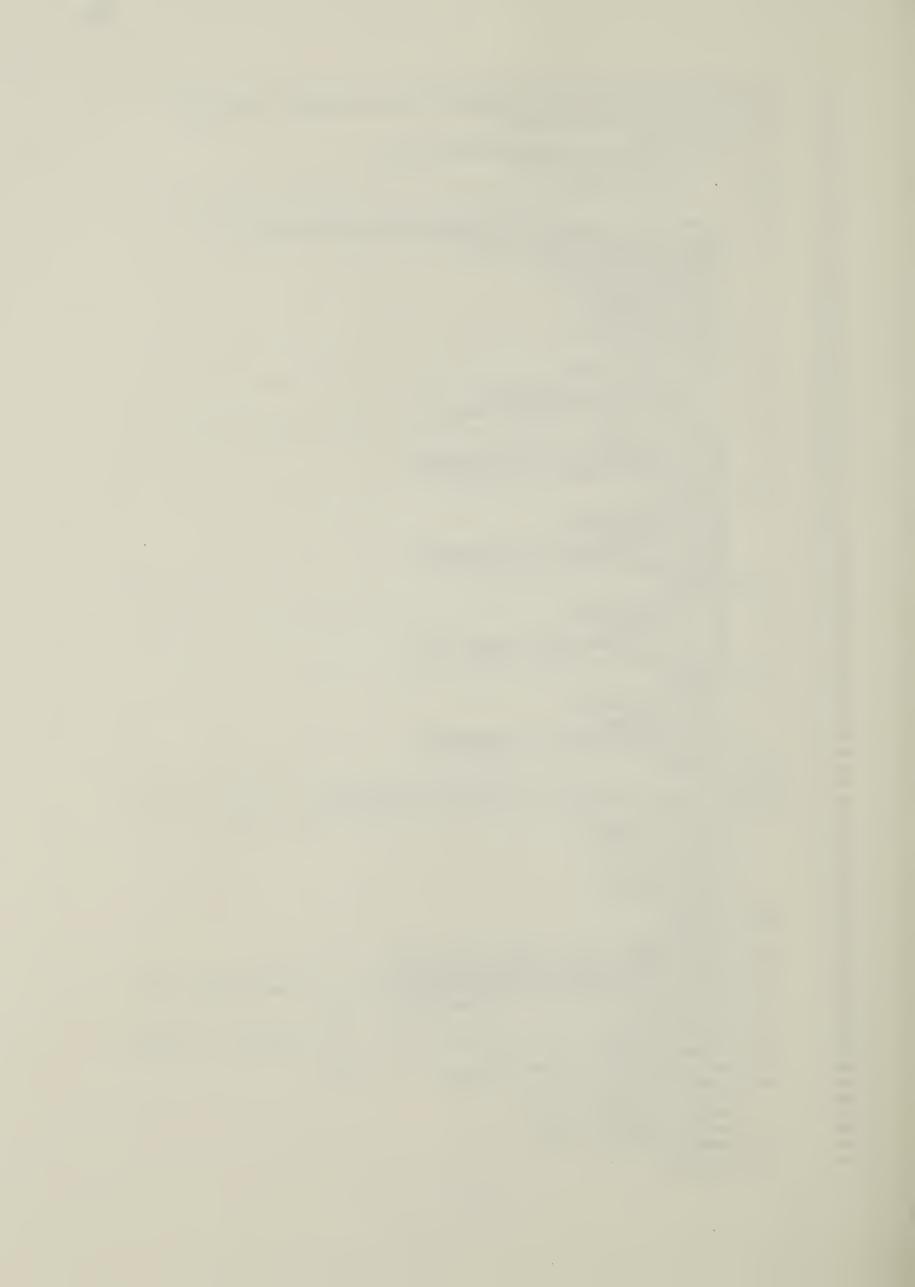
```
 1       C------------------------------------------------------------------
 2       C   SUBROUTINE FOR GENERATING A SET OF RAYS FOLLOWING THE GAUSSIAN
 3       C   DISTRIBUTION
 4       C
 5       C   DEVICE 1:STORE R**2,Z
 6       C          2:STORE AVERAGE R**2,Z
 7       C          3:STORE NO. OF RAYS WITHIN REGION, RADIUS SQUARE
 8       C          4:STORE X,Y CO-ORDINATE OF VARIOUS RAYS
 9       C          6:LIST OF DATA FOR RAY POSITIONS,NO.OF RAYS IN DISTINCT REGION
10       C          7:STORE X,Y CO-ORDINATES OF VARIOUS RAYS AT LENS PLANE
11       C          8:STORE TRANSVERSE DIRECTIONS OF RAYS--THETAX,THETAY
12       C         10:STORE 3DB POWER POINTS,Z
13       C------------------------------------------------------------------
14       C
15             SUBROUTINE DRAY(F,LAMDA,AO,TOTAL)
16             DIMENSION X(100),Y(100),THETAX(100),THETAY(100),NPT(50),P(100),
17            *RSQ(50),RNEW(50,100)
18             DOUBLE PRECISION DSEED,DELT
19             REAL LAMDA,AO
20             INTEGER TOTRAY,TOTAL
21             NAMELIST /RAYDAT/ N,DSEED,NRING,NPLANE,NEXTRA,NPLAN1,FACTOR
22             COMMON /DRAYP/X,Y,THETAX,THETAY,P,TOTRAY,ENIN,P1,EN(100)
23             READ(5,RAYDAT)
24             TOTRAY=TOTAL
25             WN=2*3.14159/(LAMDA*1.0E-4)*FACTOR
26             WNAO=WN*AO
27             FSPOT=F/WNAO
28             DZ=F/(NPLANE*1.0-1.0)
29             NRINP5=NRING+5
30             WRITE(6,604)DSEED,FSPOT,AO
31         604 FORMAT(/'DATA FROM PROGRAM DRAY',/'DSEED=',D15.8,/,'FOCAL SPOT SIZ
32            *E=',E15.8,/,'BEAM RADIUS AT LENS PLANE=',E15.8)
33       C------------------------------------------------------------------
34       C         TO GENERATE ALL RAY LOCATIONS AND DIRECTIONS AT LENS PLANE
35       C         THE CHOICE OF RAY LOCATIONS AND DIRECTIONS OBEYS A GAUSSIA
36       C         N DISTRIBUTION. SUBROUTINE GGNML GIVES A RANGE OF RANDOM
37       C         NORMAL DEVIATES WITHIN THE RANGE (0,1)
38       C------------------------------------------------------------------
39             CALL GGNML(DSEED,N,X)
40             CALL GGNML(DSEED,N,Y)
41             CALL GGNML(DSEED,N,THETAX)
42             CALL GGNML(DSEED,N,THETAY)
43       C------------------------------------------------------------------
44       C         TO CONVERT THE NORMALIZED VALUES TO ACTUAL VALUES
45       C         RAY DIRECTIONS ALWAYS TAKE OPPOSITE SIGNS TO LOCATIONS
46       C------------------------------------------------------------------
47             DO 201 I=1,N
48             X(I)=X(I)*AO/1.4142136
49             THETAX(I)=THETAX(I)/WNAO/1.4142136-X(I)/F
50             Y(I)=Y(I)*AO/1.4142136
51             THETAY(I)=THETAY(I)/WNAO/1.4142136-Y(I)/F
52             P(I)=P1/(N*1.0)
53             EN(I)=ENIN/(N*1.0)
54             WRITE(4,401)X(I),Y(I)
55             WRITE(8,401)THETAX(I),THETAY(I)
56         401 FORMAT(2E18.10)
57         201 CONTINUE
58       C------------------------------------------------------------------
59       C         TO TRACE THE RAY PATH (R**2) ALONG AXIS
60       C------------------------------------------------------------------
61             NPLANE=NPLANE+NEXTRA
62             FINALZ=(NPLANE*1.0-1.0)*DZ
63             DO 202 J=1,N
64             DO 203 I=NPLAN1,NPLANE
65             DELT=(I-1)*DZ*1.0D0
66             XNEW=X(J)+THETAX(J)*DELT
67             YNEW=Y(J)+THETAY(J)*DELT
68             RNEW(I-NPLAN1+1,J)=XNEW**2+YNEW**2
69             DELT1=SNGL(DELT)
70             IF (ABS(DELT1-FINALZ).LT.10E-3) WRITE(7,701)XNEW,YNEW
71         701 FORMAT(2E18.10)
```

```
 72             WRITE(1,101)RNEW(I-NPLAN1+1,J),DELT
 73         101 FORMAT(2E18.10)
 74         203 CONTINUE
 75             X(J)=XNEW
 76             Y(J)=YNEW
 77         202 CONTINUE
 78     C-------------------------------------------------------------------
 79     C          TO CALCULATE THE AVERAGE SPOT SIZE AT EACH AXIAL PLANE
 80     C          AND NO. OF RAY POINTS WITHIN A DEFINED BEAM AREA AT A
 81     C          PARTICULAR PLANE
 82     C-------------------------------------------------------------------
 83             DO 204 I=NPLAN1,NPLANE
 84             RSQSUM=0.0
 85             DELT=(I-1)*DZ*1.0D0
 86             WRITE(6,606)
 87         606 FORMAT(/' AVE. SPOT SIZE',5X,' AXIAL DISTANCE')
 88     C-------------------------------------------------------------------
 89     C          AVERAGE SPOTSIZE SQUARE
 90     C-------------------------------------------------------------------
 91             DO 205 J=1,N
 92         205 RSQSUM=RSQSUM+RNEW(I-NPLAN1+1,J)
 93             RSQAVE=RSQSUM/(N*1.0)
 94             WRITE(2,101)RSQAVE,DELT
 95             WRITE(6,101) RSQAVE,DELT
 96     C-------------------------------------------------------------------
 97     C          CORRESPONDING RADIAL DISTANCE
 98     C-------------------------------------------------------------------
 99             SPOTSQ=FSPOT**2+(DELT-F)**2/WN**2/FSPOT**2
100             SPOTSQ=SPOTSQ/NRING
101             DO 206 K=1,NRINP5
102             RSQ(K)=K*SPOTSQ
103             NPT(K)=0
104         206 CONTINUE
105     C-------------------------------------------------------------------
106     C          TO CATEGORIZE RAY LOCATIONS INTO VARIOUS REGIONS
107     C-------------------------------------------------------------------
108             DO 207 L=1,N
109             DO 208 M=1,NRINP5
110             IF (RNEW(I-NPLAN1+1,L).GT.RSQ(M)) GOTO 208
111             NPT(M)=NPT(M)+1
112             GOTO 207
113         208 CONTINUE
114         207 CONTINUE                                              .
115     C-------------------------------------------------------------------
116     C          SUM UP POINTS AT CORRESPONDING RADIUS
117     C-------------------------------------------------------------------
118             WRITE(6,607)
119         607 FORMAT(//'   RAY PTS. DIST.  ','   RADIUS SQUARE  ',
120            *'THEORETICAL POINTS')
121             SUM=0.0
122             VAR=0.0
123             DO 209 II=1,NRINP5
124             SUM=SUM+NPT(II)
125             RAD=N*(1-EXP(-RSQ(II)/RSQAVE))
126             VAR=VAR+(RAD-SUM)**2/RAD**2
127             WRITE(3,101)SUM,RSQ(II)
128             IF (ABS(SUM-63.0).LE.2.0) WRITE(10,101)RSQ(II),DELT
129             WRITE(6,605)SUM,RSQ(II),RAD
130         605 FORMAT(3E18.10)
131         209 CONTINUE
132             VAR=VAR/NRINP5
133             WRITE(6,608)VAR
134         608 FORMAT(/'VARIANCE=',E15.8)
135         204 CONTINUE
136             RETURN
137             END
```
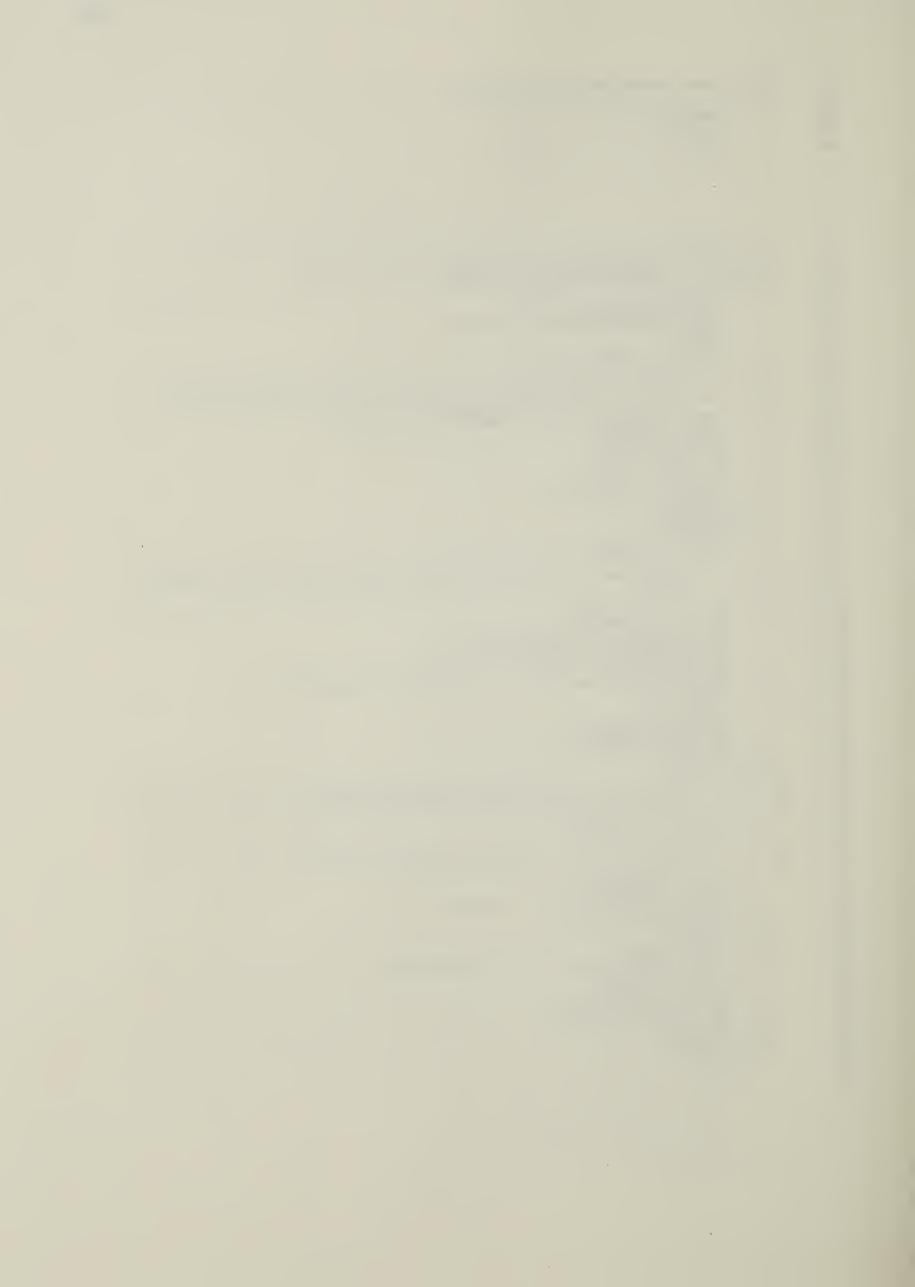
```
1       C----------------------------------------------------------------------
2       C SUBROUTINE FOR CALCULATING DENSITIES AND TEMPERATURE IN EACH CELL
3       C AND THE CORRESPONDING RADIUS
4       C
5       C   DEVICE 2:DENSITY VALUE,NORMALIZED RADIUS,
6       C           6:LISTING OF DATA
7       C          11:TAPE DEVICE
8       C----------------------------------------------------------------------
9       C
10            SUBROUTINE MHDDEN(R,N,TE,AXIDEN,PASRAD,ZSTEP,PLASEL)
11            REAL R(30,60),N(30,60),TE(30,60)
12            INTEGER ZSTEP,PLASEL
13            DR=PASRAD/(PLASEL*1.0)
14            A1=0.337769221**2
15            A2=0.185919614**2
16            A3=1.887104451**2
17            A4=0.356427765**2
18            DO 201 I=1,6
19            R(I,1)=I*DR/PASRAD
20      C----------------------------------------------------------------------
21      C           CCR--CELL CENTRE RADIUS
22      C           N-- PARABOLIC DENSITY PROFILE
23      C----------------------------------------------------------------------
24            CCR=(I-0.5)*DR
25            N(I,1)=(1+CCR**2/A1)*0.997362083E18
26            TE(I,1)=50/(1+EXP((CCR-2.0)/0.1))
27       201 CONTINUE
28            DO 204 I=7,9
29            R(I,1)=I*DR/PASRAD
30            CCR=(I-0.5)*DR
31            N(I,1)=(1-A2/CCR**2)*3.059522465E18
32            TE(I,1)=50/(1+EXP((CCR-2.0)/0.1))
33       204 CONTINUE
34            DO 205 I=10,14
35            R(I,1)=I*DR/PASRAD
36            CCR=(I-0.5)*DR
37            N(I,1)=(1-CCR**2/A3)*2.588205127E18
38            TE(I,1)=50/(1+EXP((CCR-2.0)/0.1))
39       205 CONTINUE
40            DO 206 I=15,30
41            R(I,1)=I*DR/PASRAD
42            CCR=(I-0.5)*DR
43            N(I,1)=(1+A4/CCR**2)*1.763802596E18
44            TE(I,1)=50/(1+EXP((CCR-2.0)/0.1))
45       206 CONTINUE
46      C----------------------------------------------------------------------
47      C ASSIGN RADIUS AND DENSITY IN THE AXIAL DIRECTION
48      C----------------------------------------------------------------------
49            DO 202 J=2,ZSTEP
50            DO 203 I=1,PLASEL
51            R(I,J)=R(I,1)
52            N(I,J)=N(I,1)
53            TE(I,J)=TE(I,1)
54       203 CONTINUE
55       202 CONTINUE
56            WRITE(6,604)
57       604 FORMAT(/'DATA FROM PROGRAM:RICKMHDDEN')
58            WRITE(6,605)AXIDEN,PASRAD,ZSTEP,PLASEL
59       605 FORMAT(/'AXIAL DENSITY(NORMALIZED)=',E15.8,/,'PLASMA RADIUS=',E15.
60          *8,/,'AXIAL STEPS=',I3,/,'PLASMA SHELLS=',I3/)
61            WRITE(6,602)
62       602 FORMAT('  SHELL RADIUS(NORMALIZED) ',5X,' SHELL DENSITY ',5X,'SHEL
63          *L TEMPERATURE')
64            WRITE(6,603)(R(I,1),N(I,1),TE(I,1),I=1,PLASEL)
65       603 FORMAT(E15.8,15X,E15.8,7X,E15.8)
66            DO 20 I=1,PLASEL
67            RN=R(I,1)*PASRAD-0.5*DR
68            WRITE(2,103)N(I,1),RN
69       103 FORMAT(2E18.10)
70        20 CONTINUE
```
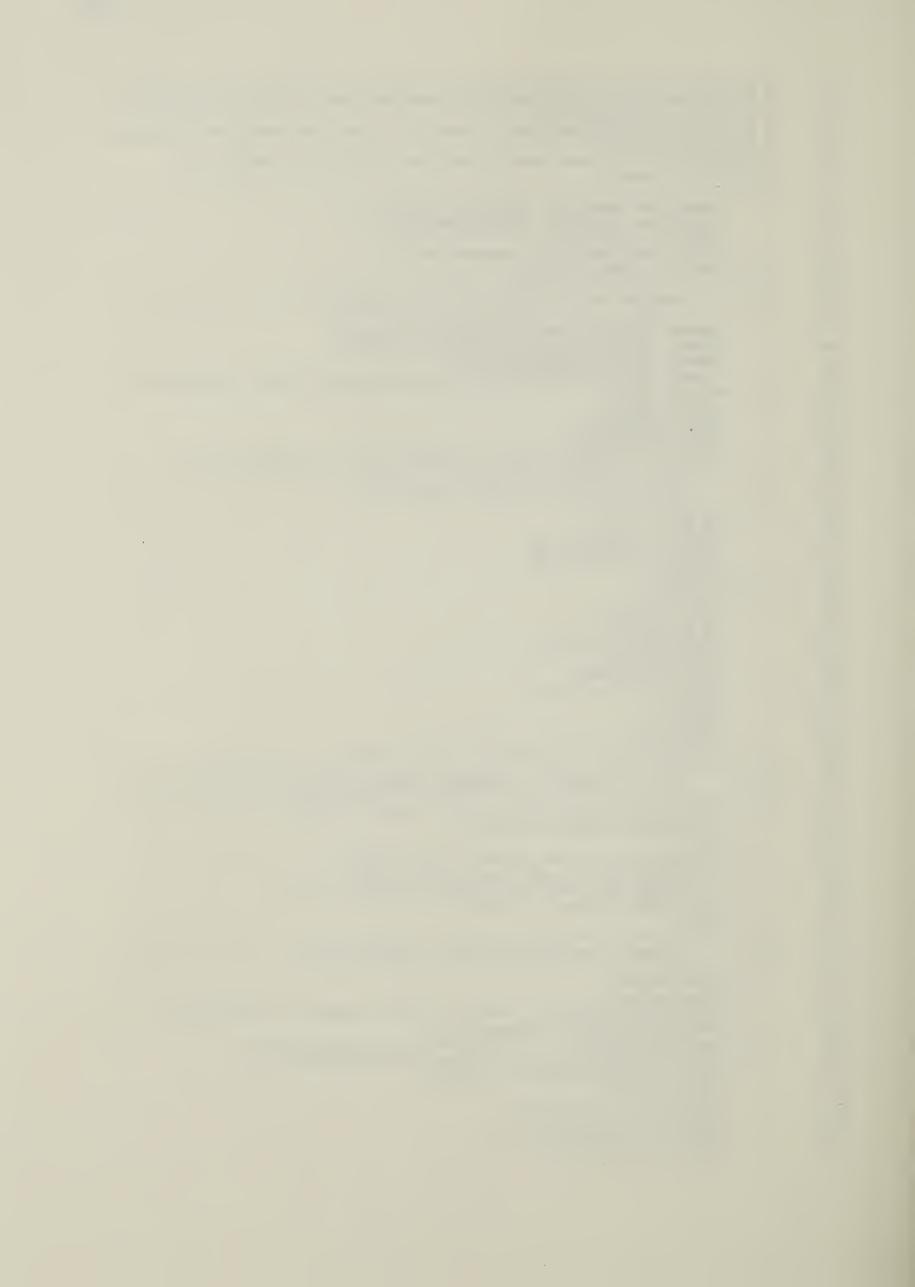
```
71    C
72    C TO STORE UNFORMATED DATA ON TAPE
73    C
74          WRITE(11) N
75          RETURN
76          END




 1    C ---------------------------------------------------------------------
 2    C ALGORITHM FOR DIVIDING THE PLASMA LAYERS INTO FINER
 3    C SHELLS (2 SUBSHELLS FOR EACH LAYER)
 4    C ---------------------------------------------------------------------
 5          SUBROUTINE GRID(R,NX,RO)
 6          DIMENSION RDENOR(30,60),R(30,60)
 7          REAL N
 8          NAMELIST /GRIDAT/LASHEL
 9    C ---------------------------------------------------------------------
10    C          LASHEL---NO. OF PLASMA SHELLS TAKEN FOR A FINER DIVISION
11    C ---------------------------------------------------------------------
12          COMMON /GRIDP/R2(60,60),OMEGA(60,60),LASHEL
13          READ(5,GRIDAT)
14          WRITE(6,GRIDAT)
15          DO 208 J=1,NX
16          DO 209 I=1,LASHEL
17          RDENOR(I,J)=R(I,J)*RO
18      209 CONTINUE
19      208 CONTINUE
20          DO 201 J=1,NX
21    C ---------------------------------------------------------------------
22    C          DIVIDE EACH OF THE 3RD AND ABOVE PLASMA LAYER INTO 2 SMALLER
23    C          LAYERS
24    C ---------------------------------------------------------------------
25          DO 202 I=3,LASHEL
26          DRI=RDENOR(I,J)-RDENOR(I-1,J)
27          DRIM1=RDENOR(I-1,J)-RDENOR(I-2,J)
28          DRS=DRI+DRIM1
29          RMID=(DRI/DRS)*RDENOR(I-1,J)+(DRIM1/DRS)*RDENOR(I,J)
30          I2M1=2*I-1
31          I2M2=2*I-2
32          R2(I2M1,J)=RMID
33          R2(I2M2,J)=RDENOR(I-1,J)
34      202 CONTINUE
35    C ---------------------------------------------------------------------
36    C          DIVIDE THE 1ST LAYER INTO 2 SMALLER LAYERS
37    C ---------------------------------------------------------------------
38          R2(1,J)=0.5*RDENOR(1,J)
39    C ---------------------------------------------------------------------
40    C          DIVIDE THE 2ND LAYER INTO 2 SMALLER LAYERS
41    C ---------------------------------------------------------------------
42          R2(2,J)=RDENOR(1,J)
43          R2(3,J)=0.5*(RDENOR(2,J)+RDENOR(1,J))
44          R2(60,J)=RDENOR(30,J)
45      201 CONTINUE
46          WRITE (6,601)
47      601 FORMAT('SHELL LAYER',5X,' SHELL RADIUS   ')
48          LIMIT=2*LASHEL
49          DO 203 I=1,LIMIT
50          WRITE(6,602)I,R2(I,1)
51      602 FORMAT(8X,I3,5X,E15.8)
52      203 CONTINUE
53          RETURN
54          END
```
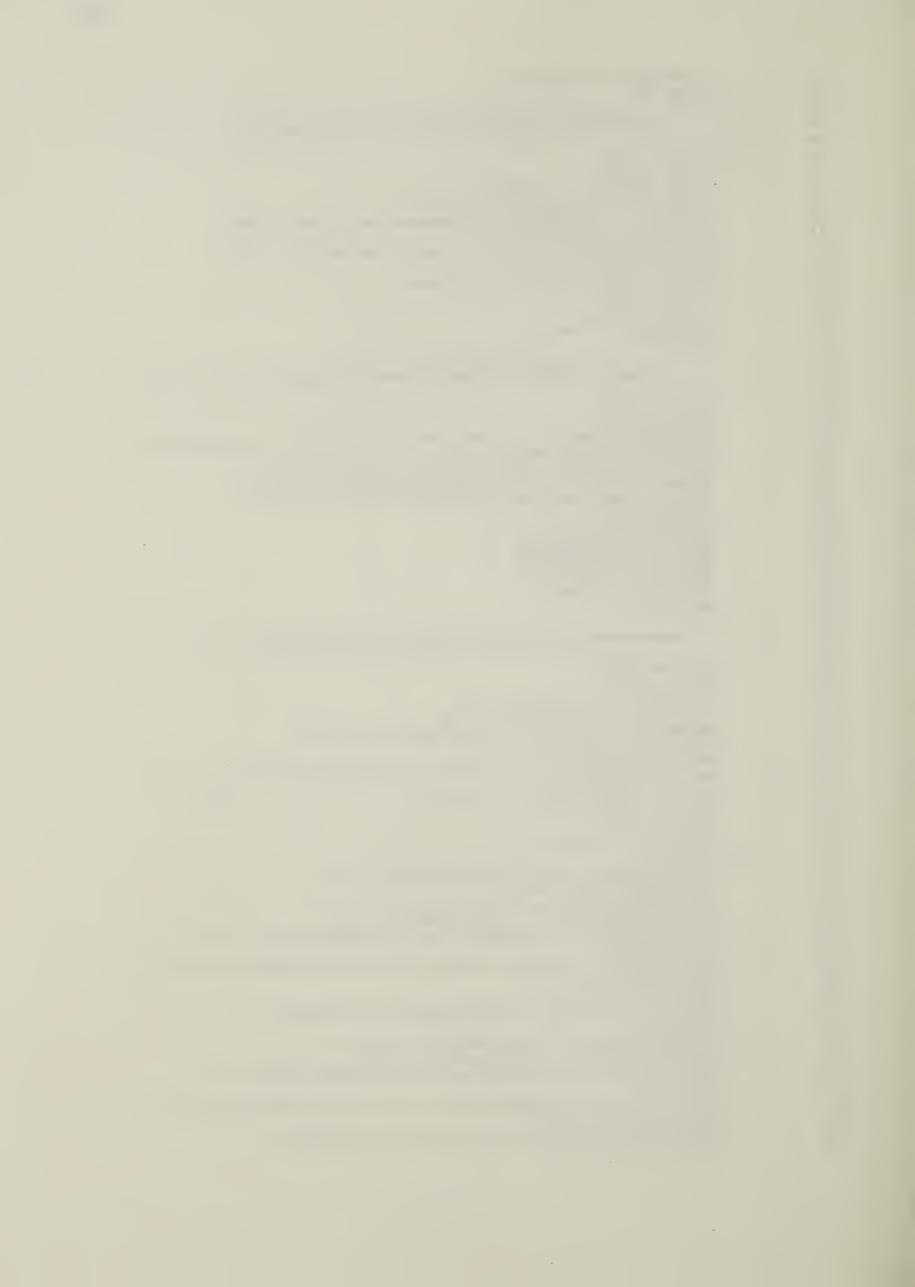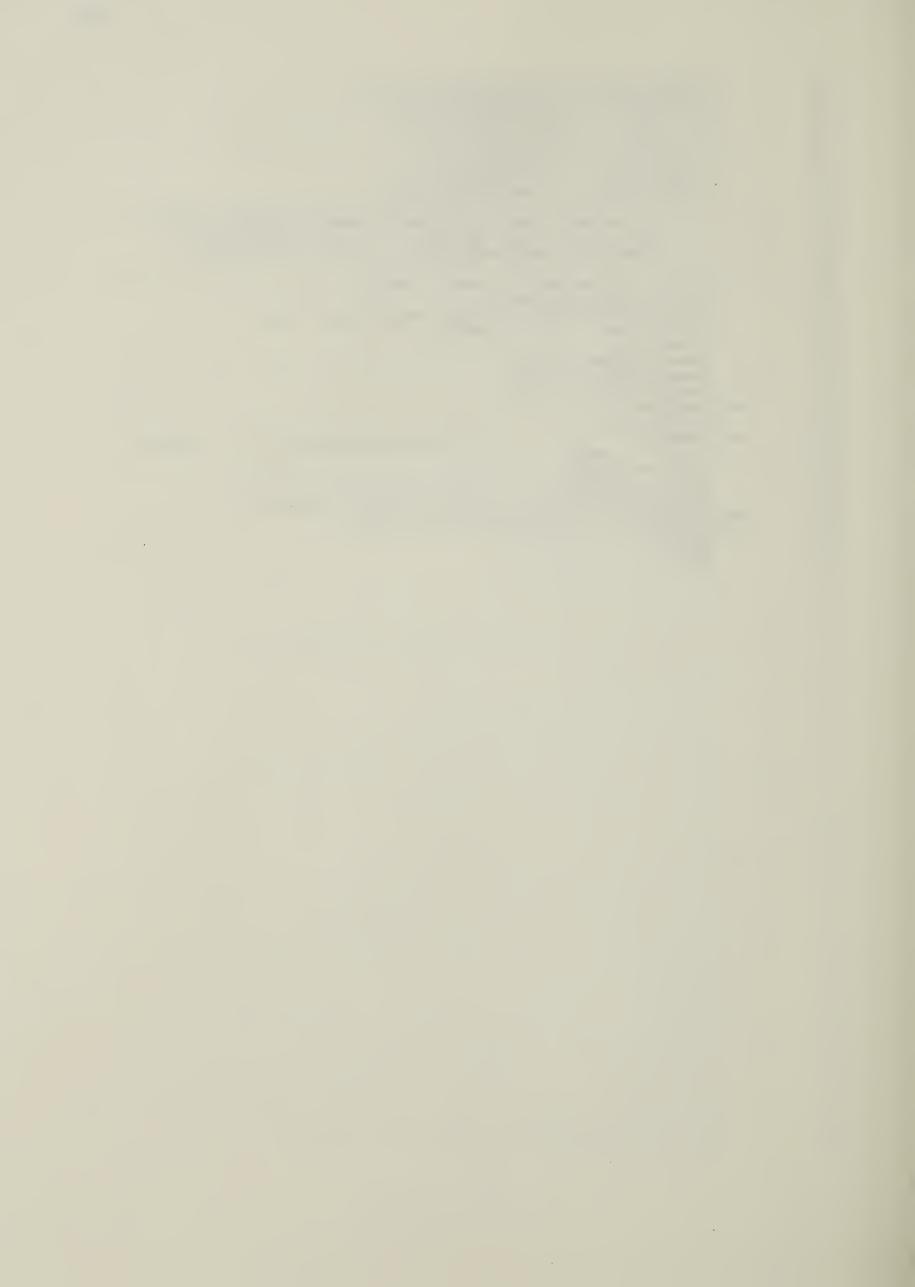
```
 1     C ----------------------------------------------------------------
 2     C SUBPROGRAM FOR CALCULATING DENSITY GRADIENT AND REFRACTIVE INDEX BET-
 3     C WEEN TWO KNOWN DENSITIES
 4     C A PARABOLIC INCREASING DENSITY PROFILE IS USED FOR APPROXIMATION,NAMELY,
 5     C N=NO(1+R**2/AO**2)
 6     C CONSTANTS NOI,AOI ARE COMPUTED FOR THE EVALUATION OF OMEGA (THE
 7     C SPATIAL FREQUENCY)
 8     C ----------------------------------------------------------------
 9           SUBROUTINE DNGR(R,N,LAMDA,NX,RO,NO)
10           DIMENSION RDENOR(30,60),N(30,60),R(30,60)
11           INTEGER ZSTEP,FLAG
12           REAL N,NOI,LAMDA,LAMTA,NDENOR,NO,KA
13           NAMELIST /DNGDAT/FRACTN          .
14     C ----------------------------------------------------------------
15     C           FRACTN---AXIAL DENSITY/1ST SHELL DENSITY
16     C ----------------------------------------------------------------
17           COMMON /GRIDP/R2(60,60),DMEGA(60,60),LASHEL
18           COMMON /DNGRP/RI(60,60),CRIDEN,FLAG(60,60)
19           COMMON /DNGRP1/NDENOR(30,60)
20           COMMON /ABSOB/AOISQ(60,60),NOI(60,60),LOCX(100,100),LOCY(100,100),
21     5     *KA(100,100)
22           READ(5,DNGDAT)
23           WRITE(6,DNGDAT)
24           LAMTA=LAMDA*1.OE-4
25           CRIDEN=9.1095E-28*3.14159*9.OE20/(LAMTA**2*(4.8032E-10)**2)
26     C ----------------------------------------------------------------
27     C           DENORMALIZING THE RADIUS AND DENSITY
28     C ----------------------------------------------------------------
29           DD 210 J=1,NX
30           DD 211 I=1,LASHEL
31           RDENOR(I,J)=R(I,J)*RO
32           NDENOR(I,J)=N(I,J)*NO
33     211 CDNTINUE
34     210 CONTINUE
35           LIMIT=LASHEL-2
36           DO 205 J=1,NX
37           SLOPE1=N(2,J)-N(1,J)
38           SLDPE3=SLOPE1
39           DO 201 I=1,LIMIT
40           SLOPE2=N(I+2,J)-N(I+1,J)
41           I2M1=2*I-1
42           I2=2*I
43           I2P1=2*I+1
44           IF (SLOPE1.LT.O.O.OR.SLOPE2.LT.O.O) GOTO 5
45     C----------------------------------------------------------------
46     C           TEST FOR DENSITY AT BOUNDARY REGION BETWEEN TWO SHELLS
47     C----------------------------------------------------------------
48           IF(SLOPE2.LT.SLOPE1.AND.SLOPE3.LT.SLOPE1) GOTO 1
49           IF (SLDPE2.LT.SLDPE1) GOTO 2
50           GOTO 1
51     5 IF(SLOPE1.GT.O.O.AND.SLOPE2.LT.O.O) GOTO 2
52           IF (SLDPE1.LT.O.O.AND.SLOPE2.GT.O.O) GOTO 4
53           IF (SLOPE2.GT.SLOPE1.AND.SLOPE3.GT.SLOPE1) GOTO 3
54           IF (SLDPE2.GT.SLOPE1) GOTO 4
55           GOTO 3
56     C ----------------------------------------------------------------
57     C           PARABOLIC INCREASING DENSITY APPROXIMATION
58     C ----------------------------------------------------------------
59     1 SLOPE3=SLOPE1
60           SLOPE1=SLOPE2
61           AOISQ(I2,J)=(NDENOR(I,J)*R2(I2P1,J)**2-NDENOR(I+1,J)*R2(I2M1,J
62     *)**2)/(NDENOR(I+1,J)-NDENOR(I,J))
63           NOI(I2,J)=NDENOR(I,J)/(1+R2(I2M1,J)**2/AOISQ(I2,J))
64           OMEGA(I2,J)=SQRT(NOI(I2,J)*9E20/(CRIDEN*AOISQ(I2,J)))
65           RI(I2,J)=SQRT(1-NOI(I2,J)/CRIDEN)
66           FLAG(I2,J)=1
67           AOISQ(I2P1,J)=ADISQ(I2,J)
68           NOI(I2P1,J)=NOI(I2,J)
69           OMEGA(I2P1,J)=DMEGA(I2,J)
70           RI(I2P1,J)=RI(I2,J)
```
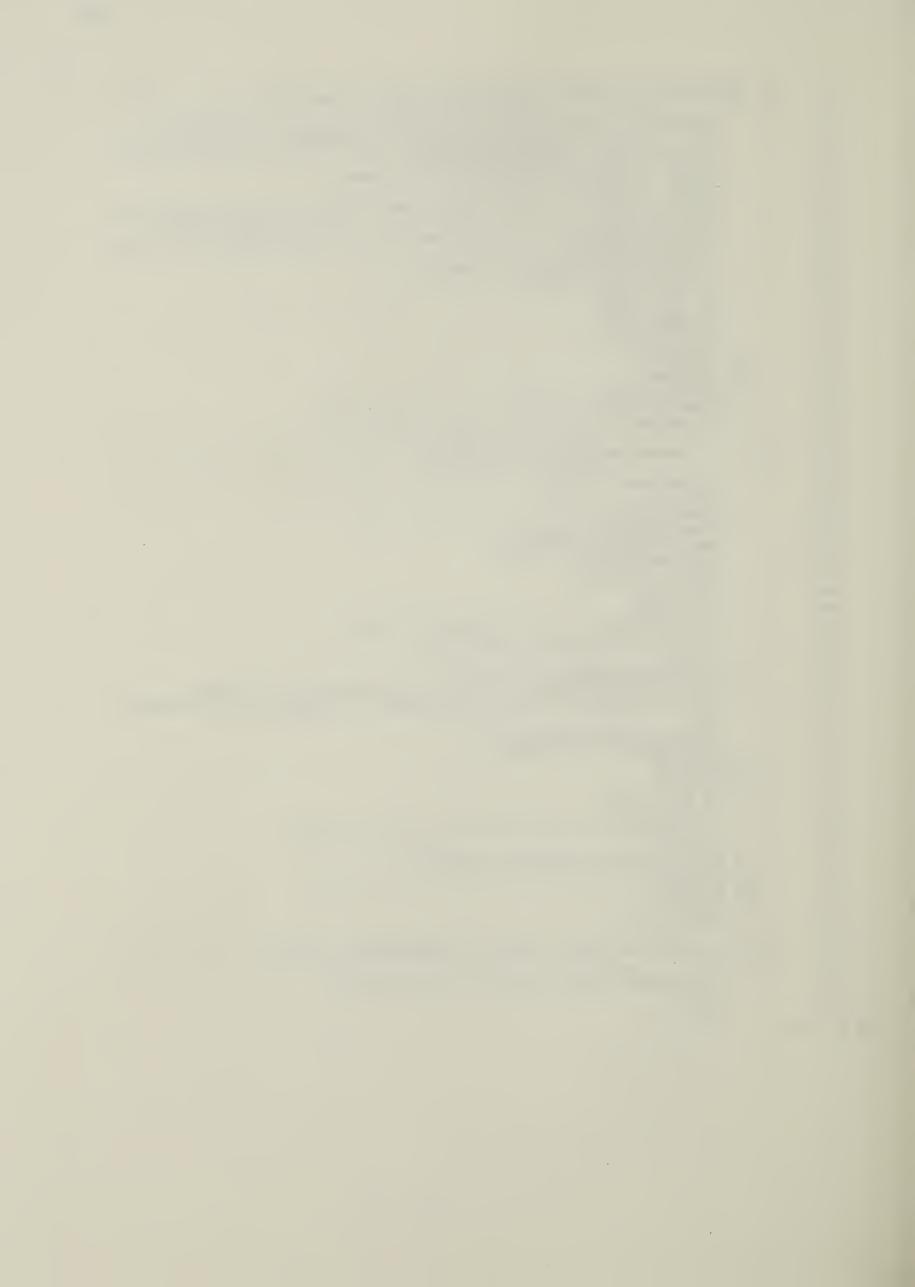
```
71              FLAG(I2P1,J)=FLAG(I2,J)
72              GOTO 201
73      C  ------------------------------------------------------------------
74      C               NON-PARABOLIC INCREASING DENSITY APPROXIMATION
75      C  ------------------------------------------------------------------
76          2 SLOPE3=SLOPE1
77              SLOPE1=SLOPE2
78              TERM1=NOENOR(I+1,J)/R2(I2-1,J)**2
79              TERM2=NDENOR(I,J)/R2(I2P1,J)**2
80              AOISQ(I2,J)=(NDENOR(I+1,J)-NOENOR(I,J))/(TERM1-TERM2)
81              AOISQ(I2P1,J)=AOISQ(I2,J)
82              NOI(I2,J)=NOENOR(I,J)/(1-AOISQ(I2,J)**2/R2(I2M1,J)**2)
83              NOI(I2P1,J)=NOI(I2,J)
84              RI(I2,J)=SQRT(1-NOI(I2,J)/CRIDEN)
85              RI(I2P1,J)=RI(I2,J)
86              FLAG(I2,J)=2
87              FLAG(I2P1,J)=FLAG(I2,J)
88              GOTO 201
89      C  ------------------------------------------------------------------
90      C               PARABOLIC DECREASING OENSITY APPROXIMATION
91      C  ------------------------------------------------------------------
92          3 SLOPE3=SLOPE1
93              SLOPE1=SLOPE2
94              AOISQ(I2,J)=(NOENOR(I,J)*R2(I2P1,J)**2-NOENOR(I+1,J)*R2(I2M1,J)**
95             *2)/(NOENOR(I,J)-NOENOR(I+1,J))
96              NOI(I2,J)=NOENOR(I,J)/(1-R2(I2M1,J)**2/AOISQ(I2,J))
97              OMEGA(I2,J)=SQRT(NOI(I,J)*9E2O/(CRIOEN*AOISQ(I2,J)))
98              RI(I2,J)=SQRT(1-NOI(I2,J)/CRIOEN)
99              FLAG(I2,J)=3
100             AOISQ(I2P1,J)=AOISQ(I2,J)
101             NOI(I2P1,J)=NOI(I2,J)
102             OMEGA(I2P1,J)=OMEGA(I2,J)
103             RI(I2P1,J)=RI(I2,J)
104             FLAG(I2P1,J)=FLAG(I2,J)
105             GOTO 201
106     C  ------------------------------------------------------------------
107     C               NON-PARABOLIC OECREASING OENSITY APPROXIMATION
108     C  ------------------------------------------------------------------
109         4 SLOPE3=SLOPE1
110             SLOPE1=SLOPE2
111             T1=NOENOR(I,J)/R2(I2P1,J)**2
112             T2=NOENOR(I+1,J)/R2(I2M1,J)**2
113             AOISQ(I2,J)=(NDENOR(I+1,J)-NOENOR(I,J))/(T1-T2)
114             AOISQ(I2P1,J)=AOISQ(I2,J)
115             NOI(I2,J)=NOENOR(I,J)/(1+AOISQ(I2,J)/R2(I2M1,J)**2)
116             NOI(I2P1,J)=NOI(I2,J)
117             RI(I2,J)=SQRT(1-NOI(I2,J)/CRIOEN)
118             RI(I2P1,J)=RI(I2,J)
119             FLAG(I2,J)=4
120             FLAG(I2P1,J)=FLAG(I2,J)
121     201 CONTINUE
122             SLOPE1=NOENOR(LASHEL,J)-NDENOR(LASHEL-1,J)
123             IF (SLOPE1.LT.0.0) GOTO 7
124             TERM1=NOENOR(LASHEL,J)/R2(LASHEL*2-3,J)**2
125             TERM2=NOENOR(LASHEL-1,J)/R2(LASHEL*2-1,J)**2
126             AOISQ(LASHEL*2-2,J)=(NOENOR(LASHEL,J)-NDENOR(LASHEL-1,J))/
127            *(TERM1-TERM2)
128             NOI(LASHEL*2-2,J)=NDENOR(LASHEL-1,J)/(1-AOISQ(LASHEL*2-2,J)**
129            *2/R2(LASHEL*2-3,J)**2)
130             FLAG(LASHEL*2-2,J)=2
131             RI(LASHEL*2-2,J)=SQRT(1-NOI(LASHEL*2-2,J)/CRIOEN)
132             GOTO 8
133         7 T1=NOENOR(LASHEL-1,J)/R2(LASHEL*2-1,J)**2
134             T2=NOENOR(LASHEL,J)/R2(2*LASHEL-3,J)**2
135             AOISQ(LASHEL*2-2,J)=(NDENOR(LASHEL,J)-NDENOR(LASHEL-1,J))
136            */(T1-T2)
137             NOI(LASHEL*2-2,J)=NOENOR(LASHEL-1,J)/(1+AOISQ(LASHEL*2-2,J)**2
138            */R2(LASHEL*2-1,J)**2)
139             RI(LASHEL*2-2,J)=SQRT(1-NOI(LASHEL*2-2,J)/CRIOEN)
140             FLAG(LASHEL*2-2,J)=4
```

```
141        8 AOISQ(LASHEL*2-1,J)=AOISQ(LASHEL*2-2,J)
142          AOISQ(LASHEL*2,J)=AOISQ(LASHEL*2-2,J)
143          NOI(LASHEL*2-1,J)=NOI(LASHEL*2-2,J)
144          NOI(LASHEL*2,J)=NOI(LASHEL*2-2,J)
145          RI(LASHEL*2-1,J)=RI(LASHEL*2-2,J)
146          RI(LASHEL*2,J)=RI(LASHEL*2-2,J)
147          FLAG(LASHEL*2-1,J)=FLAG(LASHEL*2-2,J)
148          FLAG(LASHEL*2,J)=FLAG(LASHEL*2-2,J)
149     C --------------------------------------------------------------------
150     C          THE INNERMOST SHELL IS ASSUMED TO HAVE A PARABOLIC DENSITY
151     C          THE OUTERMOST SHELL IS ASSUMED TO HAVE A NON-PARABOLIC
152     C          DECREASING DENSITY PROFILE
153     C --------------------------------------------------------------------
154          AOISQ(1,J)=FRACTN*R2(1,J)**2/(1-FRACTN)
155          NOI(1,J)=FRACTN*NDENOR(1,J)
156          OMEGA(1,J)=SQRT(NOI(1,J)*9E20/(CRIDEN*AOISQ(1,J)))
157          RI(1,J)=SQRT(1-NOI(1,J)/CRIDEN)
158          FLAG(1,J)=1
159          OMEGA(2*LASHEL,J)=0.0
160          OMEGA(2*LASHEL-1,J)=0.0
161          OMEGA(2*LASHEL-2,J)=0.0
162      205 CONTINUE
163          WRITE(6,601)
164      601 FORMAT('      FLAG      ',5X,'REFRACTIVE INDEX',5X,'      AOI**2
165         *',5X,'      NOI      ')
166          LASH2=2*LASHEL
167          DO 206 I=1,LASH2
168          WRITE (6,602) FLAG(I,1),RI(I,1),AOISQ(I,1),NOI(I,1)
169      602 FORMAT(8X,I3,9X,E16.8,5X,E15.8,5X,E15.8)
170      206 CONTINUE
171          RETURN
172          END
```
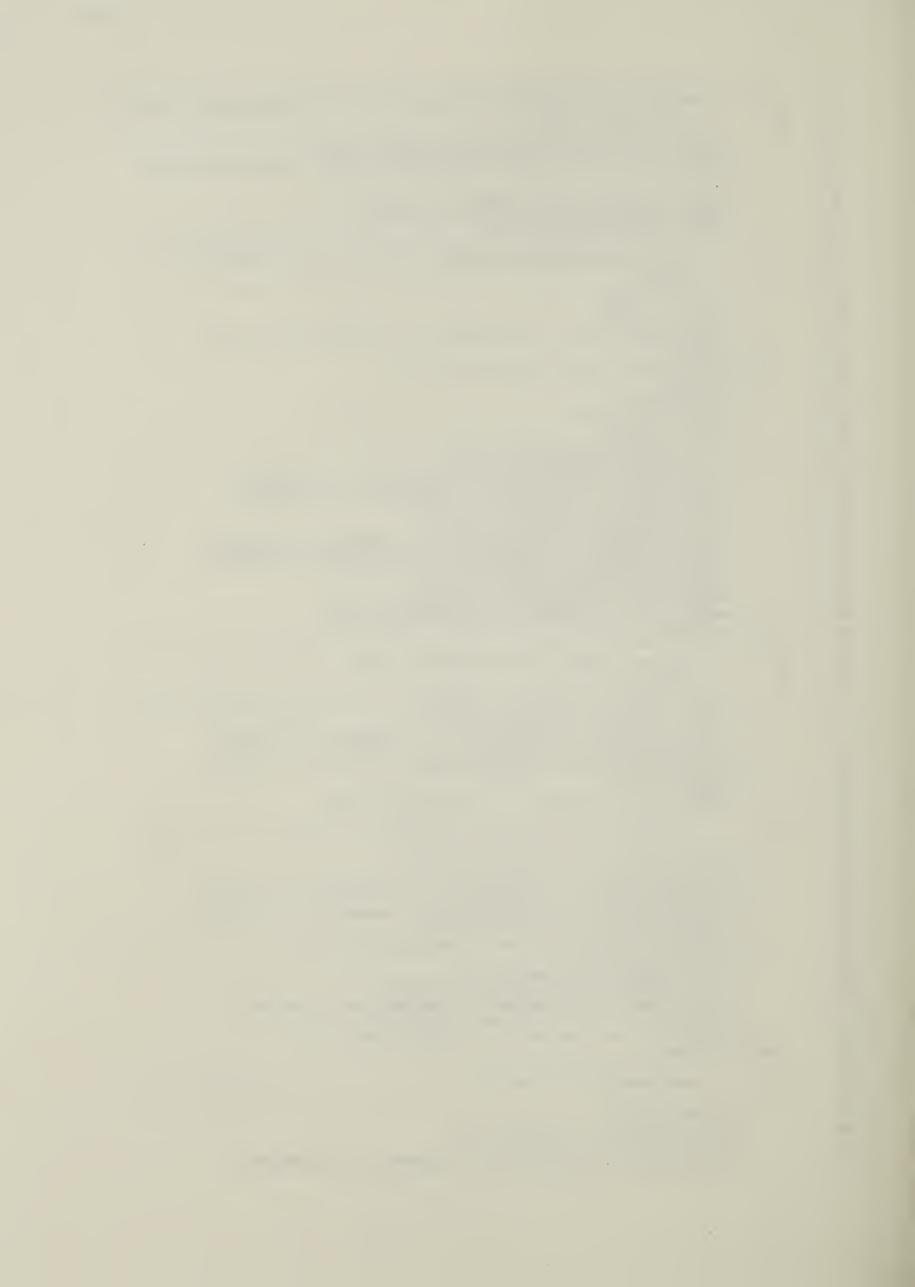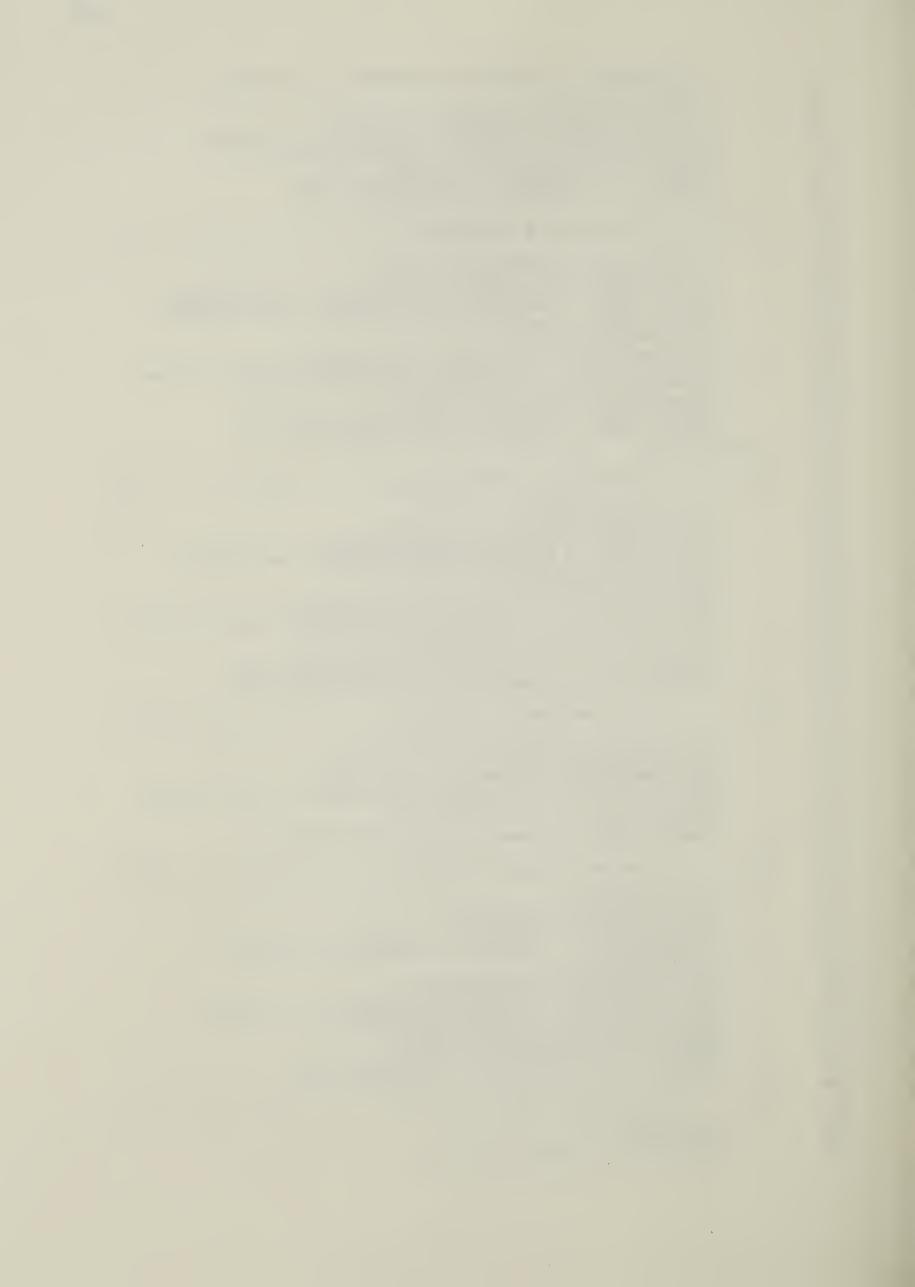
```
 1      C -----------------------------------------------------------------
 2      C SUBROUTINE FOR ENERGY ABSORPTION IN CORR. PLASMA CELLS
 3      C -----------------------------------------------------------------
 4              SUBROUTINE ENERGY(TIME,STEP,XMIN,NX,XLAS,VLAS,DX,EP,LASPWR,N)
 5              REAL LASPWR(30,60),EP(30,60),KA,N(30,60),PONOR(30,60),PONDZ(30,60)
 6              INTEGER TOTRAY,STEP,X,RXMIN,XMIN
 7              COMMON /LASP/L3,RLO,BMS,NCRIT,TL,DTL,MRMAX
 8              COMMON /PWRAY/AO
 9              COMMON /ABSOB/AOISQ(60,60),NOI(60,60),LOCX(100,100),LOCY(100,100)
10             *,KA(100,100)
11              COMMON /DRAYP/XO(100),YO(100),THETAX(100),THETAY(100),P(100),TOTRA
12             *Y,ENIN,P1,EN(100)
13              COMMON /RAYENP/NPTS(100),VSUM(100)
14              IF (STEP.EQ.1) GOTO 1
15              DO 207 J=1,60
16              DO 208 I=1,30
17              LASPWR(I,J)=0.0
18              EP(I,J)=0.0
19        208 CONTINUE
20        207 CONTINUE
21          1 WRITE(6,601)
22        601 FORMAT(/' CELL LOCATION ',5X,' POWER IN CELL ',
23             *5X,'ENERGY IN CELL ',5X,/,3X,'X',7X,'Y')
24      C -----------------------------------------------------------------
25      C            POWER AND ENERGY CALCULATION
26      C -----------------------------------------------------------------
27              OO 204 MARK=1,TOTRAY
28              NLAS=60
29              JJ=NPTS(MARK)-1
30              PIN=P(MARK)/NPTS(MARK)
31              ENINI=EN(MARK)/NPTS(MARK)
32              LIMIT=NPTS(MARK)
33              DO 202 K=2,LIMIT
34              POWER=PIN
35              ENER=ENINI
36              IF (LOCX(MARK,K-1).LT.LOCX(MARK,K)) GOTO 2
37              IX=IFIX((LOCX(MARK,K-1)-1)/2.0)+1
38              GOTO 3
39          2 IX=IFIX(LOCX(MARK,K-1)/2.0)+1
40          3 LASPWR(IX,LOCY(MARK,K-1))=LASPWR(IX,LOCY(MARK,K-1))+POWER
41              EP(IX,LOCY(MARK,K-1))=EP(IX,LOCY(MARK,K-1))+ENER*(1-EXP(-KA(MARK,K
42             *)))
43              ENER=ENER*EXP(-KA(MARK,K))
44              POWER=POWER*EXP(-KA(MARK,K))
45        202 CONTINUE
46        204 CONTINUE
47              DO 205 J=1,60
48              DO 206 I=1,30
49              IF (LASPWR(I,J).NE.0.0.OR.EP(I,J).NE.0.0) GOTO 4
50              GOTO 206
51          4 WRITE(6,602)I,J,LASPWR(I,J),EP(I,J)
52        602 FORMAT(1X,I3,5X,I3,8X,E15.8,5X,E15.8,5X,E15.8)
53        206 CONTINUE
54        205 CONTINUE
55              WRITE(12) EP
56      C-----------------------------------------------------------------
57      C TO CALCULATE THE RAOIAL ANO AXIAL PONOEROMOTIVE FORCE
58      C-----------------------------------------------------------------
59              CALL PONDER(LASPWR,VLAS,NLAS,OX,PONOR,PONDZ)
60              RETURN
61              END
END OF FILE
```
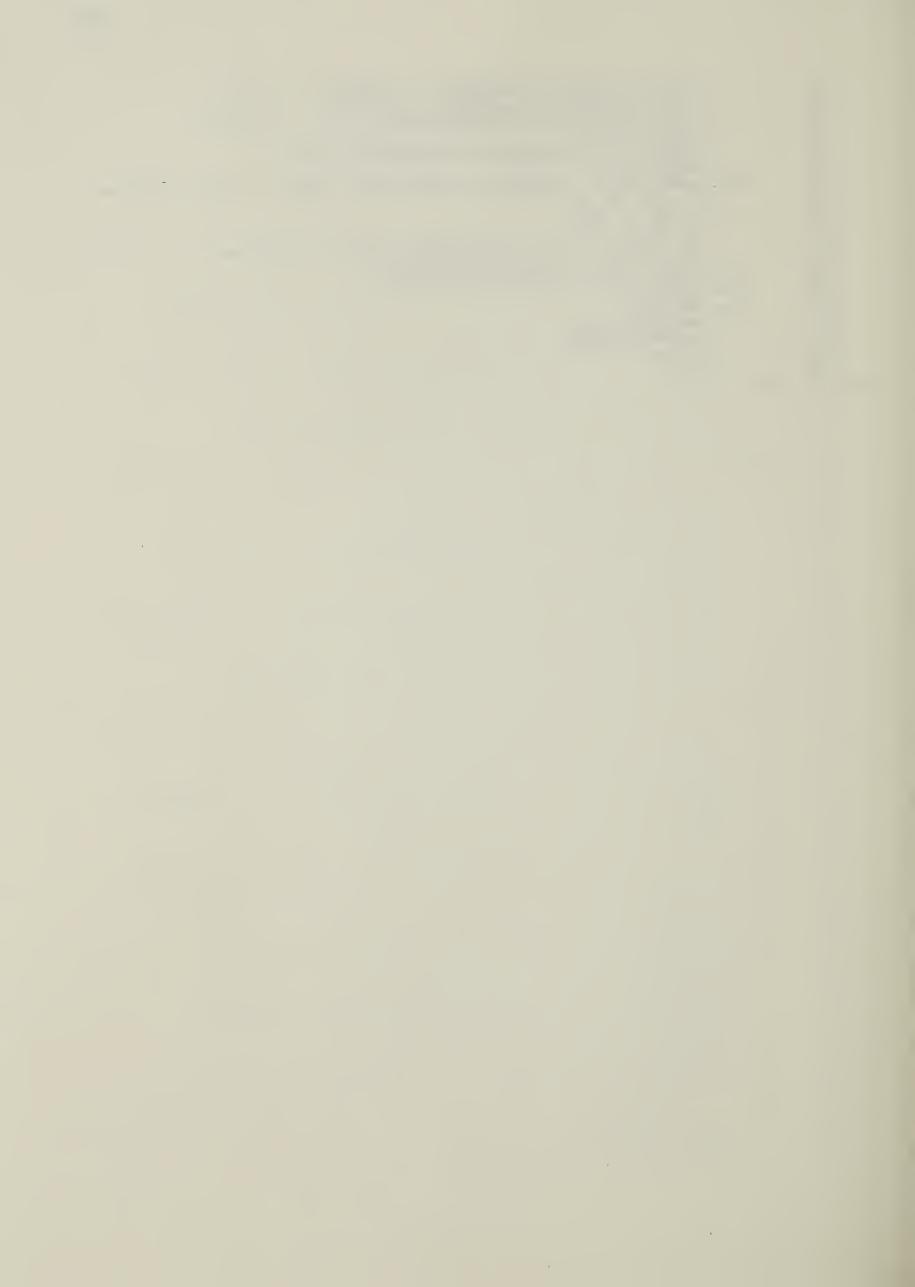
```
 1      C---------------------------------------------------------------------
 2      C           PROGRAM FOR CALCULATING THE RADIAL AND AXIAL PONDEROMOTIVE FORCE
 3      C           IN INDIVIDUAL CELLS
 4      C---------------------------------------------------------------------
 5              SUBROUTINE PONDER(P,VLAS,NLAS,DX,PONDR,PONDZ)
 6              REAL P(30,60),PONDR(30,60),PONDZ(30,60),LASHEL,NDENOR,AVEI(30,60
 7           *)
 8              COMMON /GRIDP/R2(60,60),OMEGA(60,60),LASHEL
 9              COMMON /DNGRP/RI(60,60),CRIDEN,FLAG(60,60)
10              COMMON /DNGRP1/NDENDR(30,60)
11      C---------------------------------------------------------------------
12      C          TO FIND PONDEROMOTIVE FORCES AT THE CELLS AWAY FROM THE
13      C          BOUNDARY
14      C---------------------------------------------------------------------
15              DO 201 J=1,NLAS
16              DO 202 I=2,30
17              AVEI(I,J)=P(I,J)/(3.14159*(R2(2*I,J)**2-R2(2*(I-1),J)**2))
18        202 CONTINUE
19              AVEI(1,J)=P(1,J)/(3.14159*R2(2,J)**2)
20        201 CONTINUE
21              NLASM1=NLAS-1
22              DO 203 J=2,NLASM1
23              DO 204 I=2,29
24              PIU=0.5*(AVEI(I+1,J)+AVEI(I,J))
25              PIL=0.5*(AVEI(I,J)+AVEI(I-1,J))         '
26              CU=VLAS*SQRT(1-0.5*(NDENOR(I,J)+NDENOR(I+1,J))/CRIDEN)
27              CL=VLAS*SQRT(1-0.5*(NDENOR(I,J)+NDENOR(I-1,J))/CRIDEN)
28              PILEFT=(AVEI(I,J-1)+AVEI(I,J))*0.5
29              PIRITE=(AVEI(I,J+1)+AVEI(I,J))*0.5
30              CLEFT=VLAS*SQRT(1-0.5*(NDENDR(I,J-1)+NDENOR(I,J))/CRIDEN)
31              CRITE=VLAS*SQRT(1-0.5*(NDENOR(I,J+1)+NDENOR(I,J))/CRIDEN)
32              DIDR=(PIU/CU-PIL/CL)/(R2(2*I,J)-R2(2*(I-1),J))
33              DIDZ=(PIRITE/CRITE-PILEFT/CLEFT)/DX
34              PONDR(I,J)=-0.5*NDENDR(I,J)/CRIDEN*DIDR*1.0E7
35              PONDZ(I,J)=-0.5*NDENOR(I,J)/CRIDEN*DIDZ*1.0E7
36        204 CONTINUE
37      C---------------------------------------------------------------------
38      C          TO FIND VALUES AT THE INNERMOST LAYER
39      C          LAYER 1
40      C---------------------------------------------------------------------
41              PILEFT=(AVEI(1,J-1)+AVEI(1,J))*0.5
42              PIRITE=(AVEI(1,J+1)+AVEI(1,J))*0.5
43              CLEFT=VLAS*SQRT(1-0.5*(NDENOR(1,J-1)+NDENOR(1,J))/CRIDEN)
44              CRITE=VLAS*SQRT(1-0.5*(NDENDR(1,J+1)+NDENOR(1,J))/CRIDEN)
45              DIDZ=(PIRITE/CRITE-PILEFT/CLEFT)/DX
46              PONDR(1,J)=0.0
47              PONDZ(1,J)=-0.5*NDENOR(1,J)/CRIDEN*DIDZ*1.0E7
48      C---------------------------------------------------------------------
49      C          TO FIND POND. FORCES FOR LAYER 30
50      C---------------------------------------------------------------------
51              PILEFT=(AVEI(30,J-1)+AVEI(30,J))*0.5
52              PIRITE=(AVEI(30,J+1)+AVEI(30,J))*0.5
53              CLEFT=VLAS*SQRT(1-0.5*(NDENOR(30,J-1)+NDENOR(30,J))/CRIDEN)
54              CRITE=VLAS*SQRT(1-0.5*(NDENDR(30,J+1)+NDENOR(30,J))/CRIDEN)
55              DIDZ=(PIRITE/CRITE-PILEFT/CLEFT)/DX
56              PONDZ(30,J)=-0.5*NDENDR(30,J)/CRIDEN*DIDZ*1.0E7
57              PIU=0.5*AVEI(30,J)
58              PIL=0.5*(AVEI(30,J)+AVEI(29,J))
59              CU=VLAS*SQRT(1-0.5*NDENDR(30,J)/CRIDEN)
60              CL=VLAS*SQRT(1-0.5*(NDENOR(30,J)+NDENOR(29,J))/CRIDEN)
61              DIDR=(PIU/CU-PIL/CL)/(R2(60,J)-R2(58,J))
62              PONDR(30,J)=-0.5*NDENDR(30,J)/CRIDEN*DIDR*1.0E7
63        203 CONTINUE
64      C---------------------------------------------------------------------
65      C          POND.FORCES AT COLUMN ONE
66      C---------------------------------------------------------------------
67              DO 207 I=2,29
68              PIU=0.5*(AVEI(I+1,1)+AVEI(I,1))
69              PIL=0.5*(AVEI(I,1)+AVEI(I-1,1))
70              CU=VLAS*SQRT(1-0.5*(NDENDR(I,1)+NDENDR(I+1,1))/CRIDEN)
```

```
 71            CL=VLAS*SQRT(1-0.5*(NDENOR(I,1)+NDENOR(I-1,1))/CRIDEN)
 72            PILEFT=AVEI(I,1)
 73            PIRITE=(AVEI(I,2)+AVEI(I,1))*0.5
 74            CLEFT=VLAS*SQRT(1-0.5*NDENOR(I,1)/CRIDEN)
 75            CRITE=VLAS*SQRT(1-0.5*(NDENDR(I,2)+NDENOR(I,1))/CRIDEN)
 76            DIDR=(PIU/CU-PIL/CL)/(R2(2*I,1)-R2(2*(I-1),1))
 77            DIDZ=(PIRITE/CRITE-PILEFT/CLEFT)/DX
 78            PONDR(I,1)=-0.5*NDENOR(I,1)/CRIDEN*DIDR*1.0E7
 79            PONDZ(I,1)=-0.5*NDENOR(I,1)/CRIDEN*DIDZ*1.0E7
 80      C-----------------------------------------------------------------
 81      C         TD FIND FDRCES AT CDLUMN NLAS
 82      C-----------------------------------------------------------------
 83            PIU=0.5*(AVEI(I+1,NLAS)+AVEI(I,NLAS))
 84            PIL=0.5*(AVEI(I,NLAS)+AVEI(I-1,NLAS))
 85            CU=VLAS*SQRT(1-0.5*(NDENOR(I,NLAS)+NDENOR(I+1,NLAS))/CRIDEN)
 86            CL=VLAS*SQRT(1-0.5*(NDENOR(I,NLAS)+NDENOR(I-1,NLAS))/CRIDEN)
 87            PILEFT=(AVEI(I,NLASM1)+AVEI(I,NLAS))*0.5
 88            PIRITE=AVEI(I,NLAS)*0.5
 89            CRITE=VLAS*SQRT(1-0.5*NDENDR(I,NLAS)/CRIDEN)
 90            CLEFT=VLAS*SQRT(1-0.5*(NDENOR(I,NLAS)+NDENOR(I,NLASM1))/CRIDEN)
 91            DIDR=(PIU/CU-PIL/CL)/(R2(2*I,NLAS)-R2(2*(I-1),NLAS))
 92            DIDZ=(PIRITE/CRITE-PILEFT/CLEFT)/DX
 93            PDNDR(I,NLAS)=-0.5*NDENOR(I,NLAS)/CRIDEN*DIDR*1.0E7
 94            PONDZ(I,NLAS)=-0.5*NDENDR(I,NLAS)/CRIDEN*DIDZ*1.0E7
 95        207 CDNTINUE
 96      C---------------------------------------------------------------
 97      C         TD FIND FDRCES AT CDRNER CELLS
 98      C---------------------------------------------------------------
 99            PIU=0.5*AVEI(30,NLAS)
100            PIL=0.5*(AVEI(30,NLAS)+AVEI(29,NLAS))
101            CU=VLAS*SQRT(1-0.5*NDENOR(30,NLAS)/CRIDEN)
102            CL=VLAS*SQRT(1-0.5*(NDENOR(30,NLAS)+NDENOR(29,NLAS))/CRIDEN)
103            PILEFT=(AVEI(30,NLASM1)+AVEI(30,NLAS))*0.5
104            PIRITE=AVEI(30,NLAS)*0.5
105            CRITE=VLAS*SQRT(1-0.5*NDENDR(30,NLAS)/CRIDEN)
106            CLEFT=VLAS*SQRT(1-0.5*(NDENDR(30,NLAS)+NDENOR(30,NLASM1))/CRIDEN)
107            DIDR=(PIU/CU-PIL/CL)/(R2(60,NLAS)-R2(58,NLAS))
108            DIDZ=(PIRITE/CRITE-PILEFT/CLEFT)/DX
109            PDNDR(30,NLAS)=-0.5*NDENDR(30,NLAS)/CRIDEN*DIDR*1.0E7
110            PONDZ(30,NLAS)=-0.5*NDENOR(30,NLAS)/CRIDEN*DIDZ*1.0E7
111      C------------------------------------------------------------------
112      C         TO FIND PDND.FORCES AT CELL(1,30)
113      C------------------------------------------------------------------
114            PILEFT=(AVEI(1,NLASM1)+AVEI(1,NLAS))*0.5
115            PIRITE=AVEI(1,NLAS)*0.5
116            CRITE=VLAS*SQRT(1-0.5*NDENOR(1,NLAS)/CRIDEN)
117            CLEFT=VLAS*SQRT(1-0.5*(NDENOR(1,NLAS)+NDENOR(1,NLASM1))/CRIDEN)
118            DIDZ=(PIRITE/CRITE-PILEFT/CLEFT)/DX
119            PDNDR(1,NLAS)=0.0
120            PONDZ(1,NLAS)=-0.5*NDENOR(1,NLAS)/CRIDEN*DIDZ*1.0E7
121      C-----------------------------------------------------------------
122      C         TD FIND PDND.FDRCES AT CELL(30,1)
123      C-----------------------------------------------------------------
124            PIU=0.5*AVEI(30,1)
125            PIL=0.5*(AVEI(30,1)+AVEI(29,1))
126            CU=VLAS*SQRT(1-0.5*NDENDR(30,1)/CRIDEN)
127            CL=VLAS*SQRT(1-0.5*(NDENOR(30,1)+NDENOR(29,1))/CRIDEN)
128            PILEFT=AVEI(30,1)
129            PIRITE=(AVEI(30,2)+AVEI(30,1))*0.5
130            CLEFT=VLAS*SQRT(1-0.5*NDENOR(30,1)/CRIDEN)
131            CRITE=VLAS*SQRT(1-0.5*(NDENOR(30,2)+NDENOR(30,1))/CRIDEN)
132            DIDR=(PIU/CU-PIL/CL)/(R2(60,1)-R2(58,1))
133            DIDZ=(PIRITE/CRITE-PILEFT/CLEFT)/DX
134            PDNDR(30,1)=-0.5*NDENDR(30,1)/CRIDEN*DIDR*1.0E7
135            PDNDZ(30,1)=-0.5*NDENDR(30,1)/CRIDEN*DIDZ*1.0E7
136      C-----------------------------------------------------------------
137      C         TD FIND PDND. FORCES AT CELL(1,1)
138      C-----------------------------------------------------------------
139            PILEFT=AVEI(1,1)
140            PIRITE=(AVEI(1,2)+AVEI(1,1))*0.5
```
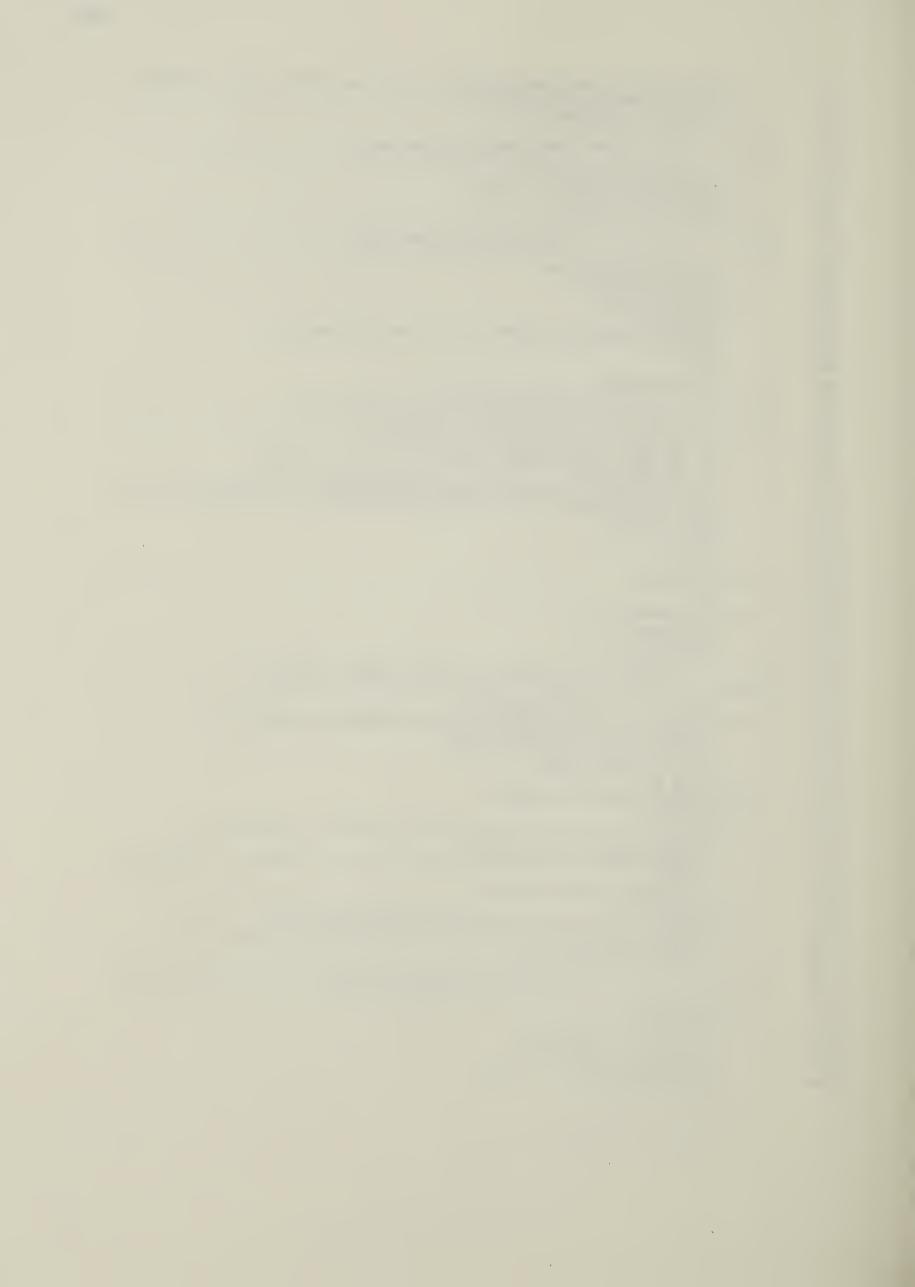
```
141            CLEFT=VLAS*SQRT(1-0.5*NDENOR(1,1)/CRIDEN)
142          . CRITE=VLAS*SQRT(1-0.5*(NDENOR(1,2)+NDENOR(1,1))/CRIDEN)
143            DIDZ=(PIRITE/CRITE-PILEFT/CLEFT)/DX
144            PONDR(1,1)=0.0
145            PONDZ(1,1)=-0.5*NDENOR(1,1)/CRIDEN*DIDZ*1.0E7
146            WRITE(6,600)
147       600 FORMAT(/'CELL LOCATION',5X,'RADIAL POND.FORCE',5X,'AXIAL POND.FORC
148          *E',/,3X,'X',5X,'Y')
149            DO 205 J=1,NLAS
150            DO 206 I=1,30        .
151            IF (PONDR(I,J).EQ.0.0.AND.PONDZ(I,J).EQ.0.0) GOTO 206
152            WRITE(6,601)I,J,PONDR(I,J),PONDZ(I,J)
153       601 FORMAT(I4,2X,I4,10X,E15.8,6X,E15.8)
154       206 CONTINUE
155       205 CONTINUE
156            WRITE(13) PONDR
157            WRITE(14) PONDZ
158            RETURN
159            END
END OF FILE
```
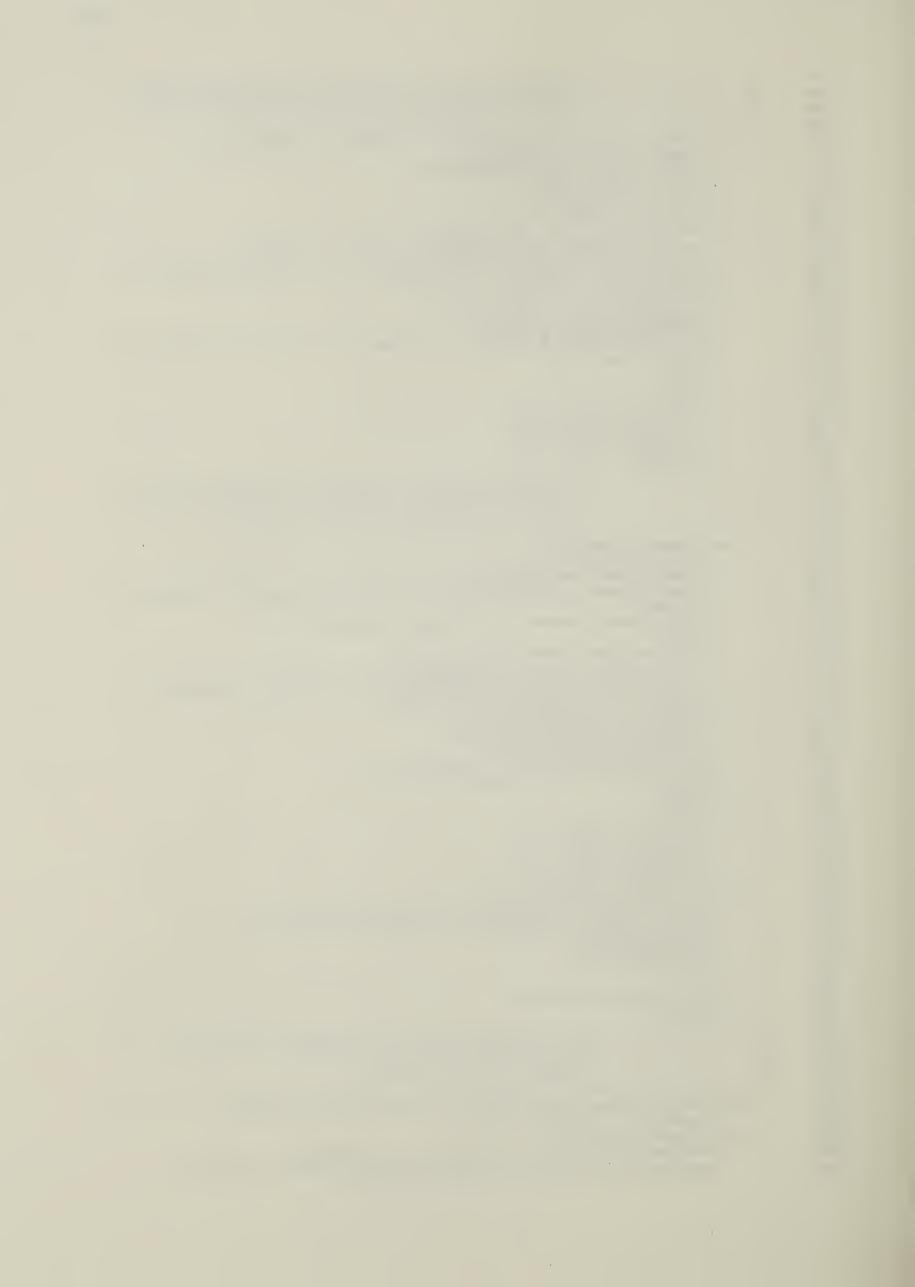
```
 1        C -----------------------------------------------------------------
 2        C SUBPROGRAM FOR FINDING THE RAY PATH IN A PLASMA COLUMN WITH A GIVEN
 3        C DENSITY DISTRIBUTION
 4        C GEOMETRICAL APPROACH IS USED
 5        C THE INTERSECTING POINT BETWEEN THE TRAJECTORY AND THE HORIZONTAL
 6        C OR VERTICAL GRID IS COMPUTED
 7        C THE SPATIAL ADVANCEMENT OF THE RAY IS DONE BY INCREASING THE RADIAL
 8        C DISTANCE UNTIL MAXIMUM VALUE IS ACHIEVED
 9        C THE ANALYTICAL EXPRESSIONS USED ARE BASED ON A PARABOLIC DENSITY
10        C DISTRIBUTION
11        C BOTH CARTESIAN AND CYLINDRICAL CO-ORDINATES ARE USED
12        C -----------------------------------------------------------------
13              SUBROUTINE RAYABS(M,NX1,TDENOR,TO,LAMTA,ZL,ZATOM,XLAS,VLAS,TIME,
14             *DX,XMIN)
15              DOUBLE PRECISION X,Y,VX,VY,DHETAY,DHETAX,DTZ,DTR,Y112,FETA1
16              DOUBLE PRECISION FETA2,FETA3,FETA4
17              DIMENSION R1(100,100),THETA(100,100),Z(100,100),TE(30,60),
18             *TDENOR(30,60)
19              REAL MTHETA,NDI,LAMDA,LAMTA,KA
20              INTEGER FLAG,TOTRAY,MARK,ZATOM,XMIN,RXMIN
21              COMMON /GRIDP/R2(60,60),OMEGA(60,60),LASHEL
22              COMMON /DNGRP/RI(60,60),CRIDEN,FLAG(60,60)
23              COMMON /DRAYP/XO(100),YO(100),THETAX(100),THETAY(100),P(100),TOTRA
24             *Y,ENIN,P1,EN(100)
25              COMMON /ABSOB/ADISQ(60,60),NDI(60,60),LOCX(100,100),LOCY(100,100),
26             *KA(100,100)
27              COMMON /LASP/L3,RLO,BMS,NCRIT,TL,DTL,MRMAX
28              COMMON /RAYENP/NPTS(100),VSUM(100)
29              EXTERNAL FETA1
30              EXTERNAL FETA2
31              EXTERNAL FETA3
32              EXTERNAL FETA4
33        C-----------------------------------------------------------------
34        C                       INITIALIZATION
35        C-----------------------------------------------------------------
36              NX=NX1
37              C=3.0E10
38              LAMDA=LAMTA*1.0E-4
39              DO 203 I=1,TOTRAY
40          203 VSUM(I)=0.0
41        C-----------------------------------------------------------------
42        C                 DENORMALIZING THE ELECTRON TEMPERATURE
43        C-----------------------------------------------------------------
44              DO 205 J=1,NX
45              DO 206 I=1,M
46              TE(I,J)=TDENOR(I,J)*TO
47          206 CONTINUE
48          205 CONTINUE
49              MARK=O
50           12 MARK=MARK+1
51              IF (MARK.GT.TOTRAY) RETURN
52              KA(MARK,1)=O.O
53              IF (XO(MARK).EQ.O.O.AND.YO(MARK).EQ.O.O.AND.THETAX(MARK).EQ.O.O.AN
54             *D.THETAY(MARK).EQ.O.O) GOTO 110
55              X=XO(MARK)
56              Y=YO(MARK)
57              R1(MARK,1)=SQRT(XO(MARK)*XO(MARK)+YO(MARK)*YO(MARK))
58              THETA(MARK,1)=ANGLE(X,Y)
59              IF (THETAX(MARK).EQ.O.O.OR.(THETAX(MARK).EQ.O.O.AND.THETAY(MARK).E
60             *Q.O.O)) GOTO 13
61              DTHETA=ATAN(THETAX(MARK)/THETAY(MARK))
62              GOTO 16
63           13 VX=O.O
64              VY=C*SIN(THETAY(MARK))
65              VZ=C*COS(THETAY(MARK))
66              GOTO 15
67           14 VX=C*SIN(THETAX(MARK))
68              VY=O.O
69              VZ=C*COS(THETAX(MARK))
70              GOTO 15
```
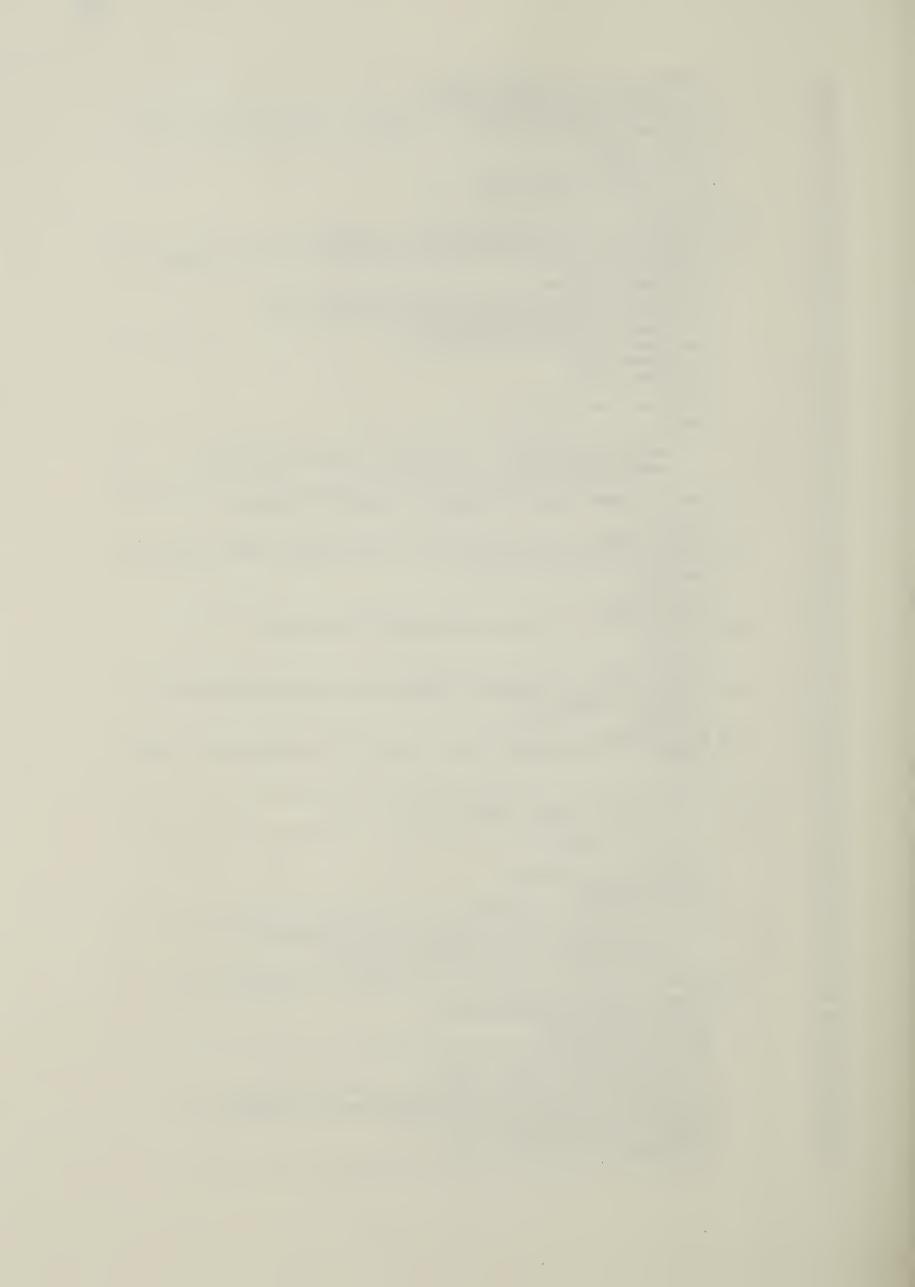
```
 71      16 MTHETA=SQRT(THETAX(MARK)*THETAX(MARK)+THETAY(MARK)*THETAY(MARK))
 72         VY=C*SIN(MTHETA)*COS(DTHETA)
 73         DHETAY=THETAY(MARK)
 74   C-----------------------------------------------------------------------
 75   C           VY HAS THE SAME SIGN AS VECTOR THETAY
 76   C-----------------------------------------------------------------------
 77         VY=DSIGN(VY,DHETAY)
 78         VX=C*SIN(MTHETA)*SIN(DTHETA)
 79         DHETAX=THETAX(MARK)
 80   C-----------------------------------------------------------------------
 81   C           VX HAS THE SAME SIGN AS VECTOR THETAX
 82   C-----------------------------------------------------------------------
 83         VX=DSIGN(VX,DHETAX)
 84         VZ=C*COS(MTHETA)
 85      15 Z(MARK,1)=0.0
 86         DZ=ZL/NX1
 87         ANGVEL=VX*COS(THETA(MARK,1))-VY*SIN(THETA(MARK,1))
 88         JJ=1
 89         J=1
 90         LAST=2*LASHEL
 91   C-----------------------------------------------------------------------
 92   C           SCAN OVER WHICH PLASMA SHELL THE RAY HITS
 93   C-----------------------------------------------------------------------
 94         IF (R1(MARK,1).GT.R2(LAST,1)) GOTO 38
 95         IF (R1(MARK,1).GT.O.AND.R1(MARK,1).LT.R2(1,1))GOTO 1
 96         DO 201 II=2,LAST
 97         IF ((R1(MARK,1).GT.R2(II-1,1).OR.ABS(R1(MARK,1)-R2(II-1,1)).LT.1.0
 98        *E-3).AND.(R1(MARK,1).LT.R2(II,1).OR.ABS(R2(II,1)-R1(MARK,1)).LT.1.
 99        *OE-3)) GOTO 2
100         GOTO 201
101       2 I=II
102         GOTO 31
103     201 CONTINUE
104       1 I=1
105      31 LOCX(MARK,1)=I
106         LOCY(MARK,1)=J
107         IVAR=FLAG(I,J)
108   C-----------------------------------------------------------------------
109   C           CHOOSE THE APPROPRIATE KIND OF DENSITY PROFILE
110   C-----------------------------------------------------------------------
111         GO TO (311,100,33,100),IVAR
112     311 TERM1=(X*X+Y*Y)/2-(VX*VX+VY*VY)/(2*OMEGA(I,J)*OMEGA(I,J))
113         TERM2=(X*VX+Y*VY)/OMEGA(I,J)
114         D=SQRT(TERM1*TERM1+TERM2*TERM2)
115         PHI=FI(TERM1,TERM2)
116         GOTO 34
117     100 ANGMOM=R1(MARK,1)*ANGVEL
118         GOTO 34
119      33 TERM1=(X*X+Y*Y)/2+(VX*VX+VY*VY)/(2*OMEGA(I,J)*OMEGA(I,J))
120         TERM2=(X*VX+Y*VY)/OMEGA(I,J)
121         TERM3=R1(MARK,JJ)*R1(MARK,JJ)+(VX*VX+VY*VY)/(OMEGA(I,J)*OMEGA(I,J)
122        *)-TERM1
123         IF (TERM2.LT.O.O) GOTO 4
124         GOTO 3
125      34 VR=VX*SIN(THETA(MARK,JJ))+VY*COS(THETA(MARK,JJ))
126         IF(ABS(R1(MARK,1)-R2(I,1)).LT.1.OE-3.AND.(VR.GT.O.O)) I=I+1
127         IF (VR.LT.O.O) GOTO 4
128   C-----------------------------------------------------------------------
129   C                   RAY GOES AWAY FROM THE AXIS
130   C-----------------------------------------------------------------------
131       3 JJ=JJ+1
132         IF (JJ.GT.100) GOTO 37
133         IF (I.EQ.1) GOTO 993
134         IVAR=FLAG(I,J)
135         GO TO(30,101,35,111),IVAR
```

```
136        C-------------------------------------------------------------------
137        C                      RAY CALC.(UP) WITH A PARABOLIC INCREASING DENSITY
138        C                      PROFILE APPROXIMATION N=NO(1+R**2/A**2)
139        C-------------------------------------------------------------------
140           30 TERM1=(X*X+Y*Y)/2-(VX*VX+VY*VY)/(2*OMEGA(I,J)*OMEGA(I,J))
141              TERM2=(X*VX+Y*VY)/OMEGA(I,J)
142              D=SQRT(TERM1*TERM1+TERM2*TERM2)
143              PHI=FI(TERM1,TERM2)
144              RMAX=BIGR(R1(MARK,JJ-1),VX,VY,D,I,J)
145              R1(MARK,JJ)=R2(I,J)
146              IF (R1(MARK,JJ).GT.RMAX) GOTO 5
147              TR=RTIME(R1(MARK,JJ-1),R1(MARK,JJ),VX,VY,I,J,PHI,D)
148              VZ=DSQRT(RI(I,J)*RI(I,J)*9.0D20-VX*VX-VY*VY-OMEGA(I,J)*OMEGA(I,J)
149             **R1(MARK,JJ-1)*R1(MARK,JJ-1)*1.0D0)
150              Z(MARK,JJ)=VZ*TR+Z(MARK,JJ-1)
151              IF (Z(MARK,JJ).GT.J*DZ) GOTO 6
152              VSUM(MARK)=VSUM(MARK)+VZ
153              CALL ABSORB(MARK,R1(MARK,JJ-1),Z(MARK,JJ-1),DZ,TR,VX,VY,PHI,LAMDA,
154             *TE,D,I,J,JJ,ZATOM)
155              VXO=VX
156              VYO=VY
157              VX=XVEL(X,VXO,TR,I,J)
158              VY=YVEL(Y,VYO,TR,I,J)
159              X=XCOOR(X,VXO,TR,I,J)
160              Y=YCOOR(Y,VYO,TR,I,J)
161              GOTO 36
162        C-------------------------------------------------------------------
163        C                      RAY CALC.(UP) WITH A PARABOLIC DECREASING DENSITY
164        C                      PROFILE APPROXIMATION N=NO(1-R**2/A**2)
165        C-------------------------------------------------------------------
166           35 R1(MARK,JJ)=R2(I,J)
167              TERM1=(X*X+Y*Y)/2+(VX*VX+VY*VY)/(2*OMEGA(I,J)*OMEGA(I,J))
168              TERM2=(X*VX+Y*VY)/OMEGA(I,J)
169              TERM3=R1(MARK,JJ)*R1(MARK,JJ)+(VX*VX+VY*VY)/(OMEGA(I,J)*OMEGA(I,J)
170             *)-TERM1
171              TERM4=TERM1-(VX*VX+VY*VY)/(OMEGA(I,J)*OMEGA(I,J))
172              NC=0
173              TR=HTIME(TERM1,TERM2,TERM3,I,J,NC)
174              IF (TR.LT.0.0.OR.NC.EQ.1)GOTO 39
175              VZ=DSQRT(RI(I,J)*RI(I,J)*9D20-VX*VX-VY*VY+OMEGA(I,J)*OMEGA(I,J)
176             **R1(MARK,JJ-1)*R1(MARK,JJ-1)*1.0D0)
177              Z(MARK,JJ)=VZ*TR+Z(MARK,JJ-1)
178              IF(Z(MARK,JJ).GT.J*DZ) GOTO 11
179              VSUM(MARK)=VSUM(MARK)+VZ
180              CALL ABSOB1(MARK,TR,VX,VY,VZ,LAMDA,TE,
181             *TERM1,TERM2,I,J,JJ,ZATOM,Z(MARK,JJ-1),DZ)
182              VXO=VX
183              VYO=VY
184              VX=HXVEL(X,VXO,TR,I,J)
185              VY=HYVEL(Y,VYO,TR,I,J)
186              X=HXCOOR(X,VXO,TR,I,J)
187              Y=HYCOOR(Y,VYO,TR,I,J)
188           36 THETA(MARK,JJ)=ANGLE(X,Y)
189              VR=VX*SIN(THETA(MARK,JJ))+VY*COS(THETA(MARK,JJ))
190              ANGVEL=VX*COS(THETA(MARK,JJ))-VY*SIN(THETA(MARK,JJ))
191              ANGMOM=R1(MARK,JJ)*ANGVEL
192              LOCX(MARK,JJ)=I
193              LOCY(MARK,JJ)=J
194              I=I+1
195              IF (I.GT.LAST) GOTO 32
196              GOTO 3
197        C-------------------------------------------------------------------
198        C                      RAY CALC.(UP) WITH A NON-PARABOLIC INCREASING
199        C                      DENSITY PROFILE N=NO(1-A**2/R**2)
200        C                      CONST>0.0 OR <0.0, VR>0.0
201        C-------------------------------------------------------------------
202          101 CONST=(ANGMOM*ANGMOM-9E20*NOI(I,J)*AOISQ(I,J)/CRIDEN)
203              IF(CONST.LT.0.0) GOTO 105
204          112 R1(MARK,JJ)=R2(I,J)
205              TR=TIMEPP(R1(MARK,JJ-1),R1(MARK,JJ),VR,CONST)
206              VZ=SQRT((RI(I,J)*3E10)**2-VR*VR-(ANGMOM/R1(MARK,JJ-1))**2)
```

```
207            Z(MARK,JJ)=VZ*TR+Z(MARK,JJ-1)
208            IF (Z(MARK,JJ).GT.J*DZ) GOTO 102
209            VSUM(MARK)=VSUM(MARK)+VZ
210            CALL ABOB2P(MARK,R1(MARK,JJ-1),Z(MARK,JJ-1),OZ,TR,VR,CONST,LAMDA,
211           *TE,I,J,JJ,ZATOM)
212            OTR=TR*1.000
213            IF (IVAR.EQ.2) GOTO 1121
214            CALL DQG32(0.DO,DTR,FETA3,Y112)
215            GOTO 1122
216       1121 CALL DQG32(0.OO,OTR,FETA1,Y112)
217       1122 THETA(MARK,JJ)=THETA(MARK,JJ-1)+Y112*ANGMOM
218            VR=SQRT(VR*VR-CONST*(1/(R1(MARK,JJ)*R1(MARK,JJ))-1/(R1(MARK,JJ-1)*
219           *R1(MARK,JJ-1))))
220            VT=ANGMOM/R1(MARK,JJ)
221            VX=VR*SIN(THETA(MARK,JJ))+VT*COS(THETA(MARK,JJ))
222            VY=VR*COS(THETA(MARK,JJ))-VT*SIN(THETA(MARK,JJ))
223            X=R1(MARK,JJ)*SIN(THETA(MARK,JJ))
224            Y=R1(MARK,JJ)*COS(THETA(MARK,JJ))
225            LOCX(MARK,JJ)=I
226            LOCY(MARK,JJ)=J
227            I=I+1
228            IF (I.GT.LAST) GOTO 32
229            GOTO 3
230    C---------------------------------------------------------------------
231    C         RAY CALC.(UP) FOR A NON-PARABOLIC DECREASING PROFILE
232    C         N=NO(1+A**2/R**2)
233    C---------------------------------------------------------------------
234      111 CONST=(ANGMOM*ANGMOM+9E20*NOI(I,J)*AOISQ(I,J)/CRIDEN)
235            GOTO 112
236       32 WRITE(6,604)
237      604 FORMAT(/'***** THE RAY GOES OFF THE PRESCRIBED PLASMA SHELLS FOR
238           *BEAM CALCULATION *****'/)
239            GOTO 666
240       39 JJ=JJ-1
241            WRITE(6,606)
242      606 FORMAT(/'***** RAY DOES NOT PENETRATE THE PLASMA *****'/)
243            GOTO 666
244       37 JJ=JJ-1
245            WRITE(6,610)
246      610 FORMAT(/'***** ATTENTION---STORAGE FOR RAY LOCATION OVERFLOW *****
247           *,INCREASE STORAGE '/)
248            GOTO 666
249       38 WRITE(6,611)
250      611 FORMAT(/'*****ATTENTION---RAY IS OUT OF THE PLASMA SHELLS RANGE***
251           ***'/)
252            GOTO 12
253    C---------------------------------------------------------------------
254    C         RAY GOES TOWARDS INNER SHELLS
255    C---------------------------------------------------------------------
256        4 IF (I.EQ.1) GOTO 9
257            JJ=JJ+1
258            IF (JJ.GT.100) GOTO 37
259            IVAR=FLAG(I,J)
260            GO TO (42,103,41,113),IVAR
261    C---------------------------------------------------------------------
262    C         RAY CALC.(UP) WITH A PARABOLIC INCREASING DENSITY
263    C         PROFILE APPROXIMATION N=NO(1+R**2/A**2)
264    C---------------------------------------------------------------------
265       42 TERM1=(X*X+Y*Y)/2-(VX*VX+VY*VY)/(2*OMEGA(I,J)*OMEGA(I,J))
266            TERM2=(X*VX+Y*VY)/OMEGA(I,J)
267            D=SQRT(TERM1*TERM1+TERM2*TERM2)
268            PHI=FI(TERM1,TERM2)
269            RMIN=SMALR(R1(MARK,JJ-1),VX,VY,D,I,J)
270            R1(MARK,JJ)=R2(I-1,J)
271            IF (R1(MARK,JJ).LE.RMIN) GOTO 7
272            TR=RTIME(R1(MARK,JJ-1),R1(MARK,JJ),VX,VY,I,J,PHI,D)
273            VZ=DSQRT(RI(I,J)**2*9D20-VX*VX-VY*VY-OMEGA(I,J)*OMEGA(I,J)
274           **R1(MARK,JJ-1)*R1(MARK,JJ-1)*1.000)
275            Z(MARK,JJ)=VZ*TR+Z(MARK,JJ-1)
276            IF (Z(MARK,JJ).GT.J*DZ) GOTO 6
```

```
277            VSUM(MARK)=VSUM(MARK)+VZ
278            CALL ABSORB(MARK,R1(MARK,JJ-1),Z(MARK,JJ-1),DZ,TR,VX,VY,PHI,LAMDA,
279           *TE,D,I,J,JJ,ZATOM)
280            VXO=VX
281            VYO=VY
282            VX=XVEL(X,VXO,TR,I,J)
283            VY=YVEL(Y,VYO,TR,I,J)
284            X=XCOOR(X,VXO,TR,I,J)
285            Y=YCOOR(Y,VYO,TR,I,J)
286            GOTO 40
287      C---------------------------------------------------------------------
288      C          RAY CALC.(UP) WITH A PARABOLIC DECREASING DENSITY
289      C          PROFILE APPROXIMATION N=NO(1-R**2/A**2)
290      C---------------------------------------------------------------------
291       41 R1(MARK,JJ)=R2(I-1,J)
292            TERM1=(X*X+Y*Y)/2+(VX*VX+VY*VY)/(2*OMEGA(I,J)*OMEGA(I,J))
293            TERM2=(X*VX+Y*VY)/OMEGA(I,J)
294            IF (TERM1.LT.TERM2) GOTO 39
295            TERM3=R1(MARK,JJ)**2+(VX*VX+VY*VY)/OMEGA(I,J)**2-TERM1
296            TERM4=TERM1-(VX*VX+VY*VY)/(OMEGA(I,J)*OMEGA(I,J))
297            RMIN=TERM1-(VX*VX+VY*VY)/OMEGA(I,J)**2+SQRT(TERM1**2-TERM2**2)
298            IF (RMIN.LT.0.0) GOTO 39
299            RMIN=SQRT(RMIN)
300            IF (R1(MARK,JJ).LT.RMIN) GOTO 43
301            NC=O
302            TR=HTIME(TERM1,TERM2,TERM3,I,J,NC)
303            IF (TR.LT.0.0.OR.NC.EQ.1) GOTO 39
304            VZ=DSQRT(RI(I,J)**2*9D2O-VX*VX-VY*VY+OMEGA(I,J)*OMEGA(I,J)
305           **R1(MARK,JJ-1)*R1(MARK,JJ-1)*1.ODO)
306            Z(MARK,JJ)=VZ*TR+Z(MARK,JJ-1)
307            IF(Z(MARK,JJ).GT.J*DZ) GOTO 11
308            VSUM(MARK)=VSUM(MARK)+VZ
309            CALL ABSOB1(MARK,TR,VX,VY,VZ,LAMDA,TE,
310           *TERM1,TERM2,I,J,JJ,ZATOM,Z(MARK,JJ-1),DZ)
311            VXO=VX
312            VYO=VY
313            VX=HXVEL(X,VXO,TR,I,J)
314            VY=HYVEL(Y,VYO,TR,I,J)
315            X=HXCOOR(X,VXO,TR,I,J)
316            Y=HYCOOR(Y,VYO,TR,I,J)
317       40 THETA(MARK,JJ)=ANGLE(X,Y)
318            VR=VX*SIN(THETA(MARK,JJ))+VY*COS(THETA(MARK,JJ))
319            ANGVEL=VX*COS(THETA(MARK,JJ))-VY*SIN(THETA(MARK,JJ))
320            ANGMOM=R1(MARK,JJ)*ANGVEL             .
321            I=I-1
322            LOCX(MARK,JJ)=I
323            LOCY(MARK,JJ)=J
324            GOTO 4
325      C---------------------------------------------------------------------
326      C          RAY CALC.(DOWN) WITH NON-PARABOLIC INCREASING PROFILE
327      C          N=NO(1-A**2/R**2)
328      C          VR<0.0,CONST>0.0 OR<0.0
329      C---------------------------------------------------------------------
330      103 CONST=(ANGMOM*ANGMOM-9E2O*NOI(I,J)*AOISQ(I,J)/CRIDEN)
331            IF (CONST.LT.0.0) GOTO 107
332      104 RMIN=SQRT((R1(MARK,JJ-1)**2*CONST)/((R1(MARK,JJ-1)*VR)**2+CONST))
333            R1(MARK,JJ)=R2(I-1,J)
334            IF (R1(MARK,JJ).LT.RMIN) GOTO 106
335            TR=TIMEPN(R1(MARK,JJ-1),R1(MARK,JJ),VR,CONST)
336            VZ=SQRT((RI(I,J)*3E1O)**2-VR*VR-(ANGMOM/R1(MARK,JJ-1))**2)
337            Z(MARK,JJ)=VZ*TR+Z(MARK,JJ-1)
338            IF (Z(MARK,JJ).GT.J*DZ)GOTO 1021
339            VSUM(MARK)=VSUM(MARK)+VZ
340            CALL ABOB2P(MARK,R1(MARK,JJ-1),Z(MARK,JJ-1),DZ,TR,VR,CONST,LAMDA,
341           *TE,I,J,JJ,ZATOM)
342            DTR=TR*1.ODO
343            IF (IVAR.EQ.2) GOTO 1041
344            CALL DQG32(O.DO,DTR,FETA4,Y112)
345            GOTO 1042
346     1041 CALL DQG32(O.DO,DTR,FETA2,Y112)
347     1042 THETA(MARK,JJ)=THETA(MARK,JJ-1)+Y112*ANGMOM
```
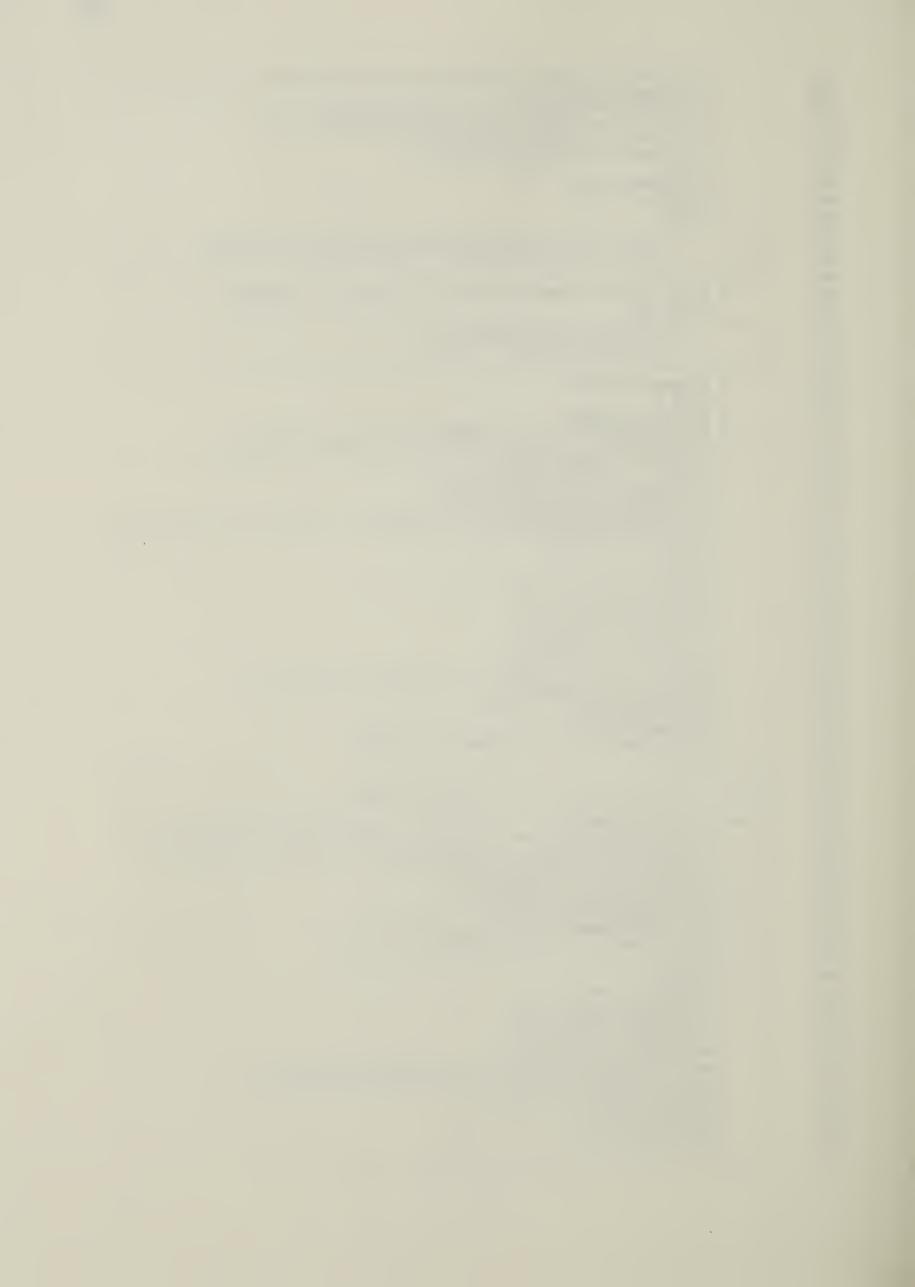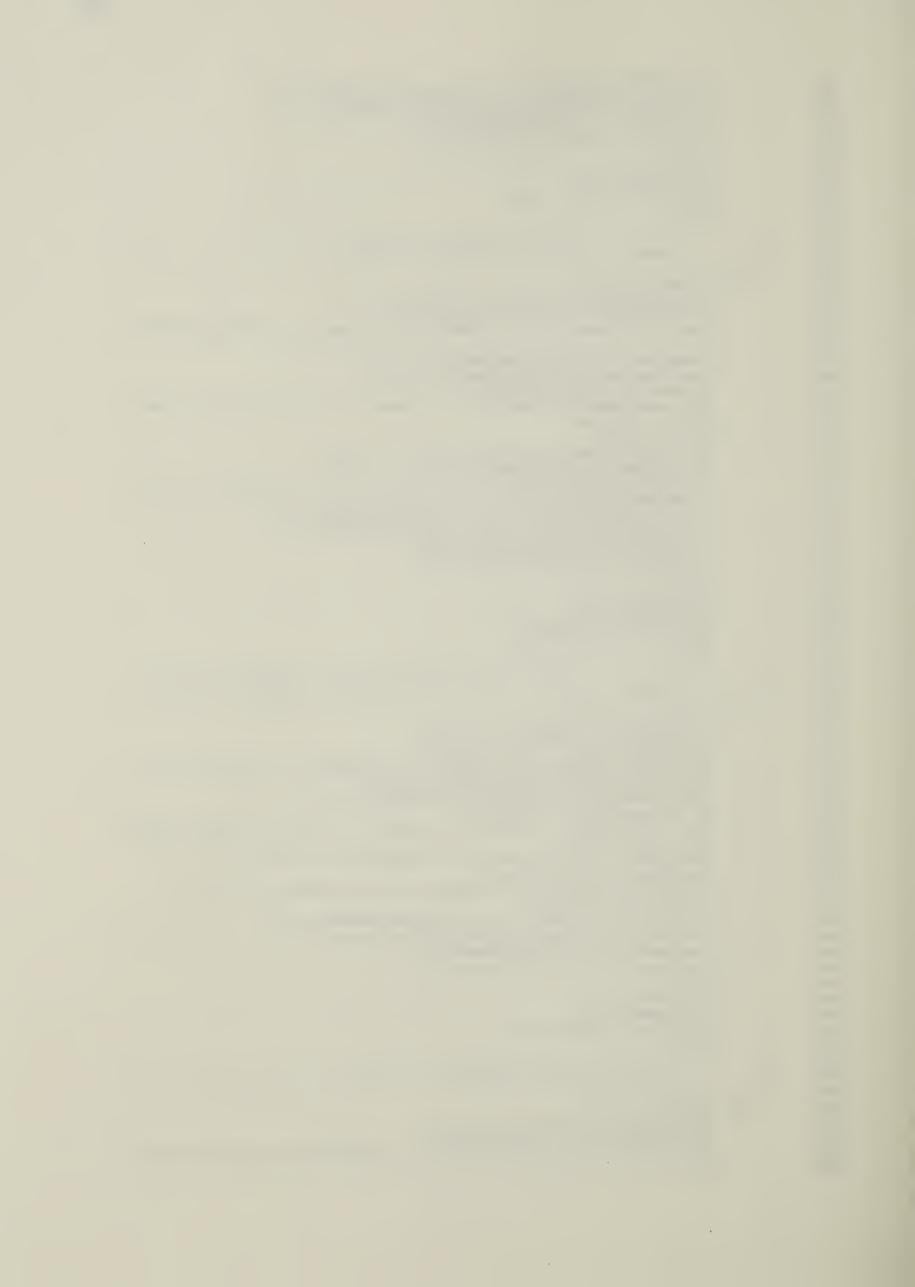
```
348          VR=-SQRT(VR*VR-CONST*(1/R1(MARK,JJ)**2-1/R1(MARK,JJ-1)**2))
349          VT=ANGMOM/R1(MARK,JJ)
350          VX=VR*SIN(THETA(MARK,JJ))+VT*COS(THETA(MARK,JJ))
351          VY=VR*COS(THETA(MARK,JJ))-VT*SIN(THETA(MARK,JJ))
352          X=R1(MARK,JJ)*SIN(THETA(MARK,JJ))
353          Y=R1(MARK,JJ)*COS(THETA(MARK,JJ))
354          I=I-1
355          LOCX(MARK,JJ)=I
356          LOCY(MARK,JJ)=J
357          GOTO 4
358    C------------------------------------------------------------------
359    C          RAY CALC.(UP) WITH NON-PARABOLIC DECREASING PROFILE
360    C          N=NO(1+A**2/R**2)
361    C------------------------------------------------------------------
362      113 CONST=(ANGMOM*ANGMOM+9E20*NOI(I,J)*AOISQ(I,J)/CRIDEN)
363          GOTO 104
364    C------------------------------------------------------------------
365    C          RAY REACHES MINIMUM/MAXIMUM
366    C          N=NO(1+R**2/A**2)
367    C------------------------------------------------------------------
368      7 R1(MARK,JJ)=RMIN
369          GOTO 8
370      5 R1(MARK,JJ)=RMAX
371      8 TR=RTIME(R1(MARK,JJ-1),R1(MARK,JJ),VX,VY,I,J,PHI,D)
372          VZ=DSQRT(RI(I,J)**2*9D20-VX*VX-VY*VY-OMEGA(I,J)*OMEGA(I,J)
373        **R1(MARK,JJ-1)**2*1.0DO)
374          Z(MARK,JJ)=VZ*TR+Z(MARK,JJ-1)
375          IF (Z(MARK,JJ).GT.J*DZ) GOTO 6
376          VSUM(MARK)=VSUM(MARK)+VZ
377          CALL ABSORB(MARK,R1(MARK,JJ-1),Z(MARK,JJ-1),DZ,TR,VX,VY,PHI,LAMDA,
378        *TE,D,I,J,JJ,ZATOM)
379          VXO=VX
380          VYO=VY
381          VX=XVEL(X,VXO,TR,I,J)
382          VY=YVEL(Y,VYO,TR,I,J)
383          X=XCOOR(X,VXO,TR,I,J)
384          Y=YCOOR(Y,VYO,TR,I,J)
385          THETA(MARK,JJ)=ANGLE(X,Y)
386          VR=0.0
387          ANGVEL=VX*COS(THETA(MARK,JJ))-VY*SIN(THETA(MARK,JJ))
388          ANGMOM=R1(MARK,JJ)*ANGVEL
389          LOCX(MARK,JJ)=I
390          LOCY(MARK,JJ)=J
391          IF (R1(MARK,JJ-1).GT.R1(MARK,JJ)) GOTO 3
392          GOTO 4
393    C -----------------------------------------------------------------
394    C          N=NO(1-R**2/A**2)    FIND MIN. RADIUS
395    C -----------------------------------------------------------------
396     43 R1(MARK,JJ)=RMIN
397          TR=0.25*ALOG(ABS(TERM1+ABS(TERM2))/(TERM1-ABS(TERM2)))/OMEGA(I,J)
398          VZ=DSQRT(RI(I,J)*RI(I,J)*9D20-VX*VX-VY*VY+OMEGA(I,J)*OMEGA(I,J)
399        **R1(MARK,JJ-1)*R1(MARK,JJ-1)*1.0DO)
400          Z(MARK,JJ)=VZ*TR+Z(MARK,JJ-1)
401          IF(Z(MARK,JJ).GT.J*DZ) GOTO 11
402          VSUM(MARK)=VSUM(MARK)+VZ
403          CALL ABSOB1(MARK,TR,VX,VY,VZ,LAMDA,TE,
404        *TERM1,TERM2,I,J,JJ,ZATOM,Z(MARK,JJ-1),DZ)
405          VXO=VX
406          VYO=VY
407          VX=HXVEL(X,VXO,TR,I,J)
408          VY=HYVEL(Y,VYO,TR,I,J)
409          X=HXCOOR(X,VXO,TR,I,J)
410          Y=HYCOOR(Y,VYO,TR,I,J)
411          THETA(MARK,JJ)=ANGLE(X,Y)
412          VR=VX*SIN(THETA(MARK,JJ))+VY*COS(THETA(MARK,JJ))
413          ANGVEL=VX*COS(THETA(MARK,JJ))-VY*SIN(THETA(MARK,JJ))
414          ANGMOM=R1(MARK,JJ)*ANGVEL
415          LOCX(MARK,JJ)=I
416          LOCY(MARK,JJ)=J
417          GOTO 3
```
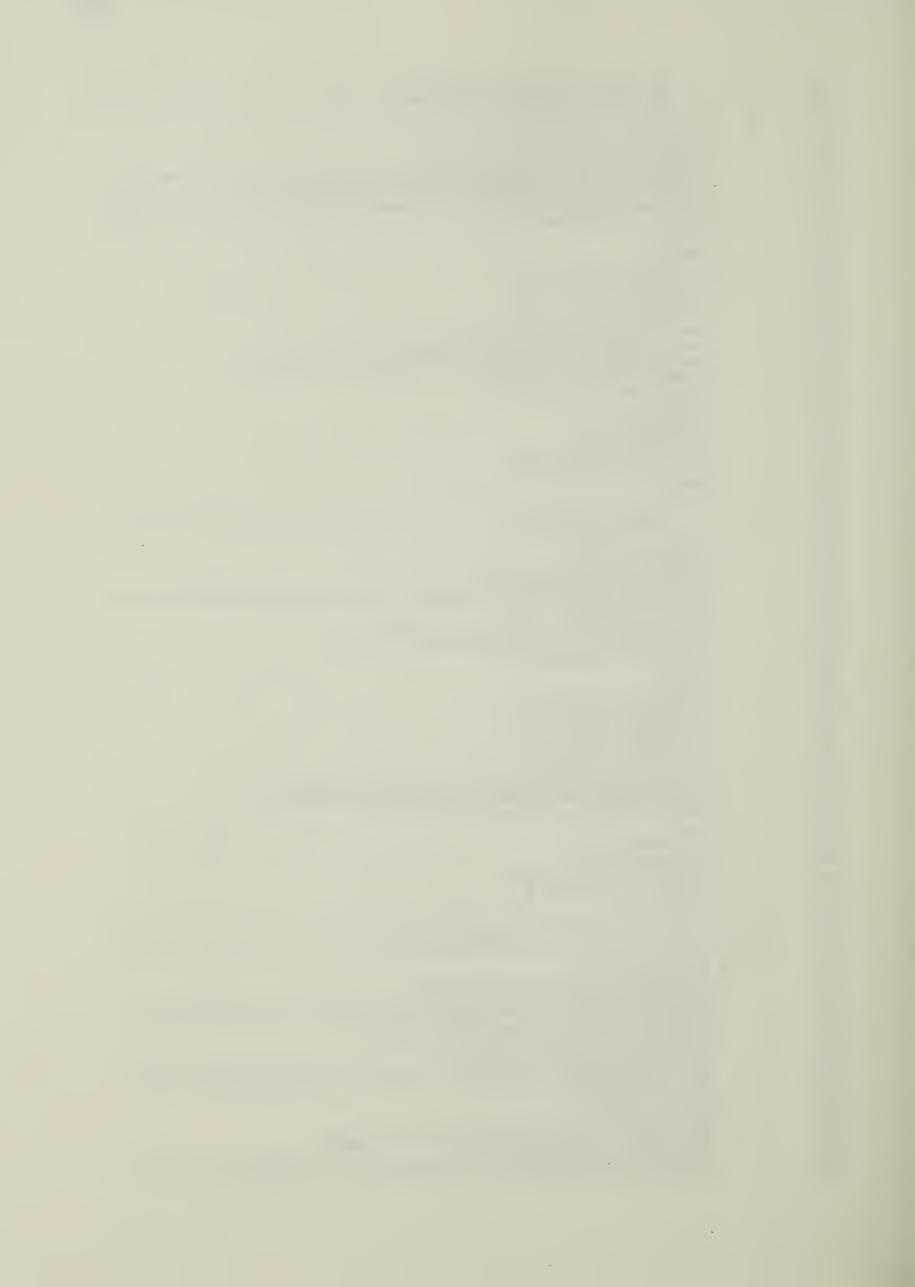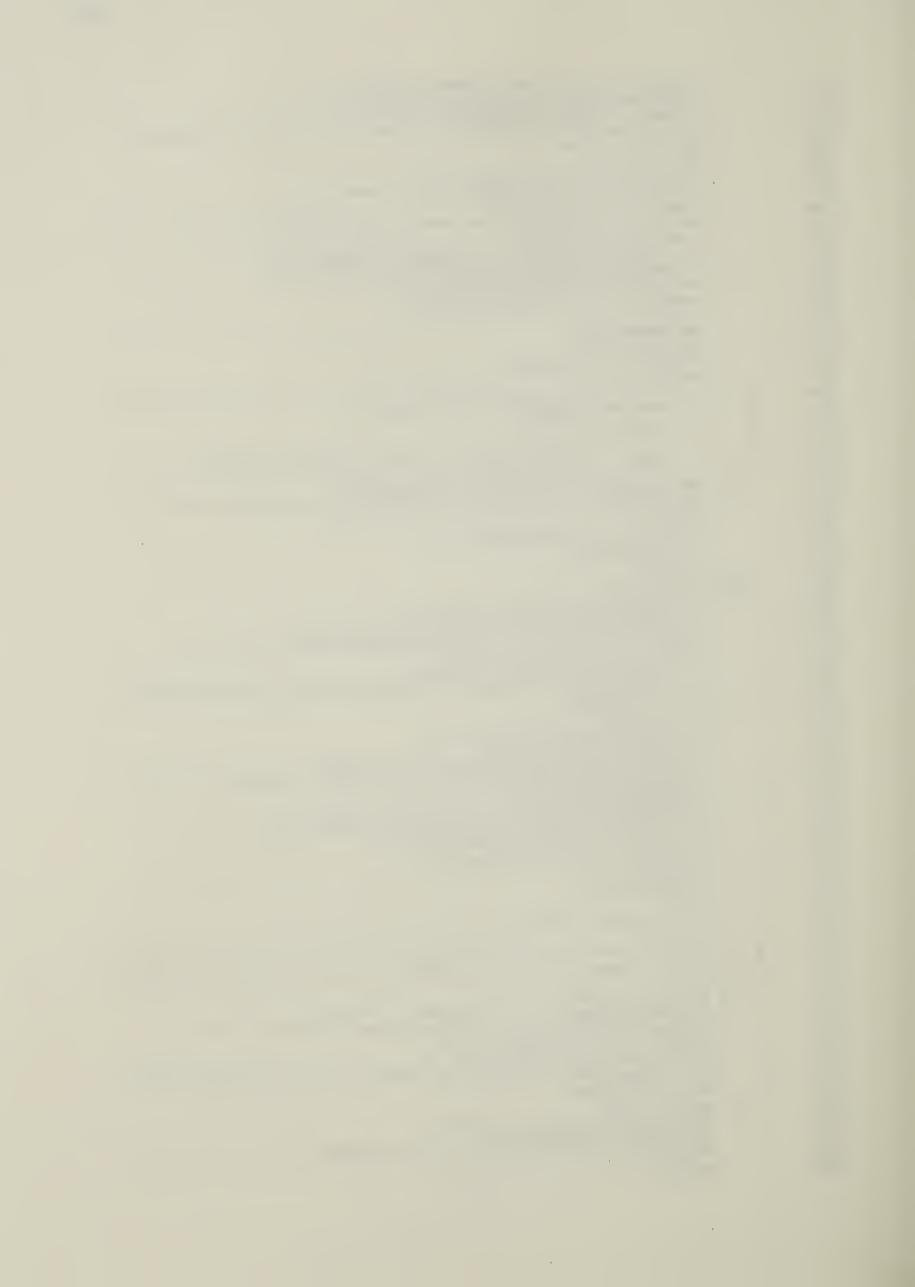
```
418      C---------------------------------------------------------------------
419      C          RAY HITS AT VERTICAL BOUNDARY
420      C          N=NO(1+R**2/A**2)
421      C ---------------------------------------------------------------------
422          6 Z(MARK,JJ)=J*DZ
423            TZ=(Z(MARK,JJ)-Z(MARK,JJ-1))/VZ
424            R1(MARK,JJ)=DSQRT(R1(MARK,JJ-1)**2/2.DO+(VX*VX+VY*VY)/(2*OMEGA(I,J
425           *)*OMEGA(I,J))+D*1.ODO*SIN(2*OMEGA(I,J)*TZ+PHI))
426            CALL ABSORB(MARK,R1(MARK,JJ-1),Z(MARK,JJ-1),DZ,TZ,VX,VY,PHI,LAMDA,
427           *TE,D,I,J,JJ,ZATOM)
428            VXO=VX
429            VYO=VY
430            VX=XVEL(X,VXO,TZ,I,J)
431            VY=YVEL(Y,VYO,TZ,I,J)
432            X=XCOOR(X,VXO,TZ,I,J)
433            Y=YCOOR(Y,VYO,TZ,I,J)
434            THETA(MARK,JJ)=ANGLE(X,Y)
435            VR=VX*SIN(THETA(MARK,JJ))+VY*COS(THETA(MARK,JJ))
436            ANGVEL=VX*COS(THETA(MARK,JJ))-VY*SIN(THETA(MARK,JJ))
437            ANGMOM=R1(MARK,JJ)*ANGVEL
438            VSUM(MARK)=VSUM(MARK)+VZ
439            J=J+1
440            LOCX(MARK,JJ)=I
441            LOCY(MARK,JJ)=J
442            IF (J.GT.NX) GOTO 666
443            IF (VR.LT.O.O)GOTO 4
444            GOTO 3
445      C ---------------------------------------------------------------------
446      C          N=NO(1-R**2/A**2)
447      C ---------------------------------------------------------------------
448         11 Z(MARK,JJ)=J*DZ
449            TZ=(Z(MARK,JJ)-Z(MARK,JJ-1))/VZ
450            ARG=SINH(2*OMEGA(I,J)*TZ)
451            R1(MARK,JJ)=DSQRT(TERM1*(1+DSQRT(1+1.ODO*ARG*ARG))+TERM2*ARG-(VX**
452           *2+VY**2)/OMEGA(I,J)**2)
453            CALL ABSOB1(MARK,TZ,VX,VY,VZ,LAMDA,TE,
454           *TERM1,TERM2,I,J,JJ,ZATOM,Z(MARK,JJ-1),DZ)
455            VSUM(MARK)=VSUM(MARK)+VZ
456            VXO=VX
457            VYO=VY
458            VX=HXVEL(X,VXO,TZ,I,J)
459            VY=HYVEL(Y,VYO,TZ,I,J)
460            X=HXCOOR(X,VXO,TZ,I,J)
461            Y=HYCOOR(Y,VYO,TZ,I,J)
462            THETA(MARK,JJ)=ANGLE(X,Y)
463            VR=VX*SIN(THETA(MARK,JJ))+VY*COS(THETA(MARK,JJ))
464            ANGVEL=VX*COS(THETA(MARK,JJ))-VY*SIN(THETA(MARK,JJ))
465            ANGMOM=R1(MARK,JJ)*ANGVEL
466            J=J+1
467            LOCX(MARK,JJ)=I
468            LOCY(MARK,JJ)=J
469            IF (J.GT.NX) GOTO 666
470            IF (VR.LT.O.O)GOTO 4
471            GOTO 3
472      C ---------------------------------------------------------------------
473      C          N=NO(1-A**2/R**2), CONST<O.O, VR>O.O,
474      C ---------------------------------------------------------------------
475        109 Z(MARK,JJ)=J*DZ
476            TZ=(Z(MARK,JJ)-Z(MARK,JJ-1))/VZ
477            TEMP1=(R1(MARK,JJ-1)*VR)**2-ABS(CONST)
478            TEMP=(TZ+R1(MARK,JJ-1)*R1(MARK,JJ-1)*R1(MARK,JJ-1)*VR/TEMP1)**2
479            TEMP=TEMP1*TEMP1*TEMP/R1(MARK,JJ-1)**2
480            TEMP=TEMP-ABS(CONST)*R1(MARK,JJ-1)**2
481            R1(MARK,JJ)=SQRT(TEMP/TEMP1)
482            CALL ABOB2N(MARK,R1(MARK,JJ-1),Z(MARK,JJ-1),DZ,TZ,VR,CONST,LAMDA,
483           *TE,I,J,JJ,ZATOM)
484            DTZ=TZ*1.ODO
485            CALL DQG32(O.DO,DTZ,FETA1,Y112)
486            THETA(MARK,JJ)=THETA(MARK,JJ-1)+Y112*ANGMOM
487            VSUM(MARK)=VSUM(MARK)+VZ
488            VR=SQRT(VR*VR+ABS(CONST)*(1/R1(MARK,JJ)**2-1/R1(MARK,JJ-1)**2))
```

```
489              VT=ANGMOM/R1(MARK,JJ)
490              VX=VR*SIN(THETA(MARK,JJ))+VT*COS(THETA(MARK,JJ))
491              VY=VR*COS(THETA(MARK,JJ))-VT*SIN(THETA(MARK,JJ))
492              X=R1(MARK,JJ)*SIN(THETA(MARK,JJ))
493              Y=R1(MARK,JJ)*COS(THETA(MARK,JJ))
494              J=J+1
495              LOCX(MARK,JJ)=I
496              LOCY(MARK,JJ)=J
497              IF (J.GT.NX) GOTO 666
498              GOTO 3
499        C -------------------------------------------------------------
500        C         N=NO(1-A**2/R**2), CONST<0.0, VR<0.0,
501        C -------------------------------------------------------------
502        1091 Z(MARK,JJ)=J*DZ
503              TZ=(Z(MARK,JJ)-Z(MARK,JJ-1))/VZ
504              TEMP1=(R1(MARK,JJ-1)*VR)**2-ABS(CONST)
505              TEMP=(TZ-R1(MARK,JJ-1)*R1(MARK,JJ-1)*R1(MARK,JJ-1)*ABS(VR)/TEMP1)*
506              **2
507              TEMP=TEMP1*TEMP1*TEMP/R1(MARK,JJ-1)**2
508              TEMP=TEMP-ABS(CONST)*R1(MARK,JJ-1)**2
509              R1(MARK,JJ)=SQRT(TEMP/TEMP1)
510              CALL ABOB2N(MARK,R1(MARK,JJ-1),Z(MARK,JJ-1),DZ,TZ,VR,CONST,LAMDA,
511              *TE,I,J,JJ,ZATOM)
512              DTZ=TZ*1.0DO
513              CALL DQG32(0.DO,DTZ,FETA2,Y112)
514              THETA(MARK,JJ)=THETA(MARK,JJ-1)+Y112*ANGMOM
515              VR=-SQRT(VR*VR+ABS(CONST)*(1/R1(MARK,JJ)**2-1/R1(MARK,JJ-1)**2))
516              VT=ANGMOM/R1(MARK,JJ)
517              VX=VR*SIN(THETA(MARK,JJ))+VT*COS(THETA(MARK,JJ))
518              VY=VR*COS(THETA(MARK,JJ))-VT*SIN(THETA(MARK,JJ))
519              X=R1(MARK,JJ)*SIN(THETA(MARK,JJ))
520              Y=R1(MARK,JJ)*COS(THETA(MARK,JJ))
521              J=J+1
522              LOCX(MARK,JJ)=I
523              LOCY(MARK,JJ)=J
524              VSUM(MARK)=VSUM(MARK)+VZ
525              IF (J.GT.NX) GOTO 666
526              GOTO 4
527        C -------------------------------------------------------------
528        C         N=NO(1-A**2/R**2), OR N=NO(1+A**2/R**2), CONST>0.0, VR>0.0
529        C -------------------------------------------------------------
530        102 Z(MARK,JJ)=J*DZ
531              TZ=(Z(MARK,JJ)-Z(MARK,JJ-1))/VZ
532              TEMP1=(R1(MARK,JJ-1)*VR)**2+CONST
533              TEMP=(TZ+R1(MARK,JJ-1)*R1(MARK,JJ-1)*R1(MARK,JJ-1)*VR/TEMP1)**2
534              TEMP=TEMP1*TEMP1*TEMP/R1(MARK,JJ-1)**2
535              TEMP=TEMP+CONST*R1(MARK,JJ-1)*R1(MARK,JJ-1)
536              R1(MARK,JJ)=SQRT(TEMP/TEMP1)
537              CALL ABOB2P(MARK,R1(MARK,JJ-1),Z(MARK,JJ-1),DZ,TZ,VR,CONST,LAMDA,
538              *TE,I,J,JJ,ZATOM)
539              THETA(MARK,JJ)=THETA(MARK,JJ-1)+ANGMOM*TR/R1(MARK,JJ)**2
540              VSUM(MARK)=VSUM(MARK)+VZ
541              VR=SQRT(VR*VR-CONST*(1/R1(MARK,JJ)**2-1/R1(MARK,JJ-1)**2))
542              VT=ANGMOM/R1(MARK,JJ)
543              VX=VR*SIN(THETA(MARK,JJ))+VT*COS(THETA(MARK,JJ))
544              VY=VR*COS(THETA(MARK,JJ))-VT*SIN(THETA(MARK,JJ))
545              X=R1(MARK,JJ)*SIN(THETA(MARK,JJ))
546              Y=R1(MARK,JJ)*COS(THETA(MARK,JJ))
547              J=J+1
548              LOCX(MARK,JJ)=I
549              LOCY(MARK,JJ)=J
550              IF (J.GT.NX) GOTO 666
551              GOTO 3
552        C -------------------------------------------------------------
553        C         N=NO(1-A**2/R**2), CONST>0.0, VR<0.0
554        C -------------------------------------------------------------
555        1021 Z(MARK,JJ)=J*DZ
556              TZ=(Z(MARK,JJ)-Z(MARK,JJ-1))/VZ
557              TEMP1=(R1(MARK,JJ-1)*VR)**2+CONST
558              TEMP=(TZ-R1(MARK,JJ-1)*R1(MARK,JJ-1)*R1(MARK,JJ-1)*ABS(VR)/TEMP1)*
559              **2
```
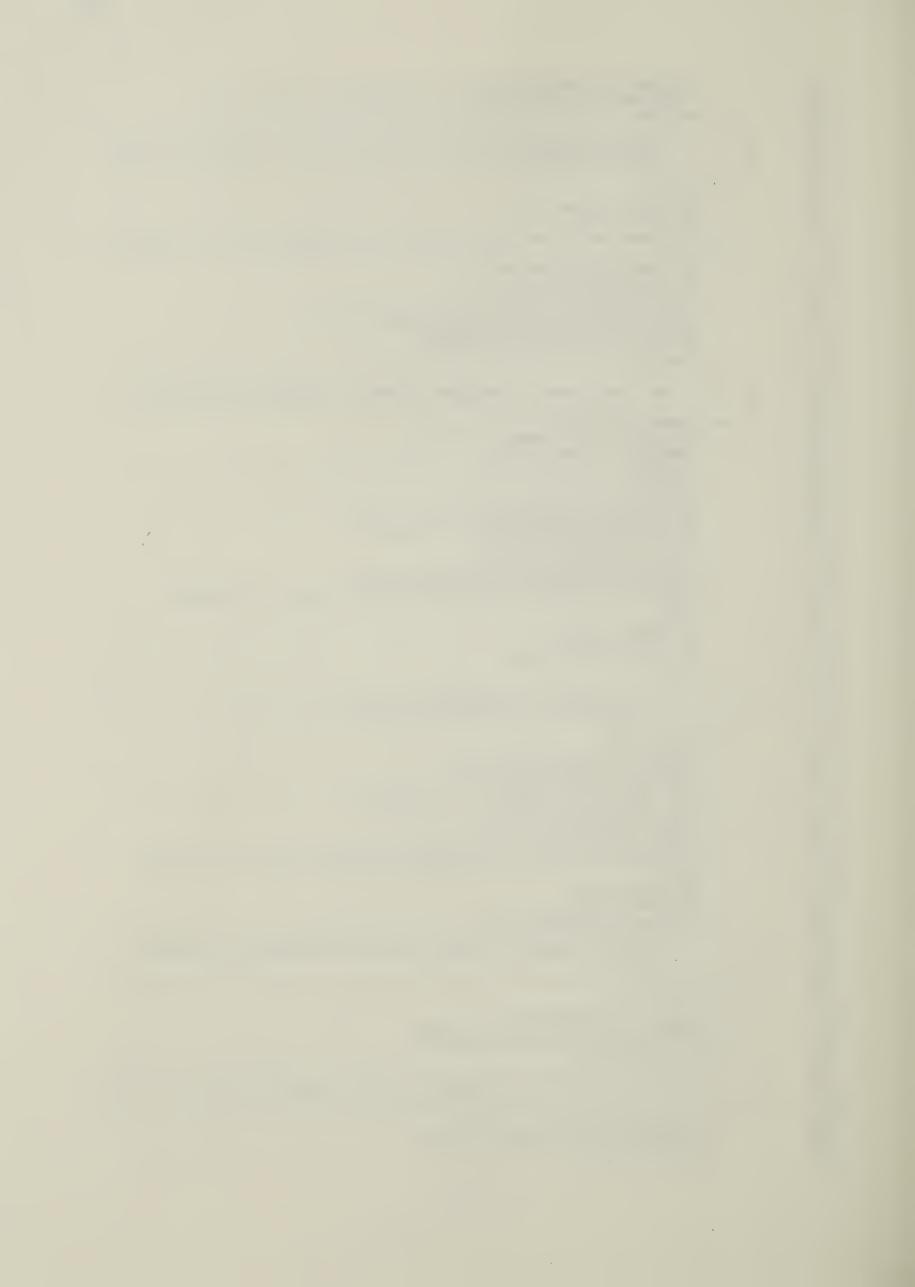
```
560              TEMP=TEMP1*TEMP1*TEMP/R1(MARK,JJ-1)**2
561              TEMP=TEMP+CONST*R1(MARK,JJ-1)*R1(MARK,JJ-1)
562              R1(MARK,JJ)=SQRT(TEMP/TEMP1)
563              CALL ABOB2P(MARK,R1(MARK,JJ-1),Z(MARK,JJ-1),DZ,TZ,VR,CONST,LAMDA,
564             *TE,I,J,JJ,ZATOM)
565              DTZ=TZ*1.0DO
566              CALL DQG32(0.DO,DTZ,FETA3,Y112)
567              THETA(MARK,JJ)=THETA(MARK,JJ-1)+ANGMOM*Y112
568              VSUM(MARK)=VSUM(MARK)+VZ
569              VR=-SQRT(VR**2-CONST*(1/R1(MARK,JJ)**2-1/R1(MARK,JJ-1)**2))
570              VT=ANGMOM/R1(MARK,JJ)
571              VX=VR*SIN(THETA(MARK,JJ))+VT*COS(THETA(MARK,JJ))
572              VY=VR*COS(THETA(MARK,JJ))-VT*SIN(THETA(MARK,JJ))
573              X=R1(MARK,JJ)*SIN(THETA(MARK,JJ))
574              Y=R1(MARK,JJ)*COS(THETA(MARK,JJ))
575              J=J+1
576              LOCX(MARK,JJ)=I
577              LOCY(MARK,JJ)=J
578              IF (J.GT.NX) GOTO 666
579              GOTO 4
580       C-----------------------------------------------------------------
581       C         FIND MAX./MIN.RADIUS FOR THE PROFILE
582       C         N=NO(1-A**2/R**2)
583       C
584       C         CASE 1 : CONST<0.0 OR 0.0, VR>0.0, FIND MAX. RADIUS
585       C -----------------------------------------------------------------
586         105 IF (R1(MARK,JJ-1).LE.R2(1,J)) VR=ABS(VR)
587              RMAX=R1(MARK,JJ-1)**2*ABS(CONST)/(ABS(CONST)-(R1(MARK,JJ-1)*
588             *VR)**2)
589              IF (RMAX.LT.0.0) GOTO 1052
590              RMAX=SQRT(RMAX)
591              GOTO 1051
592        1052 RMAX=1.0E6
593        1051 R1(MARK,JJ)=R2(I,J)
594              IF (R1(MARK,JJ).GT.RMAX) GOTO 108
595              TR=TIMENP(R1(MARK,JJ-1),R1(MARK,JJ),VR,CONST)
596              VZ=SQRT((RI(I,J)*3E10)**2-VR*VR-(ANGMOM/R1(MARK,JJ-1))**2)
597              Z(MARK,JJ)=Z(MARK,JJ-1)+VZ*TR
598              IF (Z(MARK,JJ).GT.J*DZ) GOTO 109
599              CALL ABOB2N(MARK,R1(MARK,JJ-1),Z(MARK,JJ-1),DZ,TR,VR,CONST,LAMDA,
600             *TE,I,J,JJ,ZATOM)
601              DTR=TR*1.0DO
602              CALL DQG32(0.DO,DTR,FETA1,Y112)
603              VSUM(MARK)=VSUM(MARK)+VZ
604              THETA(MARK,JJ)=THETA(MARK,JJ-1)+Y112*ANGMOM
605              VR=SQRT(VR*VR+ABS(CONST)*(1/R1(MARK,JJ)**2-1/R1(MARK,JJ-1)**2))
606              VT=ANGMOM/R1(MARK,JJ)
607              VX=VR*SIN(THETA(MARK,JJ))+VT*COS(THETA(MARK,JJ))
608              VY=VR*COS(THETA(MARK,JJ))-VT*SIN(THETA(MARK,JJ))
609              X=R1(MARK,JJ)*SIN(THETA(MARK,JJ))
610              Y=R1(MARK,JJ)*COS(THETA(MARK,JJ))
611              LOCX(MARK,JJ)=I
612              LOCY(MARK,JJ)=J
613              I=I+1
614              IF (I.GT.LAST) GOTO 32
615              GOTO 3
616       C -----------------------------------------------------------------
617       C     CASE 2 : N=NO(1-A**2/R**2), CONST<0.0, VR>0.0, FIND MAX. RADIUS
618       C -----------------------------------------------------------------
619         108 R1(MARK,JJ)=RMAX
620              TR=TIMENP(R1(MARK,JJ-1),R1(MARK,JJ),VR,CONST)
621              VZ=SQRT((RI(I,J)*3E10)**2-VR*VR-(ANGMOM/R1(MARK,JJ-1))**2)
622              Z(MARK,JJ)=VZ*TR+Z(MARK,JJ-1)
623              IF (Z(MARK,JJ).GT.J*DZ) GOTO 109
624              CALL ABOB2N(MARK,R1(MARK,JJ-1),Z(MARK,JJ-1),DZ,TR,VR,CONST,LAMDA,
625             *TE,I,J,JJ,ZATOM)
626              DTR=TR*1.0DO
627              CALL DQG32(0.DO,DTR,FETA1,Y112)
628              VSUM(MARK)=VSUM(MARK)+VZ
629              THETA(MARK,JJ)=THETA(MARK,JJ-1)+Y112*ANGMOM
630              VR=0.0
```
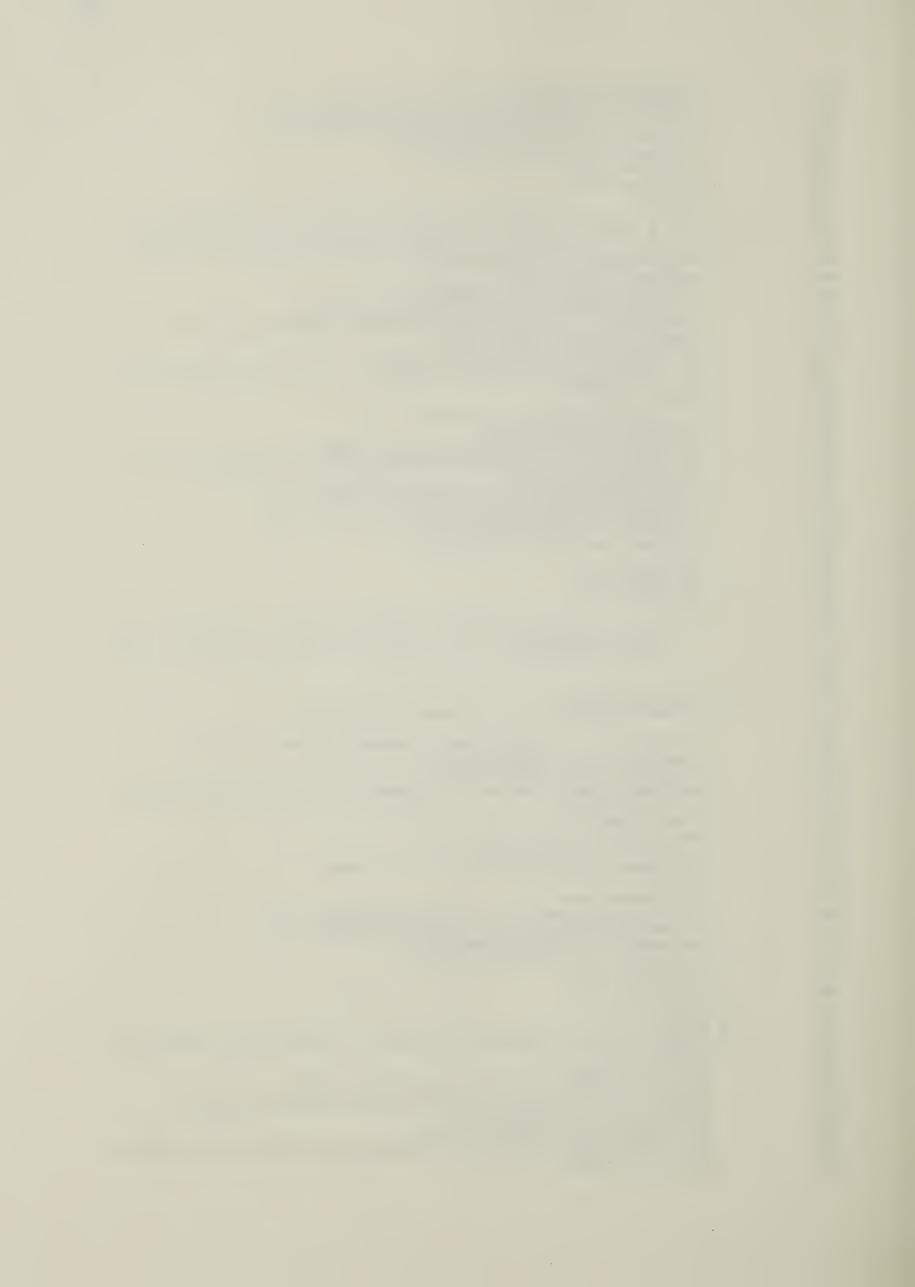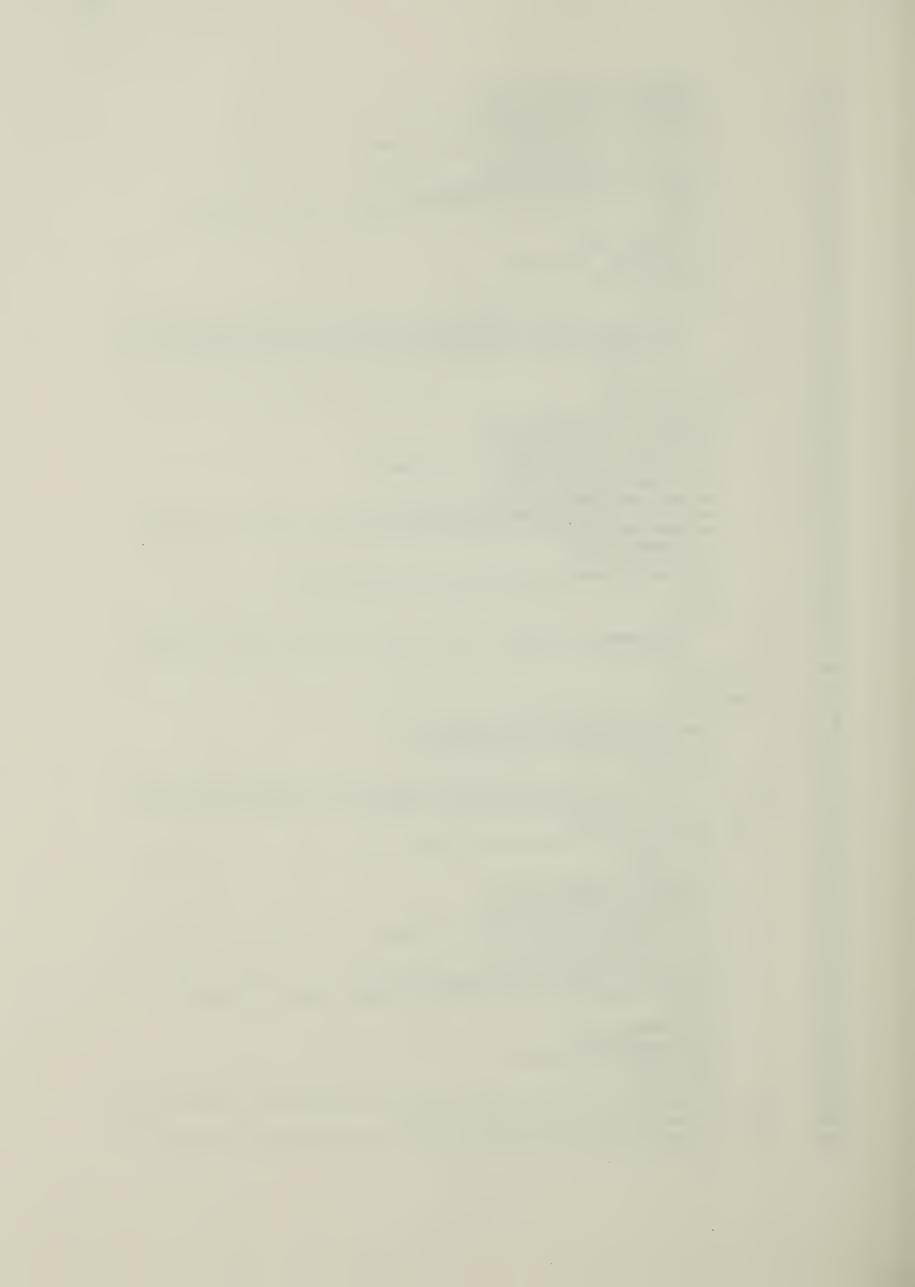
```
631              VT=ANGMOM/R1(MARK,JJ)
632              VX=VR*SIN(THETA(MARK,JJ))+VT*COS(THETA(MARK,JJ))
633              VY=VR*COS(THETA(MARK,JJ))-VT*SIN(THETA(MARK,JJ))
634              X=R1(MARK,JJ)*SIN(THETA(MARK,JJ))
635              Y=R1(MARK,JJ)*COS(THETA(MARK,JJ))
636              LOCX(MARK,JJ)=I
637              LOCY(MARK,JJ)=J
638              GOTO 4
639    C --------------------------------------------------------------------
640    C        CASE 3: N=NO(1-A**2/R**2), CONST<0.0, VR<0.0, FIND MIN. RADIUS
641    C --------------------------------------------------------------------
642      107 RMIN=ABS(ANGMOM/(RI(I,J)*3E10))
643              R1(MARK,JJ)=R2(I-1,J)
644              IF (R1(MARK,JJ).LT.RMIN) GOTO 120
645              TR=TIMENN(R1(MARK,JJ-1),R1(MARK,JJ),VR,CONST)
646              VZ=SQRT((RI(I,J)*3E10)**2-VR*VR-(ANGMOM/R1(MARK,JJ-1))**2)
647              Z(MARK,JJ)=VZ*TR+Z(MARK,JJ-1)
648              IF (Z(MARK,JJ).GT.J*DZ) GOTO 1091
649              CALL ABOB2N(MARK,R1(MARK,JJ-1),Z(MARK,JJ-1),DZ,TR,VR,CONST,LAMDA,
650     *TE,I,J,JJ,ZATOM)
651              DTR=TR*1.0DO
652              CALL DQG32(0.DO,DTR,FETA2,Y112)
653              VSUM(MARK)=VSUM(MARK)+VZ
654              THETA(MARK,JJ)=THETA(MARK,JJ-1)+Y112*ANGMOM
655              VR=-SQRT(VR*VR+ABS(CONST)*(1/R1(MARK,JJ)**2-1/R1(MARK,JJ-1)**2))
656              VT=ANGMOM/R1(MARK,JJ)
657              VX=VR*SIN(THETA(MARK,JJ))+VT*COS(THETA(MARK,JJ))
658              VY=VR*COS(THETA(MARK,JJ))-VT*SIN(THETA(MARK,JJ))
659              X=R1(MARK,JJ)*SIN(THETA(MARK,JJ))
660              Y=R1(MARK,JJ)*COS(THETA(MARK,JJ))
661              I=I-1
662              LOCX(MARK,JJ)=I
663              LOCY(MARK,JJ)=J
664              GOTO 4
665    C ---------------------------------------------------------------------
666    C          CASE 4 :N=NO(1-A**2/R**2), CONST>0.0, VR<0.0, FIND MIN. RADIUS
667    C          N=NO(1+A**2/R**2)
668    C ---------------------------------------------------------------------
669
670      106 R1(MARK,JJ)=RMIN
671              TR=TIMEPN(R1(MARK,JJ-1),R1(MARK,JJ),VR,CONST)
672
673              VZ=SQRT((RI(I,J)*3E10)**2-VR*VR-(ANGMOM/R1(MARK,JJ-1))**2)
674              Z(MARK,JJ)=VZ*TR+Z(MARK,JJ-1)
675              IF (Z(MARK,JJ).GT.J*DZ) GOTO 102
676              CALL ABOB2P(MARK,R1(MARK,JJ-1),Z(MARK,JJ-1),DZ,TR,VR,CONST,LAMDA,
677     *TE,I,J,JJ,ZATOM)
678              DTR=TR*1.0DO
679              CALL DQG32(0.ODO,DTR,FETA2,Y112)
680              VSUM(MARK)=VSUM(MARK)+VZ
681              THETA(MARK,JJ)=THETA(MARK,JJ-1)+Y112*ANGMOM
682              VR=0.0
683              VT=ANGMOM/R1(MARK,JJ)
684              VX=VR*SIN(THETA(MARK,JJ))+VT*COS(THETA(MARK,JJ))
685              VY=VR*COS(THETA(MARK,JJ))-VT*SIN(THETA(MARK,JJ))
686              X=R1(MARK,JJ)*SIN(THETA(MARK,JJ))
687              Y=R1(MARK,JJ)*COS(THETA(MARK,JJ))
688              LOCX(MARK,JJ)=I
689              LOCY(MARK,JJ)=J
690              GOTO 3
691      120 WRITE(6,612)
692      612 FORMAT(/'*****RAY REACHES THE LOWEST LIMIT AND ROTATES AROUND THE
693     *AXIS*****'/)
694              R1(MARK,JJ)=RMIN
695              TR=TIMENN(R1(MARK,JJ-1),R1(MARK,JJ),VR,CONST)
696              VZ=SQRT((RI(I,J)*3E10)**2-VR*VR-(ANGMOM/R1(MARK,JJ-1))**2)
697              Z(MARK,JJ)=VZ*TR+Z(MARK,JJ-1)
698              IF (Z(MARK,JJ).GT.J*DZ) GOTO 1091
699              CALL ABOB2N(MARK,R1(MARK,JJ-1),Z(MARK,JJ-1),DZ,TR,VR,CONST,LAMDA,
700     *TE,I,J,JJ,ZATOM)
```
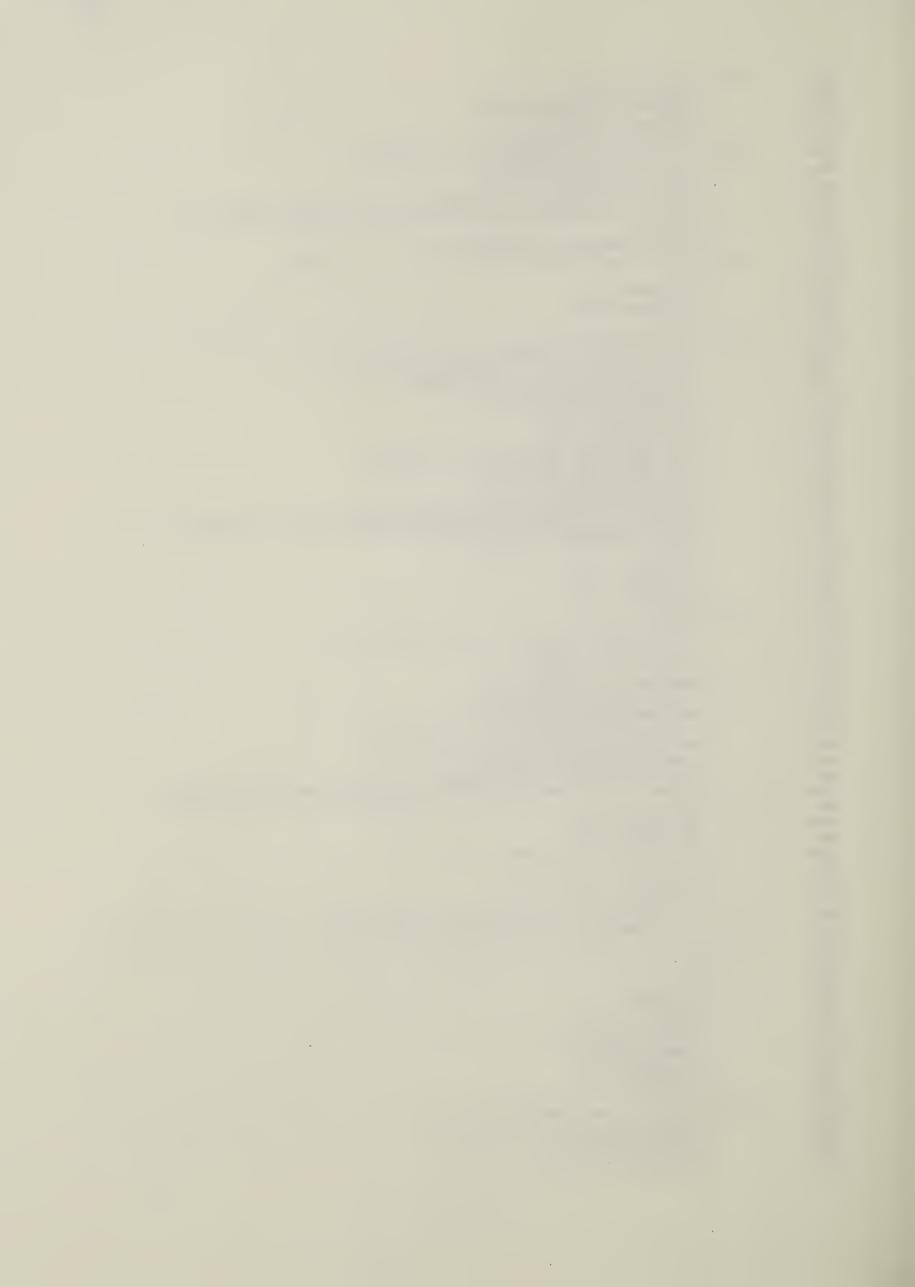
```
701            VSUM(MARK)=VSUM(MARK)+VZ
702            THETA(MARK,JJ)=THETA(MARK,JJ-1)+ANGMOM*TR/R1(MARK,JJ)**2
703            GOTO 666
704    C-------------------------------------------------------------------
705    C            ALGORITHM FOR FINDING RAY LOCATIONS WHEN IT REACHES THE INNER
706    C            MOST CORE SHELL
707    C-------------------------------------------------------------------
708          9 JJ=JJ+1
709            IF (JJ.GT.100)GOTO 37
710            VDOTR=X*VX+Y*VY
711            TR1=DSQRT(VDOTR*VDOTR+(R2(1,J)*R2(1,J)-R1(MARK,JJ-1)**2)*(VX*VX+VY
712        **VY))
713            TR1=-VDOTR-SIGN(TR1,VDOTR)
714            TR1=TR1/(VX*VX+VY*VY)
715            TR=-2*VDOTR/(VX**2+VY**2)
716            VZ=DSQRT(RI(I,J)*RI(I,J)*9E20-VX*VX-VY*VY)
717            Z(MARK,JJ)=Z(MARK,JJ-1)+VZ*TR/2
718            IF (Z(MARK,JJ).GT.J*DZ) GOTO 94
719            GOTO 96
720    C -------------------------------------------------------------------
721    C            RAY HITS VERTICAL BOUNDARY BEFORE IT REACHES THE MINIMUM
722    C -------------------------------------------------------------------
723         94 Z(MARK,JJ)=J*DZ
724            TZ=(Z(MARK,JJ)-Z(MARK,JJ-1))/VZ
725            VSUM(MARK)=VSUM(MARK)+VZ
726            X=X+VX*TZ
727            Y=Y+VY*TZ
728            R1(MARK,JJ)=DSQRT(X*X+Y*Y)
729            THETA(MARK,JJ)=ANGLE(X,Y)
730            A1=2.19E3*TE(1,J)*SQRT(TE(1,J))*LAMDA
731            A2=1.14E4*LAMDA*TE(1,J)
732            ALAMDA=ALOG(AMIN1(A1,A2))
733            A3=8.67E-30*LAMDA*LAMDA*ALAMDA/TE(1,J)
734            KA(MARK,JJ)=A3*NOI(1,J)**2*3E10*TZ/SQRT(1-NOI(1,J)/CRIDEN)
735            J=J+1
736            LOCX(MARK,JJ)=I
737            LOCY(MARK,JJ)=J
738            IF (J.GT.NX) GOTO 666
739            GOTO 9
740    C -------------------------------------------------------------------
741    C            TO CALCULATE THE MINIMUM POINT IN R
742    C -------------------------------------------------------------------
743         96 X=X+VX*TR/2
744            Y=Y+VY*TR/2
745            R1(MARK,JJ)=DSQRT(X**2+Y**2)
746            THETA(MARK,JJ)=ANGLE(X,Y)
747            A1=2.19E3*TE(1,J)*SQRT(TE(1,J))*LAMDA
748            A2=1.14E4*LAMDA*TE(1,J)
749            ALAMDA=ALOG(AMIN1(A1,A2))
750            A3=8.67E-30*LAMDA*LAMDA*ALAMDA/TE(1,J)
751            KA(MARK,JJ)=A3*NOI(1,J)**2*3E10*(TR/2)/SQRT(1-NOI(1,J)/CRIDEN)
752            TR2=TR
753            LOCX(MARK,JJ)=I
754            LOCY(MARK,JJ)=J
755            VSUM(MARK)=VSUM(MARK)+VZ
756    C -------------------------------------------------------------------
757    C            TO LOCATE THE NEXT POINT AFTER HAVING REACHED THE MINIMUM
758    C            POINT
759    C -------------------------------------------------------------------
760        994 JJ=JJ+1
761            IF (JJ.GT.100) GOTO 37
762            Z(MARK,JJ)=Z(MARK,JJ-1)+VZ*TR2/2
763         99 IF (Z(MARK,JJ).GT.J*DZ) GOTO 97
764            GOTO 98
765    C -------------------------------------------------------------------
766    C            RAY HITS VERTICAL BOUNDARY BEFORE IT REACHES THE SHELL SURFACE
767    C -------------------------------------------------------------------
768         97 Z(MARK,JJ)=J*DZ
769            TZ=(Z(MARK,JJ)-Z(MARK,JJ-1))/VZ
770            X=X+VX*TZ
```
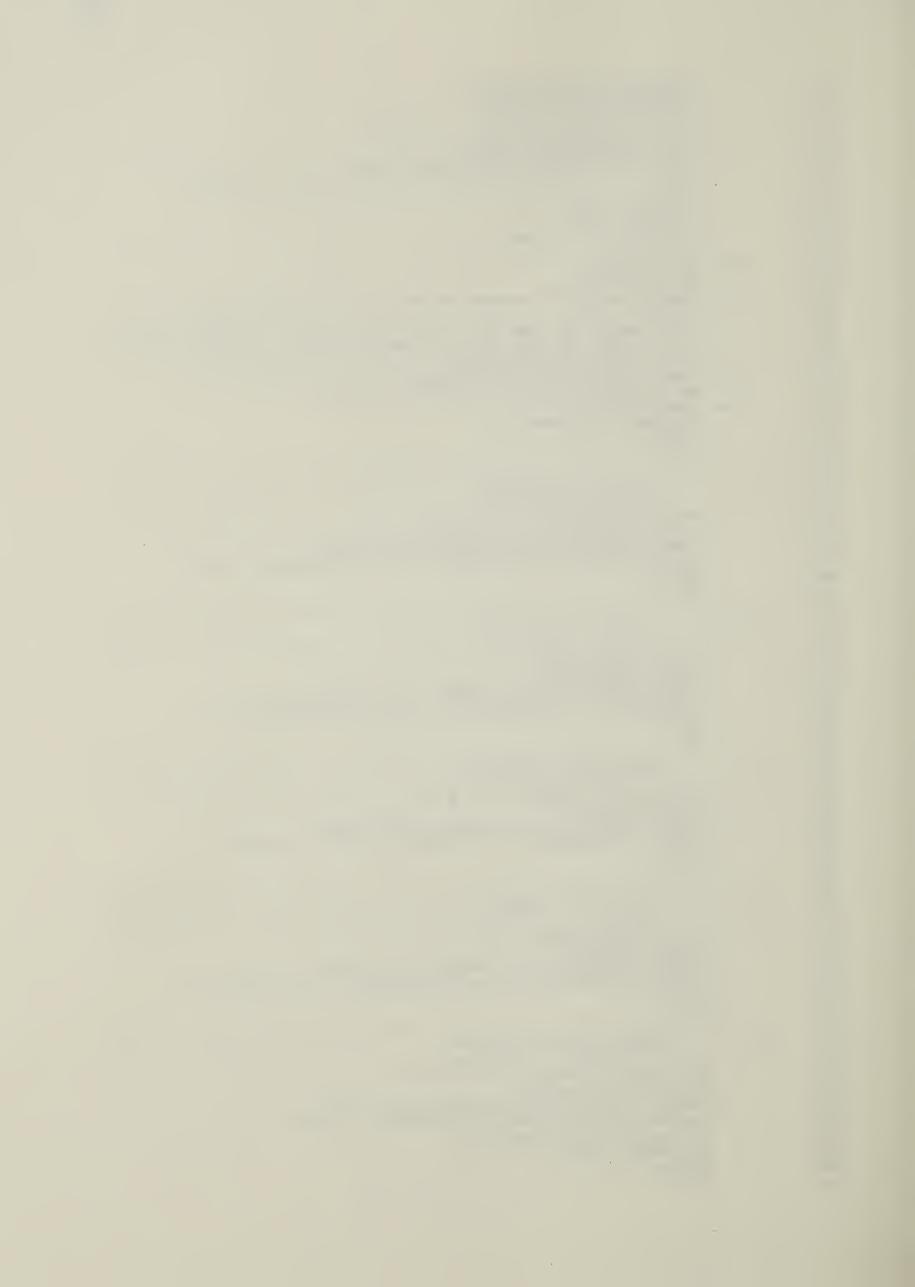
```
771              Y=Y+VY*TZ
772              VSUM(MARK)=VSUM(MARK)+VZ
773              R1(MARK,JJ)=DSQRT(X*X+Y*Y)
774              THETA(MARK,JJ)=ANGLE(X,Y)
775              A1=2.19E3*TE(1,J)*SQRT(TE(1,J))*LAMDA
776              A2=1.14E4*LAMDA*TE(1,J)
777              ALAMDA=ALOG(AMIN1(A1,A2))
778              A3=8.67E-30*LAMDA*LAMDA*ALAMDA/TE(1,J)
779              KA(MARK,JJ)=A3*NOI(1,J)**2*3E10*TZ/SQRT(1-NOI(1,J)/CRIDEN)
780              J=J+1
781              LOCX(MARK,JJ)=I
782              LOCY(MARK,JJ)=J
783              IF (J.GT.NX) GOTO 666
784              TR2=TR2-2*TZ
785              GOTO 994
786     C --------------------------------------------------------------------
787     C        TO FIND THE POINT SYMMETRICAL TO THE FIRST ENTRY POINT AT THE
788     C        INNER MOST CORE (ITS RADIUS MIGHT BE SMALLER THAN THAT OF THE
789     C        1ST SHELL)
790     C --------------------------------------------------------------------
791      98 X=X+VX*TR2/2
792              Y=Y+VY*TR2/2
793              VSUM(MARK)=VSUM(MARK)+VZ
794              R1(MARK,JJ)=DSQRT(X*X+Y*Y)
795              THETA(MARK,JJ)=ANGLE(X,Y)
796              A1=2.19E3*TE(1,J)*SQRT(TE(1,J))*LAMDA
797              A2=1.14E4*LAMDA*TE(1,J)
798              ALAMDA=ALOG(AMIN1(A1,A2))
799              A3=8.67E-30*LAMDA*LAMDA*ALAMDA/TE(1,J)
800              KA(MARK,JJ)=A3*NOI(1,J)**2*3E10*(TR2/2)/SQRT(1-NOI(1,J)/CRIDEN)
801              LOCX(MARK,JJ)=I
802              LOCY(MARK,JJ)=J
803              IF (ABS(R1(MARK,JJ)-R2(1,J)).GT.1.0E-4) GOTO 92
804              I=2
805              GOTO 3
806     C --------------------------------------------------------------------
807     C        THE SYMMETRICAL POINT IS NOT RIGHT AT THE 1ST SHELLLAYER BUT
808     C        WITHIN IT
809     C --------------------------------------------------------------------
810      92 TZZ=0
811     995 JJ=JJ+1
812              IF (JJ.GT.100) GOTO 37
813              Z(MARK,JJ)=Z(MARK,JJ-1)+VZ*(TR1-TR)
814              IF (Z(MARK,JJ).GT.J*DZ) GOTO 991
815              GOTO 992
816     C --------------------------------------------------------------------
817     C        RAY HITS THE COLUMN BEFORE IT REACHES THE SYMMETRICAL POINT
818     C --------------------------------------------------------------------
819     991 Z(MARK,JJ)=J*DZ
820              TZZ=(Z(MARK,JJ)-Z(MARK,JJ-1))/VZ
821              X=X+VX*TZZ
822              Y=Y+VY*TZZ
823              VSUM(MARK)=VSUM(MARK)+VZ
824              R1(MARK,JJ)=DSQRT(X*X+Y*Y)
825              THETA(MARK,JJ)=ANGLE(X,Y)
826              A1=2.19E3*TE(1,J)*SQRT(TE(1,J))*LAMDA
827              A2=1.14E4*LAMDA*TE(1,J)
828              ALAMDA=ALOG(AMIN1(A1,A2))
829              A3=8.67E-30*LAMDA*LAMDA*ALAMDA/TE(1,J)
830              KA(MARK,JJ)=A3*NOI(1,J)**2*3E10*TZZ/SQRT(1-NOI(1,J)/CRIDEN)
831              J=J+1
832              LOCX(MARK,JJ)=I
833              LOCY(MARK,JJ)=J
834              IF (J.GT.NX) GOTO 666
835              TR=TR+TZZ
836              GOTO 995
837     C --------------------------------------------------------------------
838     C        RAY HITS AT THE 1ST SHELL LAYER
839     C --------------------------------------------------------------------
```
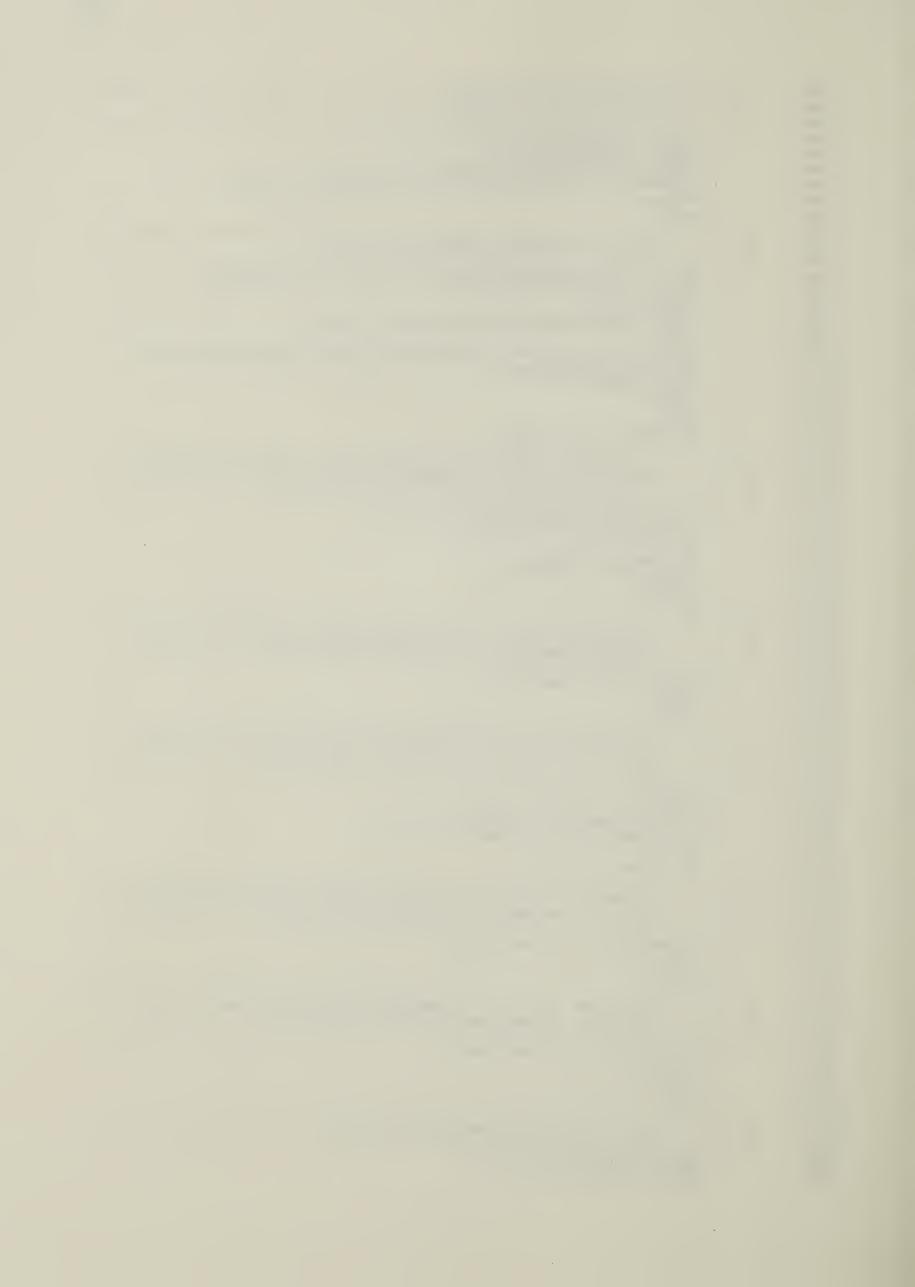
```
840        992 X=X+VX*(TR1-TR)
841            Y=Y+VY*(TR1-TR)
842            VSUM(MARK)=VSUM(MARK)+VZ
843            R1(MARK,JJ)=R2(1,J)
844            THETA(MARK,JJ)=ANGLE(X,Y)
845        999 A1=2.19E3*TE(1,J)*SQRT(TE(1,J))*LAMDA
846            A2=1.14E4*LAMDA*TE(1,J)
847            ALAMDA=ALOG(AMIN1(A1,A2))
848            A3=8.67E-30*LAMDA*LAMDA*ALAMDA/TE(1,J)
849            KA(MARK,JJ)=A3*NOI(1,J)**2*3E10*(TR1-TR)/SQRT(1-NOI(1,J)/
850           *CRIDEN)
851            WRITE(6,605)MARK,J,KA(MARK,JJ)
852        605 FORMAT(/'ABS.COEFF.(',I2,',  1,',I2,')=',E15.8)
853            I=2
854            LOCX(MARK,JJ)=I
855            LOCY(MARK,JJ)=J
856            GOTO 3
857        993 R1(MARK,JJ)=R2(1,J)
858            TR=(R1(MARK,JJ)-R1(MARK,JJ-1))/(VR*RI(1,J))
859            Z(MARK,JJ)=Z(MARK,JJ-1)+TR*VZ*RI(1,J)
860            IF (Z(MARK,JJ).GT.J*DZ) GOTO 996
861            VSUM(MARK)=VSUM(MARK)+VZ
862            X=X+VX*TR*RI(1,J)
863            Y=Y+VY*TR*RI(1,J)
864            THETA(MARK,JJ)=ANGLE(X,Y)
865            A1=2.19E3*TE(1,J)*SQRT(TE(1,J))*LAMDA
866            A2=1.14E4*LAMDA*TE(1,J)
867            ALAMDA=ALOG(AMIN1(A1,A2))
868            A3=8.67E-30*LAMDA*LAMDA*ALAMDA/TE(1,J)
869            KA(MARK,JJ)=A3*NOI(1,J)**2*3E10*TR/SQRT(1-NOI(1,J)/CRIDEN)
870            WRITE(6,605)MARK,J,KA(MARK,JJ)
871            I=2
872            LOCX(MARK,JJ)=I
873            LOCY(MARK,JJ)=J
874            GOTO 999
875        996 Z(MARK,JJ)=J*DZ
876            TZZ=(Z(MARK,JJ)-Z(MARK,JJ-1))/(VZ*RI(1,J))
877            X=X+VX*RI(1,J)*TZZ
878            Y=Y+VY*RI(1,J)*TZZ
879            VSUM(MARK)=VSUM(MARK)+VZ
880            R1(MARK,JJ)=DSQRT(X*X+Y*Y)
881            THETA(MARK,JJ)=ANGLE(X,Y)
882            A1=2.19E3*TE(1,J)*SQRT(TE(1,J))*LAMDA
883            A2=1.14E4*LAMDA*TE(1,J)
884            ALAMDA=ALOG(AMIN1(A1,A2))
885            A3=8.67E-30*LAMDA*LAMDA*ALAMDA/TE(1,J)
886            KA(MARK,JJ)=A3*NOI(1,J)**2*3E10*TZZ/SQRT(1-NOI(1,J)/CRIDEN)
887            J=J+1
888            LOCX(MARK,JJ)=I
889            LOCY(MARK,JJ)=J
890            IF (J.GT.NX) GOTO 666
891            JJ=JJ+1
892            IF (JJ.GT.100) GOTO 37
893            GOTO 993
894    C-------------------------------------------------------------------
895    C          ALGORITHM FOR RAYS GOING ALONG Z-AXIS
896    C-------------------------------------------------------------------
897        110 JJ=1
898            J=1
899            VZ=3.0E10
900            DZ=ZL/NX1
901            R1(MARK,1)=0.0
902            THETA(MARK,1)=0.0
903            Z(MARK,1)=0.0
904            LOCX(MARK,1)=1
905            LOCY(MARK,1)=1
906       1101 JJ=JJ+1
907            IF (JJ.GT.100) GOTO 37
908            TZ=DZ/(VZ*RI(1,J))
909            R1(MARK,JJ)=0.0
910            THETA(MARK,JJ)=0.0
```
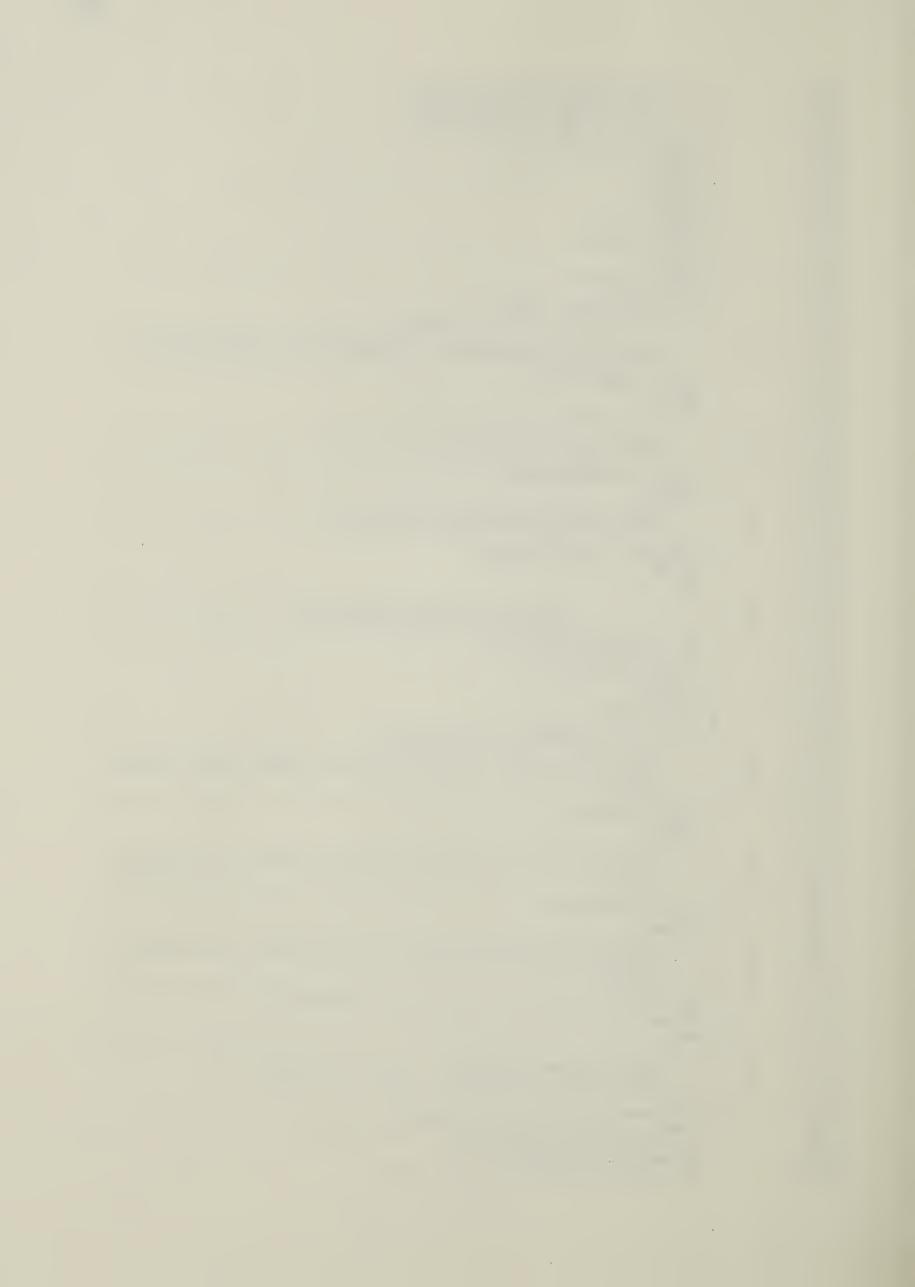
```
911             Z(MARK,JJ)=Z(MARK,JJ-1)+DZ
912             VSUM(MARK)=VSUM(MARK)+VZ
913             A1=2.19E3*TE(1,J)*SQRT(TE(1,J))*LAMDA
914             A2=1.14E4*LAMDA*TE(1,J)
915             ALAMDA=ALOG(AMIN1(A1,A2))
916             A3=8.67E-30*LAMDA*LAMDA*ALAMDA/TE(1,J)
917             KA(MARK,JJ)=A3*NOI(1,J)**2*3E10*TZ/SQRT(1-NOI(1,J)/CRIDEN)
918             J=J+1
919             LOCX(MARK,JJ)=1
920             LOCY(MARK,JJ)=J
921             IF (J.GT.NX) GOTO 666
922             GOTO 1101
923       666 NPTS(MARK)=JJ
924             WRITE(6,601)MARK
925       601 FORMAT(/'DATA FROM PROGRAM:RAYABS',/'RAY',1X,I3/' RAD.POS. ',2X,
926          *'ANG.POS. ',2X,
927          *'AXIAL POSI.',2X,'ABS.COEF. ',2X,'X CELL LOC.',2X,'Y CELL LOC.')
928             WRITE(6,602) (R1(MARK,J),THETA(MARK,J),Z(MARK,J),KA(MARK,J),LOCX(M
929          *ARK,J),LOCY(MARK,J),J=1,JJ)
930       602 FORMAT(E10.3,2X,E10.3,2X,E10.3,2X,E10.3,2X,7X,I3,2X,7X,I3)
931             WRITE(2,603) (R1(MARK,J),Z(MARK,J),J=1,JJ)
932       603 FORMAT(2E18.10)
933             VSUM(MARK)=VSUM(MARK)/JJ
934             GOTO 12
935             END
936 C----------------------------------------------------------------
937 C          X VELOCITY ALGORITHM
938 C----------------------------------------------------------------
939             REAL FUNCTION XVEL(X,VX,T,I,J)
940             DOUBLE PRECISION X
941             COMMON /GRIDP/R2(60,60),OMEGA(60,60),LASHEL
942             XVEL=-OMEGA(I,J)*X*SIN(OMEGA(I,J)*T)+VX*COS(OMEGA(I,J)*T)
943             RETURN
944             END
945 C----------------------------------------------------------------
946 C          Y VELOCITY ALGORITHM
947 C----------------------------------------------------------------
948             REAL FUNCTION YVEL(Y,VY,T,I,J)
949             DOUBLE PRECISION Y
950             COMMON /GRIDP/R2(60,60),OMEGA(60,60),LASHEL
951             YVEL=-OMEGA(I,J)*Y*SIN(OMEGA(I,J)*T)+VY*COS(OMEGA(I,J)*T)
952             RETURN
953             END
954 C----------------------------------------------------------------
955 C          X COORDINATE ALGORITHM
956 C----------------------------------------------------------------
957             REAL FUNCTION XCOOR(X,VX,T,I,J)
958             DOUBLE PRECISION X
959             COMMON /GRIDP/R2(60,60),OMEGA(60,60),LASHEL
960             XCOOR=X*COS(OMEGA(I,J)*T)+VX*SIN(OMEGA(I,J)*T)/OMEGA(I,J)
961             RETURN
962             END
963 C----------------------------------------------------------------
964 C          Y COORDINATE ALGORITHM
965 C----------------------------------------------------------------
966             REAL FUNCTION YCOOR(Y,VY,T,I,J)
967             DOUBLE PRECISION Y
968             COMMON /GRIDP/R2(60,60),OMEGA(60,60),LASHEL
969             YCOOR=Y*COS(OMEGA(I,J)*T)+VY*SIN(OMEGA(I,J)*T)/OMEGA(I,J)
970             RETURN
971             END
972 C----------------------------------------------------------------
973 C          MINIMUM RADIUS ALGORITHM
974 C----------------------------------------------------------------
975             REAL FUNCTION SMALR(R,VX,VY,D,I,J)
976             DOUBLE PRECISION VX,VY
977             COMMON /GRIDP/R2(60,60),OMEGA(60,60),LASHEL
978             SMALR=R**2/2+(VX**2+VY**2)/(2*OMEGA(I,J)**2)-D
979             IF (SMALR.LT.0.0) SMALR=0.0
980             SMALR=SQRT(SMALR)
981             RETURN
982             END
```
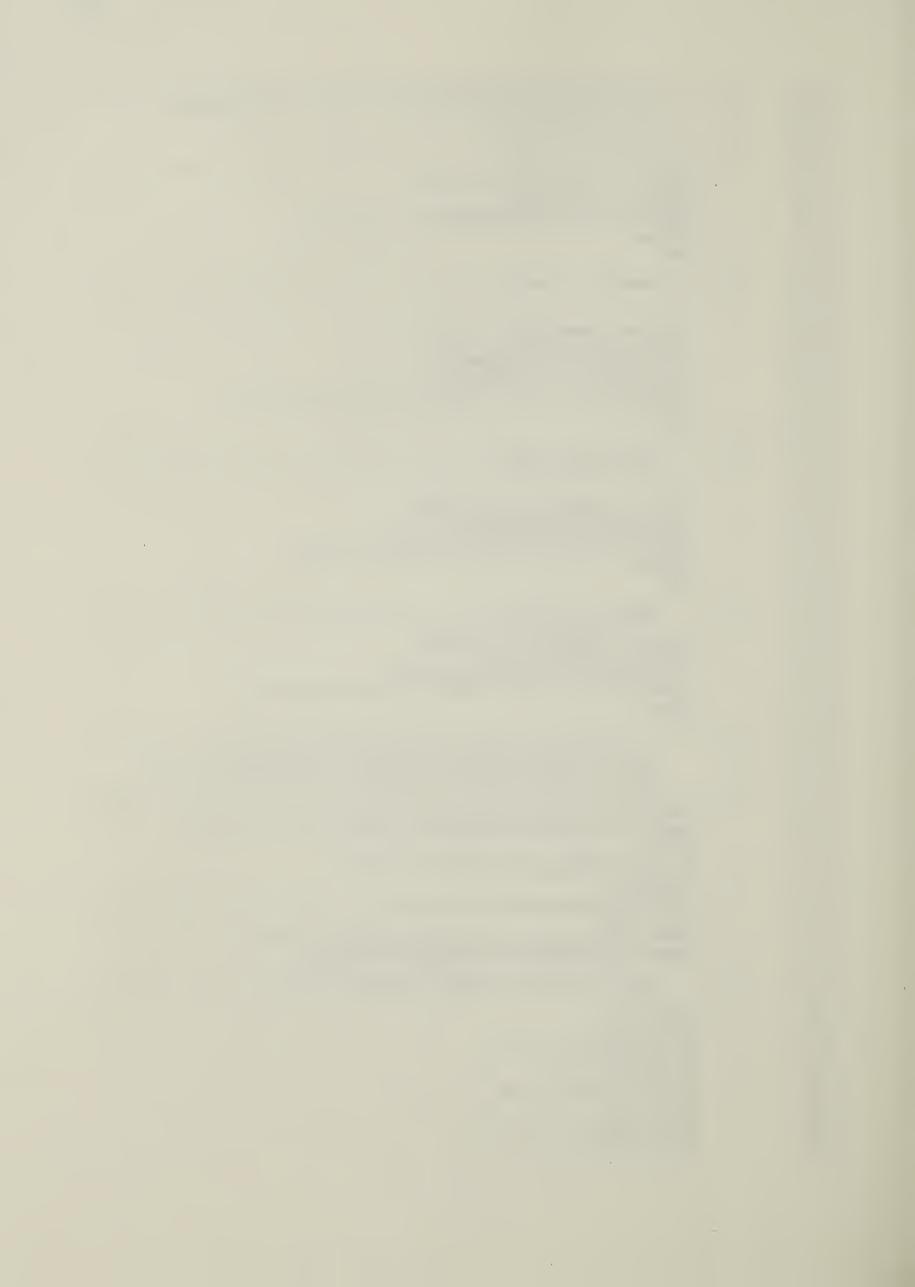
```
983      C----------------------------------------------------------------------
984      C           MAXIMUM RADIUS ALGORITHM
985      C----------------------------------------------------------------------
986            REAL FUNCTION BIGR(R,VX,VY,D,I,J)
987            DOUBLE PRECISION VX,VY
988            COMMON /GRIDP/R2(60,60),OMEGA(60,60),LASHEL
989            BIGR=DSQRT(R**2/2+(VX**2+VY**2)/(2*OMEGA(I,J)**2)+D)
990            RETURN
991            END
992      C----------------------------------------------------------------------
993      C           TIME FOR TRAVERSING FROM SHELL TO SHELL
994      C----------------------------------------------------------------------
995            REAL FUNCTION RTIME(RNOT,RNEW,VELX,VELY,ID,JD,PHIO,DD)
996            DOUBLE PRECISION VELX,VELY
997            INTEGER FLAG
998            COMMON /GRIDP/R2(60,60),OMEGA(60,60),LASHEL
999            IO=ID
1000           RTIME1=RNEW**2-RNOT**2/2-(VELX**2+VELY**2)/(2*OMEGA(ID,JD)**2)
1001           RTIME1=ASIN(RTIME1/DD)
1002           THETA=RTIME1
1003           FLAG=1
1004           IO=0
1005           IF (THETA.LT.0.0) GOTO 1
1006     C ---------------------------------------------------------------------
1007     C           TO CONVERT THETA TO ITS MULTIPLE ANGLE IN THE 2ND QUADRANT
1008     C           GIVEN THE ARGUMENT OF SIN(THETA) IS POSITIVE
1009     C ---------------------------------------------------------------------
1010         3 RTIME=(RTIME1-PHIO)/(2*OMEGA(ID,JD))
1011           IF (RTIME.GT.0.0) RETURN
1012           IO=IO+1
1013           IF (FLAG.EQ.0)GOTO 2
1014           RTIME1=IO*3.14159-THETA
1015           FLAG=0
1016           GOTO 3
1017     C ---------------------------------------------------------------------
1018     C           TO CONVERT THETA TO ITS MULTIPLE VALUE IN THE 3RD QUADRANT
1019     C           GIVEN THE ARGUMENT OF SIN(THETA) IS POSITIVE
1020     C ---------------------------------------------------------------------
1021         2 RTIME1=IO*3.14159+THETA
1022           FLAG=1
1023           GOTO 3
1024     C ---------------------------------------------------------------------
1025     C           TO CONVERT THETA TO ITS MULTIPLE VALUE IN THE 4TH QUADRANT
1026     C           GIVEN THE ARGUMENT OF SIN(THETA) IS NEGATIVE
1027     C ---------------------------------------------------------------------
1028         1 IO=IO+1
1029           RTIME1=3.14159+ABS(THETA)
1030         5 RTIME=(RTIME1-PHIO)/(2*OMEGA(ID,JD))
1031           IF (RTIME.GT.0.0) RETURN
1032           IO=IO+1
1033           IF (FLAG.EQ.0) GOTO 4
1034     C ---------------------------------------------------------------------
1035     C           TO CONVERT THETA TO ITS MULTIPLE VALUE IN THE 2ND QUADRANT
1036     C           GIVEN THE ARGUMENT OF SIN(THETA) IS NEGATIVE
1037     C ---------------------------------------------------------------------
1038           RTIME1=IO*3.14159-ABS(THETA)
1039           FLAG=0
1040           GOTO 5
1041     C ---------------------------------------------------------------------
1042     C           TO CONVERT THETA TO ITS MULTIPLE VALUE IN THE 3RD QUADRANT
1043     C           GIVEN THE ARGUMENT OF SIN(THETA) IS NEGATIVE
1044     C ---------------------------------------------------------------------
1045         4 RTIME1=IO*3.14159+ABS(THETA)
1046           FLAG=1
1047           GOTO 5
1048           END
1049     C----------------------------------------------------------------------
1050     C           ANGLE BETWEEN TWO CONSECUTIVE POINTS
1051     C----------------------------------------------------------------------
1052           REAL FUNCTION ANGLE(X,Y)
1053           DOUBLE PRECISION X,Y
```
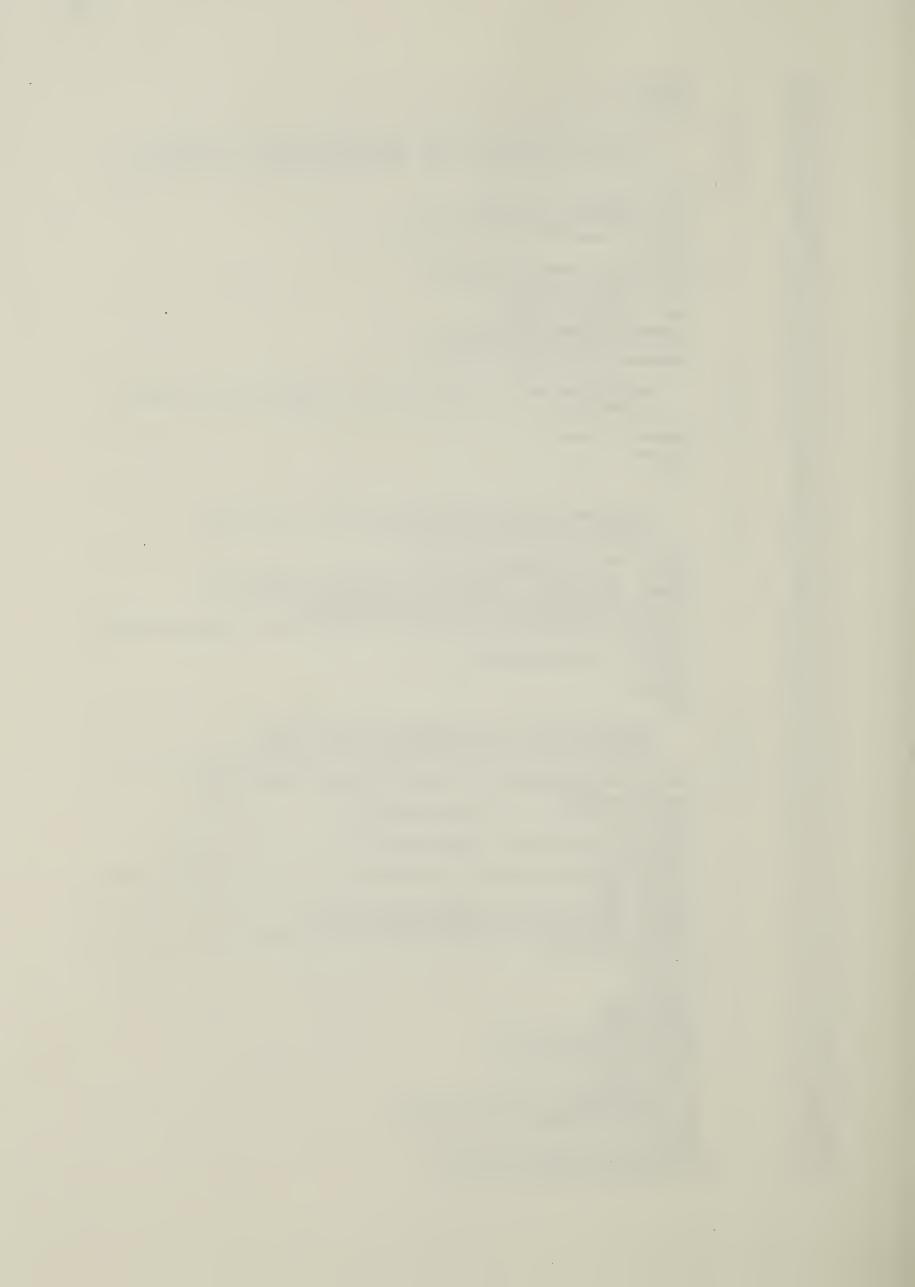
```
1054                  IF (X.EQ.O.O.AND.Y.GE.O.O) GOTO 2
1055                  IF (X.EQ.O.O.AND.Y.LT.O.O) GOTO 6
1056                  IF (Y.EQ.O.O.AND.X.GT.O.O) GOTO 4
1057                  IF (Y.EQ.O.O.AND.X.LT.O.O) GOTO 7
1058                  ANGLE=DATAN(X/Y)
1059                  GOTO 5
1060                2 ANGLE=O.O
1061                  RETURN
1062                6 ANGLE=3.14159
1063                  RETURN
1064                4 ANGLE=1.570795
1065                  RETURN
1066                7 ANGLE=4.712385
1067                  RETURN
1068                5 IF (ANGLE.LT.O.O) GOTO 1
1069                  IF (X.GT.O.O.AND.Y.GT.O.O) RETURN
1070        C -------------------------------------------------------------------
1071        C           ANGLE IN THE 3RD QUADRANT WITH ARCTAN(X/Y) BEING POSITIVE
1072        C -------------------------------------------------------------------
1073                  ANGLE=ANGLE+3.14159
1074                  RETURN
1075                1 IF (X.LT.O.O.AND.Y.GT.O.O) GOTO 3
1076        C -------------------------------------------------------------------
1077        C           ANGLE IN THE 2ND QUADRANT WITH X>O,Y<O
1078        C -------------------------------------------------------------------
1079                  ANGLE=3.14159-ABS(ANGLE)
1080                  RETURN
1081        C -------------------------------------------------------------------
1082        C           ANGLE IN THE 4TH QUADRANT WITH X<O,Y>O
1083        C -------------------------------------------------------------------
1084                3 ANGLE=2*3.14159-ABS(ANGLE)
1085                  RETURN
1086                  END
1087        C-------------------------------------------------------------------
1088        C                     ALGORITHM FOR PHASE ANGLE PHI
1089        C-------------------------------------------------------------------
1090                  REAL FUNCTION FI(T1,T2)
1091                  IF (T2.EQ.O.O) GOTO 4
1092                  FI=ATAN(T1/T2)
1093                  GOTO 3
1094                4 FI=1.570795
1095                3 IF (FI.GT.O.O) GOTO 1
1096                  IF (T1.GT.O.O.AND.T2.LT.O.O) GOTO 2
1097        C -------------------------------------------------------------------
1098        C           PHI HAS THE MULTIPLE VALUE IN THE 4TH QUADRANT FOR PHI BEING
1099        C           NEGATIVE
1100        C -------------------------------------------------------------------
1101                  FI=2*3.14159-ABS(FI)
1102                  RETURN
1103        C -------------------------------------------------------------------
1104        C           PHI HAS THE MULTIPLE VALUE IN THE 2ND QUADRANT FOR PHI BEING
1105        C           NEGATIVE
1106        C -------------------------------------------------------------------
1107                2 FI=3.14159-ABS(FI)
1108                  RETURN
1109        C -------------------------------------------------------------------
1110        C           PHI HAS THE MULTIPLE VALUEIN THE 3RD QUADRANT FOR PHI BEING
1111        C           POSITIVE
1112        C -------------------------------------------------------------------
1113                1 IF (T1.LT.O.O.AND.T2.LT.O.O) FI=3.14159+ABS(FI)
1114                  RETURN
1115                  END
1116        C-------------------------------------------------------------------
1117        C           ALGORITHM FOR FINDING THE TIME OF TRAVERSING SHELL
1118        C           WITH A DECREASING DENSITY   N=NO(1-R**2/A**2)
1119        C-------------------------------------------------------------------
1120                  REAL FUNCTION HTIME(A,B,C,I,J,NC)
1121                  COMMON /GRIDP/R2(60,60),OMEGA(60,60),LASHEL
1122                  CALL ROOT(A,B,C,R1,R22,NC)
1123                  IF (NC.EQ.1) RETURN
1124                  IF (R1.LT.O.O.AND.R22.LT.O.O) GOTO 2
```
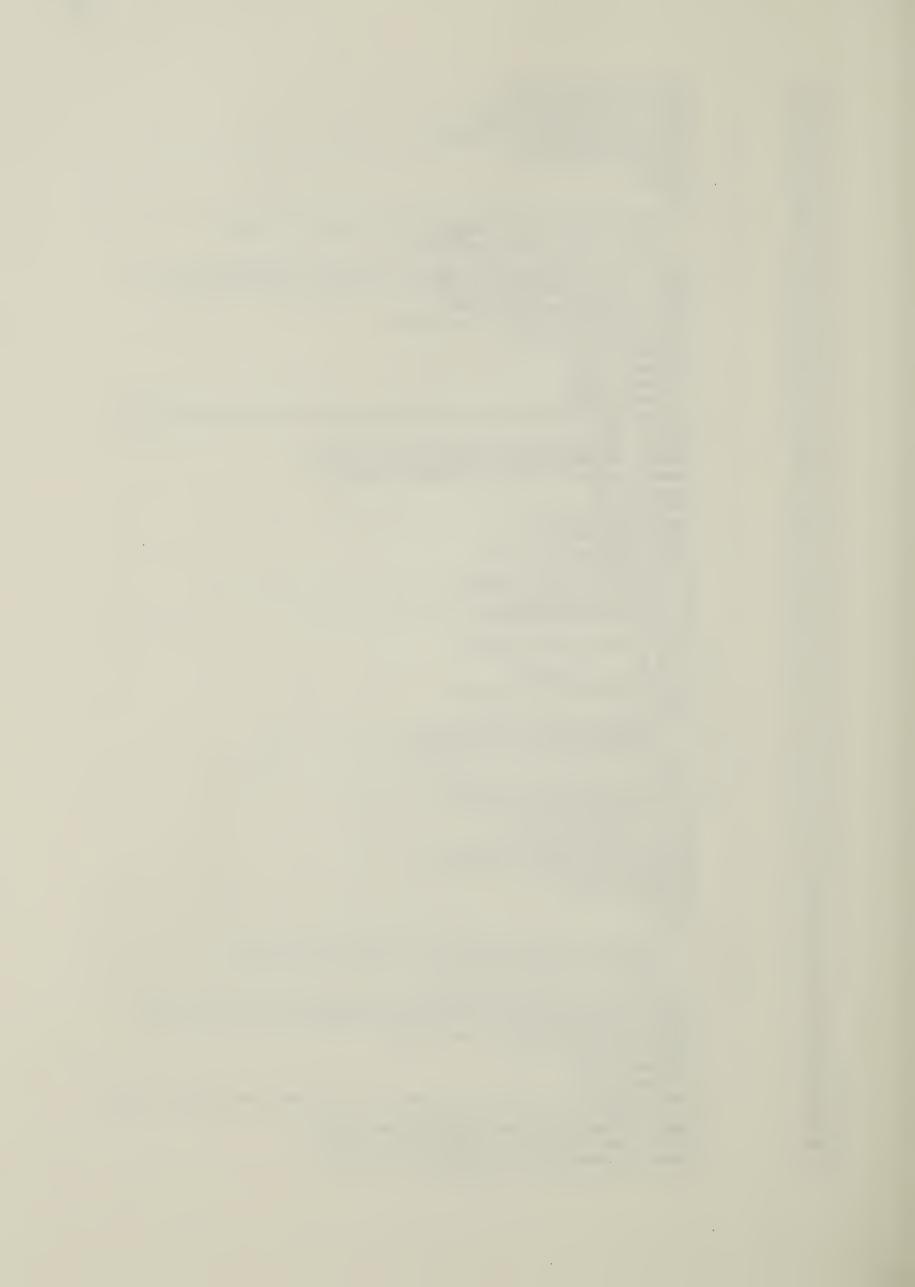
```
1191        C----------------------------------------------------------------
1192        C            TIME FUNCTION FOR NON-PARABOLIC DENSTIY APPROXIMATION
1193        C            N=NO(1-A**2/R**2)
1194        C
1195        C            CONST>O.O, VR>O.O
1196        C  ---------------------------------------------------------------
1197             FUNCTION TIMEPP(RO,R1,VR,CONST)
1198             FACT=(RO*VR)**2+CONST
1199             TIMEPP=FACT*R1**2-CONST*RO**2
1200             TIMEPP=RO/FACT*SQRT(TIMEPP)-RO*RO*RO*VR/FACT
1201             RETURN
1202             END
1203        C----------------------------------------------------------------
1204        C            CONST>O.O, VR<O.O
1205        C  ---------------------------------------------------------------
1206
1207             FUNCTION TIMEPN(RO,R1,VR,CONST)
1208             FACT=(RO*VR)**2+CONST
1209             TIMEPN=FACT*R1**2-CONST*RO**2
1210             IF (TIMEPN.LT.O.O) TIMEPN=O.O
1211             TIMEPN=RO/FACT*(-SQRT(TIMEPN))+RO*RO*RO*ABS(VR)/FACT
1212             RETURN
1213             END
1214        C  ---------------------------------------------------------------
1215        C            CONST<O.O, VR>O.O
1216        C  ---------------------------------------------------------------
1217
1218             FUNCTION TIMENP(RO,R1,VR,CONST)
1219             FACT=(RO*VR)**2-ABS(CONST)
1220             TIMENP=FACT*R1**2+ABS(CONST)*RO**2
1221             TIMENP=RO/FACT*SQRT(TIMENP)-RO*RO*RO*VR/FACT
1222             RETURN
1223             END
1224        C  ---------------------------------------------------------------
1225        C            CONST<O.O, VR<O.O,
1226        C  ---------------------------------------------------------------
1227             FUNCTION TIMENN(RO,R1,VR,CONST)
1228             FACT=(RO*VR)**2-ABS(CONST)
1229             TIMENN=FACT*R1**2+ABS(CONST)*RO**2
1230             TIMENN=RO/FACT*(-SQRT(TIMENN))+RO*RO*RO*ABS(VR)/FACT
1231             RETURN
1232             END
1233        C----------------------------------------------------------------
1234        C            ALGORITHM FOR FINDING THE ABSORPTION COEFFICIENTS
1235        C            IN THE PLASMA CELLS WITH A RADIALLY INCREASING PARABOLIC
1236        C            DENSITY PROFILE N=NO(1+R**2/A**2)
1237        C----------------------------------------------------------------
1238             SUBROUTINE ABSORB(MRAY,RO,ZO,DZ,T1,VX,VY,PHI,LAMDA,TE,D,I,J,JJ,Z)
1239             DOUBLE PRECISION DRO,DOMEGA,DAOISQ,DNOI,DD,F,Y,VX,T2,VY,
1240            *DVX,DVY
1241             REAL NOI,LAMDA,A1,A2,LLAMDA,KA,TE(30,60)
1242             INTEGER TOTRAY,MRAY,Z
1243             EXTERNAL F
1244             COMMON /ABSOB/AOISQ(60,60),NOI(60,60),LOCX(100,100),LOCY(100,100),
1245            *KA(100,100)
1246             COMMON /FUNCF/DRO,DVX,DVY,DOMEGA,DAOISQ,DNOI,DD,FI
1247             COMMON /GRIDP/R2(60,60),OMEGA(60,60),LASHEL
1248        C  ---------------------------------------------------------------
1249        C            CHANGE VALUES INTO DOUBLE PRECISION VALUES
1250        C  ---------------------------------------------------------------
1251             DRO=RO*1.DO
1252        C    DR1=R1*1.DO
1253             DAOISQ=AOISQ(I,J)*1.DO
1254             DNOI=NOI(I,J)*1.DO
1255        C    DVZ=VZ*1.DO
1256        C    DVT=(VX**2+VY**2)*1.DO
1257             DD=D*1.DO
1258             DOMEGA=OMEGA(I,J)*1.DO
1259             T2=T1*1.ODO
```
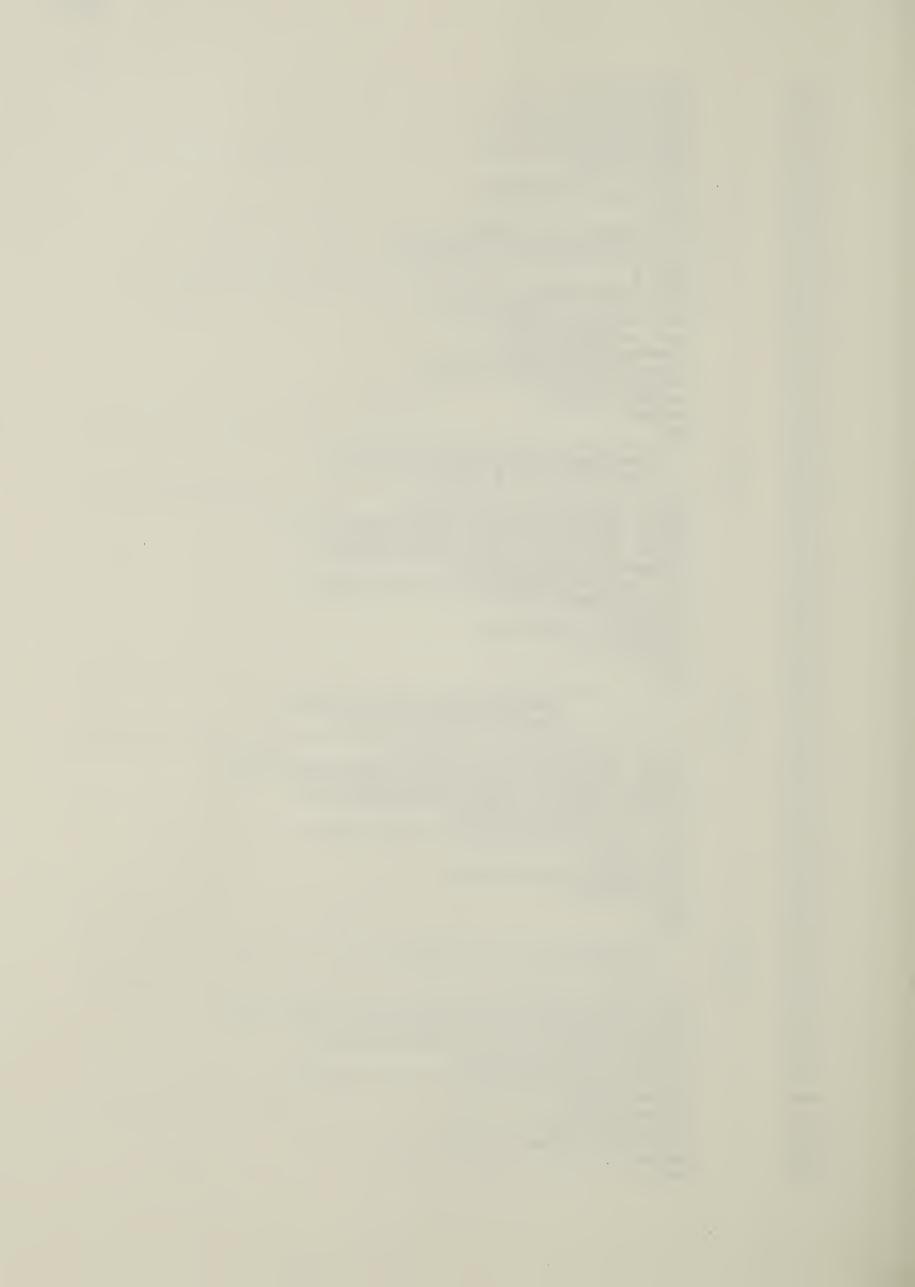
```
1260            DVX=VX
1261            OVY=VY
1262            FI=PHI
1263      C ------------------------------------------------------------
1264      C           FINO THE INTEGRAL PATH OF ABSORPTION BETWEEN TWO POINTS
1265      C           LOCX(MRAY,JJ) OENOTES THE CORRESPONOING CELL IN A PLASMA SHELL
1266      C           LAYER
1267      C ------------------------------------------------------------
1268            CALL OQG32(0.OO,T2,F,Y)
1269            IF (LOCX(MRAY,JJ-1).LT.I) GOTO 3
1270            IX=INT((LOCX(MRAY,JJ-1)-1)/2.O)+1
1271            GOTO 4
1272          3 IX=INT(LOCX(MRAY,JJ-1)/2.O)+1
1273          4 TE15=TE(IX,J)*SQRT(TE(IX,J))
1274            A1=2.19E3*TE15*LAMOA
1275            A2=1.14E4*LAMOA*TE(IX,J)
1276            LLAMOA=ALOG(AMIN1(A1,A2))
1277            A3=26.O1E-2O*LAMOA**2*LLAMDA*Z
1278            TKA=OABS(Y)*A3/TE15
1279      C ------------------------------------------------------------
1280      C           ABSORPTION COEF. IS THE SUM OF ALL SEGMENT LENGTHS WITHIN A
1281      C           PLASMA CELL
1282      C ------------------------------------------------------------
1283            KA(MRAY,JJ)=TKA
1284            RETURN
1285            END
1286
1287      C------------------------------------------------------------
1288      C           ALGORITHM  FOR THE FUNCTION USEO IN THE ABSORPTION
1289      C           INTEGRAL   N=NO(1+R**2/A**2)
1290      C------------------------------------------------------------
1291            DOUBLE PRECISION FUNCTION F(T)
1292            DOUBLE PRECISION T,RSQ,ORO,VX,VY,OOMEGA,ONOI,OAOISQ,DD
1293            COMMON /FUNCF/DRO,VX,VY,DOMEGA,DAOISQ,ONOI,DO,PHI
1294            COMMON /ONGRP/RI(60,60),CRIOEN,FLAG(60,60)
1295            RSQ=DRO**2/2.ODO+(VX**2+VY**2)/(2*OOMEGA**2)+DO*1.ODO*OSIN(2*OOMEG
1296           *A*T+PHI)
1297            F=ONOI*(1.OOO+RSQ/OAOISQ)
1298            F=F*F
1299            RETURN
1300            END
1301      C------------------------------------------------------------
1302      C           ALGORITHM FOR FINOING ABSORPTION COEF. FOR A
1303      C           PARABOLIC DENSITY PROFILE   N=NO(1-R**2/A**2)
1304      C------------------------------------------------------------
1305            SUBROUTINE ABSOB1(MARK,T1,VX,VY,VZ,LAMDA,TE,TERM1,TERM2,
1306           *I,J,JJ,Z,ZO,OZ)
1307            REAL NOI,LAMOA,A1,A2,LLAMOA,KA,TE(30,60)
1308            INTEGER Z
1309            DOUBLE PRECISION DOMEGA,DAOISQ,DNOI,T2,G,Y,VX,VY,VELX,VELY
1310            EXTERNAL G
1311            COMMON /ABSOB/AOISQ(60,60),NOI(60,60),LOCX(100,100),LOCY(100,100),
1312           *KA(100,100)
1313            COMMON /FUNCG/VELX,VELY,OOMEGA,OAOISQ,DNOI,TEM1,TEM2
1314            COMMON /GRIDP/R2(60,60),OMEGA(60,60),LASHEL
1315            COMMON /DRAYP/XO(100),YO(100),THETAX(100),THETAY(100),P(100),TOTRA
1316           *Y,ENIN,P1,EN(100)
1317            VELX=VX
1318            VELY=VY
1319            TEM1=TERM1
1320            TEM2=TERM2
1321            DAOISQ=AOISQ(I,J)*1.DO
1322            ONOI=NOI(I,J)*1.DO
1323            DOMEGA=OMEGA(I,J)*1.DO
1324            T2=T1*1.OOO
1325            CALL OQG32(0.DO,T2,G,Y)
1326            IF (LOCX(MARK,JJ-1).LT.I) GOTO 3
1327            IX=IFIX((LOCX(MARK,JJ-1)-1)/2.O)+1
1328            GOTO 4
1329          3 IX=IFIX(LOCX(MARK,JJ-1)/2.O)+1
1330          4 TE15=TE(IX,J)*SQRT(TE(IX,J))
```
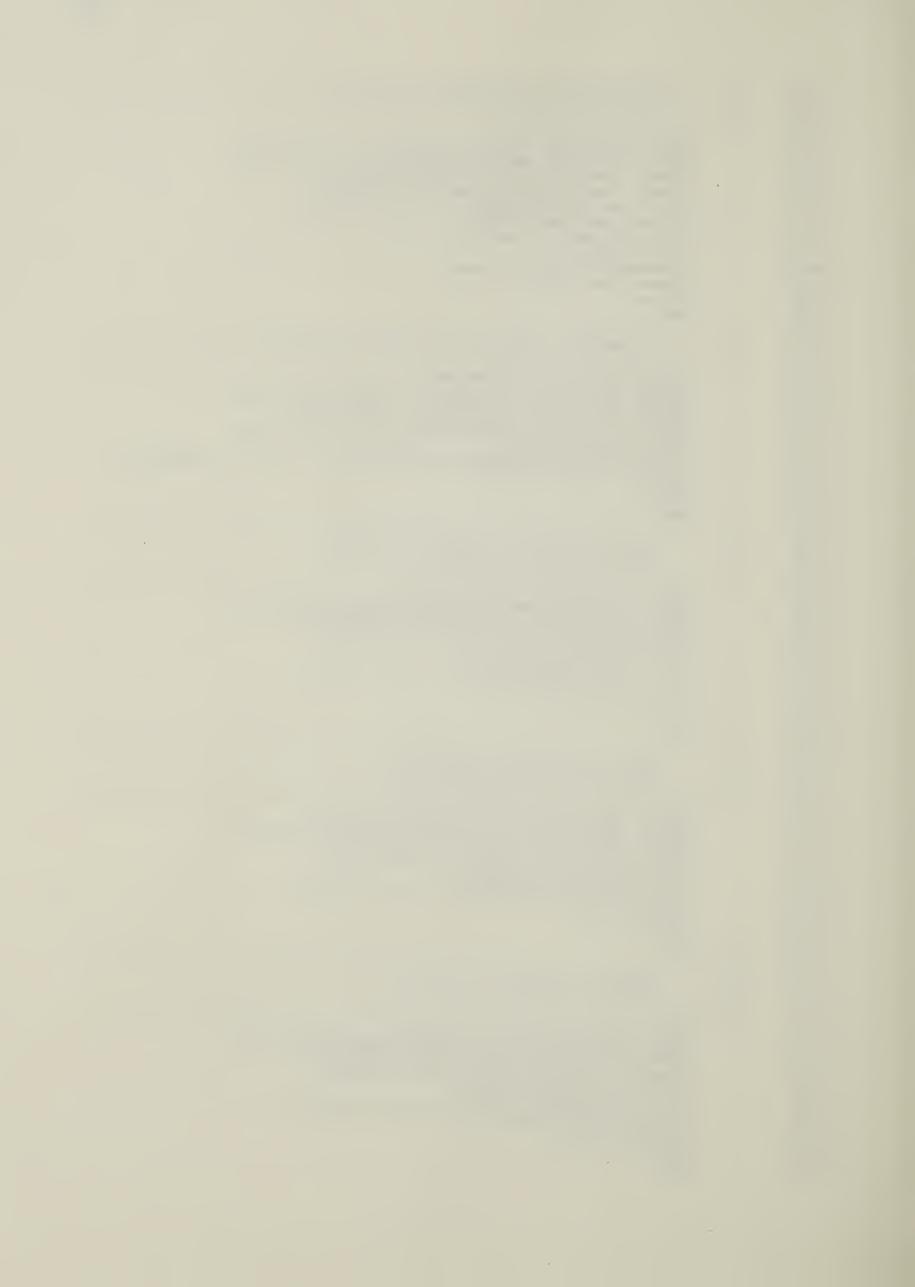
```
1331          A1=2.19E3*TE15*LAMDA
1332          A2=1.14E4*LAMDA*TE(IX,J)
1333          LLAMDA=ALOG(AMIN1(A1,A2))
1334          A3=26.01E-20*LAMDA**2*LLAMDA*Z
1335          TKA=DABS(Y)*A3/TE15
1336          KA(MARK,JJ)=TKA
1337          RETURN
1338          END
1339     C --------------------------------------------------------------
1340     C          FUNCTION FOR NON-PARABOLIC DE/IN-CREASING DENSITY
1341     C          N=NO(1-A**2/R**2),CONST>0.0
1342     C --------------------------------------------------------------
1343          SUBROUTINE ABOB2P(MRAY,RO,ZO,DZ,T1,VR,CONST,LAMDA,TE,I,J,JJ,Z)
1344          DOUBLE PRECISION DRO,DVR,DCONST,DNOI,DAOISQ,Y,F2P,T2,F2PN
1345          DOUBLE PRECISION F2PPN,F2PNN
1346          REAL NOI,LAMDA,TE(30,60),KA,LLAMDA
1347          INTEGER MRAY,Z,FLAG
1348          EXTERNAL F2P
1349          EXTERNAL F2PN
1350          EXTERNAL F2PPN
1351          EXTERNAL F2PNN
1352          COMMON /ABSOB/AOISQ(60,60),NOI(60,60),LOCX(100,100),LOCY(100,100),
1353         *KA(100,100)
1354          COMMON /FUNF2P/DRO,DNOI,DAOISQ,DCONST,DVR
1355          COMMON /GRIDP/R2(60,60),OMEGA(60,60),LASHEL
1356          COMMON /DNGRP/RI(60,60),CRIDEN,FLAG(60,60)
1357          DRO=RO*1.DO
1358          DVR=VR*1.DO
1359          DNOI=NOI(I,J)*1.DO
1360          DCONST=CONST*1.DO
1361          DAOISQ=AOISQ(I,J)*1.DO
1362          T2=T1*1.ODO
1363          IF (FLAG(I,J).EQ.4) GOTO 6
1364          IF (VR.LT.0.0) GOTO 5
1365          CALL DQG32(0.DO,T2,F2P,Y)
1366          GOTO 2
1367        5 CALL DQG32(0.DO,T2,F2PN,Y)
1368          GOTO 2
1369        6 IF (VR.LT.0.0) GOTO 7
1370          CALL DQG32(0.DO,T2,F2PPN,Y)
1371          GOTO 2
1372        7 CALL DQG32(0.DO,T2,F2PNN,Y)
1373        2 IF (LOCX(MRAY,JJ-1).LT.I) GOTO 3
1374          IX=INT((LOCX(MRAY,JJ-1)-1)/2.0)+1
1375          GOTO 4
1376        3 IX=INT(LOCX(MRAY,JJ-1)/2.0)+1
1377        4 TE15=TE(IX,J)*SQRT(TE(IX,J))
1378          A1=2.19E3*TE15*LAMDA
1379          A2=1.14E4*LAMDA*TE(IX,J)
1380          LLAMDA=ALOG(AMIN1(A1,A2))
1381          A3=26.01E-20*LAMDA**2*LLAMDA*Z
1382          TKA=DABS(Y)*A3/TE15
1383          KA(MRAY,JJ)=TKA
1384          RETURN
1385          END
1386     C--------------------------------------------------------------
1387     C          FUNCTION FOR NON-PARABOLIC DE/INCREASING DENSITY
1388     C          N=NO(1-A**2/R**2) CONST<0.0
1389     C--------------------------------------------------------------
1390          SUBROUTINE ABOB2N(MRAY,RO,ZO,DZ,T1,VR,CONST,LAMDA,TE,I,J,JJ,Z)
1391          DOUBLE PRECISION DRO,DVR,DCONST,DNOI,DAOISQ,Y,F2N,T2,F2P,F2PN
1392          REAL NOI,LAMDA,TE(30,60),KA,LLAMDA
1393          INTEGER MRAY,Z,FLAG
1394          EXTERNAL F2P
1395          EXTERNAL F2PN
1396          COMMON /ABSOB/AOISQ(60,60),NOI(60,60),LOCX(100,100),LOCY(100,100),
1397         *KA(100,100)
1398          COMMON /FUNF2P/DRO,DNOI,DAOISQ,DCONST,DVR
1399          COMMON /GRIDP/R2(60,60),OMEGA(60,60),LASHEL
1400          COMMON /DNGRP/RI(60,60),CRIDEN,FLAG(60,60)
```
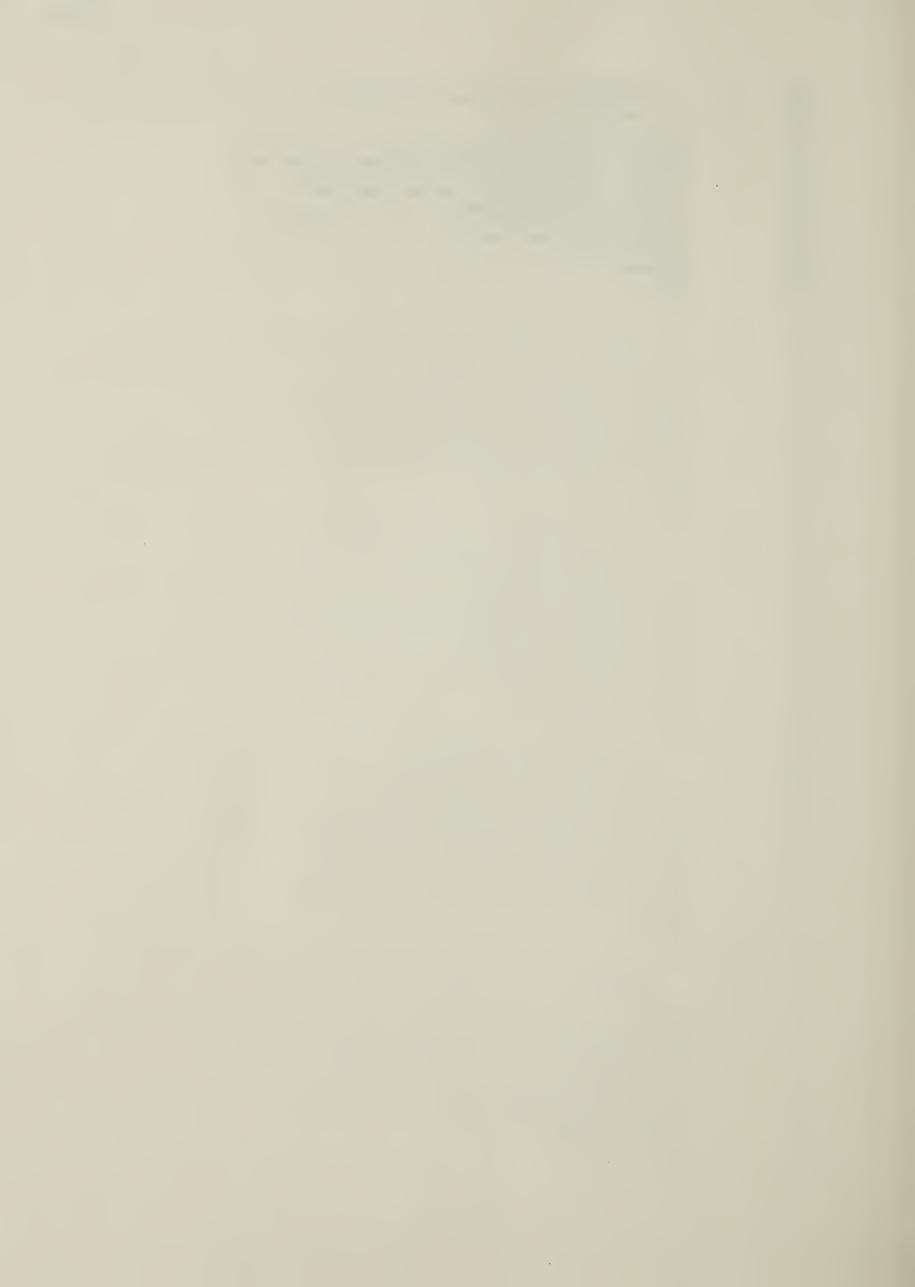
```
1401            DRO=RO*1.DO
1402            DVR=VR*1.DO
1403            DNOI=NOI(I,J)*1.DO
1404            DCONST=CONST*1.DO
1405            DAOISQ=AOISQ(I,J)*1.DO
1406            T2=T1*1.ODO
1407            IF (VR.LT.O.O) GOTO 5
1408            CALL DQG32(O.DO,T2,F2P,Y)
1409            GOTO 2
1410          5 CALL DQG32(O.DO,T2,F2PN,Y)
1411          2 IF (LOCX(MRAY,JJ-1).LT.I) GOTO 3
1412            IX=INT((LOCX(MRAY,JJ-1)-1)/2.0)+1
1413            GOTO 4
1414          3 IX=INT(LOCX(MRAY,JJ-1)/2.0)+1
1415          4 TE15=TE(IX,J)*SQRT(TE(IX,J))
1416            A1=2.19E3*TE15*LAMDA
1417            A2=1.14E4*LAMDA*TE(IX,J)
1418            LLAMDA=ALOG(AMIN1(A1,A2))
1419            A3=26.O1E-2O*LAMDA**2*LLAMDA*Z
1420            TKA=DABS(Y)*A3/TE15
1421            KA(MRAY,JJ)=TKA
1422            RETURN
1423            END
1424    C----------------------------------------------------------------
1425    C          FUNCTION F2P FOR N=NO(1-A**2/R**2)
1426    C          CONST>O.O OR <O.O   VR>O.O
1427    C----------------------------------------------------------------
1428            DOUBLE PRECISION FUNCTION F2P(T)
1429            DOUBLE PRECISION DRO,DNOI,DAOISQ,DCONST,DVR,O1
1430            COMMON /DNGRP/RI(60,60),CRIDEN,FLAG(60,60)
1431            COMMON /FUNF2P/DRO,DNOI,DAOISQ,OCONST,OVR
1432            D1=DRO*DRO*DVR*DVR+DCONST
1433            F2P=(T+DRO*DRO*DRO*DVR/D1)**2*D1*D1/DRO**2
1434            F2P=F2P+DCONST*DRO**2
1435            F2P=F2P/D1
1436            F2P=DNOI*(1-DAOISQ/F2P)
1437            F2P=F2P*F2P
1438            RETURN
1439            END
1440    C----------------------------------------------------------------
1441    C                  FUNCTION FOR N=NO(1-A**2/R**2)
1442    C                  CONST>O.O OR <O.O VR<O.O
1443    C----------------------------------------------------------------
1444            DOUBLE PRECISION FUNCTION F2PN(T)
1445            DOUBLE PRECISION DRO,DNOI,DAOISQ,DARG,DCONST,OVR,O1
1446            COMMON /DNGRP/RI(60,60),CRIDEN,FLAG(60,60)
1447            COMMON /FUNF2P/DRO,DNOI,DAOISQ,DCONST,DVR
1448            D1=DRO*DRO*DVR*DVR+DCONST
1449            F2PN=(T-DRO*DRO*DRO*DVR/D1)**2*D1*D1/ORO**2
1450            F2PN=F2PN+DCONST*DRO**2
1451            F2PN=F2PN/D1
1452            F2PN=DNOI*(1-DAOISQ/F2PN)
1453            F2PN=F2PN*F2PN
1454            RETURN
1455            END
1456    C----------------------------------------------------------------
1457    C          FUNCTION FOR N=NO(1+A**2/R**2)
1458    C          CONST>O.O VR<O.O
1459    C----------------------------------------------------------------
1460            DOUBLE PRECISION FUNCTION F2PNN(T)
1461            DOUBLE PRECISION ORO,DNOI,DAOISQ,DARG,DCONST,OVR,O1
1462            COMMON /DNGRP/RI(60,60),CRIDEN,FLAG(60,60)
1463            COMMON /FUNF2P/DRO,DNOI,DAOISQ,DCONST,OVR
1464            D1=DRO*DRO*DVR*DVR+DCONST
1465            F2PNN=(T-DRO*DRO*DRO*DVR/D1)**2*D1*D1/DRO**2
1466            F2PNN=F2PNN+DCONST*DRO**2
1467            F2PNN=F2PNN/D1
1468            F2PNN=DNOI*(1+DAOISQ/F2PNN)
1469            F2PNN=F2PNN*F2PNN
1470            RETURN
1471            END
```

181

```fortran
      C----------------------------------------------------------------------
      C         FUNCTION F2PPN FOR N=NO(1+A**2/R**2)
      C         CONST>0.0 VR>0.0
      C----------------------------------------------------------------------
              DOUBLE PRECISION FUNCTION F2PPN(T)
              DOUBLE PRECISION DRO,DNOI,DAOISQ,DARG,DCONST,DVR,D1
              COMMON /DNGRP/RI(60,60),CRIDEN,FLAG(60,60)
              COMMON /FUNF2P/DRO,DNOI,DAOISQ,DCONST,DVR
              D1=DRO*DRO*DVR*DVR+DCONST
              F2PPN=(T+DRO*DRO*DRO*DVR/D1)**2*D1*D1/DRO**2
              F2PPN=F2PPN+DCONST*DRO**2
              F2PPN=F2PPN/D1
              F2PPN=DNOI*(1+DAOISQ/F2PPN)
              F2PPN=F2PPN*F2PPN
              RETURN
              END
      C----------------------------------------------------------------------
      C         ABSORPTION ALGORITHM FOR N=NO(1-R**2/A**2)
      C----------------------------------------------------------------------
              DOUBLE PRECISION FUNCTION G(T)
              DOUBLE PRECISION T,ARG,RSQ,VX,VY,DOMEGA,DNOI,DAOISQ
              COMMON /DNGRP/RI(60,60),CRIDEN,FLAG(60,60)
              COMMON /FUNCG/VX,VY,DOMEGA,DAOISQ,DNOI,TERM1,TERM2
              ARG=DSINH(2*DOMEGA*T)
              RSQ=TERM1*(1+DSQRT(1+ARG**2))+TERM2*ARG-(VX**2+VY**2)/DOMEGA**2
              G=DNOI*(1.D0-RSQ/DAOISQ)
              G=G*G
              RETURN
              END
      C----------------------------------------------------------------------
      C         FUNCTION FETA1 FOR N=NO(1-A**2/R**2)
      C         CONST>0.0 OR <0.0   VR>0.0
      C----------------------------------------------------------------------
              DOUBLE PRECISION FUNCTION FETA1(T)
              DOUBLE PRECISION DRO,DNOI,DAOISQ,DARG,DCONST,DVR,D1
              COMMON /DNGRP/RI(60,60),CRIDEN,FLAG(60,60)
              COMMON /FUNF2P/DRO,DNOI,DAOISQ,DCONST,DVR
              D1=DRO*DRO*DVR*DVR+DCONST
              FETA1=(T+DRO*DRO*DRO*DVR/D1)**2*D1*D1/DRO**2
              FETA1=FETA1+DCONST*DRO**2
              FETA1=D1/FETA1
              RETURN
              END
      C----------------------------------------------------------------------
      C         FUNCTION FOR N=NO(1-A**2/R**2)
      C         CONST>0.0 OR <0.0 VR<0.0
      C----------------------------------------------------------------------
              DOUBLE PRECISION FUNCTION FETA3(T)
              DOUBLE PRECISION DRO,DNOI,DAOISQ,DARG,DCONST,DVR,D1
              COMMON /DNGRP/RI(60,60),CRIDEN,FLAG(60,60)
              COMMON /FUNF2P/DRO,DNOI,DAOISQ,DCONST,DVR
              D1=DRO*DRO*DVR*DVR+DCONST
              FETA3=(T-DRO*DRO*DRO*DVR/D1)**2*D1*D1/DRO**2
              FETA3=FETA3+DCONST*DRO**2
              FETA3=D1/FETA3
              RETURN
              END
      C----------------------------------------------------------------------
      C         FUNCTION FOR N=NO(1+A**2/R**2)
      C         CONST>0.0 VR<0.0
      C----------------------------------------------------------------------
              DOUBLE PRECISION FUNCTION FETA4(T)
              DOUBLE PRECISION DRO,DNOI,DAOISQ,DARG,DCONST,DVR,D1
              COMMON /DNGRP/RI(60,60),CRIDEN,FLAG(60,60)
              COMMON /FUNF2P/DRO,DNOI,DAOISQ,DCONST,DVR
              D1=DRO*DRO*DVR*DVR+DCONST
              FETA4=(T-DRO*DRO*DRO*DVR/D1)**2*D1*D1/DRO**2
              FETA4=FETA4+DCONST*DRO**2
              FETA4=D1/FETA4
              RETURN
              END
```

```
1543      C------------------------------------------------------------------------
1544      C          FUNCTION FETA2 FOR N=NO(1+A**2/R**2)
1545      C          CONST>0.0 VR>0.0
1546      C------------------------------------------------------------------------
1547          DOUBLE PRECISION FUNCTION FETA2(T)
1548          DOUBLE PRECISION DRO,DNOI,DAOISQ,DARG,DCONST,DVR,D1
1549          COMMON /DNGRP/RI(60,60),CRIDEN,FLAG(60,60)
1550          COMMON /FUNF2P/DRO,DNOI,DAOISQ,DCONST,DVR
1551          D1=DRO*DRO*DVR*DVR+DCONST
1552          FETA2=(T+DRO*DRO*DRO*DVR/D1)**2*D1*D1/DRO**2
1553          FETA2=FETA2+DCONST*DRO**2
1554          FETA2=D1/FETA2
1555          RETURN
1556          END
```